Investigation of Low Cost Infrared Sensing for Intelligent Deployment of Occupant Restraints

by

Amjad Juna

A Doctoral Thesis
Submitted in partial fulfilment of the requirements
for the award of

Doctor of Philosophy
of Loughborough University

May 2005

Loughborough University

CONTENTS LIST

List of Figures..1

Nomenclature..6

Glossary..8

Abstract 10

Acknowledgements..11

Chapter 1 Introduction..12

1.1 Description of the Research Work......................................12

1.2 Structure of the Thesis......................................12

1.3 Motivation for the Research......................................14

1.4 Accident Statistics......................................16

1.5 Importance of Airbag Safety......................................18

1.6 Scope of the Research......................................20

Chapter 2 Literature Review..23

2.1 A History of Car Safety......................................24

2.2 Accident Analysis and Cause and Effect of Airbag Related Injury......................................26

2.3 Advances In Airbag Technology......................................36

2.4 Sensors......................................42

2.5 Methods to Measure Height......................................45

2.6 Methods to Measure Weight......................................45

2.7 Out of Position Measurement......................................48

2.8 Video Systems for Occupant Detection......................................48

2.9 Safety Through Improved Design....................................54

2.10 The History and Theory of Thermal Imaging........................55

2.11 Pyroelectric Detectors..57

2.12 The IRISYS Thermal Imager...57

2.13 Applications of Thermography......................................58

2.14 Advantages of Thermography.......................................65

2.15 Advantages of Thermal Imager over a Standard Camera.....65

2.16 Summary of Literature Review.......................................66

2.17 The Scope of the Research..67

Chapter 3 Context of Research..69

3.1 Introduction..69

3.2 The Need for an Intelligent Airbag Deployment System.........69

3.3 The Advantages of Using Vision Based Systems.................75

3.4 Advantages of Using Thermography.................................76

3.5 Out of Position (OOP) Occupant......................................78

3.6 Other Developments in Advanced Vehicle Systems.............79

3.7 Potential Problems with the Intelligent Vehicle Concept.........84

3.8 Summary of Chapter 3..91

Chapter 4 Experimental Work..93

4.1 Preliminary Work...93

4.2 ITAI Crash Test Event...103

4.3 Experiment Using Talley Pressure Monitor for Occupant Seating Position Measurement...109

4.4 Operation of the Talley Pressure Monitor (TPM)..................110

4.5 Talley Pressure Monitor Results......................................113

4.6 Driving Simulator Trials..123

Chapter 5 Image Processing..128

5.1 Image Processing Techniques..128

5.2 Image Processing of the Data from the STISIM Car Simulator Experiments..130

5.3 Threshold Images..134

5.4 Analysis of Threshold Images..142

5.5 MatLab Region Properties of Threshold Images..143

5.6 Graphical Treatment of the Images..145

5.7 Discussion of the Graphs..153

5.8 MatLab Detection System..156

5.9 Visual Warning System..158

5.10 MatLab Functions..158

5.11 Summary..163

Chapter 6 Use of Artificial Neural Networks (ANN)..164

6.1 Background..164

6.2 Definition of an Artificial Neuron..165

6.3 Why Use ANN?..165

6.4 The Backpropagation Neural Network..167

6.5 Issues with ANN..169

6.6 Neural Network Analysis Results – In-Car Driver Activity Detection..170

6.7 Discussion of Accuracy of Neural Network Analysis for the Detection of In-Car Driver Activity..201

6.8 Neural Network Verification..202

6.9 Discussion of Possible Causes and Solutions of Neural Network Analysis Inaccuracy..203
6.10 Detection of Tall and Short Drivers...............................205

Chapter 7 Conclusions...208

Chapter 8 Future Work...211

References...214

Appendix 1 List of Papers..228

Appendix 2 Tables of Image Properties Data.................................246

Appendix 3 Tables of ANN Results...292

List of Figures

Figure 1-1 Crash test vehicle after side impact with 'bullet' vehicle.

Figure 1-2 Passenger compartment deformation after crash.

Figure 1-3 Table of pros and cons of the IRISYS thermal imager.

Figure 2-1 Deflated airbags.

Figure 2-2 Driver and passenger inflated airbags.

Figure 2-3 Diagram showing forward head displacement with respect to time (Reproduced from Mackay et al).

Figure 2-4 Equipment used in Facelab.

Figure 2-5 Schematic cross-section of detector array, reference [88].

Figure 2-6 Table describing uses of thermal imaging.

Figure 2-7 Thermal image of a patient with varicose veins.

Figure 2-8 Thermal image of a patient with a back spasm.

Figure 2-9 Motor and gearbox of baggage handling machine at Heathrow Airport.

Figure 2-10 Thermal image of the motor and gearbox showing internal winding problem.

Figure 3-1 Table showing fracture force of facial bones.

Figure 3-2 Table showing the fracture force of the skull.

Figure 3-3 Table showing the stiffness of the face and skull.

Figure 3-4 Diagram showing the breadth of activity within the 'intelligent vehicle' field.

Figure 4-1 Diagram showing set up of preliminary testing
Figure 4-2 Test rig used for preliminary work
Figure 4-3 Volunteer inside test rig
Figure 4-4 Large male adult
Figure 4-5 Child in infant seat
Figure 4-6 Driver looking right
Figure 4-7 Driver looking straight
Figure 4-8 Driver looking left
Figure 4-9 Driver holding cold drink
Figure 4-10 Driver leaning left
Figure 4-11 Driver smoking
Figure 4-12 Driver using mobile phone
Figure 4-13 Drowsy driver
Figure 4-14 Short driver
Figure 4-15 Medium driver/spectacles
Figure 4-16 Tall driver with spectacles
Figure 4-17 Female driver
Figure 4-18 Alsatian dog
Figure 4-19 Diagram of locations of bullet car and target car.
Figure 4-20 Thermal and visible image of Rusty Haight inside car cabin.
Figure 4-21 Diagram of TPM pressure pad
Figure 4-22 Picture of pressure pad on car seat
Figure 4-23 TPM control unit
Figure 4-24 TPM Results for Volunteer No.1
Figure 4-25 TPM Results for Volunteer No.2
Figure 4-26 TPM Results for Volunteer No.3
Figure 4-27 TPM Results for Volunteer No.4
Figure 4-28 TPM Results for Volunteer No.5
Figure 4-29 TPM Results for Volunteer No.6
Figure 4-30 TPM Results for Volunteer No.7

Figure 4-31 TPM Results for Volunteer No.8
Figure 4-32 TPM Results for Volunteer No.9
Figure 4-33 TPM Results for Volunteer No.10
Figure 4-34 TPM Results for Volunteer No.11
Figure 4-35 TPM Results for Volunteer No.12
Figure 4-36 TPM Results for Volunteer No.13
Figure 4-37 TPM Results for Volunteer No.14
Figure 4-38 TPM Results for Volunteer No.15
Figure 4-39 TPM Results for Volunteer No.16
Figure 4-40 Diagram of experimental set-up
Figure 4-41 Computers used for running simulator software
Figure 4-42 Driving simulator in action

Figure 5-1 Graphical User Interface used for the selection of thermal images.
Figure 5-2 Surface temperatures of various body parts for selected volunteers.
Figure 5-3 Thermal image and threshold image of driver looking straight.
Figure 5-4 Thermal image and threshold image of driver looking right.
Figure 5-5 Thermal image and threshold image of driver looking left.
Figure 5-6 Thermal image and threshold image of driver leaning forward
Figure 5-7 Thermal image and threshold image of driver with head on steering wheel.
Figure 5-8 Thermal image and threshold image of driver leaning right.
Figure 5-9 Thermal image and threshold image of driver reaching right.
Figure 5-10 Thermal image and threshold image of driver leaning left.
Figure 5-11 Table of region properties of threshold shape when looking straight.
Figure 5-12 Table of region properties of threshold shape when looking left.
Figure 5-13 Table of region properties of threshold shape when looking right.
Figure 5-14 Table of region properties of threshold shape when leaning left.
Figure 5-15 Table of region properties of threshold shape when leaning right.

Figure 5-16 Table of region properties of threshold shape when looking up.
Figure 5-17 Table of region properties of threshold shape when head is on steering wheel.
Figure 5-18 Centroid positions when looking straight ahead.
Figure 5-19 Area variation when looking straight ahead.
Figure 5-20 Minor axis length variation when looking straight ahead.
Figure 5-21 Centroid variation when looking to the left.
Figure 5-22 Centroid position for multiple driver scenarios.
Figure 5-23 Centroid position when looking to the left, right, and straight ahead.
Figure 5-24 Average centroid positions for multiple driver scenarios.
Figure 5-25 Area variation for multiple driver scenarios.
Figure 5-26 Minor axis length variation for multiple driver scenarios.

Figure 6-1 Schematic diagram of a feed-forward neural network
Figure 6-2 GUI of MatLab neural network toolbox being used.
Figure 6-3 MatLab neural network training in progress.
Figure 6-4 ANN Results to Detect 'Look Straight' Scenario
Figure 6-5 ANN Results to Detect 'Look Up' Scenario
Figure 6-6 ANN Results to Detect 'Look Right' Scenario
Figure 6-7 ANN Results to Detect 'Look Left' Scenario
Figure 6-8 ANN Results to Detect 'Lean Forward' Scenario
Figure 6-9 ANN Results to Detect 'Head on Wheel' Scenario
Figure 6-10 ANN Results to Detect 'Lean Right' Scenario
Figure 6-11 ANN Results to Detect 'Lean Left' Scenario
Figure 6-12 ANN Results to Detect 'Reach Right' Scenario
Figure 6-13 ANN Results to Detect 'Use Mobile Phone' Scenario
Figure 6-14 ANN Results to Detect 'Look Back' Scenario
Figure 6-15 ANN Results to detect OOP Scenarios for Volunteer 1
Figure 6-16 ANN Results to detect OOP Scenarios for Volunteer 2
Figure 6-17 ANN Results to detect OOP Scenarios for Volunteer 3

Figure 6-18 ANN Results to detect OOP Scenarios for Volunteer 4
Figure 6-19 ANN Results to detect OOP Scenarios for Volunteer 5
Figure 6-20 ANN Results to detect OOP Scenarios for Volunteer 6
Figure 6-21 ANN Results to detect OOP Scenarios for Volunteer 7
Figure 6-22 ANN Results to detect OOP Scenarios for Volunteer 8
Figure 6-23 ANN Results to detect OOP Scenarios for Volunteer 9
Figure 6-24 ANN Results to detect OOP Scenarios for Volunteer 10
Figure 6-25 ANN Results to detect OOP Scenarios for Volunteer 11
Figure 6-26 ANN Results to detect OOP Scenarios for Volunteer 12
Figure 6-27 ANN Results to detect OOP Scenarios for Volunteer 13
Figure 6-28 ANN Results to detect OOP Scenarios for Volunteer 14
Figure 6-29 ANN Results to detect OOP Scenarios for Volunteer 15
Figure 6-30 ANN Results to detect OOP Scenarios for Volunteer 16
Figure 6-31 ANN Results to detect OOP Scenarios for Volunteer 17
Figure 6-32 ANN Results to detect OOP Scenarios for Volunteer 18
Figure 6-33 ANN Results to detect OOP Scenarios for Volunteer 19
Figure 6-34 ANN Results to detect OOP Scenarios for Volunteer 20
Figure 6-35 ANN Results to detect OOP Scenarios for Volunteer 21
Figure 6-36 ANN Results to detect OOP Scenarios for Volunteer 22
Figure 6-37 ANN Results to detect OOP Scenarios for Volunteer 23
Figure 6-38 Table showing accuracy of revised ANN analysis
Figure 6-39 ANN Results to detect Tall and Short Drivers

Nomenclature

F	force		(N.
m	mass		(Kg)
v	velocity		(m/s)
r	radius		(m)
q	blackbody radiation emitted		$(W.m^2)$
σ	Stefan-Boltzmann Constant	5.67×10^{-8}	$(W/m^2.K^4)$
T_s	absolute temperature		(K)
T_{sf}	surface temperature		(K)
T_{sur}	surrounding temperature		(K)
α	absorptivity, where 1.0 = ideal blackbody.		
ε	emissivity (fraction).		
Vo	initial velocity		(m/s)
Vf	final velocity		(m/s)
L	length		(m)
h	height		(m)
a	acceleration		(m/s^2)
u	initial velocity		(m/s)
s	distance		(m)
t	time		(s)
P	pixel value after modification		

P'	pixel value before modification
A	constant
l	number of grey bits

Glossary

US	United States (of America)
EU	European Union
UK	United Kingdom
NHTSA	National Highway Traffic Safety Administration
GDP	Gross Domestic Product
SAE	Society of Automotive Engineers
BMI	Body Mass Index
CDS	Crashworthiness Data System
AIS	Abbreviated Injury Scale
BCR	Benefit to Cost Ratio
FARS	Fatal Accident Reporting System
SWI	Steering Wheel Involvement
CPI	Control Panel Involvement
WSI	Windshield Involvement
OOP	Out of Position
NASS CDS	National Automotive Sampling System Crashworthiness Data System
FMVSS	Federal Motor Vehicle Safety Standard
ICT	Institute for Chemical Technology
ISS	Integrated Safety System
PASS	Proximity Array Sensing System
IR	Infrared

MRI	Magnetic Resonance Imaging
FEF	Frontal Eye Field
RFIS	Rear Facing Infant Seat
BBC	British Broadcasting Corporation
CCD	Charged Coupled Device
FEA	Finite Element Analysis
C-PET	Calendered Polyester
U-PET	Uncalendered Polyester
ITAI	Institute of Road Traffic Safety Research Institute
ESRI	Ergonomics and Safety Research Institute
TPM	Talley Pressure Monitor
GUI	Graphical User Interface
ANN	Artificial Neural Network
NN	Neural Network
FFBP	Feed Forward Backpropagation
MLP	Multi Layer Perceptron

Abstract

In automotive transport, airbags and seatbelts are effective at restraining the driver and passenger in the event of a crash, with statistics showing a dramatic reduction in the number of casualties from road crashes.

However, statistics also show that a small number of these people have been injured or even killed from striking the airbag, and that the elderly and small children are especially at risk of airbag-related injury. This is the result of the fact that in-car restraint systems were designed for the average male at an average speed of 50 km/hr, and people outside these norms are at risk. Therefore one of the future safety goals of the car manufacturers is to deploy sensors that would gain more information about the driver or passenger of their cars in order to tailor the safety systems specifically for that person, and this is the goal of this project.

This thesis describes a novel approach to occupant detection, position measurement and monitoring using a low cost thermal imaging based system, which is a departure from traditional video camera based systems, and at an affordable price. Experiments were carried out using a specially designed test rig and a car driving simulator with members of the public.

Results have shown that the thermal imager can detect a human in a car cabin mock up and provide crucial real-time position data, which could be used to support intelligent restraint deployment. Other valuable information has been detected such as whether the driver is smoking, drinking a hot or cold drink, using a mobile phone, which can help to infer the level of driver attentiveness or engagement.

Keywords: Airbag safety, infrared, thermal imaging, image processing, occupant detection and classification.

Acknowledgments

I would like to first of all thank to my supervisors Professor Robert Parkin and Dr Mike Jackson for their continued support throughout the duration of the project.

I would like to thank IRISYS Ltd for their help and assistance in providing equipment and expertise to this project.

Thanks also go to my colleagues at the Loughborough University Mechatronics Research Group who have helped me along the way.

And finally, thanks also go to the Ergonomics and Safety Research Institute (ESRI) for their generous assistance towards this project.

Chapter 1 Introduction

1.1 Description of the Research Work

The research described in this thesis is work done with the intention of reducing the effects of airbag-induced injury and death. It is not a widely known fact that in the United States of America, there have been over 100 fatalities and thousands more injuries as a direct result of the impact between the inflated driver or passenger side airbag and the vehicle occupant.

This issue was addressed in three ways. Firstly, a comprehensive review of the available literature concerning this problem was done in order to identify the specific causes, most 'at risk' occupants, types of injury sustained, methods to reduce such injuries, and methods or design employed by other researchers to lessen the damaging effects of this problem.

Secondly, a novel method was identified and research objectives were set from the outset. Experimental work was designed and conducted using bespoke built test rigs and volunteer members of the public, to obtain data about seating and driving habits, and to test out theories and ideas. Finally, analysis of the data was done using Artificial Neural networks (ANN) and the results laid out in an accepted format. The results were discussed at length, and conclusions were drawn from them.

1.2 Structure of the Thesis

The structure of this thesis, 'Investigation of Low Cost Infrared Sensing for Intelligent Deployment of Occupant Restraints' follows a traditional linear pattern.

Chapter 1 introduces the research field that the author has chosen. The reader is given relevant information such as mortality rates, incidence of injury and the economic cost of vehicle crash incidents from major automobile owning geographical areas such as the U.S and the E.U. An explanation is given as to the importance of conducting research into this field in the first instance, and why there is the need to carry out the research at this time rather than at a later date.

Chapter 2 encompasses an extensive Literature Review including Journal papers and information from other sources of media such as published magazine articles, conference papers and articles from the internet, which are all related to the topic of airbag safety. It will also provide the basis upon which to build the proposal for the current research.

This review includes topics such as traffic accident data, current and future road safety legislation, airbag related injury and fatality statistics, injury causes and mechanisms. A comparison is made between the research conducted and published previously to the work that will be conducted within the scope of this project. The scope of the project is given at the end of chapter 2, and also a methodology of the work that will be done is described briefly.

Chapter 3 compares the research work proposed in this thesis to the work being done in the field of the 'intelligent automobile'. It also provides additional justification for conducting the research in this thesis.

Chapter 4 provides a description of the experimental design for the trials undertaken, the procedure followed and a description of the equipment used. The results of the experiments conducted are also discussed.

Chapter 5 presents the image processing techniques used in this thesis and the MatLab functions created for the purpose of processing the data obtained from the experiments.

Chapter 6 describes the neural network analysis that was done using the data collected from the experiments described in chapter 4. This chapter will describe how the data was processed, why it was done and also explain what the results show.

Chapter 7 is a brief statement of the conclusions that can be drawn from the thesis, and also whether the original objectives have been met.

Finally, chapter 8 will describe some of the work that should be done in order to progress the work even further, towards the goal of an intelligent deployment system for airbags.

1.3 Motivation for the Research

Although the title of the project states that it is concerned with the 'Investigation of Low Cost Infrared Sensing for Intelligent Deployment of Occupant Restraints', it should be noted that the term 'occupant restraints' covers restraints such as the safety harness belt (or seatbelt), the child safety seat and the occupant airbag. This project is primarily concerned with the advancement of current airbag technology and to develop a system that could deploy it in a more sophisticated way. The airbag design, construction or method of inflation is not the concern with this project, but sensing the correct scenario in which to deploy the airbag was the field of research to be investigated. In an intelligent system it would be beneficial to integrate the airbag, seatbelt and child safety seat deployment.

The desire to develop a new and improved airbag deployment system was motivated by events occurring in the field of automobile safety in the U.S, as well as growing concern in Europe. Much controversy was generated in the U.S by 'pressure groups' comprised of accident victims and researchers alike who have highlighted the potentially fatal consequences of current airbag design. It was found from reviewing accident statistics that rear facing infant seats and small female drivers were the two types of vehicle occupant that were most at risk of suffering a fatal injury as a direct result of an airbag being activated and deployed. This caused a dilemma for the automobile industry: the fact that a system designed to protect the car occupant from severe head injury in a crash situation, was itself responsible for causing the deaths of a number of occupants, and causing injuries to many others as well. Although the number of people killed as a result of airbag activation was relatively small compared with the number of lives saved as a result of airbag deployment, nevertheless it has been a source of acute embarrassment and concern that a safety device was responsible for the deaths of a number of people. This would also have had an impact on the confidence of the automobile consumer who would be wary of such new innovations in the automobile industry, and also the fear of successful litigation against the car manufacturers brought to Court by victims and their relatives could result in extremely high damages being paid by them, and these concerns, have brought the car manufacturers to the point of needing to rectify these problems.

For the purpose of highlighting the dangers of car impacts, Figure 1-1 shows the results of a side impact on a saloon car. Side impacts are an increasingly common type of car accident, and it is thought that these are the result of inattention by the driver at a T-junction, as they proceed to make a left or right turn and make an error of judgement. The occurrence of such incidents could be reduced by developing a system which is able to monitor whether the driver is alert during critical situations during a car journey, such as a T-junction. Figures 1-1 to 1-3 were freely available on the internet and were reproduced as examples of the type of damage that can occur during a car crash. It can be seen from the photos just how far the bodywork of the 'target' car has intruded into the occupant cabin space.

Figure 1-1: Crash test vehicle after side impact with 'bullet' vehicle

1.4 Accident Statistics

The statistics within this section were obtained from a number of sources **[1 – 4]**. The figures and statistics quoted in this section are from references 1 to 4, and these are reliable as they are official EU and UK governmental documents that have been published in the public domain. In the year 2001, the total number of fatalities recorded as a result of road accidents was 39,849 in the EU-15, the 15 member states that comprised the European Union at that time. These states were Austria, Belgium, Germany, Denmark, Spain, Greece, France, Finland, Italy, Ireland, Luxembourg, The Netherlands, Portugal, Sweden and the UK. In the year 2002, this equated to 102 people being killed per million of the population or approximately 1 in 10,000. Although there has been substantial progress since 1970, where the road fatality rate in the EU-15 countries stood at 77,831 people killed in that year, there is still scope for improvement in bringing the figures down. Other figures, however, also give concern. The total number of accidents occurring per year in the EU-15 nation states stood at 1,230,616 for the period 2001-2002. The number of vehicles involved in theses accidents was 2,290,067 and the number of people seriously injured and slightly injured as a result of these accidents was 1,669,772. The age categories of people killed were mostly of the 26-50 age group in which 6,963 people died. This suggests that road accidents, although decreasing ever more every year, are still a major cause of death in many countries.

It is, perhaps, unrealistic to ever expect there to be zero numbers of casualties, as cars are in the short and medium term still going to be controlled by human drivers who make human errors, and with hundreds of millions of vehicles being driven worldwide, there will always be accidents as a result of human mistakes. But there is a great deal of scope for reducing the numbers of casualties even further.

Another important point to realise is that it is not just the human cost that is important, but also the economic cost that is also worth considering, not only for the automobile industry but for the Government and consumer alike. According to the UK Department for Transport data published in the 'Highways Economics Note No.1 2002', there were a total of 221,751 road accidents which resulted in injury, with 3,124 fatal accidents, 30,521 serious and 188,106 slight accidents that occurred in the year 2002. These accidents, if prevented, would have a value of £12,808 million in 2002 prices and values. Also, the value of prevention in cost-benefit terms of the 3.3 million damage only accidents is valued at £4,951 million, giving a combined total of £17,760 million for that year. This is a huge economic cost, and explains why the UK government is keen to see a reduction of this figure by reducing the number of road accidents.

The statistics from the US are even worse than those of the EU. According to the US department of Transportation, 'National Highway Traffic Safety Administration (NHTSA), the year 2002 saw an increase of 1.5% from the previous year, up from 42,196 people killed in motor vehicle crashes in 2001 to 42,815 in the year 2002.

The number of people injured in 2002 in the US was 2,926,000, and the economic cost was also larger. According to the NHTSA, the economic cost of speeding related car crash incidents alone was estimated to be $40.4 billion per year, with speeding related incidents accounting for 31% of all fatal crashes. In many fatal crashes, the cabin occupant compartment would have had to deform and show deep intrusion. Figure 1-2 shows exactly how the cabin can be deformed. This image was reproduced from the www.car-accidents.com website, and is shown here for illustration purposes only. Figure 1-2 clearly shows the passenger compartment of the car deformed after a serious impact:

Figure 1-2: Passenger compartment deformation after crash

1.5 Importance of Airbag Safety

Advanced airbag safety systems are important because they are part of the wider effort in reducing the road accident casualty figures, and the reasons why car manufacturers and researchers alike would want to try to do this are:

- Legislation issues
- Economic reasons
- Publicity reasons
- Moral issues

The first reason is perhaps the most important. The new legislation described by the NHTSA of the U.S requires that all new automobiles for sale at the start of September 1st, 2005, must be fitted with advanced airbag technologies. A car manufacturer has no option other than to comply with the rule changes fully in order to have their vehicles legally fit for sale to the general public. If this was not done, the car manufacturer could not sell their products to the general public without finding themselves in breach of the law and be subject to legal action.

The second reason, the economic argument, is very important for a number of reasons. The first reason is the cost of an airbag deployment incident which causes injury or a fatality. It is likely, from similar cases in the U.S that this could lead to legal action against the car manufacturer for damages for negligence and for the injuries caused. Another consideration is the economic cost incurred by the government and ultimately the taxpayer for treating the injured, repairing damage to the road infrastructure (road surface, road furniture etc), damage to property, and the overall cost to the economy due to the road being partly closed to clear the debris and for the police accident traffic investigators to complete their work. Thirdly, there is a cost incurred by the driver himself in having to pay for the airbag to be reset after deployment has occurred, with costs in 1997 estimated to be approximately US$2000. The third reason, publicity reasons, is also important. Today, people are more aware of issues and current affairs than they have ever been previously, and it has been said that this is the result of the increase in the number of media outlets (print and television). Also, people have been galvanised into creating consumer groups, particularly in the US, and these are willing to challenge major companies about health and safety issues. One recent example is negative publicity about the high content of salt in certain foodstuffs, which has persuaded food manufacturers to reduce portion sizes and salt content in their products.

It is also a moral obligation on the car manufacturer to fix a fault of their own making, if they have the capability to do so, regardless of cost. In the US, there was an infamous case where a major car manufacturer discovered a potentially lethal fault in their fuel tank design, and instead of recalling all the vehicles sold and retrofitting the new part which would correct the fault, they calculated that it would be cheaper to leave the cars unchanged and pay for all the potential compensation claims which may result in case of an accident. This disregard of safety was punished in the aforementioned case.

However, it should be acknowledged that the vehicle safety is not high up on all country's lists of priorities. In some countries, airbags are not a common feature amongst the vehicles being driven, and this is particularly relevant in developing countries encompassing most of Africa, Asia and parts of South and Central America, where the average GDP per person is below US$1000. For such people, it is enough just to own and run a motor vehicle and it is unlikely that the governments in these countries would be willing to enforce legislation that would compel drivers to pay for ever more expensive equipment. Also, it is clear that that there are more pressing issues with regard to road safety, such as the poor quality of the road surface, lack of regulated traffic control measures etc.

It is thought that consumers in developed countries, mainly in the EU and the US, would be the markets which would be more willing to embrace such safety technology. This is because there is a higher emphasis on the quality of life and a greater avoidance of risk exhibited in these societies, and where there are governmental standards and guidelines that govern many aspects of the lives of the citizens.

There have also been studies undertaken which have estimated the economic costs and that traffic accidents cause to the national economy, and in the UK alone, this has been found to cost in the region of tens of billions of pounds sterling per annum. When the reader considers that the annual GDP of the U.K is of the order of 1000 billion pounds sterling, this is a significant cost, and one that can be reduced by implementing improved technologies. The higher car ownership per population, the higher disposable incomes and the fact that more car journeys are made, mean that the EU and the US would be the two car markets where an advanced airbag system would be most welcomed.

1.6 Scope of the Research

As was explained earlier in this thesis, the scope of the title 'Investigation of Low Cost Infrared Sensing for Intelligent Deployment of Occupant Restraints' is a relatively wide area, but the focus of this project is on the investigation of sensory technology that would provide an autonomous system able to discriminate different types of occupant in order to decide whether to deploy the airbag or not.

It is proposed that the work will be carried out using a low resolution, relatively low cost pyroelectric 16 x 16 pixel array thermal imaging camera developed by IRISYS, a small to medium sized manufacturer of thermal imaging equipment, and provided to the Mechatronics Research Centre at Loughborough University, U.K.

The application of the thermal imaging camera for the purpose of vehicular occupant detection and positional tracking has, thus far, not been done before. Traditional Charged Coupled Device (CCD) cameras have been used for such an activity, but it was felt that the thermal image had the potential to be more useful than these devices by giving similar information about the scene inside the car cabin, but also with added benefits over the CCD camera. These benefits outweigh the disadvantages, as is illustrated in figure 1-3:

Pros	Cons
Works in all lighting conditions	Low resolution images, relatively low detail of images
Low level of image processing required, lower computing processing required	Cannot work in high temperature conditions
Impersonal, more likely to be accepted by car drivers	Bulky size
	Cost approximately £1000, still more than CCD cameras

Figure 1-3: Table of pros and cons of the IRISYS thermal imager

It must be stressed that a complete, fully operational, automated system, ready to be fitted into a car cabin was not the objective of this project in this time-scale, rather it was hoped that the investigation would provide data and a methodology which could be built upon in future years so that the goal of an autonomous airbag deployment system could be realised.

It is proposed that a test rig simulating a typical car cabin will be built and used for the experimental trials using members of the public volunteers. The technique used for this work is image processing, which involves the collection of image data of the volunteer drivers, and the processing of this data.

This chapter has set the scene for the reasons behind the research and the general scope of activities. A detailed history of vehicle safety developments, airbag restraint technology and research into occupant detection will be presented in chapter 2 via a literature review.

Chapter 2 Literature Review

The review of literature described in this chapter was sourced from a wide variety of different media. This included the following types of media:

- Journal Papers.
- Text Books.
- Published Print Magazines/Newspapers.
- Internet Searches: Google, Yahoo, Teoma.
- Internet Databases: Emerald, Science Direct.
- Specific Internet websites: NHTSA, SAE.

Although traditionally the review of literature was focussed on studying peer-reviewed scientific papers published in scientific and engineering journals, and which dominates the literature survey conducted for this project, nevertheless the internet was used extensively to find articles and papers which were not readily available by traditional means. Care was taken to use websites that were of reliable and renowned organisations, such as the NHTSA, and the SAE.

Specialist internet databases such as Science Direct and Emerald were invaluable as they allowed the user to obtain published scientific journal papers from a variety of different publishers and journals.

2.1 A History of Car Safety

King et al **[5]** say that early work in car safety was concerned with protecting the driver in the event of a front-impact, which led to the concept of crash energy absorbing crumple zones that we have today. In fact according to Lovsund **[6]**, the 1953 model Mercedes 180 was designed with a deformable front end, and the interior was padded with energy absorbing material to reduce the crash load exerted onto the occupants. Restraint systems such as the seatbelt came after this and finally in the last two decades, the airbag was introduced. Scholz **[7]** working for Daimler Benz explains how the company spent 14 years in research and development to be able to put their airbag system into their model year 1982 cars in the North American market. It consisted of 4 basic components: the sensor, the gas generator, the airbag and the knee bolster. They designed the driver airbag to be oval shaped; it consisted of neoprene – coated nylon and fully expanded it had a volume of 60 litres and deployed within 25-35ms. They also produced a passenger side airbag which was trapezoidal in shape, held 145 litres and deployed within 40-50ms. Both airbags were filled with 95% nitrogen gas. Fleming **[8]** describes some of the problems associated with fitting airbags into lower – class range of cars. He says that the distance between the front end and passenger compartment was shorter and therefore the passenger compartment absorbed more of the energy. The structural rigidity of joints, components and load bearing members was lower, and so the passenger compartment itself sometimes deformed. This meant that the airbags in these cars had to be of higher stiffness to absorb more of the occupants' energy.

The NHTSA of the U.S grew so concerned about the number of airbag related deaths and injuries sustained by motorists that they drew up some new requirements that the automotive manufacturers had to abide by concerning airbags. Hinger et al **[9]** explain that the new requirements of FMVSS 208 are scheduled to come into effect over a gradual seven year period, in two phases. The first phase requires light vehicle manufacturers to have 100% of their new vehicles to be compliant with such technologies as airbag suppression and multi-compartment inflation by September 1st 2006 at the latest. The second phase of the ruling concerns restrained occupants, and stipulates that the speed of the frontal barrier tests that they perform with belted 50th

percentile male dummies be raised from 48 km/hr to 56 km/hr by September 1st 2010 at the latest.

The NHTSA have also estimated some costs and benefits regarding this ruling in their Final Economic Assessment **[10]**. The benefits are that not only will up to 95% of airbag related injuries caused by low speed deployments be eliminated, but also property damage savings could reach up to US$1.3 billion for the life of the vehicle. However, it is thought that the economic cost to automobile manufacturers will be about US$2 billion annually to comply with the regulations.

Many people have studied the problem of improving the safety of airbags, seatbelt restraints and the in-car safety of the passenger and driver overall. The problem with current airbag and seatbelt technology as explained by Galer-Flyte **[11]** is that they would operate regardless of what the distance the driver was to the steering wheel, or what size the driver was. There is a general consensus that to improve safety, the individual physical characteristics of the driver or passenger needs to be measured and the safety equipment tailored exactly for his needs. But, there is disagreement within this community over how to go about collecting this data and to what degree it should influence the activation of the safety restraints. Others wish to introduce more factors into the decision making process. Breed **[12]**, for example, wishes to link the airbag inflation rate to as many different factors as is relevant such as the size, position, and relative speed of the occupant, seat and back rest positions, vehicle velocity and the severity of the crash. However, there is a danger that having too many data variables to collect and process and to decide upon may prove difficult to do within the required short space of time.

The technology that many of the researchers have proposed using in their systems is not new and has been around for many years. These include strain gauges, load cells for weight measurement and infrared and ultrasonic sensors for distance and height measurement. Visible light (standard or CCD) cameras are also being used to track the position of the car occupant in real time.

Such is the level of concern about airbag related injury that there are some companies that sell switches that turn on and off the airbag deployment mechanism. One such company is 'The Airbag Switch Company' **[13]**. It claims it can fit its airbag switches to virtually all passenger vehicles. This is useful in that it can switch off the front seat passenger airbag when there is a child safety seat or whether the driver is particularly vulnerable to airbag related injury such as the small adults, children or the elderly. However, the problem with this switch is that it is manually controlled – the driver can decide whether to switch it on or off, and so human error is always a danger. The driver may switch on the airbag when it is not needed and vice versa. The system proposed in this thesis would be able to take this decision automatically. It should be noted that some car manufacturers are providing similar technologies. For example, on some 2005 year Mercedes Benz models, there is an 'intelligent' switch which identifies whether there is a child seat on the front passenger seat and automatically deactivates the airbag. However, this will only work with the child seat provided by Mercedes Benz.

2.2 Accident Analysis and Cause and Effect of Airbag Related Injury

Accidents will always happen as long as cars are subject to human control and therefore subject to human error, and so injuries and fatalities should be expected. However, some studies have been conducted to explain the risks that the vehicle occupants undertake. Evans, in his paper published in 1994 **[14]**, used Newtonian mechanics to explain the premise that drivers in lighter/smaller vehicles are more at risk of injury and fatality than drivers in heavier/larger vehicles. This is a common view. What is surprising, however, is the scale of the risk. Evans describes how if a car crashes into a car twice its own weight, the occupant in the lighter car is approximately 12 times more likely to be killed than the occupant in the heavier car, and is given as a an equation below:

$$R=\mu^{u}$$

where:

$\mu = m_2/m_1$ = mass of heavier car / mass of lighter car

R = probability of driver fatality in lighter car/probability of driver fatality in heavier car

u = 3.53

This can be explained by the fact that the heavier car will have a higher kinetic energy and inertia compared with the smaller and lighter car, and it is these factors which will cause more damage to the lighter car.

Mock et al **[15]** in their experiment, study the relationship between body weight and the risk of death and serious injury in motor vehicle crashes. Data from the Crashworthiness Data System (CDS) from the NHTSA of the United States was obtained, specifically analysing the crash data between the years 1993-1996, and restricted to people 15 years of age or older. This meant that data on 36,206 occupants, and weight and height data for 26,727 (or 75%). Approximately 54% of the people were male, with a mean age of 34.4 years. Proper seatbelt use was reported for 76% of occupants. Airbags deployed for 74% of the crashes. The mean change in velocity in the crash was 20.1km/h, and 59% of all the crashes were frontal crashes. It was found that increased body weight and increased Body Mass Index (BMI) was associated with increased risk of mortality. The adjusted odds ratio for death was 1.007 for each kg increase in body weight, when weight was considered as a linear variable. Similarly, the adjusted odds ratio for death was 1.014 for each unit increase in BMI. Although this increased mortality was mainly due to increased co-morbid factors in overweight occupants, nevertheless Mock et al do admit that this could be due to increased severity of injury. This could confirm the hypothesis that heavier people would suffer more injuries as a result of a crash due to the theoretically higher momentum of the heavier driver hitting the steering wheel and the interior with greater force, and is partially confirmed by Mock where he states that chest injuries were more likely to occur with higher weight and BMI.

The position of car drivers sitting in cars was studied by Parkin et al **[16].** Their experiments consisted of filming drivers whilst in general traffic flow whilst the drivers were unaware of the presence of the cameras. The camera was positioned at a right angle to the direction of travel of the vehicle, in other words, the drivers were filmed side on from the driver's side. The camera was 15-20 metres away from the car, with the cars travelling at approximately 30 mph. The analysis of the results show that female drivers are much closer to the steering wheel than male drivers, by 6.2 cm at the 50 percentile level, whilst 5 percentile female drivers are 21.5 cm closer to the steering wheel than the 95 percentile female driver. Older drivers (old drivers being classified as 55 years or above) also sit closer to the steering wheel by 1cm than normal, but such a small distance is not statistically significant. However, male drivers were said to be more at risk of 'head strike'. Parkin also says that 14.6% of the male population is likely to suffer head strike with the metal structures at roof level, compared with just 2.6% of female drivers. This report adds weight to other research which argues that the small female driver is more likely to suffer airbag related injury, since they sit closer to the steering wheel than other drivers.

In a study published in 1996, Kuner et al **[17]** set out to study (in the form of a questionnaire, the effects the airbag had in affecting the incidence of certain injuries caused during a road traffic accident. One hundred and forty-seven hospitals in Germany participated in his study, as well as twenty-six car manufacturers whose combined manufacturing output amounted to 95% of the country's total output. The injuries that were attributed to the airbag itself were as follows:

- 14.8% of patients received bruises and abrasions to the face
- 5% had bruising to the thorax
- 3.3% had these injuries to the forearm and the wrists

However, the results showed that 74.6% of all head and neck injuries suffered by airbag protected victims were superficial injuries (AIS 1) whilst 67.2% were thoracic and 79% were abdominal. Nevertheless, the airbag did cause eye injuries from smashed lenses of spectacles, and this is one of the areas of concern and one which a smart airbag system would hope to detect and to prevent.

The analysis of Nirula et al **[18]** provides stark evidence of how head injuries occur to the occupant in a crash situation. They studied the 15 severe head injury cases (AIS>4) that were identified from the 101 cases in the Seattle CIREN database. There were 10 side impacts and 5 frontal impacts in the 15 that were chosen for further study, and it was found that the majority of head injuries were caused by the striking of the B-pillar inside that car by the head. It is interesting to note that of the 15, only 2 people died, one of which was an elderly woman (aged 77) who was involved in a frontal impact and the 'head contact site' (HCS) was the airbag. This confirms the dangers of airbag head strike to certain members of the driving public.

The attempts of Fildes et al **[19]** to compare the costs and benefits of the airbag and face bag was highlighted by their paper which was published in 1994. There was some argument between those advocating the use of the Euro bag (40 litre volume, 24 km/h firing threshold, slow deployment) and the American full size airbag (70 litre volume, 16 km/h firing threshold, rapid deployment) with the argument for the 'Euro bag' being that the belted European occupant would not require rapid airbag deployment, therefore the 'Eurobag' would be less injurious to the occupant. The concept of harm was introduced by Fildes as being the product of unit cost and frequency of a particular type of injury, resulting in a total cost of that injury in millions of dollars. This is an important consideration because car manufacturers will usually be looking for ways to avoid cost and risk, and this will get their attention. It was found that the full size airbag had a 'benefit to cost ratio' (BCR) of 1.17 compared to the best 'Eurobag' or 'Facebag' BCR of 0.98, which suggests that the full size airbag was the airbag worth having. It must be noted, however, that the cost data used in this study dates from as far back in time as 1993, therefore the BCR could be altered since it is probable that the manufacturing costs of both airbag types have been reduced. It is thought that an intelligent airbag deployment system would be beneficial to the car industry as it will provide an extra feature or accessory which can be used to make the car attractive to the customer. Generally, the higher the level of detail or specification a car has, the more desirable it is for the customer.

Figures 2-1 and 2-2 are pictures of automobile airbags, deflated and inflated. Figure 2-1 was taken from the website www.engine27.com and figure 2-2 was taken from the website www.peugeot.co.za and are reproduced here for illustration purposes only. The reader will notice how far the driver's airbag in figure 2-2 intrudes into the forward occupant space between the driver and the steering wheel. The depth of the inflated airbag is relatively deep, and this is because it must decelerate the forward motion of the head to a safe velocity before striking the steering wheel.

Figure 2-1: Deflated airbags

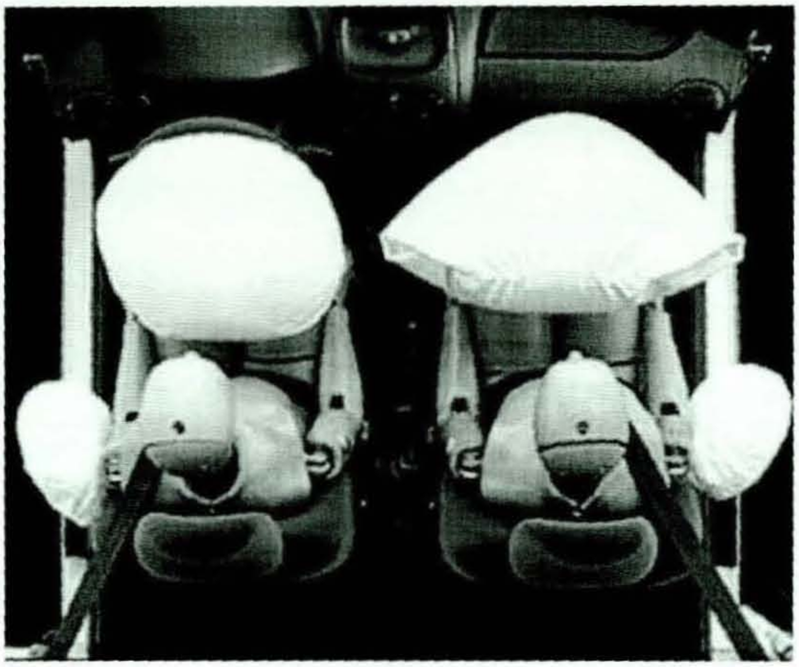

Figure 2-2: Driver and passenger inflated airbags

Lehto et al **[20]** sought to study the possible ocular (eye) injuries that were sustained from the airbag deployment during a crash situation. This was done by using observational studies and also by conducting a literature survey using databases such as the widely available MEDLINE database of medical articles. In his paper, Lehto begins by explaining that ocular injuries can be categorised in two groups:

The mechanical force of the airbag causes blunt trauma to the face and the eye regions, and also causes perforations by indirectly interacting with other objects such as spectacles or smoking pipes for example, and these are pushed up into the eye regions causing perforation injuries to occur. Chemical burns also occurred from the chemical reactions involved in the deployment of the airbag. Lehto's team studied two sets of data, the 'Fatal Accident Series', and the 'Airbag Study'. Combining this data, the results show that 4 out of 161 occupants who did not wear eyeglasses suffered eye injury, whilst 3 out of 83 who did wear eyeglasses suffered an injury to the eye, thus showing that there is not a large increase in the risk of eye injury if spectacles area worn or not. But it must be said that this is there is still the potential for eye injury to be caused, and since this is a very important organ of the body, as much care as possible should be used to protect this from damage.

Evan's study of literature and data obtained from the 'Fatal Accident Reporting System' (FARS) between the years of 1975 to 1983 produced an estimation of the effectiveness of restraint systems, lap/shoulder belts and airbags to prevent fatalities **[21]**. It was found that in frontal and near-frontal crashes that airbags were approximately 18% +/-4% effective in reducing driver fatalities, and about 13 +/- 4% effective in reducing fatalities for the right sided passenger. The total fatalities would be reduced by 6.5% if the airbag was installed for all drivers in the U.S, and this would improve to approximately 8.2% for all drivers and right sided passengers, when compared with cars with no restraint systems at all.

In another study of the available literature, Evans **[22]** attempted to investigate the links, if any, between the type of crash, driver age and alcohol concentration in the blood to airbag effectiveness. This study used FARS data from the years 1975 to 1986 inclusive, and it was found that the airbag was more effective in preventing fatality in two-car accidents (21%) than one-car accidents (16%). Driver age and alcohol concentration in the blood, however, did not greatly affect the effectiveness of the airbag for the driver.

The process, by which the occupant was injured inside the car during a car crash, was the subject of a study conducted by Stefanopoulos et al **[23]**. They used crash data from their local area, Patras in Greece, where 109 collisions were studied and 48 of which were selected for further analysis by the team. From this, they found that 41 vehicles had no compartmental intrusion (containing 70 occupants), whilst the remainder had significant compartmental intrusion, which accounted for 11 occupants. They classified the incidents into different categories, into SWI, CPI and WSI accidents, which stand for 'Steering Wheel Involvement', 'Control Panel Involvement' and 'Windshield Involvement' respectively. The team's conclusions found that in vehicles without compartmental intrusion, the more structures that are deformed, the higher severity of the injury will be to the occupant. Also, back seat occupants are not seriously injured, and WSI and SWI are more significant factors in front-seat occupant injury than CPI.

'Airbag crash investigations' was also the title of a study undertaken by Chidester and Roston **[24]**, and published by the NHTSA. They investigated car crashes which involved the airbag being deployed during the incident. From May 1998, the NHTSA started to report unconfirmed airbag fatalities in their monthly reports, and it was found that up to January 1 2001, there were a total of 232 cases (172 confirmed, 60 unconfirmed) where airbag deployment had caused a fatal injury to the occupant during a low speed crash. Out of this total, 145 were children (102 confirmed, 43 unconfirmed) and from this total, 125 (83 confirmed, 42 unconfirmed) were children in a 'rear facing child safety seat' (RFCSS). The predominance of child fatalities was to be expected because the airbag was not originally designed to protect them, they were designed to be used by the adult driver, and later for the passengers as well. In a typical airbag crash situation, the unbelted child would be moved into the 'out of position' (OOP) zone which is in front of a typical adult driver seating position. The airbag would inflate and would rapidly deploy into the face, lifting the head off the neck, resulting in atlanto-occipital fractures, with possibly a transection of the spinal cord and brain stem injuries being the other possible injuries suffered as a result. Chidester and Roston also confirm that the majority of airbag-related fatalities occur to drivers who are 66 inches or less in height, and that 60 % of the drivers who are fatally injured are 50 years of age and over.

Kang et al **[25]** studied the effects of airbag loading on the 5^{th} percentile female Hybrid 3 dummies. It was found that the neck responses of the dummy were highly dependent on the way in which the airbag came into contact with the dummy. Three different modes of airbag interaction with the dummy were investigated. The first interaction mode is where the airbag directly loads the head. The second mode is when the airbag is trapped between the chin and the jaw region of the occupant, and the third interaction mode occurs when the airbag is trapped behind the jaw, in the neck-jaw cavity. Static tests were done to investigate these airbag interactions with the dummy, with the test dummy being positioned leaning towards the instrument panel, in a full-forward passenger seat. The results showed that in the first airbag-neck interaction mode, the head is directly loaded by the airbag, and the neck shear is positive, and the head is pushed back. In the second interaction mode, the neck shear is negative, meaning that the head is pulled forward relative to the neck. However, the major part of the neck loading is due to the inertia load of the head pulling the neck forwards, and the direct loading due to the airbag on the neck. In the third interaction mode, the airbag is positioned underneath the chin of the driver, thus causing the head to be lifted up from the neck when the airbag inflates. It should be noted, however, that this study is very limited as it dealt with in-position occupants, in other words, occupants who were correctly and safely seated. Also, this study indicates that the responses of the dummy to airbag loading may not be accurate in a real-world situation, and so the design of the dummy may need to be modified.

The work done by Buzeman et al **[26]** was concerned with investigating what effects certain parameters had on the fatality rates in car crashes. He builds on the work of others who have studied this field, such as Evans, who have studied injury risk, and developed a formula for finding the predicted injury and fatality rates. This calculation, explained in this paper, calculates that there would be 235.7 severely injured occupants, and 34.8 would be killed per 100,000 registered vehicles. Other notable results are that by reducing collision speed by 10 %, this would reduce casualties by 34 % and fatalities by 40 %. However, the changes in the mass of the vehicle fleet were not as important a factor.

Hobbs **[27]** says that approximately two thirds of car occupant accidents are front impact or oblique frontal impacts. He also says that although over 90% of U.K drivers wear seatbelts, the majority of belted driver's injuries result when he comes into contact with the car interior. The airbag was designed to prevent the occupant from hitting the hard components of the steering wheel and dashboard, and has been largely successful. However, according to the National Highway Traffic Safety Administration (NHTSA) of the U.S.A **[28],** the number of deaths caused by the airbag by October 2001 was 195. There are approximately 2 deaths per 100 people saved by the airbag, and many more people have been injured by it. According to Segui-Gomez **[29],** this is because the airbag increases the amount of energy released during the crash that will act on the occupant. She says that airbags in the U.S.A were designed to meet Federal standards. These required the forces acting on a male 50^{th} percentile dummy's head, chest and thighs to not exceed a certain level when a crash occurs at 48 km/hr.

The severity of airbag related injury was evaluated by Segui-Gomez using 'The Abbreviated Injury Scale', with scores that range from 1, minor injury, to a maximum of 6. No injuries have a score of 0. She collected data from 13,092 drivers from the years 1993-1996 from the National Automotive Sampling System Crashworthiness Data System (NASS CDS). Her results show that in frontal or near-frontal crashes, the airbag is effective in reducing the most severe injuries. However, in low-severe crashes, the airbag actually causes injuries, particularly amongst females, with abbreviated injury scale scores of between 1 and 3. Huelke et al **[30]** describes in his paper 27 case studies of traffic accidents which resulted in the deployment of airbags in the U.S. The drivers sustained a variety of injuries as a result of airbag deployment. He found that 30% of drivers sustained injuries to the head, i.e. erythemia or skin abrasions to the face or neck. Burns to the hand and wrist by the venting of hot gases from the back of the airbag depends on the position where the airbag vents are located. Vents located on the 9 o'clock and 3 o'clock positions caused more incidents of burns than when the vents were located on the 11 o'clock and 1 o'clock positions at the back of the airbag. Also, tethering the centre of the airbag to stop it fully expanding can also reduce minor facial injuries. Tests conducted by other researchers have shown that the greatest risk of injury occur when the occupant's torso is positioned so that it is fully against and covering the airbag module at the time of deployment.

Langweider et al **[31]** confirms that the typical 'out of position' airbag injury situation occurs to a female front seat passenger (157cm, 67kg) who had moved her seat too far forward and therefore suffered the large force of the airbag deployment. In this case study, the victim suffered massive dislocation trauma to the head and neck; and hyperextension of the cervical spinal column caused broad dislocation between the 1^{st} and 2^{nd} cervical vertebrae. Two-thirds of all front seat passengers, he says, suffered facial injuries when the head hit the airbag, with contusions and abrasions being most common. A few suffered burns to the forearm caused by the hot gas escaping at the rear of the airbag during deflation.

Up to now, there had not been much 'real world' testing of some of the newer airbag technologies to see how they reduced the incidence of airbag-related injury. However, Augenstein et al **[32]** have recently collected crash and injury data on 141 drivers and

41 passengers during the period from the years 1992 to 2000. These included 28 cases where the newer depowered airbags were fitted. It was found that the depowered airbag has not, thus far, caused any fatalities either to the driver or to child passengers at low speeds. Also, no significant injuries occurred to belted drivers and passengers at low speeds.

2.3 Advances in Airbag Technology

Since the safety concerns about current airbag technology came to light, some companies have collaborated to develop a more sophisticated airbag. Miller et al **[33]** report that the NHTSA have in recent years revised the Final Rule for Federal Motor Vehicle Safety Standard (FMVSS 208) – Occupant Crash Protection. This specifies new safety compliance tests that airbags will have to meet and is due to come into effect for use in the year 2004 model vehicle. Hence, much research is being done in improving occupant safety technology. A case in point is the collaboration between the Fraunhofer Institute for Chemical Technology, and car and component manufacturers, as reported by 'The Engineer' website news service **[34]**. Their design incorporates sensors that locate the driver's position and a time delay mechanism which regulates the flow of gas into the airbag so that the driver does not receive the full force of the airbag straight away.

Other people are also working on reducing the force of the airbag. Ryan **[35]** explains how an airbag can be variably powered using a variety of methods e.g. separate inflators, a primary and secondary airbag inflator which operates independently of one another to provide multiple levels of airbag inflation. The primary inflator would deploy for low or medium severity impacts. But both primary and secondary inflators would deploy for high severity impacts. A similar principle is used in the 'Dual Chambered Pyrotechnic Inflators' and 'Dual Heater Hybrids'. A so called 'Pyrotechnically Actuated Venting' system controls airbag inflation by allowing a portion of the airbag gas to vent out of the airbag at a controlled rate, thus varying the pressure inside the airbag.

Rohr et al **[36]** discuss in their paper the future technologies that are being developed today. Their 'Integrated Safety System' (ISS) list of requirements after an accident has occurred contains such questions as 'what are the vital signs of the occupants?', 'how many occupants are there?', and 'is there a fire?' These could all be answered by the thermal imaging system that this research proposes. It must be stressed that some of the requirements that Rohr talks about are difficult to achieve and could take many years for car companies to perfect, particularly in the field of collision avoidance.

One problem with trying to develop the concept of an intelligent automotive occupant sensing system to monitor height, position, weight etc is the fact that the crash and deployment of an airbag takes literally fractions of a second to complete. Hollingum **[37]** says that the complete cycle from airbag triggering to full inflation takes about 50msec. In all, 150msec from the beginning, the airbag has inflated and deflated and the occupant has hit the airbag and returned to his normal upright driving position. To put this all into perspective, blinking of the human eye takes a relatively pedestrian 200msec.

To enable the reader to understand just how quickly the driver will impact with the steering wheel in the event of a car crash, figure 2-3 shows how far the driver moves forward with respect to time elapsed.

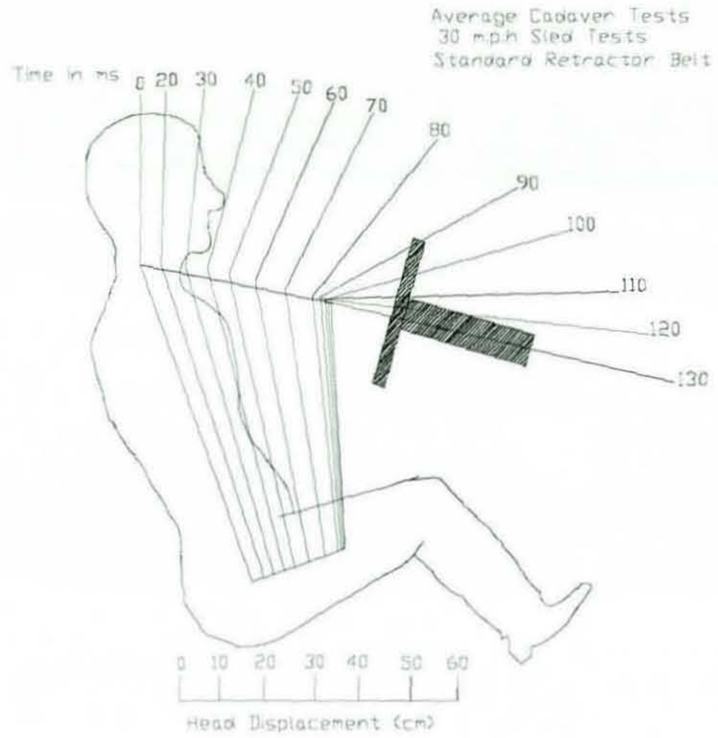

Figure 2-3: Diagram Showing Forward Head Displacement with Respect to Time (Reproduced from Mackay et al)

Mackay et al **[38]** have also observed that a more intelligent airbag is required. However, their emphasis is on a combined restraint strategy with more emphasis on smarter seatbelts, and they have only given a rudimentary description of an occupant monitoring system, and advocate an advanced collision warning system to prepare the restraints.

It is not just people with short legs (and who therefore must sit very close to the steering wheel) and small children and females who are at risk of airbag related injury. Galer and Jones **[39]** have written that for people over 60 years of age, the probability of serious injury or death increases by 70% compared with a 20 year old person. This is mainly to do with the G-forces that seatbelts exert on very small, localised areas of the body such as the neck. Although the airbag distributes these forces over a larger surface area (and so cushioning the blow), they are also dangerous for them. Libertiny **[40]** reveals that of the 70 year olds who suffered severe trauma injuries, 92% never return to their previous level of independence.

However, elderly drivers compensate for this increased risk by driving larger vehicles, using seatbelts, driving less miles and not drinking alcohol prior to driving.

Pressure sensors in the car seat are a popular method for calculating the weight of the driver. For example, on the Cadillac Seville (2000) **[41]**, there is a plastic coated pressure mat embedded into the foam of the seat. Changes in weight correspond to changes in electrical resistance in the pressure mat, and this coupled with a pattern recognition system, can detect whether an adult or a child is sitting on that seat. If it is the child, then the airbag will not deploy.

Breed et al **[42]**, whose work has been partially supported by the NHTSA and 'Autoliv', have developed a sensor system that can detect, monitor and identify objects that are in the car cabin. It uses ultrasonic transducers, together with a pattern recognition algorithm in order to differentiate between a rear facing child seat and an adult occupant out of position. The four ultrasonic transducers operate at 40 kHz and emit unfocussed wide beam pulses directly onto the occupants. The echoes are returned within 10msec, and are therefore fast enough to be used in an airbag deployment sequence, as the occupant position will hardly change within that time. However, Breed himself admits that whilst a single ultrasonic transducer can determine the distance an object is, it cannot determine its exact location within the cabin. Therefore he uses four ultrasonic transducers. This adds to the complexity and to the cost and so a one thermal camera based system may prove cheaper. Another disadvantage of Breed's ultrasonic system is that it cannot distinguish between an adult or small children or animals, which the thermal camera can.

Car manufacturers like Mercedes are not only motivated by occupant safety but also by reducing the running costs for the motorists. For example, the driver would not want his airbag to be activated unnecessarily as is sometimes the case, particularly when considering that they cost approximately US$2000 to replace and set according to Paula **[43]**. That is why they have installed a weight sensor into the driver and passenger seat, which will deploy an airbag only when there is a load greater than 26 pounds on that seat. This weight limit is set so that if a small baby is left on that seat, because he would generally weigh less than this, the airbag should not deploy and harm him. However, it doesn't take into account the fact that people may leave heavy bags of shopping or luggage on that seat, and so there is still the potential for the airbag to be activated needlessly. Mercedes have also introduced the 'BabySmart' system into its range of cars. This system sends out a low power signal and if a reply signal is sent by the resonator built into the child seat, then the airbag will not deploy and a light on the dashboard alerts the driver to this.

The theoretical application of electric fields generated around the human body was the subject of an investigation by Jinno et al **[44]**. They fitted four electrodes into a car seat, which generated very weak electrical fields, and the deflection or disturbance of these fields when an occupant or an object was on the seat was measured. It was found that a child in a safety seat could be detected, and that the system was not adversely affected by external factors such as heat, light, dust, sound, humidity, or type of clothing. This method has been used by others in the occupant safety research field to produce their own similar occupant sensing systems.

Lu et al **[45]**, working for the BMW group, use two sensing systems to classify the occupant as he sits in the car seat. A force-sensitive resistor sensor array within the seat measures the imprint of the person's buttocks. The second system uses capacitive plates within the seat to generate an electric field around the seat. This electric field will change due to the conductivity of the body, and using these two systems, Lu et al have developed an algorithm to know if there is an empty seat, a child in the seat or an adult in the seat.

Another ingenious occupant sensor is the 'Proximity Array Sensing System' (PASS) developed by Advanced Safety Concepts, Inc **[46]**. It basically uses a capacitor sensor installed in the ceiling directly above the driver's head. It measures the dielectric constant of the body (about 80), which is much higher than that of air (1) or other luggage (2-4). Therefore it is almost impossible for it to mistake a piece of luggage with a person. Also its estimated manufacturing cost is US$4 and so price is not an issue. What is an issue is that it could be fooled into thinking that an animal such as a dog is a human, because animals contain water and salts as humans do, and so the dielectric constant may be much closer. Paula also goes on to say that some have tried to modify the airbag itself by dividing it into two or more compartments with each having a gas generating chamber, and so each compartment has half the power of a conventional airbag, thus reducing the impact onto the driver. Kimberley **[46]** says that other companies have also tried to modify the airbag shape. TRW, for example, have created a 'donut airbag' so-called because its shape resembles that of a donut when inflated. Its mass is reduced, it has no direct cover contact and so it also exerts less force onto the driver's head.

Birch **[47]** has written in an article about the developments that are being made by a company renowned for its emphasis on safety: Volvo. It's 'EyeCar' system has a video camera and infrared light source, and this system is able to locate the position of the driver' eyes and to adjust the position of the seat, steering wheel and even the pedals. Another Volvo device measures the distance from the ceiling to the top of the driver's head by measuring the small electrical current of the driver. This will fluctuate according to the water content of the body. One device not directly related to airbag deployment is the 'Volvo Personal Communicator', which incorporates a heartbeat sensor which can inform the driver if a child or animal is still in the car. This could act as an occupant sensor also, although again it may have the problem of being unable to distinguish between people and animals.

Kosiak and Rohr **[48]** are attempting to combine crash sensing and severity data to predict the restraint strategies that would be required in the event of an accident. They argue that one sensor at least should be in the front end of the car, and not to rely too heavily on sensors located in the passenger compartment. This is because the front end and passenger compartment are a distance away from each other and the crash pulse from the front may dissipate as it travels along the car to give an unreliably small signal in the passenger compartment. Kosiak and Rohr argue that weight sensors are the short - term solution for occupant classification. One method is to have a fluid filled pad in the seat cushion, and the fluid pressure gives the occupants weight. A pressure sensitive mat on the backrest and seat is another suggestion. However, although weight sensing can give some information about the driver, it can be fooled into measuring objects other than the occupant, and cannot give vital occupant position measurements.

One aspect that has not been fully explored is whether the driver would want a system to deactivate the airbag. As mentioned earlier, drivers in the U.S.A are allowed to buy and install switches that manually deactivate the airbag, but this is not common in Europe. Also, manual switches put the burden of responsibility onto the driver, and humans can make mistakes. Henriksson et al **[49]** have addressed this issue. The results of their questionnaire revealed that most people preferred an automatic airbag deactivation system, but with the ability to override it manually.

One novel idea that has been researched by Mao and Appel **[50]** with regards to reducing airbag-related-injury is the airbag folding pattern. Four airbag patterns were investigated – leoprello (Conventional), raff folding, stoichiastical folding and z-folding; which can be abbreviated as L, R, S and Z folding. L-type folding means that the airbag is folded down into the airbag module in accordion type layers. R-type folding is where the airbag is formed into a concentric 3-D wave structure around the inflator and then packed radially around the centre airbag module. S-type folding has very irregular folding lines with the airbag pressed down into the centre, and Z-type folding is similar to L-type folding in that it folds down into a concertina type pattern. Tests showed that L-type folding has a higher potential for afflicting injury to the driver because it has a higher opening pressure which means that the airbag 'punches out' towards the occupant much harder than the other folded airbags do.

2.4 Sensors

Sensors have been used for decades for control and measurement purposes. However, these were usually heavy, mechanical devices and often device specific. They have also had the problem of being 'contact' sensors, in other words, they have to be in contact with the object in order to measure its length or take its temperature etc. Slazas **[51]** agrees that non contact sensors are the only viable method for some difficult data measurements. Non-contact sensors currently available include infrared, ultrasonic, acoustic technology, and they have a variety of uses. For example, Ogawa et al **[52]** have used a variety of different sensors in order to monitor the activities of people in a house, with their goal being to improve safety around the home. They use infrared sensors and carbon dioxide sensors for occupant detection, which is similar to the occupant detection work that is proposed in this project. Lambert **[53]** has also considered a similar system. He explains how the passenger side airbag could be suppressed when there is a child safety seat on the front passenger seat by using direct thermal detection. The temperature of the surface of the front passenger seat is compared with that of the driver's seat, and if the two temperatures differed by more than a predetermined amount, then the airbag would be suppressed. However, the response time for this system to detect such temperature changes is a little slow, being in the region of 5 to 10 seconds.

Teuner et al **[54]** explains that passive motion sensing (i.e. detecting motion with a stationary camera) can be performed by analysing dynamic changes in different image sequences. To do this, he suggests using such approaches as detecting pixel intensities in consecutive frames, and estimating motion vector fields. He also goes onto say that high speed imaging can be used to control airbags by recognising certain situations and depowering or deactivating them. The author agrees with a vision based system controlling airbag deployment but is wary of being involved with actual physical changes with the airbag like reducing the volume or slowing down the deployment. This is because it would add a much greater complexity, and be difficult to integrate with the airbag control system. There are infrared and other optical range finders available on the market, but they are usually used for measuring distances between large, straight walls, for example. Novotny and Ferrier **[55]** explain that in order to find the range from a particular surface, the surface properties (e.g. reflectance) have to be known. It would therefore be difficult to find the range from a human face or body for example because not all people are alike. There would be differences in contours, skin colour (hence reflectance), facial hair, and differences in the type of clothing. Others have tried different approaches to distance measurement. Miller et al **[56]** used a vision system onboard their robot. It can find its position from a single frame, and this is one of the goal's of this research – to find the position of the driver inside the passenger compartment from just one thermal image.

A related work has already been done by Fukui et al **[57]**, who have designed a side airbag occupant position detection system. This works by using a specially constructed passenger seat which has six height sensors built into the seatback in a linear pattern, and one head sensor vertically located near where the side airbag is installed. The sensory system relies on the changing impedance. For example, if the sensor detects the occupant's head near the side airbag's deployment zone, the airbag operation is inhibited to prevent the airbag firing and causing injury to the occupant's head, which, again, is similar to the research proposed in this project. The one drawback with Fukui's system is that it requires a specially built car seat so that the sensors can be fitted inside, and this would be expensive to manufacture and to maintain throughout the product's life.

It is not just the Mechatronics Centre at Loughborough University which is experimenting with infrared sensors. Hashimoto et al **[58]** explain in their paper the development of a one-dimensional eight element pyroelectric array detector which was made out of $PBTiO_3$. This was made primarily for the application of people counting in a closed space i.e. a building, or a room. Their claimed resolution is up to a maximum of 48x180 pixels, which is done by the use of interpolation methods (neighbour output averaging scheme). Using this equipment, the number of people inside a room, as well as other objects such as a lighted cigarette and high temperature regions in electrical wiring, can be detected. This work provides extra independent corroboration of the validity of using a thermal imager for use on human subjects.

In their paper, Gitelman et al **[59]** describe a long range infrared video-oculargraphic system for recording driver eye movements in real-time, in a 2-D format, using MRI technology. He describes how three volunteers were asked to perform some behavioural tasks which were intended to induce spatial attention shifts. It was found that a task based on covert shifts of spatial attention led to 'Frontal Eye Field' (FEF) activation, even though the volunteers' eyes remained centrally focussed. This work uses technology that is more advanced than the infrared thermal imager being used in this project.

Wetzel's team at the TEMIC centre **[60]** have developed and tested their occupant detection system. Their detection philosophy was to detect the rear facing child seat, the passenger and the empty seat, with the highest priority being the child safety seat. The system used optical distance measuring by triangulation. The contour image detected by the CCD array is compared to an image stored of an unoccupied seat.

Another advantage of Wetzel's system is that the optical and electronic equipment can be fitted into a package of relatively compact size (10cm x 3cm x 2.5 cm) and so can be fitted into the headrest of the car seat, for example. Other activities detected include such driver activities as newspaper reading, book reading, feet on the dashboard, crossed legs on the seta or feet on the seat, and having a bag on the lap. However, it was felt that for the purpose of this project, such driver behavioural instances were not relevant as it was felt that these were rare and unusual activities for a driver to do inside the car.

2.5 Methods to Measure Height

A driver's height, particularly the upper body height, is important to know because this determines all sorts of dashboard adjustments. For example, a taller driver would need the steering wheel angle to be raised so that it faces more upwards towards him; the seat needs to be pushed back away from the pedals etc. There is another, more important reason to want to know the height of the driver, and that is to know where the driver's head will hit the steering wheel. In the event of a crash, the head and upper body would pivot about his waist and arc towards the wheel. The head of a tall driver will be positioned higher up from the base of the seat than an average sized driver. Conversely, a short driver will have their head positioned lower down from that of an average sized driver. Therefore, in the event of an accident, the head will be forced up over the airbag (in the case of the tall driver) or forced underneath the airbag (in the case of the short driver). In both cases, the driver would suffer severe neck injuries. Traditional methods used to measure this include having pressure sensors located up along the backrest of the seat at measured intervals, and this would give a less precise but cheap estimate of height.

2.6 Methods to Measure Weight

There are three impacts that occur when a car crashes into another vehicle. Firstly, there is the impact of the two vehicles colliding with each other. Secondly, there is the impact of the head striking the steering wheel. Thirdly, and not widely known, is the internal organs jolted forwards and hitting the rib cage and skull. Parenteau et al **[61]** have analysed U.S statistics from the NASS-CDS which confirms that weight of the driver affects the severity of the injury. For example, she says that for belted drivers involved in crashes of low to moderate severity (Equivalent Test Speed less than 24 m.p.h), drivers who weighed less than 55 kg had the highest rate of severe injuries. U.S and U.K drivers who weighed more than 86 kg had the highest rate of moderate injuries.

It should be noted that the total body weight need not be measured but rather the upper body from the waist upwards as this will pivot forward in the event of a crash.

Many car manufacturers use simple instruments to measure weight. Pressure mats inserted under the driver seat give can measure the upper body weight of the occupant. For example, Billen et al **[62]** explain an occupant classification system that uses a seat pressure sensor mat which is able to identify a number of different types of occupant such as children and adults, and children in child safety seats. It analyses their pressure profiles – a compact seat pressure profile indicates a human whilst a spread out pressure profile suggests that there is a child safety seat sitting on that seat. Also the width between the buttocks is an important parameter as this is indicative of the occupant's weight.

Other researchers use variations of this technology. Kuboki et al **[63]** use a flexible tactile sensor, which is similar to the membrane switches that are used in computer keyboards. However, the difference is that whilst the keyboard membranes have only two positions, an 'on' and 'off' position, the flexible tactile sensor has electrodes with pressure sensitive ink which means that as force is applied, the electrical resistance varies proportionately and so this would produce a more accurate reading.

It must be stressed that pressure mats embedded inside the drivers seat will only give a reading of the upper body weight of the driver when he is sitting still and not touching other parts of the cabin. In a real life driving situation, some of the body weight will be exerted down onto the seat, some onto the backrest of the seat; the driver would put pressure onto the steering wheel and onto the pedals /floor through his feet. Other problems with weight sensors embedded into the seat are that they work well when the car is moving in a straight line at constant speed, but problems arise when the car is accelerating or decelerating or turning around corners. The centripetal force that occurs when the car is cornering is most troublesome because it is :

$$\mathbf{F = mv^2 / r}$$

Where

F = force (N)
m = mass (kg),
v = velocity (m/s)
r = radius (m).

The dominant factor in this equation is the velocity of the vehicle, not the mass, and so the use of weight sensors would lead to inaccuracies in some situations.

It would be ideal to have a non-contact sensor that could estimate the weight of the driver's torso as soon as he steps into the car seat for the sake of driver comfort. Also, it is desirable to use as few a number of sensors as possible since it would reduce cost and more importantly reduce the risk of systems failure by reducing the number of parts needed. One initial idea was to use the thermal imager to estimate the surface area of a part of the body such as the driver's hand, and then rearranging the equation that calculates surface area from weight and height, to find the weight of the hand and scale it up to find the whole weight of the body. However, it was soon realised that this would produce large errors since the body weight is not distributed evenly around the body, in terms of bone size and body fat. Body fat generally settles around the waist and the thighs, not in the hands or fingers, so this idea proved to be non viable.

Others have also tried to produce a non-contact weight sensor. Chandrasekaran et al **[64]** have demonstrated a system that uses two optical fibres. One carries light from a remote source to the target whose displacement is going to be measured and the other optical fibre receives the reflected light from the target. The weight sensor has a spring that allows it to displace when there is a weight acting on it, and as the weight sensor is displaced, the intensity of the light varies. However, this is not a true non-contact weight sensor since there still has to be a weight acting on the weight sensor for it to displace.

2.7 Out of Position Measurement

Height and weight measurement are important factors to be considered when developing a more intelligent system, but also the position of the driver is equally important, if not more so. It is common sense that a driver should not be too close to the steering column in the event of an airbag deployment, but the driver should also not be too far left or right laterally from the normal driving position in the car seat. This is because the head could get trapped or be pushed extremely hard between the inflated airbag and the door, for example. Another problem is that the driver may be pushed to one side, but his body would not be supported in the direction of the car's deceleration. This would result in high dynamic forces being experienced by the driver.

It is important, therefore, that the position of the diver's body, and more importantly, the driver's head, should be measured. There are many sensors that can achieve this, but deciding upon which sensor to use is dependent upon what level of sophistication the intelligent airbag system should be. It may be found that a rudimentary level of detection would be sufficient, for example, detecting whether the driver's head is leaning too close to the steering wheel or not. The level of measurement accuracy would also impact the complexity and cost of the airbag system, and this needs to be taken into account.

2.8 Video Systems for Occupant Detection

A popular way to determine if indeed there is anyone sitting inside the driver or passenger seat is to use one or two video cameras attached to the inner cabin of the car with it tilted and looking down upon the person. Krumm and Kirk **[65]** used monochrome cameras bolted onto the ceiling to view the scene inside the car. Their experimental work consisted of taking pictures over a number of days in variable lighting conditions in order to detect whether the seat was occupied or had a 'Rear-Facing Infant Seat' (RFIS). A process termed 'image matching' was used to classify the images – basically an image of an empty seat and one that had a RFIS on it were obtained as the control and subsequent images were taken. If the later images did not match that of the control images, then the image was classified as occupied.

Owechko et al **[66]** describe a system which uses a pair of vision sensors mounted near where the rear view mirror is in order to capture video footage of the driver, so that they could identify the occupant, identify an out of position occupant etc. Its real-time frame rate is quite fast at around 20 frames per second and they claim that their occupant classification system is over 98% accurate. They detect occupant motion by taking the differential measure between three successive images so that the history of the driver's movement is known and so the system can react accordingly.

Ran and Liu **[67]** have detailed their work on a vision based system to detect vehicles for hazard detection and tracking for the goal of collision warning and avoidance. Although it is to view exterior objects, whereas the focus of this project is to work on an interior imaging system, the principle is similar. However, Ran and Liu are using a single CCD camera mounted just behind the windscreen, and they admit that they are having some problems with the lighting conditions, something that does not affect the thermal imager.

Victor **[68]**, in his work at Volvo, used stereo cameras to record real-time data of the driver. Its novelty is that it can determine the direction of the driver's gaze as his head moves, thus evaluating whether he is attentive to the road or not.

It must be noted that the major problems with using video cameras to record footage of the driver in his car are that it can only work in good, constant lighting conditions and takes longer for image processing than for a thermal imager. To reduce cost and time of image processing, Haro et al **[69]** used a black and white camera with infrared lighting. They claim that they can detect the eyes of all people indoors using Kalman trackers, without any camera calibration. Their system runs at a fast 25 frames per second. Eye detection can be, and has been used in various forms to detect the presence of an occupant, and it can also be very useful in determining whether the driver is attentive or drowsy.

Russakoff and Herman **[70]** believe their stereo data head tracking system can overcome the lighting problems that Ran et al describe, by building up a 3-D model of the head. Once the head has been located, and the camera focal length and baselines are known, the head's position in 3-D co-ordinates can be determined. This stereo system does not encounter problems with differences in skin colour etc. However, the quoted processing time per frame on a dual 350MHz Pentium II processor is 1 second, and this is far too slow to use for airbag deployment strategies.

There are slight variations on this theme. Boverie **[71]** for example uses the principle of the time of flight of light to calculate the linear distance measurement between dashboard and driver. Using video cameras and a backlight, a 3-D image of the driver is built up by estimating the distance of each pixel in the array.

Siemens Automotive also demonstrates other uses for video cameras, such as 'driver vigilance monitoring', 'driver vision enhancement' and its 'electronic mirror' systems.

Other manufacturers have been involved in producing video camera systems to monitor driver fatigue. In a report by 'The Detroit News' **[72]**, Nissan's CQ-X car has a small camera mounted into the dashboard and an infrared sensor that detects whether the driver's eyes are blinking or narrowing which would suggest that he is feeling sleepy. It then sounds an alarm and finally releases a scent through the air conditioning system, which is designed to bring the driver back to full alertness.

Drowsiness is another factor which has been proven to have caused road accidents. In their paper, Verwey and Zaidel **[73]** quote research from the U.S.A where between 1.2 % and 1.6 % of all the police reported accidents, and up to 3.2 % of all fatal road accidents, are caused by driver drowsiness. Fatigue and drowsiness are defined as conditions that impair information processing of the driver, thus increasing the likelihood of various perceptual and attention errors.

There are two categories of in-vehicle driver alertness devices. One type is to detect and to warn about driver drowsiness; the second type is concerned with maintaining constant driver alertness by activation of the driver throughout the trip. Verwey and Zaidel studied this using a fixed base driving simulator to study the onset and effects of the drowsiness on 112 candidate drivers. Their results showed that providing the driver with 'mental activity' (in this case, a 'games box' where the driver was set some interesting tasks to do) helps prevent drowsiness from setting in. This work has relevance to this project because it is hoped that the thermal imager would also be able to detect some typical driver behavioural movements and signs, and to use this for the driver's benefit.

Recently, there has been an advance in the field of driver monitoring by a company called 'Seeing Machines' in Australia by a team of 20 international scientists, and they have come up with a system called 'FaceLab' **[74].** Figure 2-4 shows the arrangement of the cameras, of which there are 2 cameras spaced apart and mounted on the dashboard and connected to a computer in the boot of the car which does the processing. Two cameras give an offset of the face from which a 3-D model of the face is produced. Once this is done, the eyes and mouth are used as reference points in order to determine the driver's angle of the head and number of times the eyes are blinking, to tell whether the driver is attentive or not.

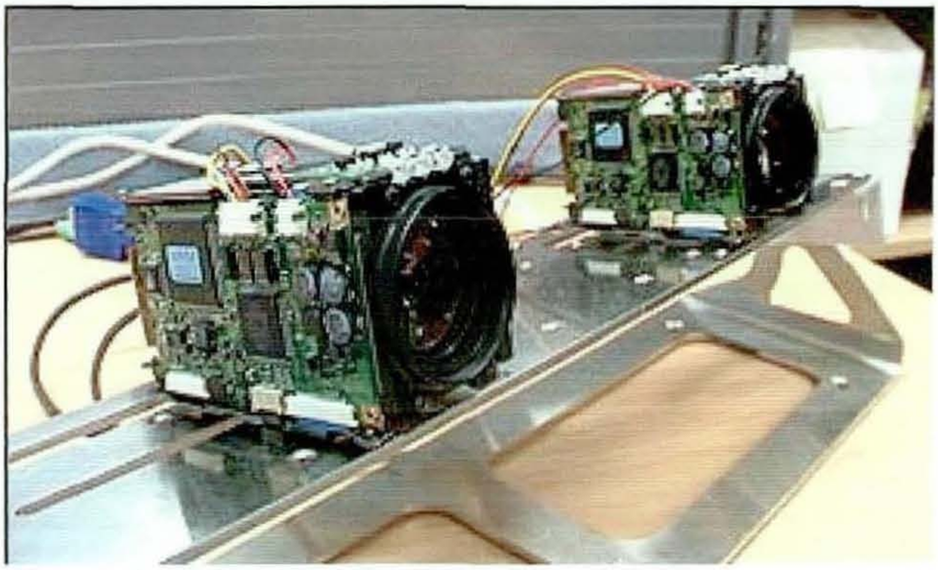

Figure 2-4: Equipment used in Facelab

Driver fatigue is a larger problem than people may think – it is estimated in this report on the BBC website that of the 700,000 road deaths that occur worldwide, as much as 30% is the result of driver fatigue, and so a system like this would be an important safety feature to have on vehicles.

There are similarities between the proposed research in this thesis and the FaceLab system in that both use a camera system connected to a computer with hopes of reducing both size and hence cost substantially in the next few years. However, the thermal imaging system will aim to derive more information about the driver than FaceLab. Also, it is believed that a thermal imager has more advantages than a normal camera or video camera system, as will be explained later.

An interesting procedure for measuring the gaze direction of the driver was described by Mita et al **[75],** where the authors make a distinction between the facial direction and eye gaze direction. They point out that a driver who turns his head 30° to the left, and the eyeball moves 30° to the right, he would still be looking towards the centre and front. In the experimental work done by Mita and his colleagues, images were captured by projecting pulsed infrared light for a short time onto the driver, and a CCD camera with polarizing film and IR pass filter combined, is used to capture the images. A separability filter is used to extract the eye area from the face of the driver.

Predicting how a driver behaves once inside the driver's seat of the car is a topic that has been examined by Liu and Salvucci **[76]**. They have attempted to model driver behaviour by assuming that the driver has a large number of internal cognitive states with their own individual control behaviour, which are in turn responsible for short term behavioural actions such as passing and turning, and also the long term behavioural actions such as lane keeping. It was found from the preliminary results that the driver changed his eye gaze direction many times when undertaking an activity such as lane changing, as well as discovering that there is increased gaze activity towards the inside mirror approximately one second before the driver executes a lane change manoeuvre. Their further work will attempt to use Markov Dynamic Models to detect these changes.

One interesting theory is expounded by the work of Wouters and Bos **[77]**. He suggests that drivers who are aware of being observed by others will tend to modify their behaviour, and it is claimed that this information can be used to encourage people to drive more safely, and could have two benefits. Firstly, drivers who know that they are being filmed or watched may improve their driving, and secondly, data recording could be used to provide feedback to the driver after their car journeys have taken place.

The work of McAllister et al **[78]** in hand and forearm tracking is interesting in its potential application as an in-vehicle driver fatigue and behaviour detection system. In the paper published, the hands of the driver were tracked by taking image sequences inside a real car and images were also taken of the driver operating the steering wheel. A 2-D geometrical model of the hand and the forearm was created and used to fit onto the hand and forearm in the image. The movement of the hands and steering wheel was found by plotting changes of the x and y co-ordinates. Using the data, simple graphs were plotted, such as the differences between the x-coordinates and the y-coordinates of the two hands. When the driver executed a right turn, for example, the y-coordinate difference shows positive maxima, thus indicating that the right hand is positioned lower than the left hand, and so this must be because the steering wheel is turned right. During a left turn, there is a negative minima, and so the driver is turning left. McAllister's research has proven that hands and forearms can be tracked in order to determine what actions the driver is doing inside the car, and this is similar to one of the goals of the work proposed in this project. The purpose of the hand and forearm tracking is that it is able to tell whether the driver is behaving in a responsible way, for example, to tell whether the driver is turning the wheel the correct direction and degree. It can be argued that a steering wheel encoder could have been used, but this would add to the cost and number of components to install into the car, which is to be avoided if possible.

2.9 Safety Through Improved Design

There have been many different approaches to solving the problem of airbag related injury. Many have concentrated their efforts on advanced sensor systems that would take into account the position of the vehicle occupant before the crash occurred, whereas others focussed on other areas, such as the airbag itself. Zhang et al **[79]** have optimised the design of an airbag using Finite Element Analysis (FEA) models, where they made simplified models of three different airbag chamber designs; H, U and A shaped chambers. Their analysis showed that the U – shaped airbag chamber design inflated with greater ease and had fewer problems with localised pressure build up. This is because the geometry of this chamber is much simpler than the other designs; there is only one bend in the chamber and so the airbag inflates at a faster rate than the other airbag designs.

Nishimura et al **[80]** also focus on improving airbag designs for occupant safety. They describe the development of new polyester fabrics to be used for the airbag itself, in order to find an improvement on the nylon 66 fabrics which were used at the time of writing. They found that calendared polyester fabric (C-PET) and uncalendered polyester fabric (U-PET) had high strength, low and stable gas permeability, longer life and had lower costs than current fabrics. Also, it was gentler to the skin and so was less prone to causing the occupant skin abrasions.

From the literature reviewed up to this point, it has been evident that the general consensus amongst researchers and car manufacturers alike, that the way forward towards an advanced airbag deployment system has been to use imaging. These imaging devices have usually been of the visible light variety, CCD cameras and such like. The proposed research has also concluded that imaging of the car occupants is the way forward, but not necessarily using the same equipment. It is proposed that a thermal imager may prove to be more beneficial with regards to occupant detection and monitoring than traditional CCD devices. The reasoning behind this decision is explained later in chapter 2.

2.10 The History and Theory of Thermal Imaging

All objects that have a higher temperature than absolute zero (-273°C) emit infrared radiation **[81]** and this is what makes infrared sensors so useful, because it means that virtually any object can be detected.

Modern thermometry really developed after Kirchoff developed his 'Kirchoff's Law' in 1859. It stated that 'a substance's capacity to emit light is equivalent to its ability to absorb light at the same temperature' **[82].** In 1860, Kirchoff introduced the 'blackbody' concept, which proved to be very important in the development of radiation thermometry. He defined a blackbody as being an object that absorbs all frequencies of radiation when it is heated, and gives off this radiation when it cools down.

Josef Stefan developed 'Stefan's Law' which stated that the total radiation that a blackbody emits is proportional and varies to the fourth power of its absolute temperature **[82]**. This law was later modified by Boltzmann, and he introduced the equation:

$$q = \sigma . T_s^{\,4}$$

where: **q** = blackbody radiation emitted ($W.m^2$).

σ = Stefan-Boltzmann Constant = 5.67×10^{-8} ($W/m^2.K^4$).

$\mathbf{T_s}$ = absolute temperature (K).

For a non – blackbody, the heat transfer rate per unit area is given as:

$$q = \alpha.\sigma.(T_{sf}^4 - T_{sur}^4)$$

where: $\mathbf{T_{sf}}$ = surface temperature (K).

$\mathbf{T_{sur}}$= surrounding temperature (K).

α = absorptivity, where 1.0 = ideal blackbody.

$\mathbf{q}$ = blackbody radiation emitted (W.m^2).

σ = Stefan-Boltzmann Constant = 5.67×10^{-8} (W/m^2.K^4).

Although ideal blackbodies have an emissivity (ε) of 1.0, all objects and surfaces have emissivity values of less than 1.0. Emissivity is defined as the ratio of thermal radiation emitted to the radiation emission of a blackbody at the same conditions. A corrected equation of heat transfer of a real surface i.e. whose objects have an emissvity of less than 0.9 is given below:

$$q = \varepsilon.\sigma.T_s^4$$

where: $\mathbf{q}$ = blackbody radiation emitted (W.m^2).

σ = Stefan-Boltzmann Constant = 5.67×10^{-8} (W/m^2.K^4).

ε = *emissivity (fraction).*

$\mathbf{T_s}$ = absolute temperature (K).

2.11 Pyroelectric Detectors

The pyroelectric effect was first discovered by the Ancient Greeks, 200 years ago **[83]**. They found that when tourmaline was placed in hot ash, there was a noticeable change in the electric charge on the surface. The tourmaline would attract the ashes when it was hot, but repel them when it was cold.

The basic operation of a pyroelectric detector, as described by Rogalski **[84]** is that they are made up of materials that exhibit a, 'temperature dependant spontaneous electrical polarization'. Under equilibrium conditions, the electrical asymmetry is balanced by the presence of free charge, but when there is a rapid temperature change which is faster than the rate at which the free charge can redistribute themselves, then an electric signal is observed in the material. One such material is lithium tantalite **[83]** and to encourage heating and absorption, the material is coated with gold black, carbon black and organic black.

Depending on the number of elements, pyroelectric detectors vary considerably in price. Porter et al **[85]** explains that this is dependent on the number of elements used. A complete unit with between 1 to 4 elements can cost under £10, whilst arrays up to 100,000 elements can cost up to £20,000.

2.12 The IRISYS Thermal Imager

IRISYS is a company that manufactures low resolution pyroelectric thermal imagers at a relatively low cost. Their imagers were used for this project.

Porter et al **[85]** describe the development of their low cost pyroelectric thermal imager. Their IRISYS thermal imager is a 2 dimensional array, which is uncooled, with an operational temperature range of -10^{o}C to 70^{o}C, and has a thermal resolution of better than 2^{o}C. Due to the fact that detection of moving objects was required for some of the applications, then it was thought that pyroelectric detectors would be the answer. The 256 pixel resolution from the 16×16 element array provides just enough resolution to be able to detect moving objects. However, the ability to 'see' moving objects is made possible by fitting a rotating 'chopper'. This is basically a plate with holes in it that spins around a shaft between the detector array and the lens. If the array were to view a static object or scene, the image would soon disappear. When the chopper is added, however, the array sees the object, then the chopper, then the object, then the chopper and so on. This constant change of scenery means that a constant image of any object, moving or static can be generated. The perceived resolution can be increased by approximating the sub-element intensities, so the viewer can effectively see a resolution of up to 128 × 128 pixels. Figure 2-5, reproduced from Porter et al, shows a simple sketch of what a pyroelectric array is composed of.

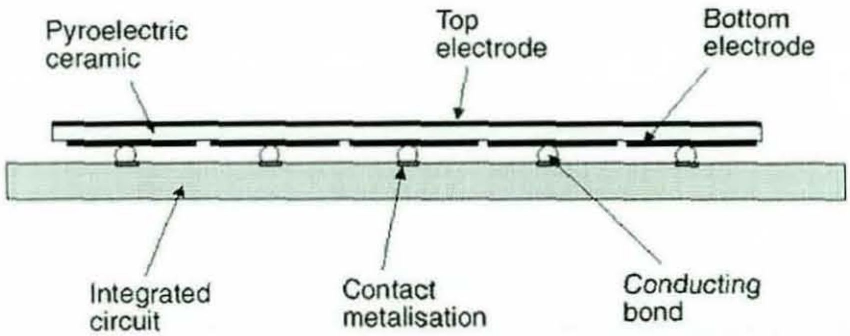

Figure 2-5: Schematic cross-section of detector array, reference **[85]**

Another useful feature of the IRISYS imager is that it can act as a radiometer, i.e. it is able to tell the temperature of the image or different parts of the image. This is done by referencing the image data to the known temperature of the chopper.

2.13 Applications of Thermography

It must be stressed that thermal imagers and infrared cameras are not a new development. Indeed, these developments were the result of military research conducted in the 1970's into thermography, and to this day, infrared technologies are used by the armed forces of principal developed countries, such as the U.S.A and much of Western Europe. The air forces in these countries, for example, use such weapons commonly known as 'heat-seeking' missiles; and thermal cameras are used by the pilots of military aircraft to detect enemy forces during missions conducted under the cover of darkness.

This is only one application of thermal imaging. Some examples of civilian use of thermography are given in the table shown in figure 2-6, reproduced from the book written by Burnay et al **[86]**, titled 'Applications of Thermal Imaging'.

Application	Industries	Description
Inspection of fluid and gas flow relief valves	Petrochemical and steel	Hotter -or-colder-than-normal temperatures can be an indication of damaged, worn or inefficient valves
Inspection of steam traps	Petrochemical	Malfunction usually shows up as higher-than-normal temperature due to steam leakage
Detection of leakage from underground pipes	Petrochemical	Leakage due to various causes (e.g. corrosion, faulty welding etc) will show up as localised surface temperature anomalies
Determination of fluid, gas or solid levels in pipes or process vessels	Petrochemical and steel	Temperature differences usually exist between different phases and this enables the presence and/or level of each phase to be determined from the outside of the vessel. Temperature differences may arise from dynamics of the process, or external heating etc.
Inspection of heat exchangers	Petrochemical and steel	Abnormal temperature distributions and hot or cold spots are an indication of a build up of solids (which could lead to reduced efficiency and flow rate), or a thinning of walls (which could lead to wall failure)
Inspection of air coolers	Petrochemical and steel	Where individual tubes are cooler than average this usually indicates that they are partially or completely blocked by a build-up of solids
Inspection of insulated vessels and pipelines	Petrochemical and steel	Damaged or inadequate insulation will show up as cold or hot areas
Evaluation and inspection of furnaces	Petrochemical and steel	Comparison of tube temperatures with design temperatures may be used as an indication of poor flame patterns, internal coking or external deposits. The adequacy of cleansing or decoking processes may also be assessed in this way
Monitoring of electrical switchgear	Various	Higher-than-normal temperatures are an indication of a changed resistance due to corrosion, defective insulation or mechanical damage
Inspection of transformers and circuit breakers	Various	Low oil levels, which could lead to failure, show up as higher-than-normal operating temperatures
Monitoring of electrolytic cells for fluorine and chlorine	Chemical	Poor connections in individual cells lead to inefficient operation
Safety of coal, slag and refuse tips	Coal and others	Potential areas of spontaneous combustion can be established by monitoring temperature of tips
Determination of thermal efficiencies	Various	Temperature measurements over reactor vessels, furnaces, etc can be used for determining heat flows (losses and gains) and hence the thermal efficiency of a particular plant
Measurement of temperature distribution in moulds and dies etc	Metal, glass and plastic	The temperature distribution can be measured during the period when they are open. Quality of mouldings is affected by temperature distribution

Figure 2-6: Table describing uses of thermal imaging

Other civilian uses of thermal imaging can be found in the building industry **[86]**, for example, where thermography has been used for boiler maintenance. The thermal imager was used to measure the rate of change of temperature decay from the walls of the boiler, which would give the user a measure of the internal corrosion of the steel pipes, and also how effective the thermal lagging of the pipes was. The corrosion of the pipes was detected because of the slower rate of temperature decay that occurs from corroded pipes.

Meteorology has also benefited by the advent of thermography **[86]**. Satellite thermal imaging has been used by civilian and military satellites to measure different aspects of the ecosystem on earth. They have been used to measure the effects of 'global warming' by detecting the levels of desertification on land, and also the rise in sea temperatures. Meteorological satellites such as Meteosat can be used to detect the presence of clouds. Land, sea and clouds have approximately the same emissivity, and the temperature differences between these bodies are used as the basis for the images. Although there is a very small temperature difference between land and sea, there is a much more noticeable difference with clouds, as clouds are generally colder than either land or sea, and so they can be readily identified. Thermal imaging has the advantage over visible light imaging as they can 'see' throughout the day and night, and also because more information can be interpreted from the image, such as cloud temperature, which also means that cloud height can also be measured. Cloud height can be measured because the way in which varying height affects temperature is well understood by meteorologists.

Medical thermography is another civilian use of thermal imaging cameras **[86]**, and is successfully used as a medical diagnosis tool. Although thermal imaging may not be as useful as an X-ray machine or an MRI scanner, which are both able to detect internal organs and other parts of the body, they are however able to measure skin surface temperature, which in turn could give some information about internal physiological problems. For example, in an ambient temperature of 22°C, the skin temperature of a healthy, unclothed, average adult would be between 22°C to 35°C, from the feet to the sternum. At this temperature range, peak infrared emission occurs at the 10 micro-metre wavelengths.

Temperature measurement is a useful diagnostic measurement **[86]**. The core temperature of a healthy human being will be 37°C. Below 35°C, hypothermia starts, whereas if the person has a severe fever or illness, then temperatures can reach up to 40°C to 41°C. Skin temperature is, however, affected by factors such as:

- Age – different thermal patterns are observed on the back of a human subject depending on the age of the person.

- Obesity – an excess of subcutaneous fat will distort the temperature profile. Areas where there are excess fat deposits will show up as cooler regions than normal.

- Environmental temperature – this would also affect the skin temperature. As the ambient temperature rises, there will be less difference in temperature between skin and the air. Sweating and evaporation may dominate body heat loss.

- Exercise – this would increase the skin temperature from the normal skin temperature, particularly in the muscle regions in the legs and arms. The increased blood flow through the body as a result of exercise would mean that more heat is released through the skin, thus increasing overall skin temperature.

Thermal imagers can be used for the following medical applications:

- Inflammatory conditions
- Pain and trauma assessment
- Vascular disorders (deep vein thrombosis, identification of varicosities, vascular disturbance syndromes, assessment of arterial disease)

This is illustrated by the thermal images shown in figure 2-7 and figure 2-8. These images were taken from the 'FLIR Systems' website, www.flir.com. Figures 2-9 and 2-10 were also taken from the 'FLIR Systems' website, and all these pictures are reproduced here for illustration purposes only.

FLIR Systems is one of the largest and most important manufacturers of thermal imagery equipment, although they usually produce equipment which has a higher resolution than the IRISYS thermal imager, although the downside to this is the extra cost of the FLIR equipment. One image shows the thermal image of a man with varicose veins, whilst the other image shows a man with a back spasm.

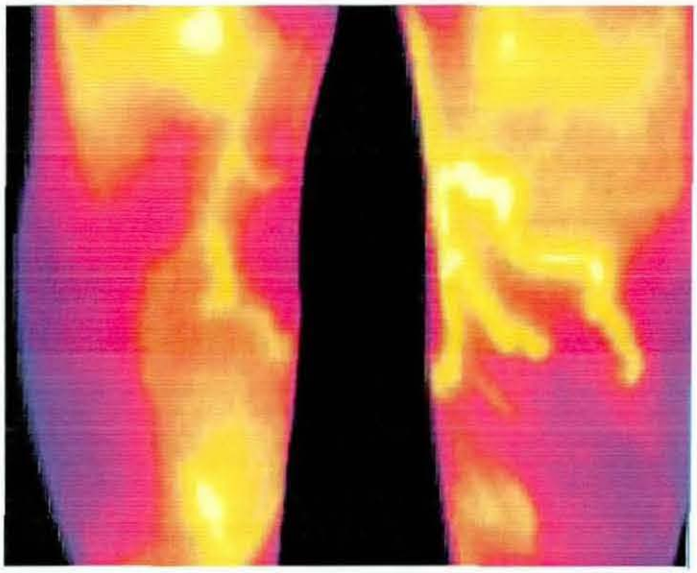

Figure 2-7: Thermal image of a patient with varicose veins

Figure 2-8: Thermal image of a patient with a back spasm

In recent times, applications of thermography have included non-contact condition monitoring for a wide range of industries such as the monitoring of bearings and belts used in the U.K Royal Mail post processing machines. Generally, they are fixed and set up to discover abnormally high temperatures emanating from the equipment. If this happens, it is usually taken to be a sign that the apparatus is malfunctioning in some way, because the temperature is outside the limits of normal operation. This is perhaps best illustrated in figure 2-9 and figure 2-10:

Figure 2-9: Motor and gearbox of baggage handling machine at Heathrow airport

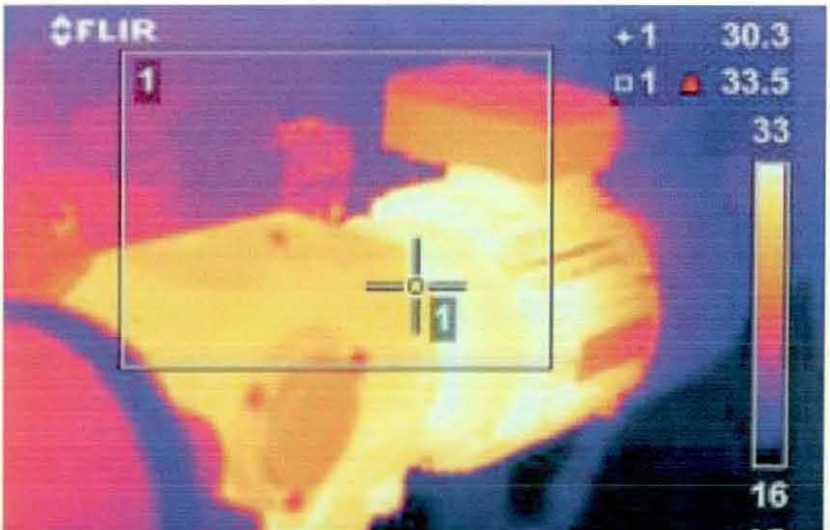

Figure 2-10: Thermal image of the motor and gearbox showing internal winding problem

Other civilian uses of thermal imaging are as follows:

- Mechatronics Centre research into applying thermal cameras for condition monitoring.

- Emergency fire services using thermal imagers to look for people in smoke filled buildings and also to detect people trapped under rubble after earthquakes.

- Police forces using thermal cameras mounted onto helicopters for traffic monitoring at night.

There remains the question of whether thermography is suited for use on people. However, it was felt that thermography was very well suited for use in detecting humans because:

- Humans are warm-blooded mammals and therefore emit constant thermal radiation.

- Important parts of the body are not usually covered by clothing, such as the head.

Thermal imagers can also be used in all lighting conditions, light or dark, day or night. Variable lighting conditions are more commonly experienced by the vehicle occupant than is initially realised, because a car journey may involve:

- Driving through tunnels.
- Poor road and street lighting.
- Height density of foliage covering the road and restricting light incidence onto the road.
- Variable cloud cover, particularly in temperate regions of Western Europe (e.g. U.K).

2.14 Advantages of Thermography

The advantages of using thermography **[86]** are listed below:

- Remote sensing – thermal imagers are able to measure temperature without direct contact with the object. It can be used to measure temperatures from long distances and also be able to be used in hazardous areas (e.g. hazardous areas where there is high voltage, poisonous gases).

- Two-dimensional data acquisition – images of two dimensions are able to be produced.

- Fast response.

However, this does not explain whether thermography is a better option than standard CCD cameras. However, the thermal imager does have advantages over the CCD camera, and these are explained in the following section.

2.15 Advantages of Thermal Imager over a Standard Camera

The majority of research done on developing a driver monitoring system involves a standard visible light or CCD camera pointing at the driver in question. There is nothing wrong with this, indeed it was considered for use for this project, but it was felt that there were other alternatives that could be suitable, such as the IRISYS thermal imager. Infrared thermal imagers are not new, but they have been in the past extremely expensive and hence not economically viable for some applications. However, the low cost thermal imager from IRISYS, although has relatively low resolution with its 16×16 pixels, does have advantages over the standard camera such as:

1. Thermal imagers work during variable natural lighting conditions i.e. during the day and night time. Visible light cameras have problems with too little sunlight or too much sunlight, and they would not work well, if at all, in the

dark. Also it would have problems when the car travels from two extremes of lighting conditions i.e. when the car enters a tunnel or is in the shade.

2. Thermal imagers only 'see' the person in front of it and very little background information, whilst the camera sees the person and everything else in the background. Therefore the thermal imager will not have the problem of separating the important image of the driver from the unnecessary background image.

3. Because the thermal imager 'sees' only the driver and little else, its images can be processed faster than those of an ordinary camera, and this is a crucial point because of the fact that airbag deployment takes place over milliseconds.

4. The cost of the thermal imaging system will therefore be cheaper because it will not need the expensive and faster computers to process the information that a CCD camera would.

5. The privacy of the driver would be protected with the thermal imager and so people would be more inclined to accept it into their cars than they would a normal camera. The driver would not feel that there is a 'Big Brother' watching over every move that the driver makes, which could be used to incriminate him in the event of an accident.

These clear advantages make thermography an attractive and novel method of occupant sensing within the car cabin, and was why it was chosen ahead of the CCD camera.

2.16 Summary of Literature Review

In summary, the review of the available literature has shown that extensive work has been carried out by other researchers in the field of occupant safety, and specifically for the aim of improving airbag safety. Injuries of differing severity are caused by the action of the occupant hitting the airbag, and the mechanisms of this process have been discussed. It has also been established that some occupants are more at risk of injury or fatality than others, and these have been identified as being infants in child safety seats, and small female drivers, although it was also realised that all front seat vehicle occupants are at risk of airbag induced injury if they are positioned within the airbag deployment zone.

The NHTSA of the United States of America has recognised the danger after keeping track of the available crash statistics, and have ultimately passed new regulations which new vehicles have to adhere to, and which will come be enforced in the coming years. This has led to various interested parties, from car manufacturers to engineering research establishments to develop methods and technologies for combating this problem. Many of the solutions proposed rely on vision systems with CCD cameras, others use weight sensors built into the car seat. However, they are also limited in their scope, and seek only to measure or detect one aspect such as the weight of the occupant. Nor do many use multiple sensors in their systems, and there are questions about the viability of the systems due to the high cost of some of the components used.

2.17 The Scope of the Research

The review of the available literature has shown the need to detect occupants inside the car cabin, and to be able to differentiate between adults and children; and between men and women, if possible. Also of equal importance is the need to obtain information on whether the driver is OOP. With these criteria, and having already discussed the reasons why infrared thermal imaging was the method of doing this, the main objectives of the proposed research were defined as:

- To detect the presence of a human being on the seat. The detection system must also be intelligent enough to detect whether the thermal profile it detects is that of an animal or another object such as luggage or bags of shopping. In these cases, the airbag should not fire.

- To measure the occupants height and position inside the car. He could be leaning forward to use the radio or to get something out of the glove compartment or could be leaning to the side for an overtaking manoeuvre. This would be termed 'out of position' and the airbag should not activate.

- To identify the type of occupant i.e. whether it is male or female and whether it is a small child or an elderly person. In some of these cases, the decision to activate the airbag would need careful consideration since it could injure the elderly and child occupants.

- To identify any other possible factors that may have safety issues such as whether the driver is smoking or not.

Some of the work described in the literature review and the work being described in the literature review and the work being proposed in this research project is perhaps leading to ever more advanced technology being developed for use inside the car. Indeed, the following chapter will present the reader with other issues of what is known in the industry as the 'intelligent vehicle' concept. The next chapter explains what developments are being made to advance the 'intelligent vehicle' concept, and where 'intelligent deployment of occupant restraints' fits in this field of research.

Chapter 3 Context of Research

3.1 Introduction

The literature survey conducted in the previous chapter has commented upon the research conducted in the field of advanced airbags and the sensors used in these systems. This chapter will put the research conducted in the field of advanced airbags into context with regards to the broader area of the 'intelligent vehicle'. The issues that will be addressed in this chapter are:

- The purpose of intelligent deployment.
- The meaning of 'Out of Position' (OOP).
- The advantages of using thermography.
- A discussion of other developments which are happening in the 'intelligent vehicle' field.

3.2 The Need For An Intelligent Airbag Deployment System

It can be demonstrated that there is a genuine need for the 'intelligent deployment of occupant restraints' for three reasons. The first reason can be explained by detailed research (as reported in chapter 2) which has shown that the airbag has caused death and injury to the car occupant. The essence of this research shows that there have been over 100 deaths and many more injuries which have been attributed directly to the act of airbag deployment, and not as a result of injuries caused by the crash itself. The research has also shown that these injuries and deaths occur mainly to a select group of vehicle occupants, and these are:

- Small female drivers under 165cm tall.
- Small children and infants in rear facing infant seats on the passenger seats.

In order to prove that the act of airbag inflation could indeed cause serious damage to an occupant, a simple calculation was carried out, taken from Frey et al. **[87]**. Actual data (e.g. type of material used, weight of material, propellant, expansion force, rate of expansion, heat discharged etc) of a real production airbag could not be obtained from car manufacturers as, naturally, they were reluctant to make such information about their components and parts open to the public and their competitors. Therefore, some assumptions about the airbag dimensions were made by Frey et al.

A basic calculation of the force required to fill an airbag is given below. It is assumed for the purposes of this calculation that a typical airbag has a weight of approximately 2.5kg. This is reasonable bearing in mind that the airbag needs to be of sufficient strength and construction to be able to withstand the initial rapid expansion of the airbag, to hold up to 60 litres of gas for a short period of time; to withstand the impact of the occupant's head and upper body, and to withstand the heat generated from the explosion of the propellant used to expand the airbag.

Assuming that the front surface of the airbag,

$u=0$ m/s

$v = 200$m.p.h or 89.4 m/s

d = thickness of fully inflated airbag = 30 cm

$v^2 = u^2 + 2ad,$

$v^2 - u^2 = 2ad,$

$a = v^2 - u^2/2d,$

$a = 89.4^2 - 0^2 / (2 \times 0.30),$

$a = 1.33 \times 10^2 \text{ m/s}^2.$

Assuming that the weight of a non-inflated airbag = 2.5 kg,

$F = ma,$

$F = 2.5 \times 1.33 \times 10^4 = 3.33 \times 10^4\text{N}.$

The next question to consider is whether this force of 33 kN is sufficient enough to cause serious damage to a car occupant. This can be answered to some degree by the research done by Nahum et al **[88]**. Their research provides some useful information on the forces required to break bones in the face and head of an average sized adult. In his book, Nahum documents some experiments which were conducted. These experiments consisted of using blunt instruments which impacted onto the skull or heads of cadavers, and then measuring the force required to fracture certain bones in the head. Similarly, the airbag could also be said to be a blunt instrument, as the pressure inside the airbag is so great at peak inflation that it acts as a hard, solid object. The results of these experiments are shown in the tables below (reproduced from Nahum et al):

Fracture Force of Facial Bones

	Force				
Bone	**Range (N)**	**Mean (N)**	**Sample size**	**Impactor area (cm^2)**	**Author (reference)**
Mandible					
Midsymphysis	1890 - 4110	2840	6	6.5	Schneider
Lateral	818 - 2600	1570	6	25.8	Schneider
Mandible	4460 - 6740	5390	5	127	Hopper
Maxilla	623 - 1980	1150	11	6.5	Schneider
Maxilla	1100 - 1800	1350	6	20 mm diam.bar	Allsop
Maxilla	788	788	1	20 mm diam.bar	Welbourne
Zygoma	970 - 2850	1680	6	6.5	Schneider
Zygoma	910 - 3470	1770	18	6.5	Nahum
Zygoma (a)	1120 - 1660	1360	4	6.5	Hodgson
Zygoma (a)	1600 - 3360	2320	6	33.2	Hodgson
Zygomas (b)	2010 - 3890	3065	4	25 mm diam.bar	Nyquist
Zygomas (b)	900 - 2400	1740	8	20 mm diam.bar	Allsop
Zygoma	1499 - 4604	2390	13	Approx. 25 mm diam.bar (steering wheel)	Yoganandan
Zygoma	1452 - 2290	1739	4	Steering wheel	Yoganandan
Naison	1875 - 3760	2630	5	25 mm diam.bar	Welbourne
Full face ©		>6300	5	181	Melvin
Superior orbits	4780 - 11040	8000	19	41 mm diam.bar	Porta

(a) Multiple imapcts prior to fracture.

(b) Both zygomas below suborbital ridges.

(c) Greater then 6300 N for fractures other than nasal.

Figure 3-1: Table showing fracture force of facial bones

Fracture Force of the Skull

Bone	Force Range (N)	Mean (N)	Sample size	Impactor area (cm^2)	Author (reference)
Frontal	2670 - 8850	4930	18	6.45	Nahum
Frontal	4140 - 9880	5780	13	6.45	Schneider
Frontal	2200 - 8600	4780	13	20 mm diam.bar	Allsop
Frontal	5920 - 7340	6370	4	6.4 mm diam.bar	Hodgson
Frontal	8760 - 8990	8880	2	25.4 mm diam.bar (saggita) (a)	Hodgson
Frontal	N/A	6550	1	50.8 mm diam.bar (90 durometer, sagittal) (a)	Hodgson
Frontal	N/A	6810	1	203 mm radius hemisphere	Hodgson
Frontal	4310 - 5070	4690	2	76 mm radius hemisphere	Hodgson
Frontal	N/A	5120	1	50.4 mm diam.bar (sagittal) (a)	Hodgson
Left frontal boss	2670 - 4450	3560	2	25.4 mm diam.bar	Hodgson
Temporoparietal	2215 - 5930	3490	18	6.45	Nahum
Temporoparietal	2110 - 5200	3630	14	6.45	Schneider
Temporoparietal	2500 - 1000	5200	20	5.07	Allsop
Temporoparietal	10976 - 11662	11388	3	176	Mcintosh
Parietal	5800 - 17000	12500	11	50	Allsop
Zygomatci arch	930 - 1930	1450	11	6.45	Schneider
Occipital	4655 - 10290	7272	4	176	Mcintosh

(a) Major axis of bar parallel to sagittal plane

Figure 3-2: Table showing the fracture force of the skull

Stiffness of the Face and Skull

Bone	Stiffness (N/mm) Range (N)	Mean (N)	Sample size	Impactor area (cm^2)	Author (reference)
Maxilla	80 - 180	120	6	20-mm-dia bar	Allsop
Zygoma	Force (N) = [displacement (mm)]^2.5		6	25-mm-dia bar	Nyquist
Zygoma	90 - 230	150	8	20-mm-dia bar	Allsop
Frontal	400 - 2200	1000	13	20-mm-dia bar	Allsop
Temporoparietal	700 - 4760	1800	20	6.45	Allsop
Parietal	1600 - 6430	4200	11	50	Allsop

Figure 3-3: Table showing the stiffness of the face and the skull

Frey's calculation of the airbag 'punch out' force (albeit using some assumptions) shows that the force is approximately 33kN. This is significant as figure 3-1 shows that the maximum recorded force required to fracture a facial bone (the 'superior orbits') was only 17kN. This proves that the airbag 'punch out' force can indeed cause severe damage to the human body if the occupant's head is positioned close enough to the airbag during its inflation phase. This certainly proves the danger of airbag deployment and highlights the necessity of having an intelligent airbag deployment system, such as the one proposed in this thesis.

The first reason why legislation was necessary in the US, and not in the UK or the EU 15, was that the US airbag was designed to be much larger than the EU airbag (inflated volume of 70 litres and 40 litres respectively). The second reason is because drivers in the US have historically tended to wear the seat belt less than their European counterparts. Traditionally, there has been less enforcement of wearing seatbelts in the US than in the UK for example. Although seatbelt wear rates have increased in the US during the 1990's, it is still lower than in the UK or the rest of the EU. Hence, the airbag designed for the US market was designed to be the primary method of protecting the driver from crashing into the dashboard and steering wheel, whereas in Europe, the airbag is seen as the secondary device. The seatbelt would prevent most drivers from striking the steering wheel in the event of a frontal impact. If it did not, the airbag would have deployed and protected the driver in this instance.

Halldin et al **[89]** have also recognized that impact to the head and associated injuries to the brain and neck regions are a major cause of death to the driver and occupant. Whilst other researchers have focused on prevention of accidents by the use of advanced systems to improve driving and reducing the number of deaths and injuries on the road, the work done by Halldin et al is involved in the protection of the driver in the event of an accident, and to try to limit the damage caused by an accident. They have developed an 'experimental head restraint concept' (EHRC), which basically works as a safety belt for the head, and was designed to reduce crash forces being exerted onto the head and neck in the event of a full frontal car crash. The purpose of doing this work is explained by Halldin et al when they say that traumatic brain injury accounts for more than 40% of all neurotrauma (injury to the central nervous system) injuries occurring in traffic accidents. They argue that by reducing the head acceleration prior to impact, brain injury can be significantly reduced. The EHRC consists of a curved aluminium pipe containing a linear elastic spring (with a spring constant of 1.5 kN/m), a vertical aluminium plate. The function of the EHRC is to decrease the G forces exerted on the head, and to prevent impact of the head with other objects inside the car cabin.

Sled tests were conducted to evaluate the effectiveness, and the readings taken were of head resultant acceleration, moment in neck around the occipital condyles, axial and shear force in the neck, and resultant acceleration in the thorax. The impact speed for these tests was 11 m/s. These results show how effective the EHRC device was. Peak translational acceleration of the centre of the head was reduced by 32%. Peak axial and shear forces in the neck were reduced by 37% and 43%. Adding the EHRC with the seatbelt and the airbag configuration improves the head injury criterion (HIC) value to 68%. These results strongly indicate that if this safety device was fitted into motor vehicles, then severe neurotrauma injuries would be significantly reduced. However, it remains to be seen whether this type of device would ever be installed inside a vehicle, regardless of its safety benefits. The major problem is that it severely restricts the movement of the driver in the car cabin, as well as causing the driver to enter and exit the vehicle slower.

The third reason why an intelligent airbag deployment system is required is because of legislation being passed in the US where the vast majority of recorded airbag-related fatality and injury incidents have occurred. The NHTSA have been forced by this mounting evidence, to pass amendments to their Federal Motor Vehicle Safety Standard (FMVSS). In particular, FMVSS No. 208, which specifies the standards which manufacturers must follow for the provision of airbag occupant protection, has been amended. In his paper 'Development of Occupant Classification System for Advanced Airbag Requirements' Nozumi **[90]** says that FMVSS No. 208 was upgraded to include 'advanced airbag requirements' which were to be designed to protect small adults and children on the front passenger seat. Nozumi, on behalf of the Mitsubishi Motors Corporation (MMC), explains that the new crash test procedures also give the car manufacturer two methods of reducing the risk of 'out of position' (OOP) occupants being injured. These methods are to either automatically suppress the inflation of the airbag, or to allow a low-risk deployment which means deploying the airbag in such a way that it minimizes the risk of airbag inflicted injuries. Due to current airbag technology not being advanced enough to satisfy the requirements of the latter, then airbag suppression was the method used. Nozumi reports that their occupant classification system (OCS) is now used in Mitsubishi GALANT vehicles produced in North America , and consists of four strain gauges (mounted in the front and rear of the seat) which produce signals that correspond to load inputs which are received from sensors located under the passenger seat rails. This load is representative of the weight of the seated occupant, and using this data, the OCS is able to determine what size of occupant is seated on the seat. Nozumi explains that this technology complies with the legislation, and indeed, other major manufacturers such as Mercedes and BMW have also introduced similar systems (based on weight sensing and measurement) as has been documented in chapter 2. It is thought that this not only provides important reasons for conducting research into intelligent deployment of occupant restraints, but also further strengthens the case for using thermography. Vision based sensing in general can be better utilized to provide occupant classification with more subtlety and accuracy than weight sensing, as well having the advantage of being non-intrusive and less expensive to maintain (over the lifetime of the product) than direct contact, seat based sensors.

3.3 The Advantages of Using Vision Based Systems

The question of why a vision based system was selected and not other methods or systems is explained by Bertozzi et al **[91]** in their paper titled 'Vision-based intelligent vehicles: State of the art and perspectives'. They argue that tactile sensors and acoustic sensors are of no use due to their low detection range. Acoustic sensors are affected by factors such as sound pressure dissipating over distance, and also by objects or barriers between the sensors and the source of the sound emitter. Also, it would be difficult to find a correlation between the sound emitted inside the car cabin and the position or the distance of the driver to the sensor. Background noise would also reduce the effectiveness of an acoustic sensor, therefore this technology is unsuitable for use in this application.

Other sensors which could be considered are laser based sensors and millimetre wave radars, which detect distance between objects by measuring their time of flight. However, as Bertozzi mentions, their disadvantages are that they have low spatial resolution and slow scanning speed. This is where vision based sensors have the advantage over laser or radar sensors in that vision based sensors can scan and acquire data in a non-invasive way.

3.4 Advantages of Using Thermography

In order to explain why the thermal imager was chosen as the main sensor in this project, it is important to consider the alternatives to this technology. These were:

- Pressure sensors/weight sensors/strain gauges/load cells.
- Ultrasonic sensors.
- CCD cameras/video cameras.

Pressure and weight sensing were not favoured because they had the major disadvantage of not being able to provide accurate positional measurement data about the occupant on the seat. This was investigated further in chapter 4, the findings of which are also discussed in chapter 4. Another disadvantage is that these types of sensors are 'direct contact' sensors, which means that they must come into contact with the occupant in order for them to produce a measurement. Although weight sensors and strain gauges could be mounted on the seat frame, this would reduce the impact on the driver but possibly at the risk of reacting slower to changes in the load exerted on the seat, as they would be mounted a distance away from the point of impact of the load. Direct contact sensors cause problems as this type of contact can affect the driver and even cause some degree of pain. This is a serious issue as it would provide an unwanted level of distraction for the driver and could compromise safety of the vehicle if driver concentration levels drop. Repeated direct contact between the occupant and the sensor may also cause damage to the sensor and possibly cause it to malfunction.

Ultrasonic sensors are non-contact sensors, just like the infrared imager, however, they too have their disadvantages, namely, that they can only provide positional measurement data. They operate by measuring the time of flight of the ultrasonic beam leaving the source, hitting its target and then returning to the detector array. Many ultrasonic sensors are required to provide a reliable measurement of distance, and this adds both to the complexity and cost. Also, the major drawback with this is that the ultrasonic sensor is unable to provide any additional information which would be useful in an airbag deployment system, such as what type of occupant was seated, whether the occupant was human or some other object etc. Vision systems, however, have the capability to provide this extra information.

Perhaps the closest challengers to the thermal imager are the CCD (Charged Couple Device) and the CMOS sensor. Supporters of this technology may argue that this technology has been 'tried and tested' and is not as new and untried as thermography. Also, CCD cameras are readily available and can be purchased for relatively small sums of money. However, the thermal imager does have one major advantage over the CCD camera and it is its ability to 'see' or obtain information in all lighting conditions, which the CCD camera cannot. This is extremely important as the advanced airbag deployment system must be able to operate all the time throughout the journey. It must operate during the day or night or during variable lighting conditions as would be experienced when driving through tunnels, or through heavily forested areas, or overcast conditions. Another significant advantage that the thermal infrared imager has over its CCD counterpart is that it is able to distinguish the human occupant far more clearly from the background, whereas the CCD camera would show not only the occupant, but also unimportant information such as the objects in the background. To process this CCD image with it's far larger number of pixels, would require longer processing time, and would require more expensive equipment and necessitate the need for more complex image processing software and/or algorithms. It is for these reasons that the decision was made to use thermography as the basis of its sensing system.

3.5 Out of Position (OOP) Occupant

The term 'out of position' (OOP) has been coined by people within the automotive safety industry to describe a driver or occupant as being not in the correct seating position for driving, or being in a potentially dangerous position should the driver or passenger side airbag deploy. As has been mentioned in previous chapters, the NHTSA have recommended that all drivers and front seat passengers should keep a distance of 10 inches from the surface of their breastplate to the front surface of the airbag module contained in the centre of the steering wheel. This advice is designed to ensure that there is a large enough space between the occupant and the steering wheel in order to ensure that the airbag is able to fully inflate without hindrance by some object, which would tend to be the occupant. This advice is necessary when one considers the deaths and injuries caused by inappropriate deployment.

In their paper titled 'Measuring Airbag Injury Risk To Out of Position Occupants', Morris et al **[92]** have explained how and why deaths and injuries occur to 'out of position' occupants. They explain that there are two phases of airbag deployment, the 'punch out' phase and the 'membrane loading phase'. The punch out phase only becomes an extreme danger when, for some reason, the occupant is leaning extremely forward of his normal sitting position and is resting on the steering wheel. This could be if the driver is unconscious. If this happens, the gas pressure within the airbag rapidly increases, resulting in a high force being exerted against the occupants' body. However, this injury risk can be significantly reduced if there is a small separation between the airbag module and the occupant, and it is for this reason that the NHTSA recommend that the occupant should be a minimum distance of 10 inches away from the airbag module at all times.

Injuries are also caused during the membrane loading phase, which occurs when the airbag has been released from the module. According to Morris et al, the injuries to the driver are caused when the inflating airbag wraps around the occupant in its path. This is very serious as there is danger even when there is some separation between the occupant and the airbag module. This is particularly worrying because there are some types of driver who have little option but to sit close to the steering wheel either because of their short stature or for medical reasons (e.g. failing eyesight). An intelligent airbag deployment system could reduce this risk, and is another reason for conducting research into this problem.

3.6 Other Developments in Advanced Vehicle Systems

The field of advanced airbags is but one of a myriad of different areas of research and development being undertaken under the umbrella of the 'intelligent vehicle' concept. There are so many different organizations involved that to keep track of all the new research ideas and developments is difficult. However, an attempt has been made in the UK to do just this very exercise. Foresight Vehicle is a collaboration between the UK Government, industry and academia, and was set up by what was known then as the UK Department of Trade and Industry. They produced a comprehensive document (which was freely available from their website) entitled 'Foresight Vehicle Technology Roadmap: Technology and Research Directions for Future Road Vehicles', and was published in August 2002 **[93]**. The document's stated aim was to identify and demonstrate technologies for sustainable road transport. More than 130 'experts' in the road transport field and 60 organizations were brought together to form views about predicting developments in vehicle markets, products, and technology in the next 20 years. Of particular interest (with regards this project) were the potential developments in the health, safety and security fields. Foresight Vehicle has estimated that the 3,500 road deaths and 40,000 serious injuries which occur in the UK each year have a huge social and economic impact. The economic impact of automobile accidents is estimated to be 2% of the Gross Domestic Product (GDP) of Europe, and this is an extremely large amount of money when considering that the GDP of the UK is approximately $1,700 BN per annum. Reducing this cost by reducing the number of people killed and injured on the roads is another important reason for conducting research into intelligent deployment of occupant restraints.

Foresight Vehicle also reveals that there are political considerations to take into account as well. The UK Government has set up a ten year transport plan, in which one target is to reduce the number of deaths and serious injuries on the road by 40% and to have 50% fewer children killed or seriously injured by 2010. The intelligent airbag deployment system will also contribute to this effort, and should ensure favorable publicity for the manufacturer(s) who install such systems into their vehicles.

In terms of technology, the Foresight Vehicle has identified that there could be advances in software and sensors that are able to provide passive warnings and information services; development of sensors for control of vehicles, and active support to the driver. These developments are expected between the years 2006 to 2013. Other aims are to have systems which are capable of driver classification; driver characterization (useful for automatic setting up of the vehicle tailored to the driver's size); and identification and characterization of the passenger. From 10 to 20 years in the future, it is hoped that there will be such features as intelligent speed adaptation; vehicle fingerprinting; dynamic route guidance; remote anti-theft (vehicle control) and vehicle to vehicle control. Beyond 20 years in the future, it is difficult to predict accurately, but the Foresight Vehicle team have identified that automated highway control driving is likely to be introduced, ostensibly to reduce congestion on the roads. This is not surprising as earlier in their report they estimate that congestion on the roads cost the UK economy between £15-20BN each year, which is just over 1% of the GDP of the UK. Indeed, the Foresight Vehicle team agrees that safety is of the utmost importance. They rated each market requirement as to what their importance in the year 2020 would be, with '5' representing the most important, and '0' the least important. Safety of the travellers and bystanders was given a rating of '5', higher than other issues such as energy use or reliability. This provides independent confirmation of how important safety related research is, and provides further justification for conducing this research into intelligent deployment of occupant restraints.

Other developments in the 'intelligent vehicle' field are given in figure 3-4. The figure shows that intelligent or advanced deployment of airbags is but one of many of different research and development topics being pursued under the banner of "intelligent vehicle". Many different sources have been used to compile this diagram, from journal papers, articles in the print media as well as from personal experience of working in this field. Although not complete, it nevertheless shows some of the major areas of research within the field of intelligent vehicle. Some of the aims of the research groups are to reduce the number of deaths on the road down to zero. Although this is a laudable aim, it is also perhaps too optimistic to hope for if vehicles are to be controlled by humans, as humans are always prone to make mistakes.

However, there is some debate as to whether some of the systems being investigated are actually necessary. Although safety systems are necessary, the driver information systems are not as important, as it could be argued that the vehicle drivers of earlier generations did not need such technology. However, it could be argued that anything which makes the task of driving easier, also makes driving safer for the driver, the occupants and other road users and pedestrians alike, therefore, such technology is worthwhile.

Vehicles of the future will not only require advanced safety systems or driver aids, as can be seen in figure 3-4. More fundamental changes will occur in the way in which the vehicle is powered, and the research and development for this to take place is already being done today. There are competing technologies for powering the vehicle of the future. These are fuel cells, batteries and highly efficient internal combustion engines. Fuel cells are popular because they can be powered by hydrogen, and they do not produce harmful 'greenhouse' gases such as carbon dioxide or nitrogen dioxide. The fuel, hydrogen, is an element which is in plentiful supply in water. Electrolysis is one method of separating the hydrogen from the oxygen molecules, however, this requires a lot of energy, and the energy required to power the electrolysis process would need to be derived from a renewable source in order to obtain the full benefits of having a fuel cell. If vehicles were fitted with fuel cells, yet the power required to produce the hydrogen came from existing coal or gas fired power stations, there would be considerable doubt as to whether there was any significant benefit to the environment from switching from the internal combustion engine to the fuel cell.

Other technical challenges are explained by Pischinger et al **[94]**. Their paper analyses the requirements of current automobile technology. For example, Pischinger writes that today's vehicles require fast response to load changes, and fast acceleration. He also gives figures for what the energy requirements could be for a future vehicle. For example, 500 kWs is required to accelerate a car (weighing 1850 Kg) from 0 to 85 Km/h as long as there is 50 kW of constant mechanical power, and also 1kWs is required for the air compressor. Other requirements include the need to heat the engine or fuel cell to a it's operating temperature, from 20°C to 80°C, and this is estimated to take up to 4000 kWs. What all these examples show is that a large quantity of electrical power is required from a future fuel cell/electric vehicle in order for it to match the performance of current vehicles. It is important for the future vehicle to at least match that of the current internal combustion engine powered cars, otherwise this would be a problem because it would be difficult to sell the fuel cell powered car if its performance was significantly poorer than that of the internal combustion engine cars.

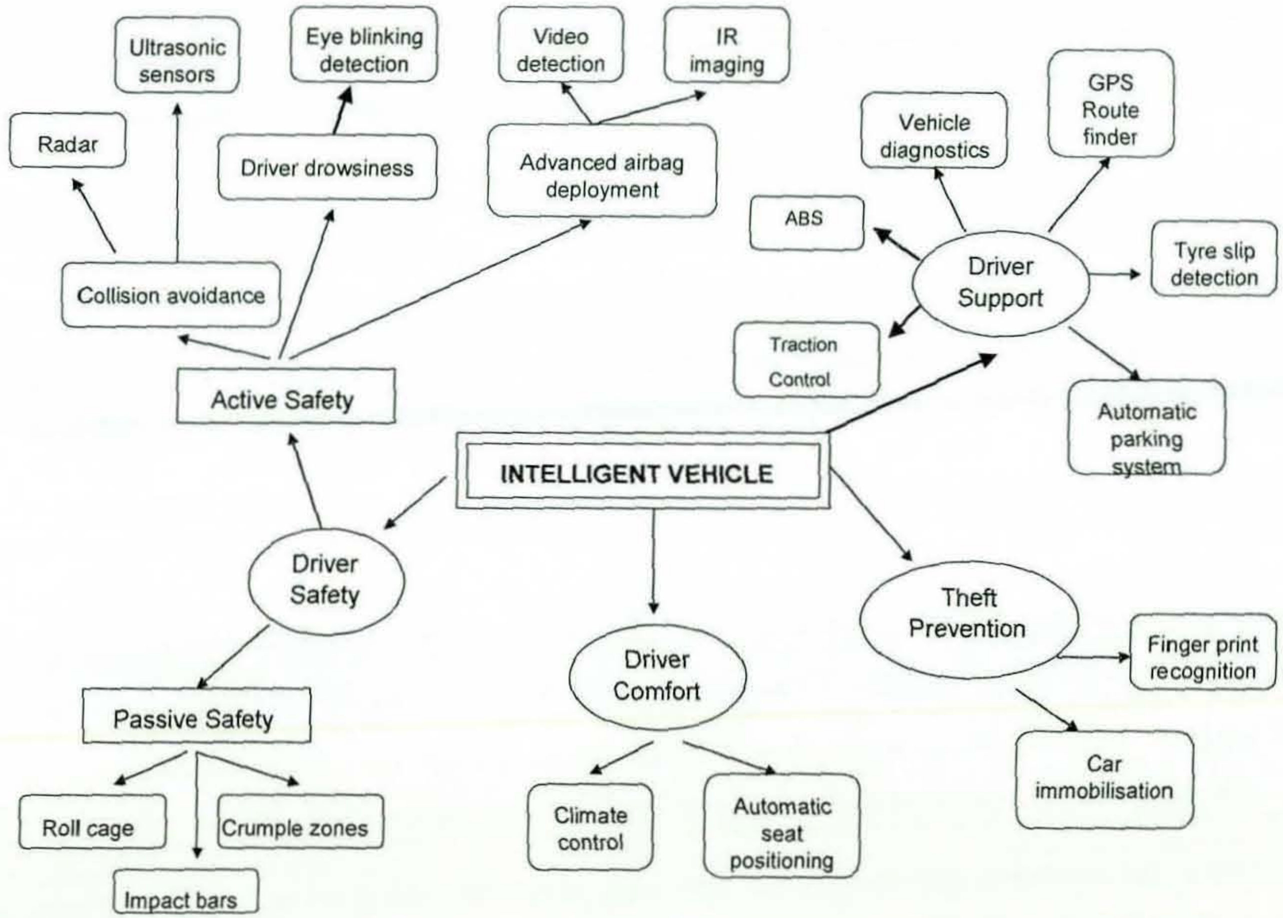

Figure 3-4: Diagram showing the breadth of activity within the 'Intelligent Vehicle' field

3.7 Potential Problems with the Intelligent Vehicle Concept

Before some of the 'intelligent vehicle' features can be installed into the vehicle, national laws governing road safety may require amendments or complete replacement. For example, some manufacturers wish to develop a vehicle which uses so called 'steer by wire' technology. This causes a problem as there is a statement in existing regulations which requires the steering wheel to have a mechanical link to the drive wheels. Also, there are potential safety concerns such as if the electrical supply to the motor vehicle is stopped mid way through a journey. It is likely that this would cause an accident, which could be fatal if it occurred in a high speed environment such as when driving on a motorway.

Some have questioned whether further research into an 'intelligent vehicle' is necessary. It is true that the large milestones in the field of occupant safety have already been made in the past 50 years. These have been, firstly, the advent of crumple zones in the front end of vehicles which were specifically designed to deform at a particular rate in order to absorb most of the crash pulse, thus protecting the occupant from the worst of the crash energy. The next major innovation was the three point safety belt, originally developed by Volvo, a Swedish manufacturer (now owned by the Ford Motor Company). The introduction of this device led to a major reduction in the number of road deaths and injuries. The third major innovation was the driver airbag. Although primarily designed as a secondary restraint device, it has nevertheless been directly responsible for saving the lives of thousands of car occupants and many more injuries. In the US, this was most useful as until recently, there was a culture where drivers and other occupants did not wear seatbelts. It can be argued that the safety features and devices which have been introduced afterwards have not been as important. These include devices such as the roll cage, passenger side airbags, side airbags and knee bolsters and side impact bars. Although these have all contributed towards making the car occupant safer in the event of a crash, these features are not standard, nor are they compulsory and so their impact on road accident statistics has been lessened.

In any future intelligent vehicle, it is desirable for all the various systems to be able to communicate with one another. This could present some problems as there are many different organizations trying to develop their own systems for a future intelligent vehicle, and they will invariably use different communication interfaces (e.g. Can BUS). The problem is that at this time, it is not clear who or which organization will produce a system which will be adopted as the industry standard, in the same way that the three point safety harness design was adopted as the standard seat belt in passenger vehicles. This means that between now and then, there will be little coordination between different systems, and this may delay the implementation of an intelligent vehicle in the near future.

However, some research is being done to prove that different motor vehicles can communicate with each other for the mutual benefit of both vehicles and their occupants. Real world trials to eliminate or reduce causes of accidents have been researched by Kato et al **[95]**. They have attempted to reduce the number of collisions that occur at intersections in the road by the use of communication between the two vehicles concerned.

They have also attempted to use this technology to implement 'platoon driving' whereby vehicles are queued up behind the lead car on a motorway, for example, and there is a constant distance between each vehicle as all the vehicles maintain a constant speed. This is not a new idea, as it has been mooted many years previously, however, Kato et al have demonstrated the technology by which 'platoon driving' may be possible. The potential benefits of such ordered driving could be in terms of lower overall vehicle fuel consumption (due to reduced braking and acceleration), and also lower vehicle accident rates.

Kato et al have shown a few potential uses of the wireless ALN and 5.8 GHz DSRC technology, and how it can benefit the driver in terms of road safety, but there are other possible applications of this technology. For example, it may be possible to use these same communication devices to alert the emergency services of a possible accident or emergency affecting that particular vehicle, and the technology would be able to guide the emergency vehicles towards it. The technology could also be used to communicate with road management co-ordinators to give up to date information about congestion on the road.

If every vehicle on the road had the ability to communicate with other vehicles, then it is likely that with this extra information, drivers of the future would be able to make more informed decisions on the road, which may be able to reduce the numbers of accidents that occur on the road. Although much work still needs to be done, the work described by Kato et al has shown that cooperative communication between vehicles is an achievable goal.

Perhaps another potential problem is that although providing information to the driver is generally thought to be a good idea, as it can improve overall safety and efficiency of travelling between locations, it must be remembered that the main purpose of the driver is to drive the vehicle. This is not meant to be a facile statement, but as a warning that there is a danger that too much visual and audible information may contribute to the driver losing concentration on viewing the road scene and controlling the vehicle to a high standard.

There have been reports in the print media in the UK over the past few years about high profile advertisements on large roadside billboards which have caused a few drivers to lose momentary concentration and to cause an accident. This phenomenon has also been scientifically researched by some, with Piechulla et al **[96]** being one such research group. Piechulla et al have also researched this in their paper and say it is commonly accepted that driver information overload can compromise driver safety. However, in their paper, they argue that a more intelligent solution to solve the problem of information overload is possible by means of an adaptive man-machine interface that is able to filter information to the driver according to situational requirements. They estimate the workload of the driver by using a software module which is able to predict the mental strain of the driver and can reduce mental workload by postponing or even cancelling what it regards as less important information and messages to the driver. Piechulla et al tested this by doing a field experiment using a mix of young drivers (aged between 21 to 29 years old), 6 male novice drivers (average age of 18.26 years old), and experienced drivers, holding a drivers license for an average length of time of 6.80 years. Each driver drove the experimental route 3 times. The tasks that the drivers had to perform were varied. For example, the drivers were asked to answer the telephone by pressing a button integrated into the steering wheel. The drivers were also set 10 simple mental arithmetic tasks, for example, adding the number 12 to a number in the range of 11 to 93 and saying the number out aloud. For the average person, these are simple to do, but it is thought that they become more challenging tasks when the person is doing another task, such as driving a motor vehicle. The driver's mental effort was measured by taking an electrocardiogram (ECG) and heart rate variability (HRV) of each of the driver. HRV was considered useful as it is known that a decrease in HRV is known to cause an increase in mental effort. The results showed that beginner drivers experienced a higher amount of mental strain than experienced drivers. However, the adaptive man-machine interface module did manage to reduce the mental workload significantly for experienced drivers, and has at lest demonstrated that this technology is available and can be useful for the driver of the future.

Although car manufacturers and researchers are keen to stress that the driver will remain in overall control of their vehicle, there is still some concern at the prospect of some decisions being taken or advised upon by a central command computer. Even if the driver has ultimate control of the vehicle, there is still bound to be a certain amount of doubt as to who is in charge of what function inside the car. This is especially pertinent when it comes to safety systems – the computer responsible for the safety system may make a decision which it feels is in the best interests of the driver, but the driver may feel differently. At one end of the scale, this would be mildly irritating to the driver, at the other end of the scale, this could have dangerous implications.

Who is ultimately in control of the vehicle has also been asked in another article titled 'Drivers Take A Back Seat' which appeared in the 'Professional Engineering magazine on the 14th December 2005 **[97]**. In it, the article explains that according to the 1965 Vienna Convention on Road Traffic, the (human) driver is required to be in overall command of the vehicle, and it is understood that this is still the case today. However, with the advent of the intelligent vehicle and systems, there is a question posed in this article as to who would take responsibility for the road accident, the driver or the driver assistance system?

The article also expresses a concern that although the technology is available, people may not be prepared to purchase the technology as the article reports that in the 10 years that Bosch first introduced the first electronic stability system, 67% of new German vehicles have been fitted with the system, compared with a relatively small 38% in the UK. This confirms that one of the fears that take up of intelligent vehicle systems would not be high is a real one, and needs to be addressed. Ways in which this could be addressed include:

- Advertising to promote the benefits of intelligent vehicles and technologies.

- Including the feature as a standard item, and increase the overall cost of the car accordingly, rather than have it as an optional extra.

- Legislation to require advanced vehicle systems to be included into all new vehicles.

- Offer the incentive of reduced insurance premiums for drivers whose cars have intelligent safety systems fitted in them.

Some of these suggestions are more feasible than others, but the onus ought to be on the vehicle manufacturer to promote these features better and to show how it can aid the driver.

Another potential problem is that having too many safety features may cause drivers to drive carelessly. It has been said before that if cars were designed to be less safe, then drivers would tend to naturally reduce speed and drive with more care and attention. However, when comparing death and injury rates from 30-40 years ago, at a time when cars were not as safe as they are today, there were far more deaths and injuries on the road than there are today. There is no evidence to suggest that drivers in previous years drove slower or more carefully as a result of the relatively high death rate. Therefore, it is thought that improving driver safety features will have a negligible impact upon the driving habits of car drivers, and in overall terms, should reduce the number of people killed and injured on the road.

Researchers and designers alike strive to anticipate and to address future eventualities. However, some of the benefits of the intelligent car program cannot be fully determined at this stage due to the early nature of the program. What can be estimated are the potential benefits which are hoped for, and these are in terms of reduced injury and death on the roads. This is perhaps the most important reason for conducting research into the field of intelligent vehicles, and it is often said that one cannot put an amount on a human life. However, this is exactly what risk analysts and cost estimators have to do. Governments and manufacturers alike have to make such decisions when it comes to implementing safety features, and they have to make a decision based on the number of lives saved for a period of time against the capital and running costs. In recent times, the UK government has delayed the installation of a comprehensive automatic train protection system because it was felt that the high cost of developing and installing such a system could not be justified against the relatively few number of train passengers it would potentially save during the lifetime of service of the system.

Finally, it is unclear what the market is for the intelligent vehicle. Part of the reason for this ambiguity is the fact that some or most of the proposed developments are still at the concept and research stage and are many years from ever being a realized. Therefore, predicting the market for such systems in the future is a risky business. However, an educated guess can be made. Since today's market has shown that car buyers do like to have added functionality installed into their cars, then there will be a large enough demand for the new intelligent vehicle features. As mentioned before in chapter 1, such vehicles will only be realistically attractive for consumers in the US or EU or in other economically and technologically advance countries such as Japan, South Korea, the Middle East. In other consumer markets, it is unlikely that such technologies can be afforded let alone required or desired.

One potential problem that has been discussed before is the lack of enthusiasm on the part of the driver for intelligent vehicle systems. Marchau et al **[98]** present results of a series of questionnaires about whether they were willing to accept some limitations in their driving control imposed by advanced technology, and whether they would be prepared to purchase such systems.

One good reason for having advanced driver assistance inside the vehicle is also given by Marchau et al, who quote another source which says that 90% of all traffic accidents can be attributed to human failure e.g. lack of alertness, fatigue, poor decision making etc. The potential benefits of 'Advanced Driver Assistance Systems' (ADAS) are potentially huge. They have estimated that if there was large scale implementation of collision avoidance systems, there could be a decrease of up to 45% in road fatalities. 'Intelligent Speed Adaptation' (ISA) could reduce injury accidents by 40% and reduce fatal accidents by 59%, which are clearly significant improvements in road safety. However, whilst these statistics are impressive, yet the problem remains of how to convince drivers to install these systems inside their vehicles, as the results given by Marchau et al in their questionnaire illustrates. Only 40% of correspondents think that speed enforcement on motorways is important, and the majority would not accept an ISA system which could not be overruled in their vehicle on a motorway, preferring instead an advisory or warning system. This shows the reluctance, still, of drivers to accept an intelligent driver aid inside their vehicle. However, 80% of correspondents would be prepared for a system which could act autonomously (i.e. make its own decisions) in exceptional weather conditions, such as when there is heavy fog or snowfall.

The work done by Garvil et al **[99]** also highlights the difficulties that intelligent automotive devices have in being installed into the vehicle. They report that of the 13,400 car owners who were contacted in their study, only 38% of them were prepared to let the 'Electronic Speed Checker' (ESC) be fitted into their car. Again, drivers had vastly different opinions on 'warning' systems and 'controlling' systems. Drivers who were speeding were more positive to the warning speed checking system. However, they did not approve (generally) of the ISA system which could intervene and control the speed of the vehicle. This study reinforces Marchau et al and confirms the problems that the intelligent vehicle will probably face.

The crucial question is whether people would buy such a system. The results show that drivers would definitely not purchase a system if it cost more than 150 Euros, and only 30% would buy a system which had the ability to make decisions independently of the driver in a non-overrule able way. This proves the difficulty that intelligent systems will have in the future of getting into the market and be used by a significant proportion of the diving public.

3.8 Summary of Chapter 3

In conclusion, the necessity of having an intelligent airbag system has been explained, and the type of sensor to be used for such a system has been justified.

Also discussed were the developments being researched and planned in the field of the 'intelligent vehicle', and this provides evidence that should the work in this project be successful, there is a probability that car manufacturers would be interested in using this work in the future.

Potential issues have been discussed such as the importance of an intelligent airbag system, the importance of vehicle safety systems in general, what other developments are being done in the field of the intelligent vehicle, and what other possible issues may arise in the near future.

As with all the systems being created for the intelligent vehicle, the way in which these systems are tested are by using members of the general driving public to test the systems in a mock up of the real vehicle. The volunteers would then be asked to use the said devices/systems and to use it whilst 'driving' the vehicle on the simulator. At the end of the test, they would then be asked to rate the system in terms of effectiveness, ease of use, in order for the system developer to see how well it is performing, and if necessary, to make some modifications to it. This principle was the basis for the experimentation which was conducted for this research project, and this is described in greater detail in the next chapter.

Chapter 4 Experimental Work

In the previous chapter, the concept of the 'intelligent vehicle and how the 'intelligent deployment of occupant restraints' concept fitted into this scheme. This chapter will focus on the experimental work which was done in order to progress the development of a smart airbag system. It is also important for there to be a realisation of the limitations of what experimental work can achieve, and this will be made clearer later in the chapter.

4.1 Preliminary Work

Initial testing using the IRISYS thermal imager was done to enable one to be familiar with the use and operation of the equipment. The preliminary work was also useful to do because it enabled one to examine the limits of the thermal imager's performance when imaging people, and would answer such questions such as whether the thermal imager could detect humans, what the range of detection was, what level of detail could be detected and so forth.

The thermal imager acquired from IRISYS Ltd is a pyroelectric, uncooled thermal imaging device. The lens has a field of view of 20°, and the imager has a temperature range of between -20°C to 90°C. It is able to capture images of 16 x 16 pixels resolution, but the software supplied by IRISYS Ltd is able to modify this to 32 x 32 pixels, 64 x64 pixels and finally up to 128 x 128 pixels resolution. This improved resolution was made possible by interpolation methods, and did not actually add any extra information; it merely was a tool designed to aid the visual perception of the user. Its maximum frame rate is 6 Hz.

The internal components of the imager are housed in a die cast aluminium box of dimensions 100 mm x 100 mm x 60 mm, which weighs approximately 1.3 kg.

For the preliminary work, the imager was mounted onto a tripod as shown in figure 4-1. This was placed approximately 140 cm away from the surface of the driver's face, facing directly towards the driver.

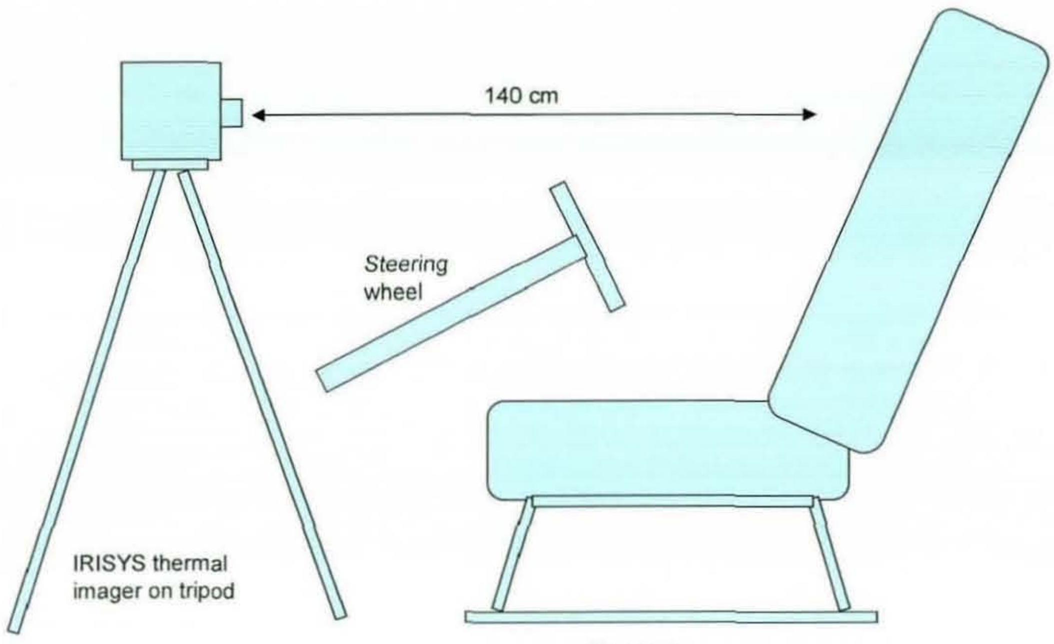

Figure 4-1: Diagram showing set up of preliminary testing.

Figure 4-2: Test rig used for preliminary work

Figure 4-3: Volunteer inside test rig.

The test rig in question was constructed to mimic a basic car cabin of a typical car. Some of the components such as the steering wheel mechanism and driver and passenger seats were taken from a real car and mounted onto the test rig. The steering wheel could be tilted up and down to suit any particular driving style and the seat was mounted on a moveable platform which was able to raise the seat up and down, and also move the seat backwards and forwards. The entire structure of the test rig was also able to be lifted, and all these options enabled drivers of differing sizes and body shape to enter the test rig comfortably.

The volunteers were selected at random and asked to perform some basic driving manoeuvres and tasks that one would expect a driver to do inside a car. These included performing a series of left and right turns, operating the gear shift lever, and looking to the left and right side and up and down. These movements were to simulate the actions that the driver is supposed to perform whilst in control of the car.

The data was then transferred via the RS232 link to a PC for storage purposes so that it could be extracted later. This initial work was done for a variety of reasons:

1. To check the resolution of the images.
2. To determine whether the driver could be distinguished from the background.
3. To check how fast the refresh rate was i.e. how long did the image on the screen take to match the real time movement of the driver?
4. To see if other objects could be detected apart from the driver such as cell phones, cigarettes etc.
5. To determine what other details could be detected.

From visual inspection of the results, it was clear that the thermal imager was capable of not only identifying the presence of the driver, but also detecting his body and facial movements and identifying other extraneous features, for example, the presence of a lighted cigarette or whether the driver was in possession of a hot and cold drink, or whether the driver was wearing spectacles.

The thermal imager was also capable of showing the differences between an adult seated in the car driver seat, and a small child and a household pet such as a dog. It was also apparent that the thermal imager could show the driver looking either to the left or right side as he would be expected to do if he was at a T-junction.

It was hoped at the beginning of the project that the thermal imager could also detect the gender of the driver and also identify exactly each driver from the image. From the male and female volunteers that sat in the test rig for the initial testing, there were slight differences between their head profiles. For example, the head profile of an adult male was on the whole larger and more square shaped, whilst the head profile of the female driver is smaller in size and also much rounder, almost oval in shape. However, with regards to identifying the specific driver exactly, this would appear from the initial results to be unattainable. The resolution of the thermal imager is only 16 x 16 pixels per frame and can be resolved greater to 256 x 256 pixels using interpolation. Even at the maximum resolution possible, the driver appears at best to be an orange/yellow shape in the middle of a dark background. There are almost no identifiable facial features such as the nose or eyes or mouth. It is only when the driver is wearing spectacles or when the diver opens his mouth that these features can be identified. Therefore detecting a specific driver inside the car driver seat would seem to be perhaps unrealistic judging by the limitations of the equipment.

Figure 4-4 to figure 4-15 illustrate clearly just how low the resolution of the thermal imager is:

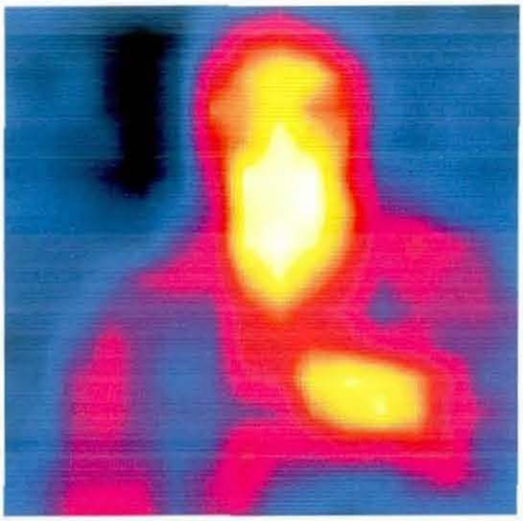

Figure 4-4 Large male adult

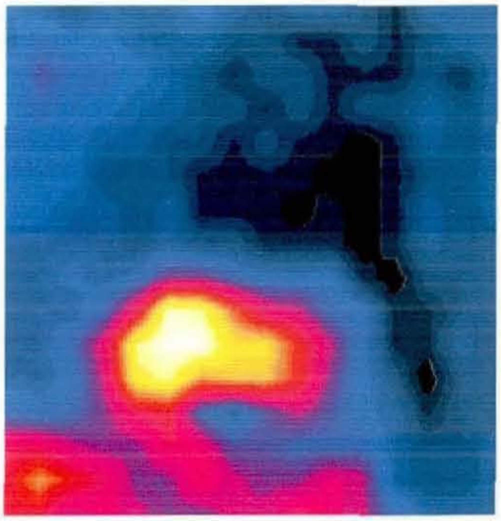

Figure 4-5: Child in infant seat

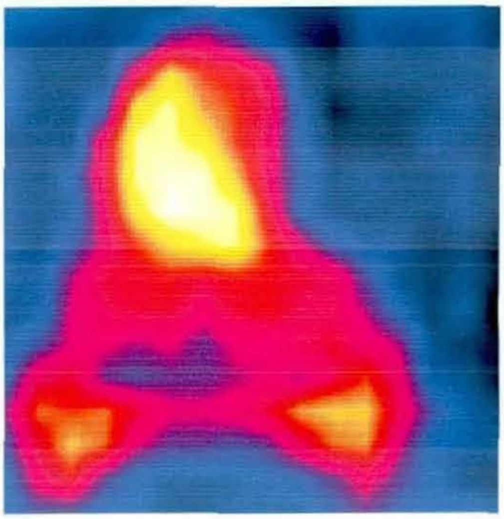

Figure 4-6: Driver looking right

Figure 4-7: Driver looking straight

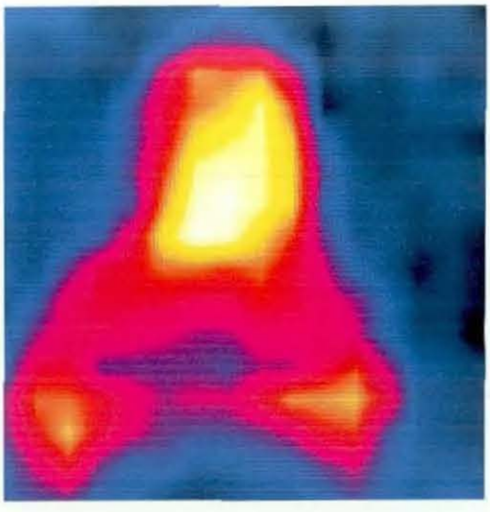

Figure 4-8: Driver looking left

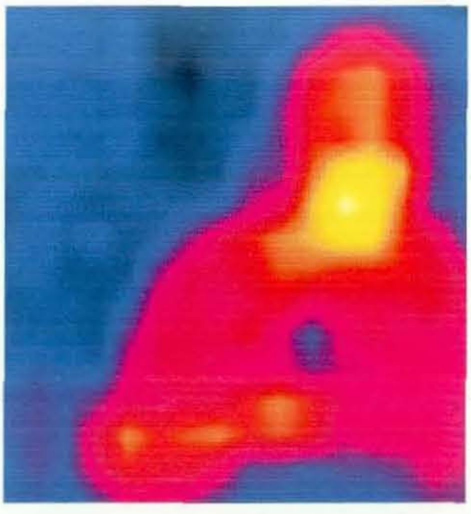

Figure 4-9: Driver holding cold drink

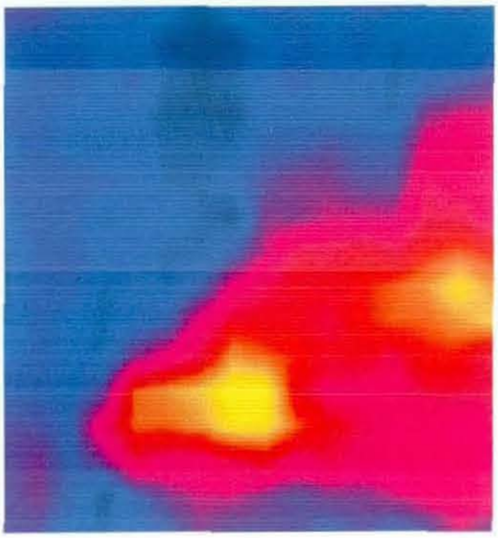

Figure 4-10: Driver leaning left

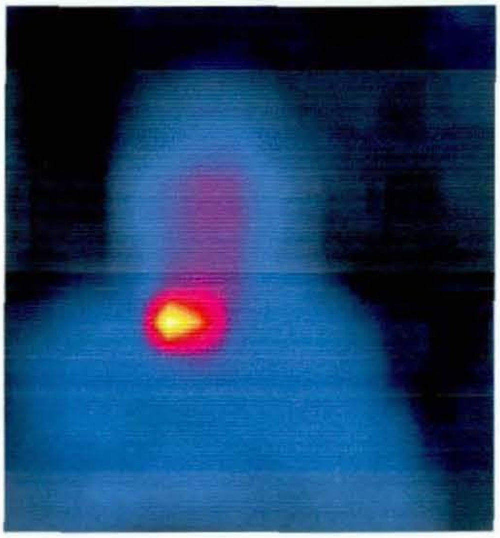

Figure 4-11: Driver smoking

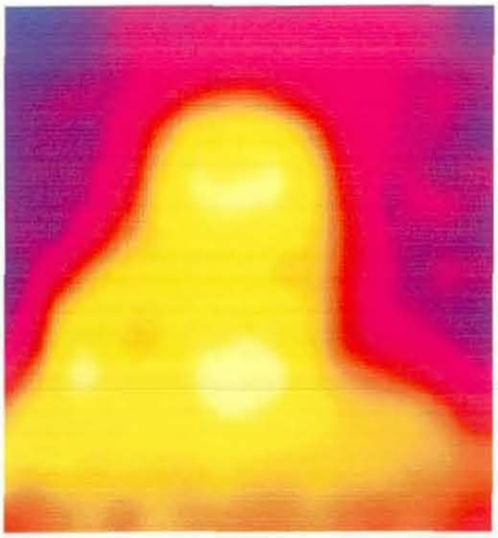

Figure 4-12: Driver using mobile phone

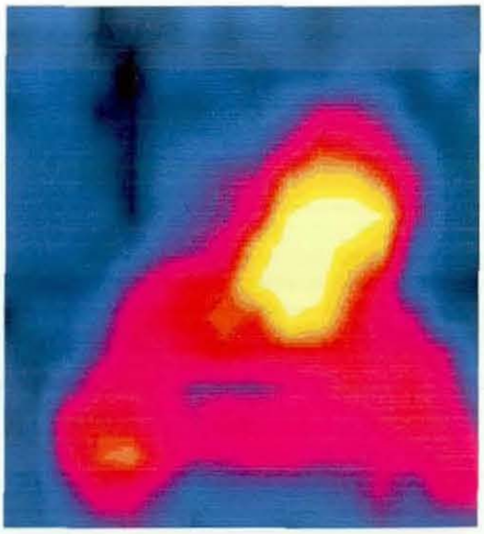

Figure 4-13: Simulated drowsy driver

Figure 4-14: Short driver

Figure 4-15: Medium driver/spectacles

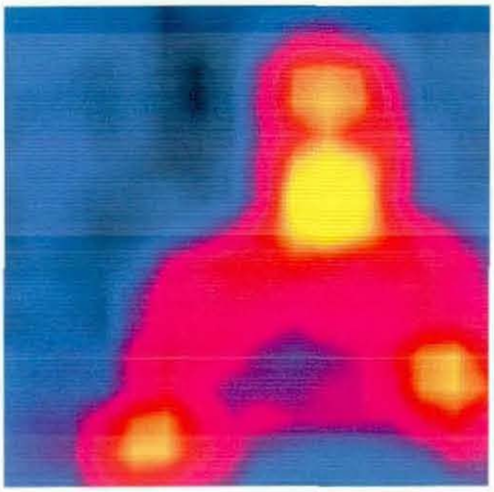

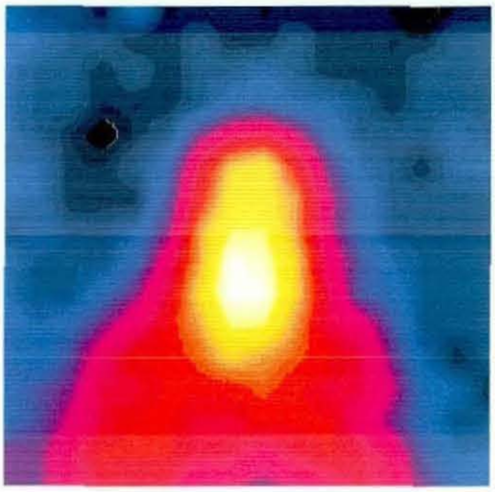

Figure 4-16: Tall driver with spectacles *Figure 4-17: Female driver*

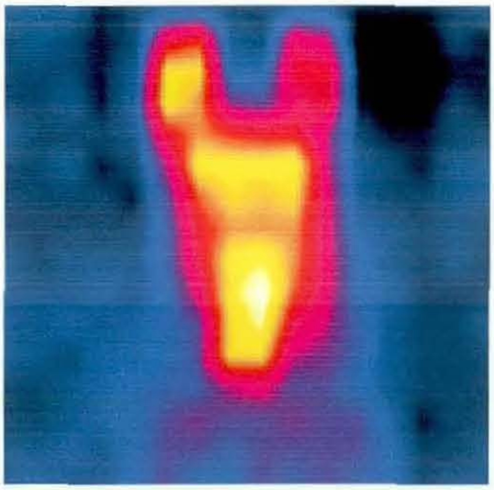

Figure 4-18: Alsatian dog

The images above were all captured using the thermal imager mounted onto a tripod and facing the driver volunteers inside the test rig. Using standard norms of visual perception, the hot areas where there is greater thermal radiation emission are represented by the 'warm' colours such as red, yellow and orange. The cooler areas of the image are represented by the 'cooler' colours such as black and blue, and the use of these two distinct sets of colours enabled the important regions of the image to be clearly defined such as the head and body of the driver volunteer from the background.

Figure 4-4 is of a tall male driver with spectacles. What is striking is that the thermal imager can clearly detect the face, the torso and even one hand on the steering wheel, whilst there is very little background information, which is useful as it is known that the less number of pixels in an image, the less amount of time it takes to process the image. Notice also how the face is elongated, and that the spectacles can be seen.

Figure 4-5 is the image of a 2 year old infant as he sits in a child safety seat. It would appear that the thermal imager is able to distinguish between a child and an adult. The child's head has a much rounder profile, when compared with that of the adult in figure 4-4.

Figures 4-6, 4-7, and 4-8 are images of the driver behaving as he should do at a junction. Figure 4-6 shows him looking to his right, figure 4-7 is him looking straight ahead, and figure 4-8 is the driver looking to his left. There is a clear difference in the shape of the head as he moves his head to either side. The image of the face is angled towards the direction he is looking in. In terms of driver monitoring, it is important to know whether the driver is performing correctly i.e. looking towards both sides at a junction, for example.

Figures 4-9, 4-10, 4-11 and 4-12 show a selection of typical in - car driver activities. Figure 4-9 shows him holding a cold drink, with the cold drink showing up as a blue area against the rest of his body in the centre. Figure 4-10 shows the driver leaning to his left, operating the radio or searching through the glove compartment. The driver is smoking a cigarette in figure 4-11, clearly seen by the very light area just below his chin. Notice that because the cigarette is so much hotter than the rest of the body, the image of the driver pales into the background. Figure 4-12 is the thermal image of the driver holding a mobile phone to his right ear. The image of the driver and the phone is very bright – perhaps the result of the radiation emitted by the phone, although this would need to be tested fully.

It is clear that the driver in figure 4-13 is not attentive, or that something is wrong with him. His head is angled down to one side and his shoulders are slumped from its normal position. This driver was mimicking the effects of drowsiness, however, some may argue that the driver in this image may have been simply leaning down to reach something, and so more work needs to be done in a controlled environment to study the body movements of a sleepy driver and to differentiate this from other situations or movements.

Figures 4-14 to 4-16 show a selection of different drivers. Figure 4-14 shows a short driver without spectacles, figure 4-15 is of a medium build driver with small spectacles, and figure 4-16 is a tall driver with large spectacles. The imager can detect the spectacles and also show slight differences in height. A woman driver is shown in figure 4-17. Notice that the profile of her face is more oval than those of the men, and women are generally shorter than men, as can be seen if one were to contrast figures 4-16 and 4-17. To be able to distinguish between a male and female would be useful for an intelligent restraint system, as women are more likely to get injured by the airbag and so the restraint strategies should be different.

It is obvious that the occupant in figure 4-18 is not human. The upside down triangular face and large ears at the top are those of a large Alsatian dog in the passenger seat. This is useful because airbags can be activated unnecessarily by a small impact from another motorist, and the driver may not want to spend US$2000 on replacing the airbag, which has fired to protect his pet.

4.2 ITAI Crash Test Event

Some of the findings that resulted from the initial experiments were shared with the transport division of the Ergonomics and Safety Research Institute (ESRI), who are working in a similar field. They were impressed with the clarity of the image data that the thermal imager could provide, and communication with a member of ESRI (Mr James Lenard) was particularly productive. The response from him was extremely encouraging, considering that he was also involved with determining European Union road safety standards. It was from this contact that an opportunity arose to participate in a car crash test meeting, which was arranged at the Darley Moor race track. A group of researchers from the Mechatronics Centre was invited to attend and to set up the thermal imaging equipment in one of the moving impact cars. Although the thermal imager worked well in the test rig, doubts were raised concerning the 'survivability' of the thermal imager and the associated equipment (laptop computers) in the event of a real – world impact.

One day before the event was due to start; the equipment was installed into the car. Due to safety concerns about placing a heavy object in the forward space of the driver, it was agreed that one imager could be set in the front passenger side foot-well. This imager was tilted at an angle and bolted into place so that it would capture the driver's head and torso at an angle. A second imager was attached to the left back - seat pillar, facing diagonally across to the left side of the driver's head and front space to the dashboard. This was a good view considering that it would capture the driver's torso and head movements and also capture the firing of the airbag. The car hit a stationary car at 45 mph with the stationary car offset at an angle of 45^{o} to the direction of the moving car, and this is best shown in figure 4-19:

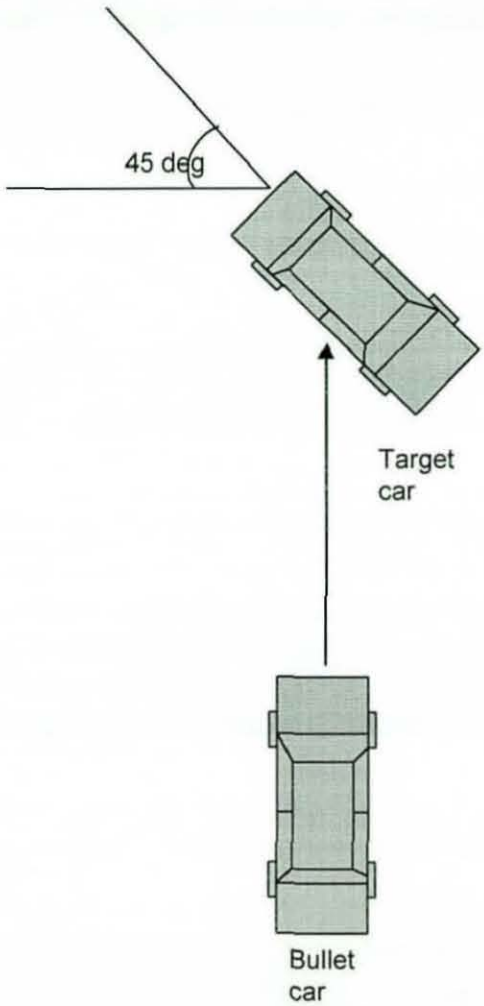

Figure 4-19: Diagram of locations of bullet car and target car.

The thermal imager and the rest of the equipment survived the impact and streaming data was captured of the events inside the passenger compartment. Figure 4-20 is a thermal image of the driver from the thermal imager located at the rear:

Figure 4-20: Thermal and visible image of Rusty Haight inside car cabin.

The ITAI crash test event and the preliminary work presented the author with the opportunity to be able to capture moving images of the driver inside the car. This was useful in the sense that this illustrated how exactly the driver would behave in a real life crash test situation. These short video films are presented on a compact disc for viewing on a personal computer using 'realplayer' software, which is freely available to be installed by the reader.

In the file 'Darley Dale/BBC-MiniCam-5B' on the compact disc, the crash test driver Rusty Haight is seen inside the car as he prepares to drive the 'bullet car' into the 'target car'. The impact is over in a split second, and both the driver and front passenger airbag inflate. The file 'Darley Dale/Crash 5' shows an external view of this crash. The video camera for this film was located on the side of the road, approximately 150 metres away. From this video, it can be seen that the crumple zones of the two cars work very well, they deform by absorbing most of the crash energy, and the cars are left a very short distance away from each other. This is an inelastic collision, whereas in an elastic collision, the cars would have collided and sprung apart with more or less the same force and be much further apart from each other.

Accident investigators and researchers from across the UK were present at this ITAI event, and it was deemed important enough that a popular and long running BBC television show called 'Tomorrow's World' attended the proceedings, interviewed the main protagonists, and set up their own equipment in one of the 'bullet cars'. File 'Darley Dale/tworld 29 May 2k2' is a video clip of the feature that aired on U.K terrestrial television on the 29th May, 2002. Also in the folder 'Darley_Dale' are two AVI files which show the moving thermal images of the actual crash, from inside the car. The file 'Infrared_camera_back' shows the test driver Rusty Haight in the bullet car, driving into and hitting the target car. There is some distortion in the image; however, the thermal imager is able to detect the action of the airbag deployment at the end of the AVI film. This sequence was filmed by another thermal imager in a different location (in the front seat passenger foot well) and is shown in the file named 'infrared_camera_front'. This AVI film also shows Rusty Haight driving towards the target car, and again there is a lot of 'noise' in the image. The driver's left arm can be seen moving and operating the steering wheel, and at the end, the airbag deployment is clearly seen. These AVI films demonstrate that firstly, the thermal imager is able to withstand the impact of a typical car accident, and secondly, it can distinguish the car driver from other objects inside the car cabin.

The AVI files in the 'Vehicle Safety' folder are taken from the NHTSA website. The file 'Vehicle Safety/crash bag' shows a crash test dummy in a saloon car which hits a wall, and shows the driver airbag inflating. Notice how large these U.S airbags are when compared with European sized airbags. The U.S airbags are larger because they are more important in the restraint strategy for the driver because U.S drivers are more reluctant to wear a seatbelt compared with European drivers. The file 'Vehicle Safety/Crash both' contains a video clip showing two crashes, one where there is an airbag, and one without an airbag. This is interesting as it allows the viewer to compare how well each driver fares after the impact. It is clear from this just how effective the airbag is in restraining the driver's natural forward momentum towards the steering wheel. The file 'Vehicle Safety/crash dummy' shows a saloon crashing into a wall, and no airbag deploys. From this video clip, it is quite clear just how extreme the damage would be caused to the driver's head in the event of an accident. The force involved is so powerful that the driver's body deforms the steering wheel and assembly, and would have definitely caused the driver severe injury, with possibly fatal consequences.

In the folder 'Preliminary work', there are some short duration thermal imaging 'movies' for the viewer to examine. The file 'Dog_animated2' shows the action of the Alsatian in the car seat of the test rig. This was done to check whether the thermal imager was able to detect difference between human and non-human facial characteristics, and this was clearly evident here. The file 'Woman1_animated' shows a medium sized female 'driving' in the test rig. It is interesting to compare this with the files 'Car3_anim' and 'Car 4_anim' where a male adult is driving in the test rig. The viewer will notice that there is a slight difference in that the female adult's head and face is more oval shaped, and smaller than that of the male adult. Other things that the viewer will notice in the latter two files, are that the male adult in question picks up a cold drink and proceeds to drink it. This is clearly shown by the blue object set against the warm red background of the male adult's body. In 'Car4_anim', the male adult exits the car seat towards the end, and it can clearly be seen that the car seat has been warmed by the driver's body, although this cannot be mistaken for the actual human driver as the temperature in this region is lower and the shape of the warm region is much different. There are also still images in the folder named 'Images' available for viewing. These are images of the ITAI car crash event, and also pictures from the preliminary work that was done.

To summarise, the information gained from the crash testing which took place at the ITAI event was useful in a number of ways. The images showed how quickly the airbag deployed, the temperature of the airbag once it had deployed. From this, it was then possible to appreciate how and why the airbag injuries described in chapter 2 could occur. Perhaps of even greater significance, the images obtained from the crash test showed that the equipment could withstand the crash impact and remain operational during this time.

4.3 Experiment Using Talley Pressure Monitor for Occupant Seating Position Measurement

It was felt that a different type of sensor system was needed in order to corroborate the data obtained from the thermal imager. Since the thermal imager was a non-contact sensor system, a direct contact sensor system would be a good alternative and would make a good comparison.. There was a slight concern that to rely on one, as yet unproven, sensor system for such a safety critical system would provide misleading results. This is why a seat pressure monitoring system was used, as it was a tried and tested commercially available product, and had a proven track record of being used by other research organisations such as the Ergonomics and Safety Research Institute (ESRI). The Talley Pressure Monitor (TPM) consists of a thin flexible pressure pad which could be fitted on top of the seat base, or seat back. The flexible mat is rectangular in shape, and fixed onto it were flexible rubber inflatable cells, circular in shape. They were placed in groups of 3 rows across, and 4 columns, giving 12 cells in total per matrix. In all, there were 8 matrices, giving a grand total of 96 pressure cells in total as shown in the figure 4-21.

These cells were able to inflate because each matrix was connected via a flexible hose to an electronic control unit. This control unit pumped air through the eight hoses and inflated the pressure cells.

matrix 4	1	2	3	10	11	12	matrix 5
	6	5	4	9	8	7	
	7	8	9	4	5	6	
	12	11	10	3	2	1	
matrix 3	1	2	3	10	11	12	matrix 6
	6	5	4	9	8	7	
	7	8	9	4	5	6	
	12	11	10	3	2	1	
matrix 2	1	2	3	10	11	12	matrix 7
	6	5	4	9	8	7	
	7	8	9	4	5	6	
	12	11	10	3	2	1	
matrix 1	1	2	3	10	11	12	matrix 8
	6	5	4	9	8	7	
	7	8	9	4	5	6	
	12	11	10	3	2	1	

Fig 4-21: Diagram of TPM pressure pad

4.4 Operation of the Talley Pressure Monitor (TPM)

The procedure to operate the TPM is described below:

- Press start to allow the cells to inflate. Once the pressures of the cells have been scanned by the internal computer housed within the control unit, a hard copy print out of the results was automatically produced. This data was used as the control data.

- When measuring the seat pressure profile of each volunteer, they were asked to remove any items from their back pockets, as this may have created an artificially high pressure concentration on a particular pressure cell when sitting on the pressure pad.

- The volunteer was asked to sit in a particular seating position and remain motionless until the TPM had completed its scan of the pressure profile. There were 3 different seating positions for the volunteer to sit in, and were as follows:

1. Volunteer sitting back, in their normal driving position, with back leaning gently along the backrest.

2. Volunteer sitting halfway between the steering wheel and the backrest of the seat.

3. Volunteer leaning forward with their head touching the centre panel of the steering wheel.

The thinking behind these seating positions was to investigate whether a seat pressure instrument could be used to detect the occupant's position on the seat, and in turn, get an estimate of the driver's position inside within the car cabin space.

The literature review in chapter 2 has already explained how similar technology has been used by certain automobile manufacturers to measure the body weight of the occupant. Using this information, they are able to make crude but informative classifications about the occupant sitting in the seat, for example whether the occupant is a child or an adult. Within this project was an attempt at using the TPM more creatively by using it to seek other information about the seated occupant, namely the detection of certain driver positions, as described above. If this was possible, then this would be useful in providing a second method of detecting the position of the occupant, thus ensuring greater reliability of the system.

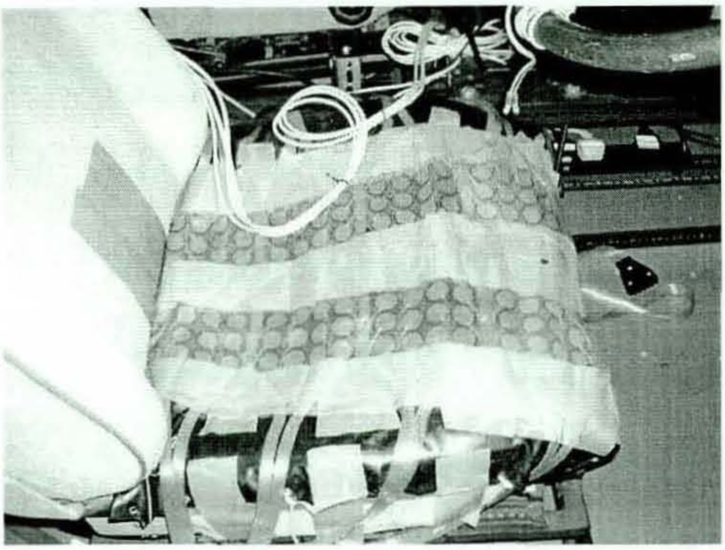

Fig 4-22: Picture of pressure pad on car seat

Fig 4-23: TPM control unit

The results were printed out in hard copy format and the data was input into a Microsoft Excel worksheet. This proved to be easier to work with and the data could be accessed and manipulated more easily. The pressure readings from the control experiment were subtracted from each of the pressure profile readings from each of the volunteers, as this would give the pressure exerted by the person onto the pressure pad.

4.5 Talley Pressure Monitor Results

The pressure readings from the TPM are presented below in a graphical format and show the comparison between the three distinct seating positions that the driver volunteers were asked to position themselves in.

The graphs show the mean average pressure reading from the back of the pressure pad, which is situated near the backrest of the driver's car seat, to the front of the pressure pad, which is located at the front of the seat, nearest to the steering wheel, and below is a diagram which shows the layout of the pressure cells within the pressure pad.

As can be seen from the figure 4-21, the pressure pad is 16 pressure cells long by 6 cells wide, and this was designed to cover the main inset base of the seat where the vehicular occupant would normally position themselves into. Although figure 4-21 does not show this, the pressure cells were slightly set apart at the front of the seat so that a V shape was produced, and this was done so that the pressure pad mirrored the shape of the legs of the human body when seated where the legs tend to position themselves outward diagonally from the waist.

Figure 4-24 to figure 4-38 show the pressure distribution for each volunteer whilst sitting in each of the three different seating positions.

Figure 4-24: TPM Results for Volunteer No.1

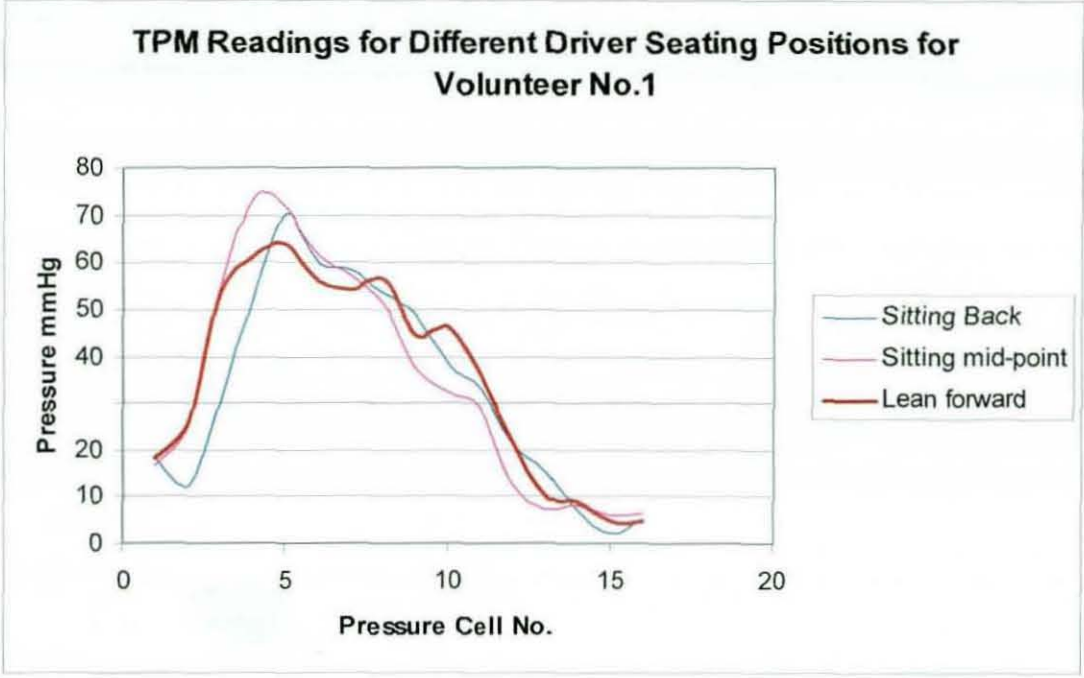

Figure 4-25: TPM Results for Volunteer No.2

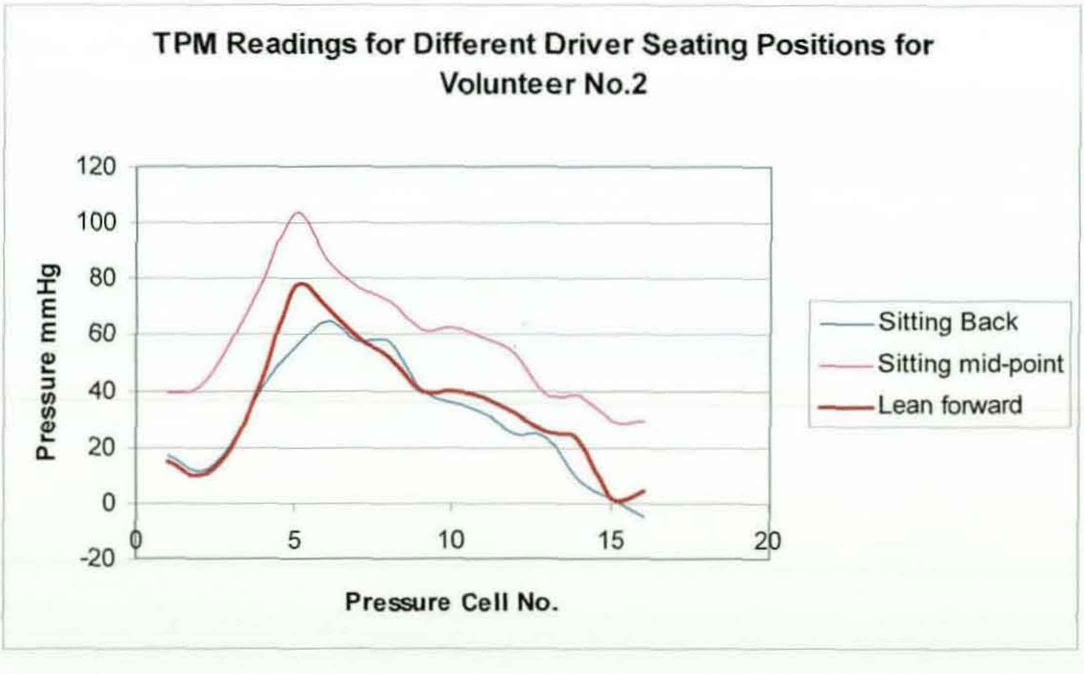

Figure 4-26: TPM Results for Volunteer No.3

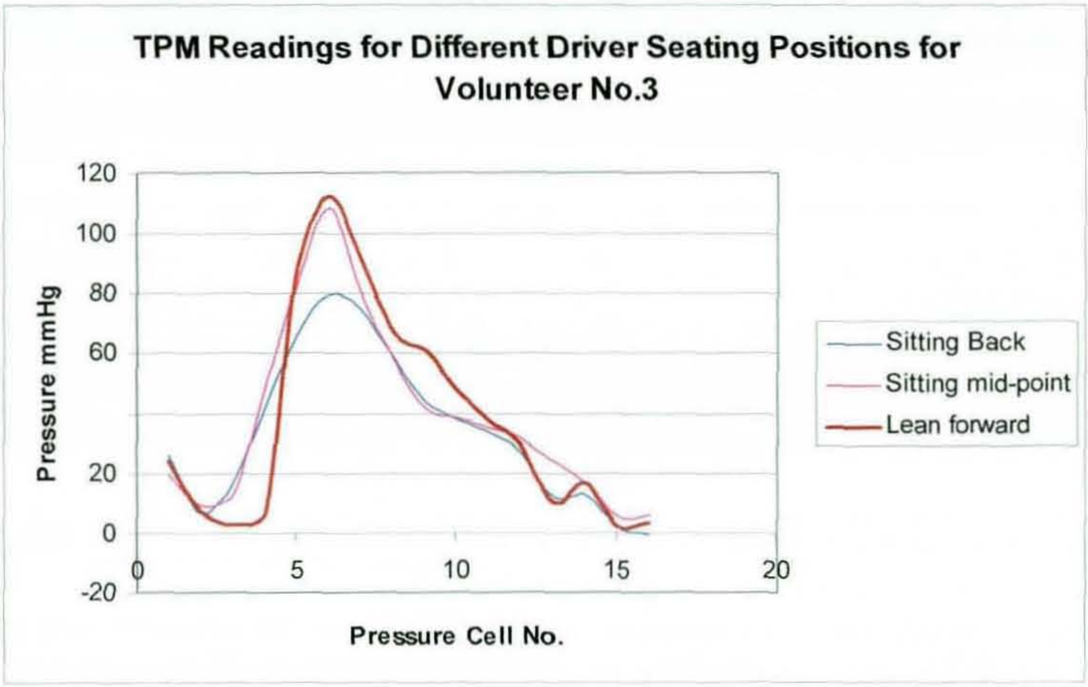

Figure 4-27: TPM Results for Volunteer No.4

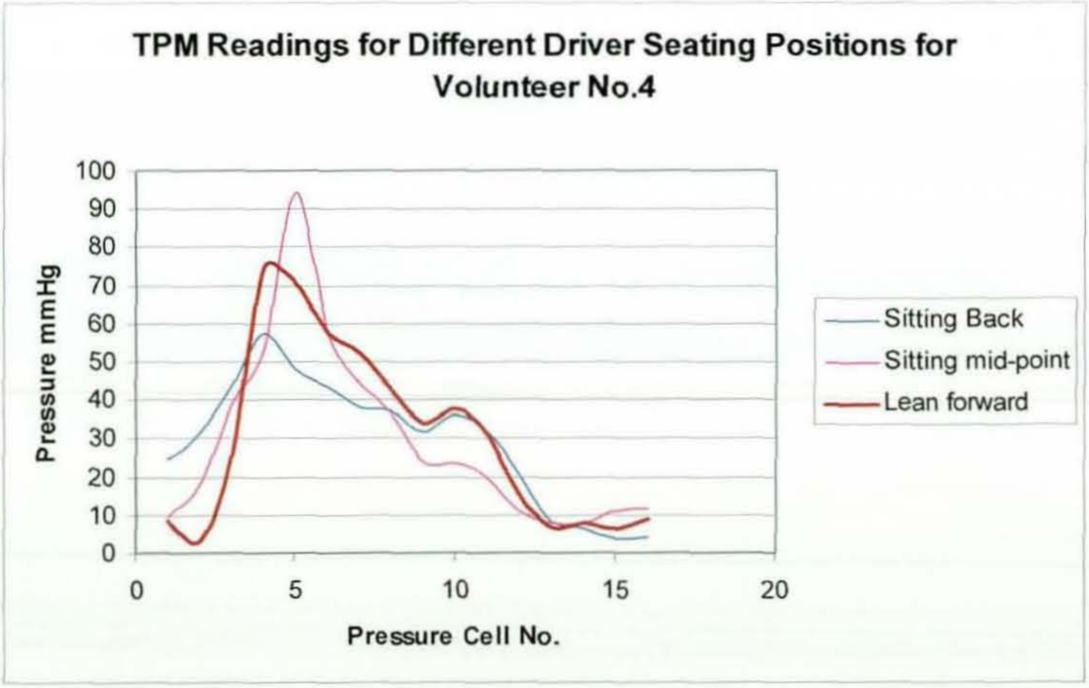

Figure 4-28: TPM Results for Volunteer No.5

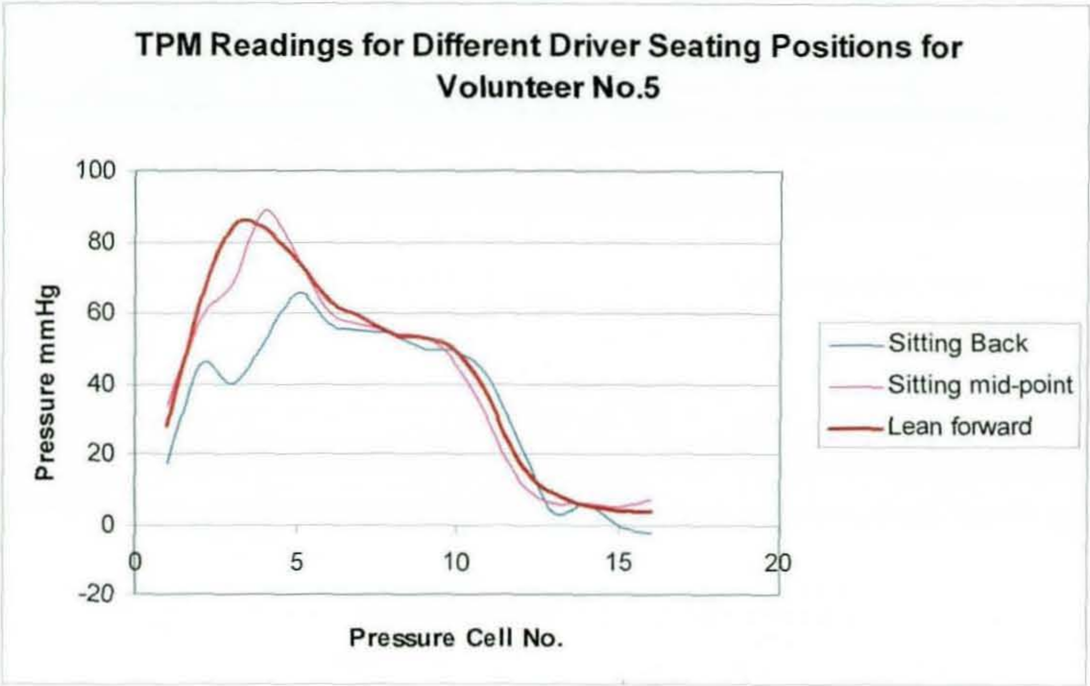

Figure 4-29: TPM Results for Volunteer No.6

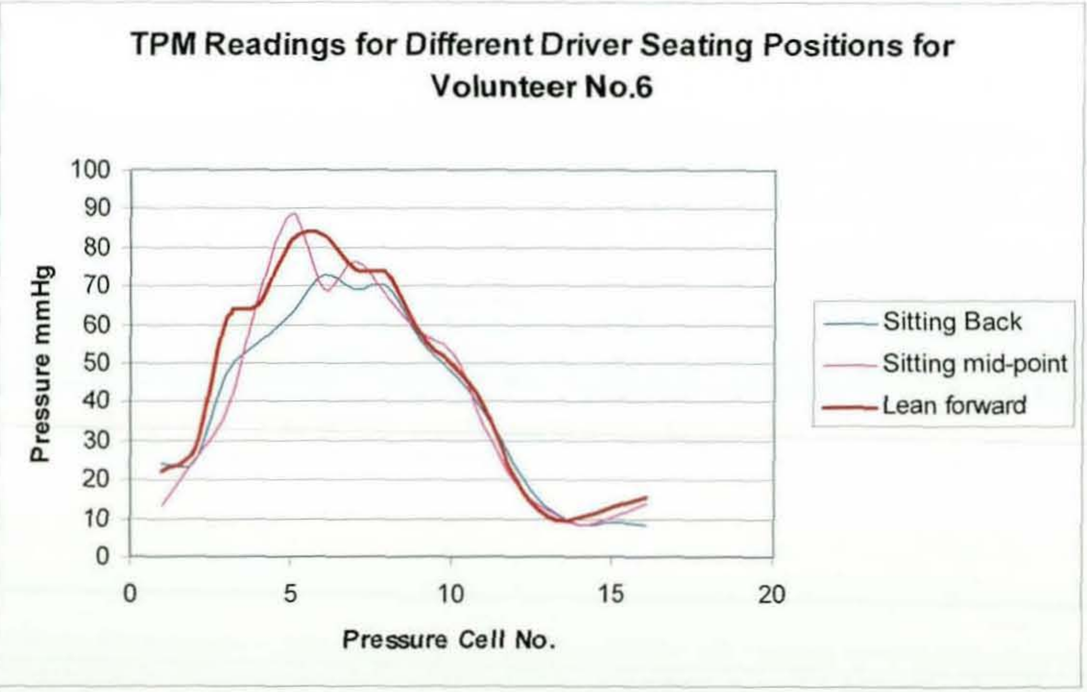

Figure 4-30: TPM Results for Volunteer No.7

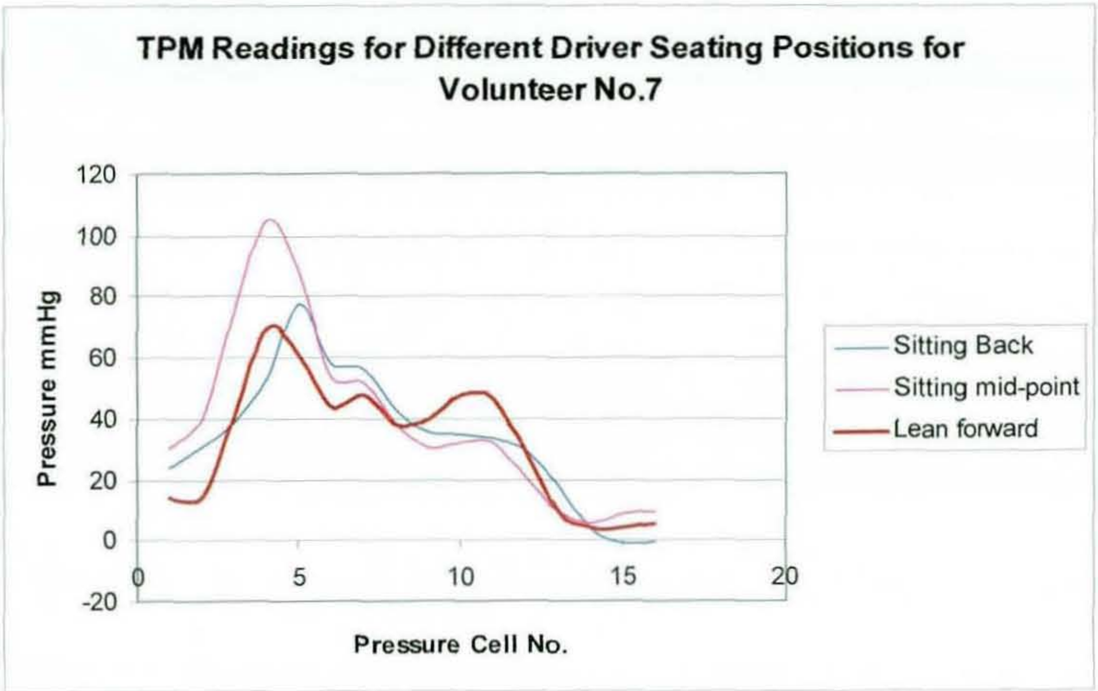

Figure 4-31: TPM Results for Volunteer No.8

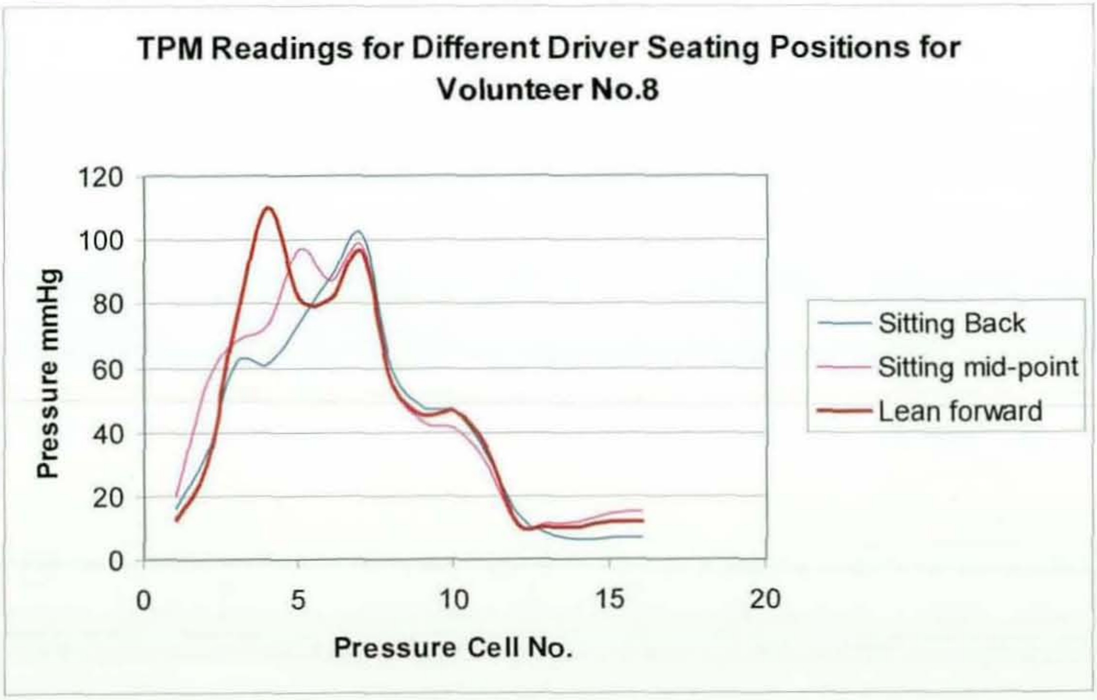

Figure 4-32: TPM Results for Volunteer No.9

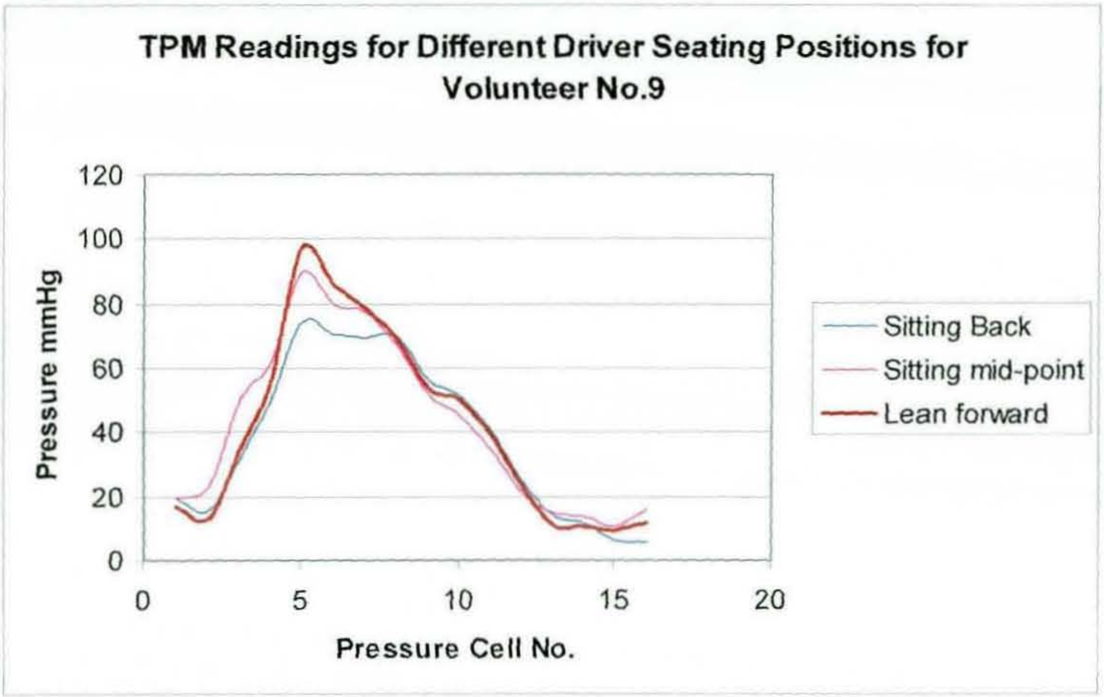

Figure 4-33: TPM Results for Volunteer No.10

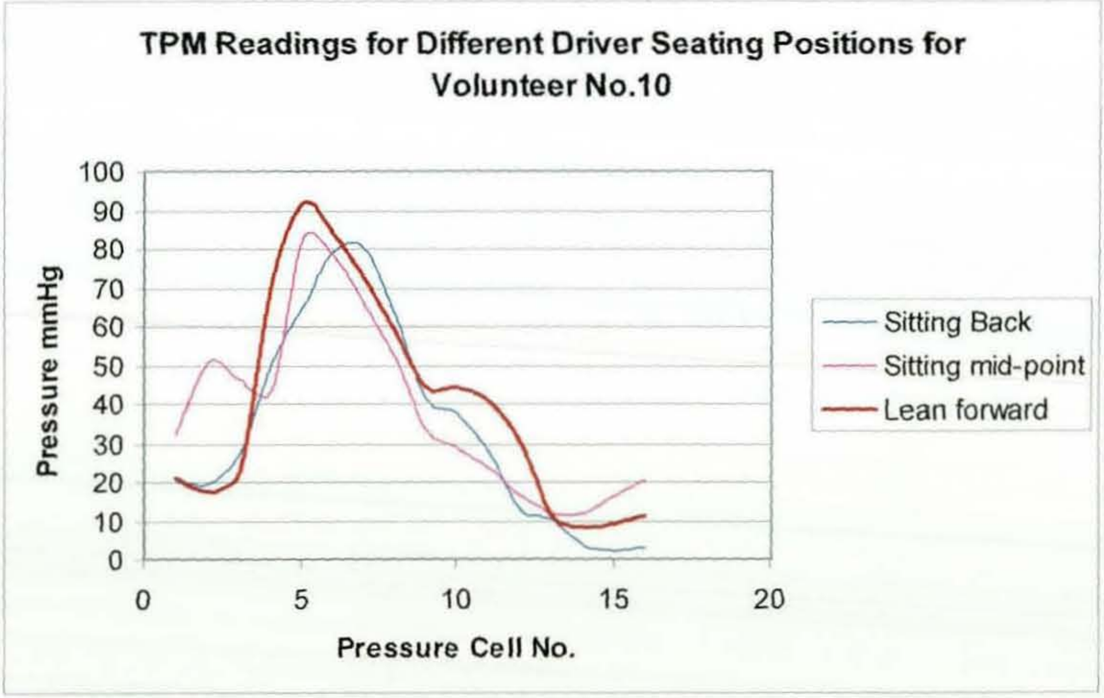

Figure 4-34: TPM Results for Volunteer No.11

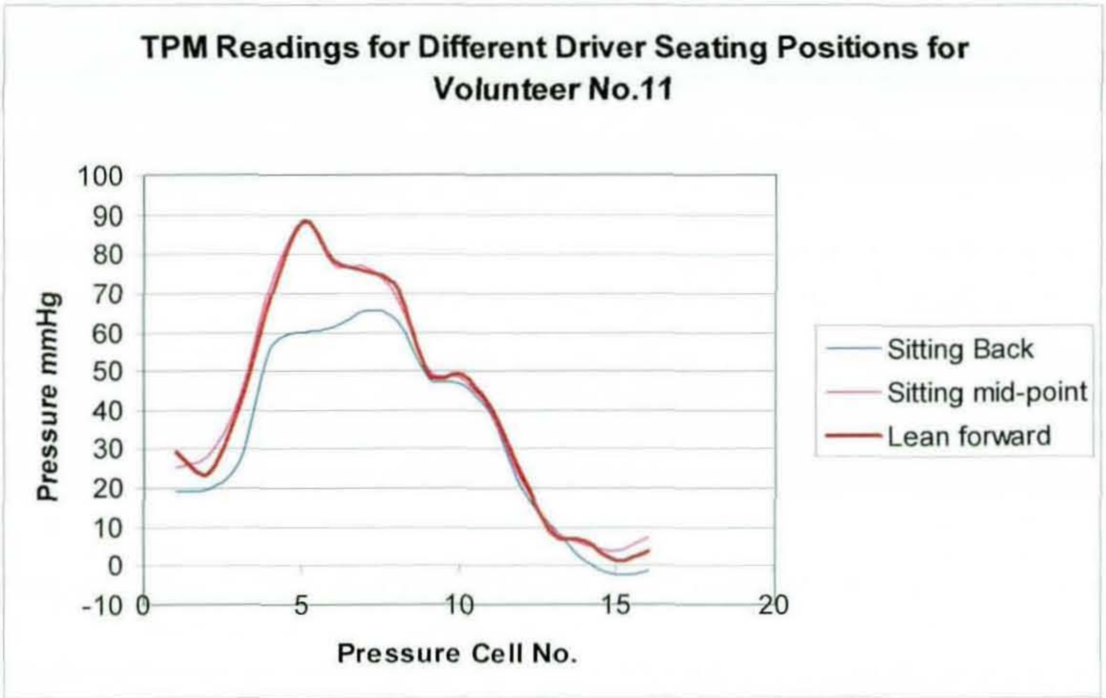

Figure 4-35: TPM Results for Volunteer No.12

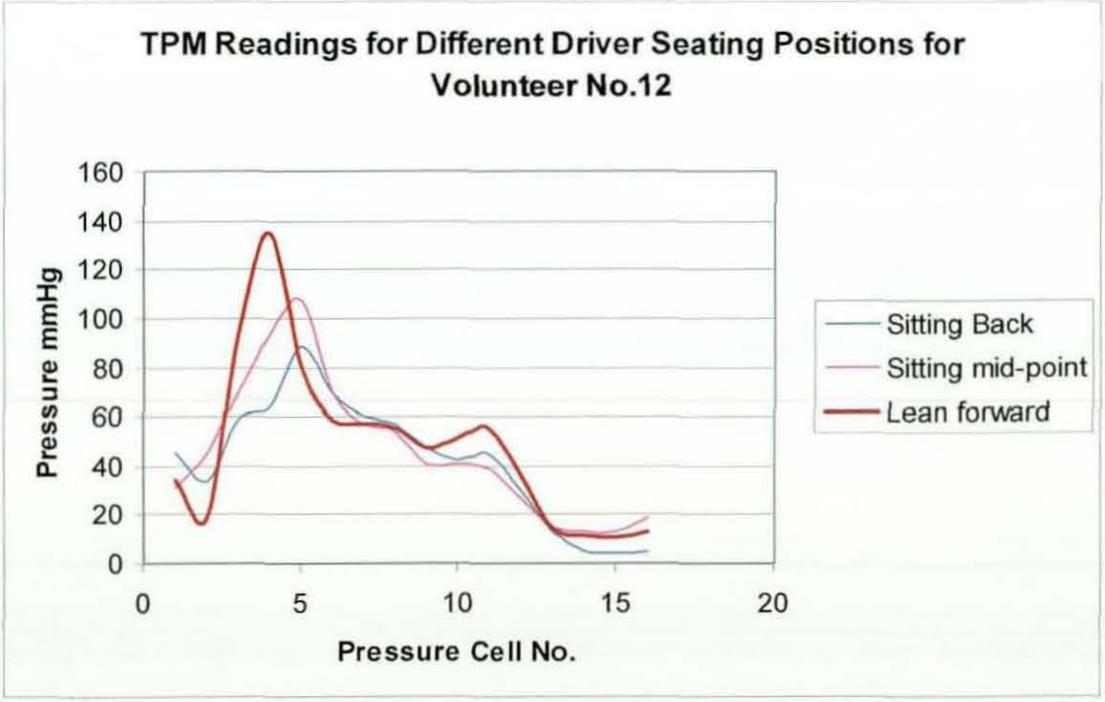

Figure 4-36: TPM Results for Volunteer No.13

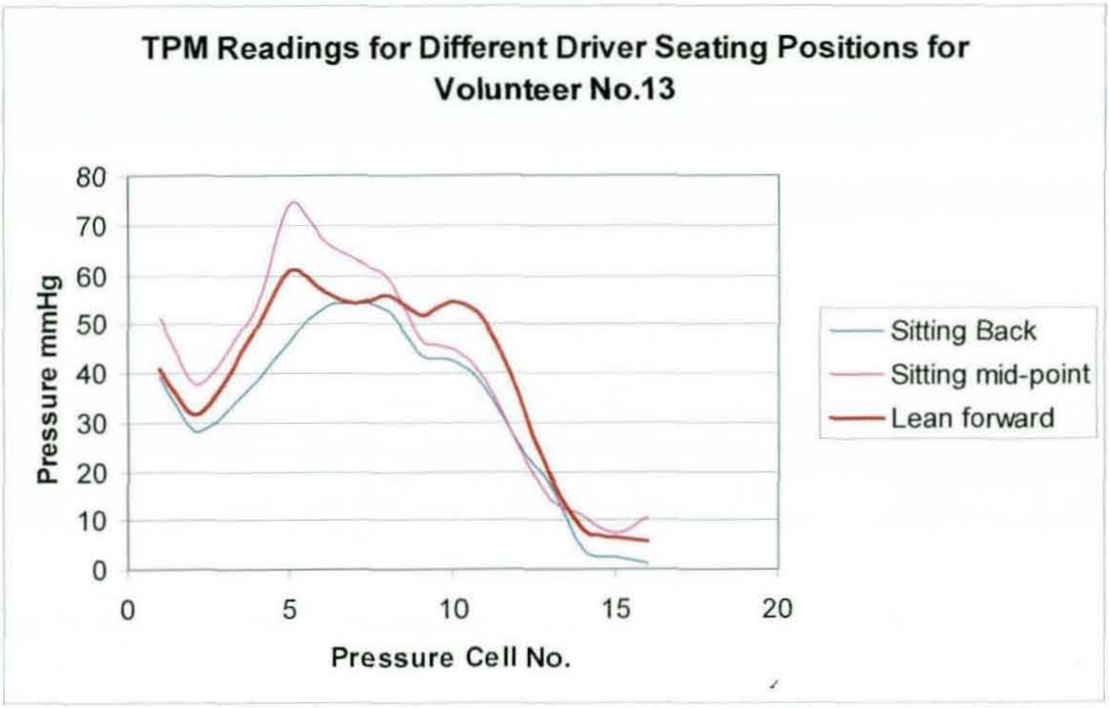

Figure 4-37: TPM Results for Volunteer No.14

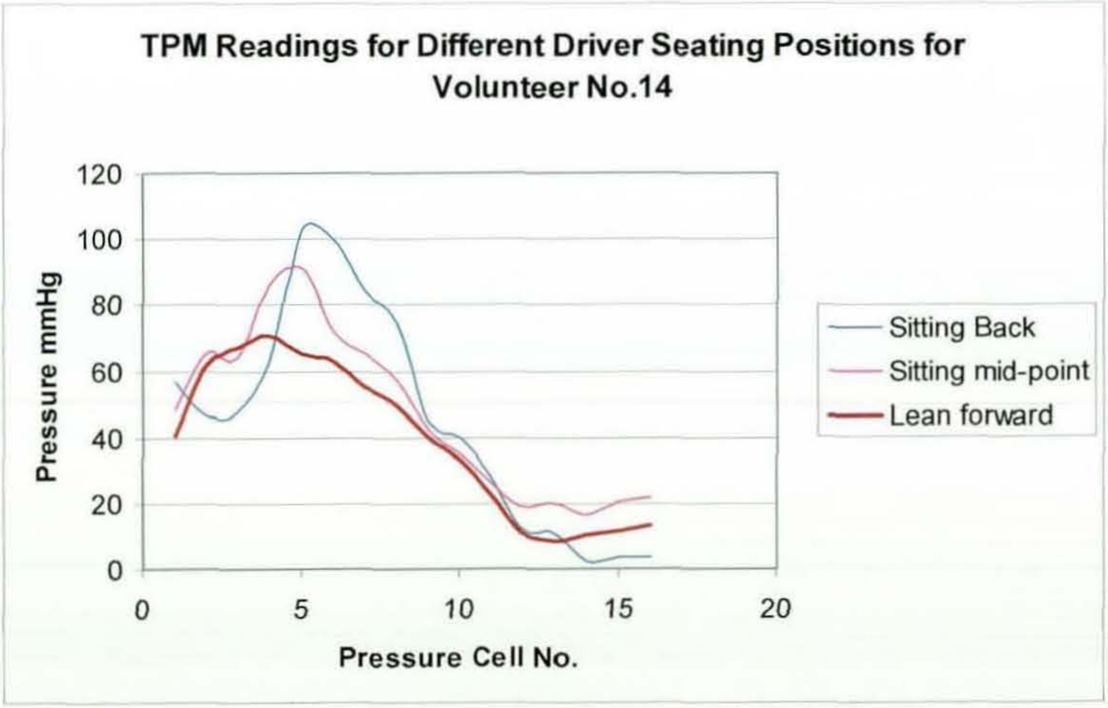

Figure 4-38: TPM Results for Volunteer No.15

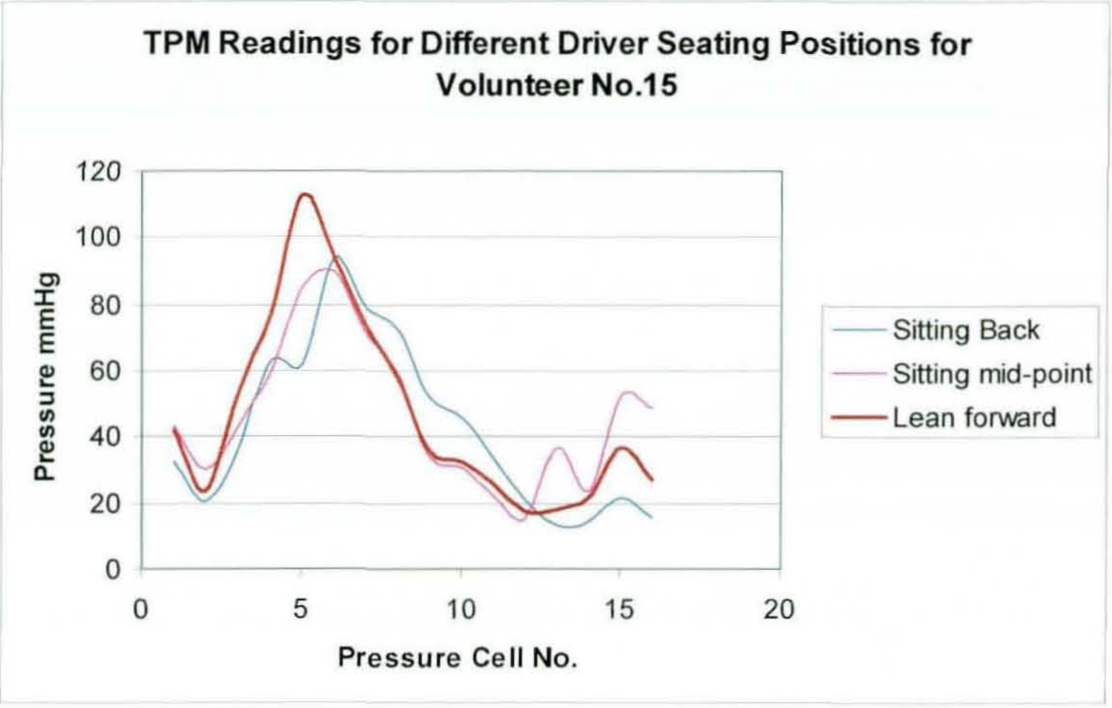

Figure 4-39: TPM Results for Volunteer No.16

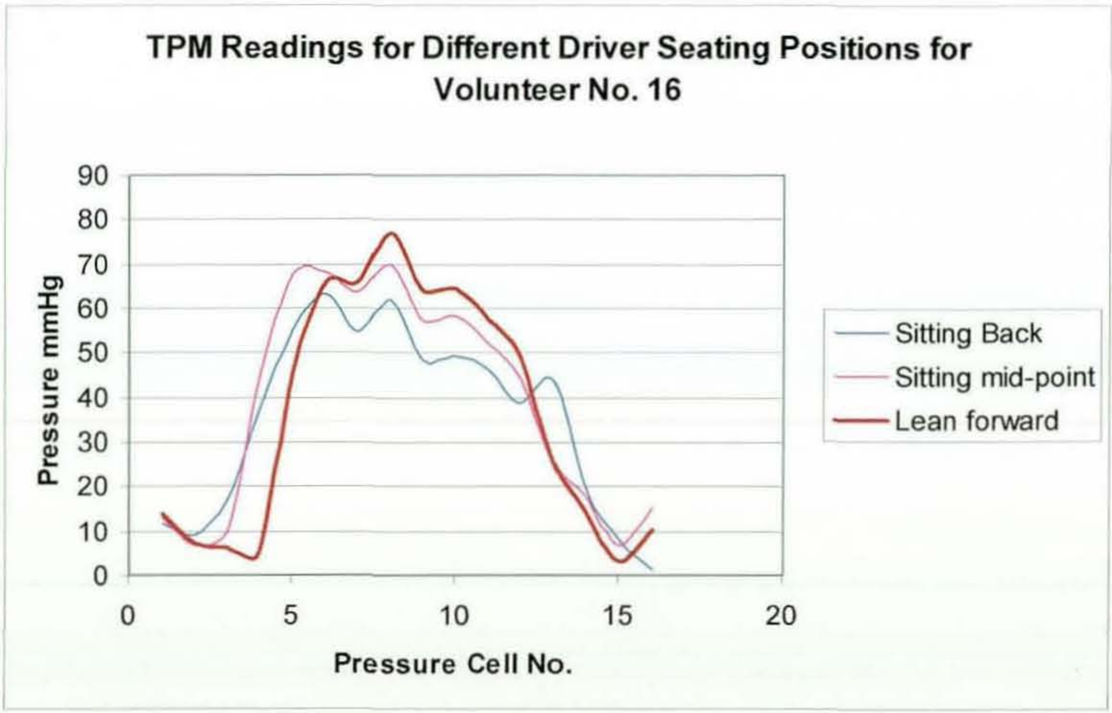

As can be seen from the majority of the TPM graphs for the various driver volunteers, there does not seem to be as large a difference between the plots of the pressure variance for the three different driver seating positions (i.e. sitting back, leaning forward to the mid-point, and finally leaning forward with head resting on the steering wheel). However, it is possible to see that there is a general trend emerging. From a cursory inspection of the results shown in the graphs, it can be seen that the peak pressure exerted by the driver occurred when the driver was sitting in position number 2, where he is sitting in the mid-point position, halfway between the furthest forward and furthest back position. This was true in 7 out of 16 cases. In 8 out of 16 cases (or 50 % of cases), the highest pressure exerted occurred when the driver was sitting in position number 3, when he is leaning forward with his head up against the steering wheel. More conclusive results are shown when taking into account the lowest pressure. For 11 out of 16 cases, or approximately 69 % of all cases, the lowest pressure occurs when the driver is in position number 1, when he is sitting back up against the backrest, in his default driving position.

This result came as a surprise because it was thought originally that the highest pressure would be exerted when the occupant is sitting back up against the backrest where his back would be in an upright position and exerting a force vertically downwards onto the pressure pad. In the other measured positions, the occupant's back is at an angle to the horizontal and so it was thought that the weight of the upper body would not exert so much pressure onto the 5th pressure cell location, but would spread the load onto other pressure cell locations further up the pressure pad.

The results are somewhat disappointing as it was hoped that there would be a larger and more significant difference between the plots for the three different seating positions that were measured by the TPM. Ideally, it was hoped that there would have been different peaks at different pressure cell references (1 to 16) along the pressure mat, and so the different seating positions could have been differentiated more straightforwardly than it can at present, and that this would have provided a secondary source of occupant position sensing within the vehicular occupant's cabin space. Nevertheless, there are some clear trends, notably that in a large majority of cases, the lowest pressure was found to be exerted by all drivers when they were sitting back up against the backrest, and this information could be used to identify when the driver is in an OOP driving scenario.

The TPM experiments have given much useful information. For example, the results have shown that it is possible to deduce occupant position inside the car cabin using pressure seat profiles. Another insight is that it is also possible to learn some extra information about the diver. When comparing the pressure profile graphs of volunteer number 15, for example, with the pressure profile graph of volunteer number 16, it is clear that the graph for volunteer number 16 has high pressure spread across more cells than volunteer 15. This would suggest that the driver is a larger or heavier person than volunteer 15. Although many more tests would need to be done in order to verify that this can be detected repeatedly, nevertheless, this information would be useful to know as a personalised restraint strategy could be developed for drivers of different body mass and shape.

4.6 Driving Simulator Trials

The main experimentation was done using a facility owned and used by ESRI, who kindly allowed it to be used as the focal point of this experimental work. The building contained a full-sized driving simulator on the first floor. It was housed inside a large darkened room, with a small room next to it where the experimental co-ordinator could monitor the experiments as they were in progress, and it also contained the major computing equipment. The driving simulator itself consisted of a Ford Scorpio model car which had its engine removed so that the major driver controls could be instrumented up. The steering, brake and accelerator were connected up to encoders and a data acquisition card. The volunteer driver would operate the controls as per usual and the movements of the steering wheel, brake and accelerator pedals would move the encoders which would then transfer a signal to the data acquisition card inside a personal computer which was running the simulation, and the software would interpret the driver's actions on the screen in front of him. This apparatus is more clearly shown in figure 4-40:

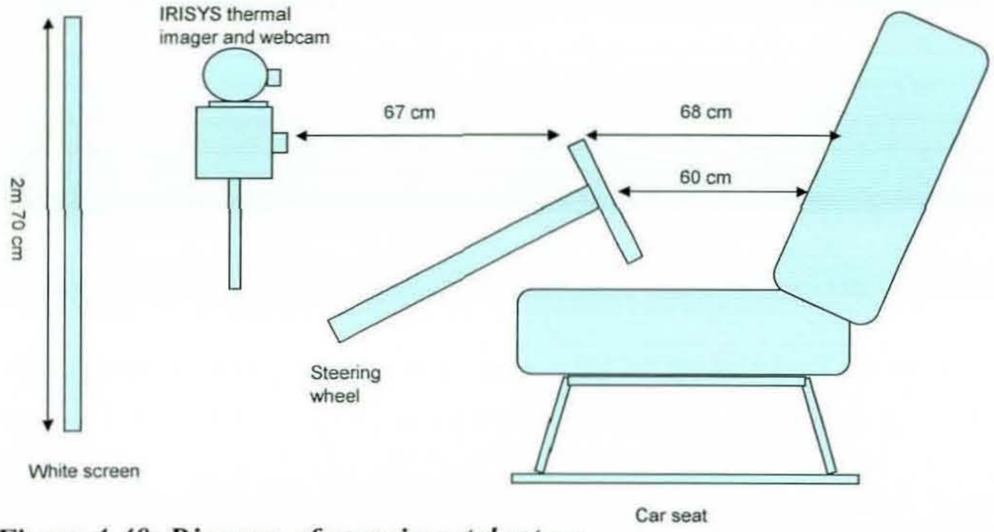

Figure 4-40: Diagram of experimental set-up.

The driving simulation software used was a commercially available simulation created by Systems Technology, Inc. This company has a long history and high reputation for making simulation software, and was chosen as the basis for this experiment. Although there are obvious shortcomings of any driving simulator such as the audio and visual scene complexity are not as high as in real life, and there is a lack of motion feedback exerted onto the driver, nevertheless, it does have some advantages. These include the fact that it is a method of doing repeatable test and results; it is relatively low cost, and it mimics a 'real life' situation, but in a controlled and safe manner. Figure 4-41 shows the computers that were used to run the simulation program, and figure 4-42 shows the actual driving simulator in action:

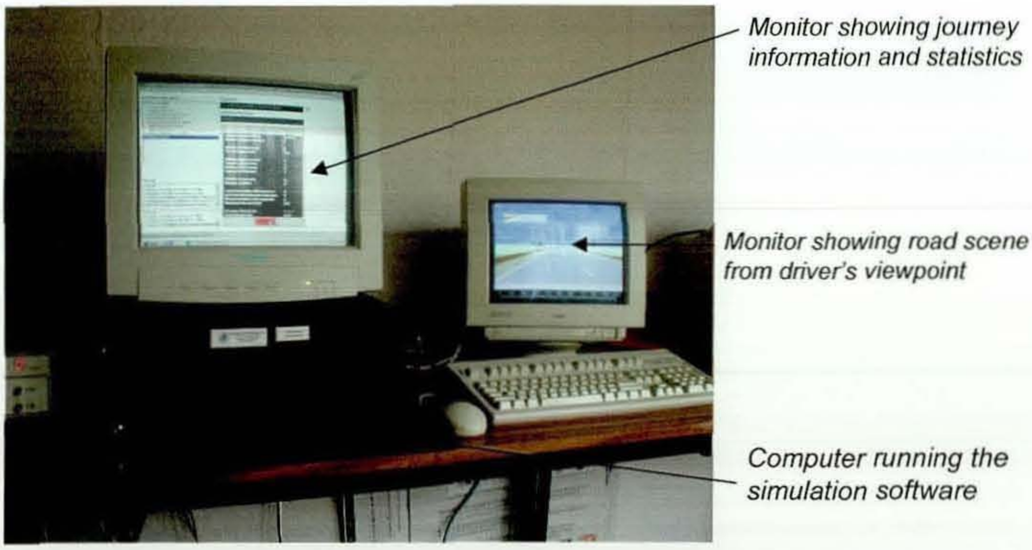

Figure 4-41: Computers used for running simulator software

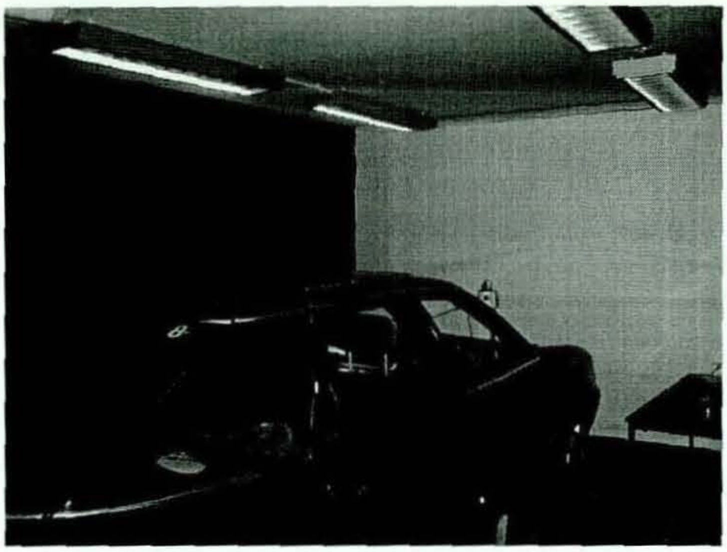

Figure 4-42: Driving simulator in action

The experimental procedure for conducting this experiment was as follows:

1. The volunteer was asked to sit inside the driver's seat. They were allowed a practice run of the driving scene, so as to be familiar with the controls and level of car response, as this was slightly different to that of a real car.

2. After approximately 5 minutes, the driver was asked to stop and exit the car.

3. The driving scenario was selected and started. The data capture software was switched on.

4. The driver was asked to sit inside the car cabin through the driver's entrance, and to put on the seatbelt. He was then told to follow the verbal instructions that would be given to him by the experimental co-ordinator who was standing outside of the car, to the side and out of the field of view of the thermal imager and webcam.

5. The driver was told to look over their shoulder and reverse the car for a small predetermined distance. The driver was also told to look in the rear-view mirror as often as necessary.

6. The driver was asked to wind down the window and reach outside with his right arm and touch a panel which was set up on the right side of the car. This was to mimic the operation of a 'swipe card' system for entering and exiting a car park, or other premises.

7. The driver was told to drive forwards and to keep to existing speed limits and traffic norms.

8. At a red traffic light, the driver was asked to slow down, stop, look to the left and to the right, before slowly accelerating upon receiving a green signal from the traffic light.

9. The driver was asked to overtake slower cars once reaching a dual carriageway, and to lean to his right side in order to view oncoming traffic in the opposite direction of travel.

10. During the course of the journey, the driver was asked to do a number of typical driver actions. He was told to lean to his left and operate the car radio on the centre console; to use a mobile phone which was placed on the front passenger seat and to lean slightly forward at random.

11. Finally, at a specific time during the driving simulation, the driver was told to increase his speed and to deliberately crash into the back of another vehicle. Upon crashing the car, the driver was told to move his upper body and head suddenly onto the steering wheel and to sit back up again, in order to mimic the driver response during a car crash.

12. The driver was told to slow down, park by the side of the road, unbuckle his seatbelt and exit the car.

The results obtained from the testing done using the driving simulator and the thermal imaging equipment was different from the data obtained from the previous trials due to a number of reasons:

- Different image acquisition software and storage.

- More sophisticated experimental procedure implemented. This meant that there was a set of repeatable instructions for the volunteers to follow, which meant that the data sets for the different volunteers could then be compared with one another. Also, the volunteer was surrounded by a more 'real life' driving situation, and the level of driver interaction with the controls was higher than it had been in the initial experiments described at the start of the chapter.

- Greater number and variance of images captured.

Now that the experiments had been completed and the data captured, the next step was to process the data. The next chapter will describe exactly what kind of processing the image data taken from this experiment was undertaken; what techniques were used and why. The reader will understand the benefits and also the limitations of what analysis was done, and will be guided through the remaining analysis done in Chapter 6.

Chapter 5 Image Processing

This chapter will describe some of the more common techniques used for the processing of images and how it could be applied to the data obtained from the experiments done in chapter 4. The experimental analysis is described later in this chapter. What is also shown is the evolution of the algorithms written in MatLab, ranging from the simple to the relatively complex. The problems encountered are highlighted and discussed, and the possible solutions to them put forward. This provides the context for the artificial neural network analysis (ANN) which was done and explained in chapter 6, as there was a clear need for a more deterministic method for recognizing and matching the images.

The purpose of Section 5.1 is that it will provide an appreciation of what work has been done previously in the field of image processing, and whether it could be used for processing infrared images. Where possible, 'tried and tested' techniques were used as it was considered that reliability was a key factor in any safety system.

5.1 Image Processing Techniques

Digital image processing has been established in research and industry for many years, with machine vision to low level image enhancement work, and as such, certain techniques have become common, and some of them will be described in this chapter.

Paraphrasing from Burdick (in his book entitled 'Digital Imaging Theory and Applications') **[100]**, neighbourhood operations are operations that use a certain area or cluster of pixels around one target pixel in order to produce an output pixel, and this differs from 'point operations' because a point operation relies on one pixel to produce one output pixel.

Convolution is perhaps the most important 'neighbourhood operator' and it works by rolling a small area of pixels to produce a resultant pixel. Convolution works by using a convolution mask, or kernel, M, which has individual elements i,j. The elements in the mask are multiplied by the corresponding pixel in the neighbourhood of the input image, P, which has elements $p_{x,y}$. These are added together and the sum is divided by the sum of the mask values to produce a pixel, $c_{x,y}$, in the convolved image, C.

Convolution presents a problem in that the computing power required is very large. For example, to perform a 3×3 convolution on a 1024×1024 pixel image would require 27 million multiplications, 24 million additions and 3 million divisions.

Point Operations

A point operation is one where the output image is a function of the grey-scale value of the pixel at the corresponding position in the input image. A histogram is a graphical representation of the frequency of the pixel intensities that occur in the image. In a typical histogram, the x-axis (or abscissa) represents the grey-level value, whilst the y-axis represents the frequency or number of pixels at that particular grey intensity level.

Image Brightness Modification

Image brightness adjustment is the simplest pixel operation. This operation would move the cluster of pixels from one end of the histogram to the other end of the histogram. This operation can be thought of as adding or subtracting a constant value from the pixel intensity values in an image, depending on whether increasing or decreasing brightness is required, and this would move the histogram to the right on the abscissa and to the left along the abscissa respectively. Image brightness modification can be expressed as:

$$P' = A + P$$

Where P' = pixel value after modification

P = pixel value before modification

A = constant

Contrast Enhancement

Contrast enhancement involves multiplying the pixel values by a factor to stretch the histogram over the full range of the abscissa. This operation ensures that the brightest pixels are set to 'peak white' intensity, and contrast enhancement is traditionally used for image restoration.

Negation

Negation is where black images or pixels are mapped as white pixels and vice versa. This can be done by subtracting the pixel value from the maximum grey-level value of the image, and can be expressed by the following equation:

$$P' = 2^l - P$$

Where l = number of grey-level bits used.

Thresholding

Thresholding is an operation where the image is segmented into a background and foreground region. Traditionally, this is done by selecting a threshold value which enables the separation of the foreground image from the background. Selection of the threshold value can be done more accurately by studying the histogram and finding the point where there is a trough in the histogram between two peaks.

From the image processing techniques described in this section, thresholding was perhaps the most appropriate technique to use as it works well with images of different resolution, is simple to incorporate into computer programmes or functions, and will be able to separate the infrared images into different regions of interest. How this was done is explained later in the chapter.

5.2 Image Processing of the Data from the STISIM Car Simulator Experiments

The dataset of each volunteer driver had been stored onto the removable hard disk using compression techniques. The data was extracted and then imported into MatLab version 6.5 using a specially coded program which had been coded using National Instruments Labview/CVI tools. This program enabled the operator to visualise both the visual light camera image of the volunteer driver next to its corresponding thermal image, as can be seen in the figure below. The figure below shows the 'graphical user interface' (GUI) software application developed for accessing the image data files and exporting the data into the MatLab software workspace. What this GUI application allowed was the ability to see each individual frame or image captured by the thermal imager and the CCD 'webcam' by the user, and to enable him to pick specific images in order to further process them.

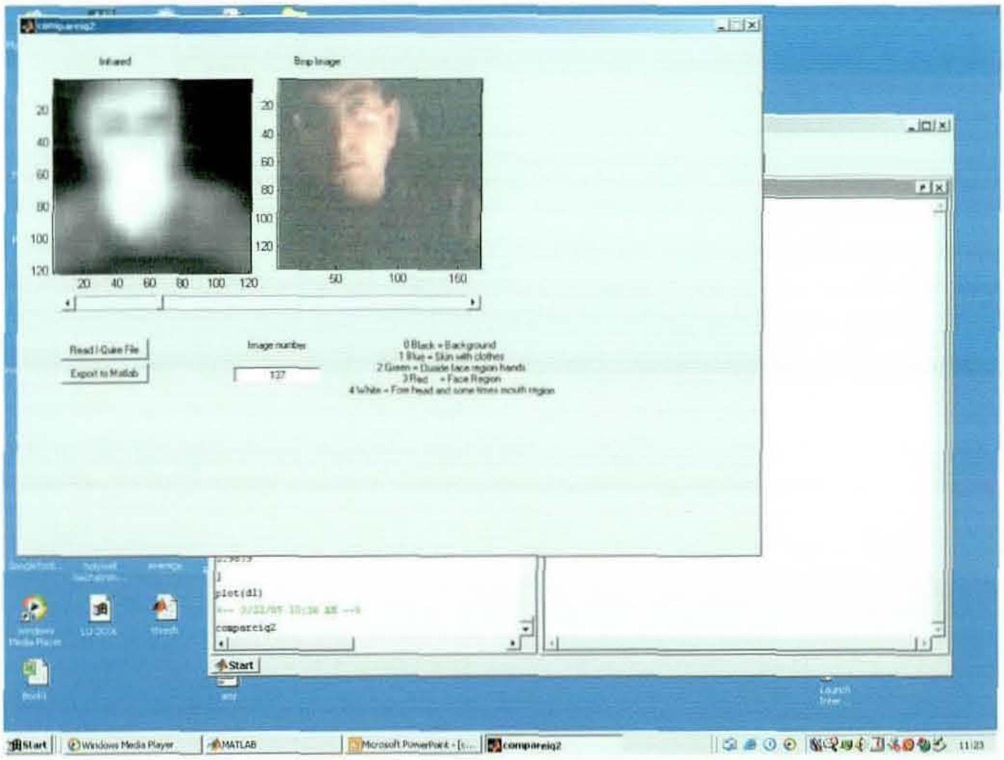

Figure 5-1: Graphical User Interface used for the selection of thermal images

The data collected posed a problem as it was found that the number of thermal images collected by the data acquisition software varied for each volunteer driver. Also, although the driver response test procedure had been the same for each of the volunteer drivers, their responses also varied significantly. For example, if the driver was asked to lean to the right to simulate the driver leaning to get a view of the opposite lane, some leaned far further than others. Another problem was that some driver's responses to the stimuli was quicker than other volunteer drivers, and all these minor differences made it difficult for 'like for like' image comparison and analysis.

It was necessary to obtain the relevant images so that they could be studied further. Although in some instances the datasets for some volunteer drivers contained over 800 thermal images, it was not necessary to use all of them because most of these images were not relevant as they were of the driver sitting upright, looking straight towards the road, hands on the steering wheel. For analysis purposes, only a handful of these images were necessary for comparison studies with images of the drivers in other situations. Although it could be argued that all the images of the same situation should have been processed for the purposes of completeness, it would have taken many more months to complete and the higher accuracy which would result was not deemed high enough to justify spending so much extra time.

The thermal images contained in each dataset for each volunteer were inspected visually one at a time for instances where the driver displayed some behaviour or action that differed from the norm. In other words, if the driver was in a different position to his standard position of sitting back in the seat, head and gaze of the driver straight towards the road scene ahead, then the frame numbers of these images, and a description of the image was tabulated so that it could be reviewed later. Once this was done for the data of all the driver volunteers, these images were extracted from their datasets once again for image processing.

The images were reshaped and imported using MatLab version 6.5 software. They were displayed as 121 x 121 pixel images and not as 16x16 pixel images because of the greater clarity and the scope for more accurate segmentation of the images.

The data acquisition program and the program used for the importing and displaying of the image data files ('compareiq2') was developed and the data acquisition code was written using commercially available 'Lab Windows/CVI' from the company 'National Instruments', and was chosen as it supported most hardware interfaces, and was relatively easy to use, and used standard ANSI C code.

The dataset for the first driver volunteer was opened up using the 'compareiq2' software program, as shown in figure 5-1. All the images were viewed manually using the scroll function of the program. Any images that were of interest were marked for further analysis later. Of particular interest were the images which showed the driver volunteer in differing positions or performing certain actions that were not the norm. These images were as follows:

1. Looking straight ahead. The driver's gaze is straight towards the scene in front of him and the head is in the centre of the image.

2. Looking up. The driver's gaze is directed upwards towards the region where the rear view mirror is located. The head is angled upwards.

3. Looking to the right. The driver's gaze is towards the right, simulating typical driver's actions at T-junctions, crossings. The head is rotated to the right.

4. Looking to the left. The driver's gaze is towards the left, simulating a typical driver's actions at T-junctions, crossing etc. The head is rotated to the left.

5. Head leaning forward, on the steering wheel. The driver's head is resting on the steering wheel, simulating the position of the driver in the event of a vehicle crash situation.

6. Leaning to the left. The head and body are positioned to the left, simulating the action of a driver reaching to buckle/unbuckle the seatbelt or operate the controls on the centre panel of the car.

7. Using mobile phone. The driver was asked to pick up a mobile phone which was placed on the passenger seat prior to the start of the experiment.

8. Reach right. This action was to mimic the operation of a barrier for entry into a car park or building.

All these images were put into a table which included information such as their frame number in the dataset, a short description of what the image showed. This process was done for all the different driver scenarios that are described above.

5.3 Threshold Images

In order to further analyse the images of the volunteer drivers, the images themselves would have to be modified in order that the important regions were given prominence, for example the head and facial areas, whilst the other sections (such as the background) were removed from the image. For the purposes of this project, the head region was the focus of the analysis because this was the part of the body which was the most likely to come into contact with the steering wheel or other parts of the dashboard, and would be most at risk from airbag related injury in the event of a crash incident.

The differences or regions in the 128x128 pixel images were clearly designated by the differences in temperatures. For example, on visually inspecting the thermal images, it was clear that the background was at a lower temperature than that of the rest of the body, and the torso of the driver was at a lower temperature than the head and hands of the driver. This was obviously because the skin on the face and hands was uncovered, whilst the rest of the driver's skin was covered by clothing, resulting in lower thermal emission.

One of the simplest methods of processing the images was to use a threshold function on them. This was a process whereby certain parts of the image, or segments, were visually enhanced, whilst other parts of the image were removed. For the purposes of the thermal images collected from the experimental work, it was clear that the most important regions of the images were:

- Head/Face regions.

- Hands.

- Upper body.

- Background.

Clearly the most important region was the head and facial regions as this was the part of the body that was most at risk from airbag related injury as it would be the first part of the body that would collide with the steering wheel first. Therefore it was thought that separating the head/facial areas from the rest of the body and the background would visually aid the analysis of the images.

The different regions were shown by the different temperatures that they were designated with. For example, on visually inspecting any thermal image, it was clear that the background was at a lower temperature than the head and facial regions, and these differences were shown up as differences in colour. The lower temperatures regions were designated the 'cooler' colours such as blue and black, whilst the higher temperatures were shown as the yellow and red regions. Using this colour scheme, it was possible to distinguish between different sections of the body. However, in order to analyse the images, temperature and not colour was used as the variable. Before this could be done, however, it was important to know what the temperature readings were for the various regions in the image were. It was also important to obtain this information from as wide a range as possible of images of as many of the volunteer drivers as possible, in order to maintain the accuracy of the results.

The first driver scenario that was examined was the driver scenario or position which would be the most common, the driver looking straight ahead, towards the road ahead and in his normal driving position. This image was viewed using the 'compareiq2' program, and the data was exported into the MatLab command environment. The command to bring up the value of any pixel of the image was called 'xval', and this enabled the researcher to use the computer mouse device to hover above any region of interest in the image, click on a particular pixel and thus find its resultant temperature reading. A number of random pixel temperatures were measured in this way for all the different regions of the image (e.g. head, upper body, hands, background), and the modal average of the temperatures were found. This process was done for a selection of the volunteers, and the results tabulated and displayed in figure 5-2.

However, it was clear that the temperatures for the same region (head, body etc) differed by a few degrees Centigrade for each different volunteer. The threshold technique chosen to distinguish the head region apart from the rest of the regions in the image was a simple one. The head region was set at a particular temperature (say 30 degrees Celsius). A short MatLab function program was written using a standard 'IF' argument structure which basically said that if the pixel was at a temperature higher than the threshold limit, then that pixel would have a value of 1, but if any pixel had a temperature less than the threshold limit, then that pixel would be set to 0. The resultant image would show the head and neck regions only, and would be set apart from the background.

Setting the threshold temperature was crucial to the success of this project as it would be written into a MatLab program which would be used to threshold all the relevant images for all the volunteers. A mean temperature may have been suitable for one of the volunteers but if used as the threshold limit for other volunteer's images, may have resulted in distorted head region sizes and shapes, because that volunteer's temperature readings were slightly lower than the norm. Therefore the temperatures of the relevant regions were checked for a selection of the volunteers and the lowest temperature was used as the threshold limit. Using the lowest temperature value for human skin was thought to be a satisfactory solution as it was found that by analysing a random selection of images from all the volunteers, the surface facial skin temperature was found to be higher than 30 degrees Celsius at standard room conditions. Of course, this would not apply where the ambient temperature was over 30 degrees Celsius, but it was rationalised that drivers would not willingly remain in a car cabin which was at this high temperature. They would probably turn on the air conditioning system in order to maintain an ambient temperature in the region of 20-25 degrees Celsius, and is therefore not a real concern.

	Amjad	Andy	Bilal	Faraz	Gavin	Imran	James	Mark	Stephen	Val	Diming	Average	Min
	deg C	deg C	deg C	deg C	deg C	deg C	deg C	deg C	deg C	deg C	deg C	deg C	deg C
	1	2	3	4	5	6	7	8	9	10	11		
Face	30-34	30-33	31-35	31-34	31-35	33-35	31-35	33-37	31-35	31-32	34	32.95455	30
Hands		28-29		30-31	30-31		26-27	33-35		31-33	30-31	30.35714	26
Hair	26-29	25-26		24-26	27-29	26-27	27-28	26-28	25-29	23-26.75	24.7-32	26.75	23
Clothed body	24-25	25-29	22-25	24-25	24-26	24-25	25-26	25-26	25-27	23-25	21.25.7	24.86364	21
Background	17-20	18-20	18-20	17-20	18-21	17-20	18-20	18-21	19-21	18-20	18-21	19.09091	17
Spectacles	25.25-26		28									26.75	25
Headrest	22		22-26			21	22-23					22.375	21
teering whee	25-26		24-25			23						24.33333	23
Seatbelt						21	21-22	23-24				22	21
Images Referenced		1, 252, 347	, 853, 95	, 257, 78	, 256, 46	1, 85, 183	15, 34, 105, 175		2	6, 72	22, 422, 405		

Figure 5-2: Surface temperatures of various body parts for selected volunteers

Using information obtained from the table given in figure 5-2, the following function was written using MatLab. This was a simple IF argument which classified individual pixels according to their temperature values. Pixels over a certain temperature threshold were assigned a value of 1, whilst pixels which were below the threshold were assigned a value of 0. The threshold value could be determined by the user by changing the value of 't', whilst the image was written as a matrix, 'x'.

The MatLab function was as follows:

```
function y = thresh(x, t)
% AVERAGE Mean of vector elements.
% AVERAGE(X), where X is a vector, is the mean of vector elements.
% Non-vector input results in an error.
[m,n] = size(x);
if (m<=1 | n<=1)
   error('Input must be a 2D matrix')
end
y=x;
for i=1:m
```

```
    for j=1:n
        if x(i,j)<t
            y(i,j)=0;
        else
            y(i,j)=1;
        end
    end
end
```

Using this threshold function, it was possible for the user to process the images, and examples of this are shown in figure 5-3 to figure 5-10:

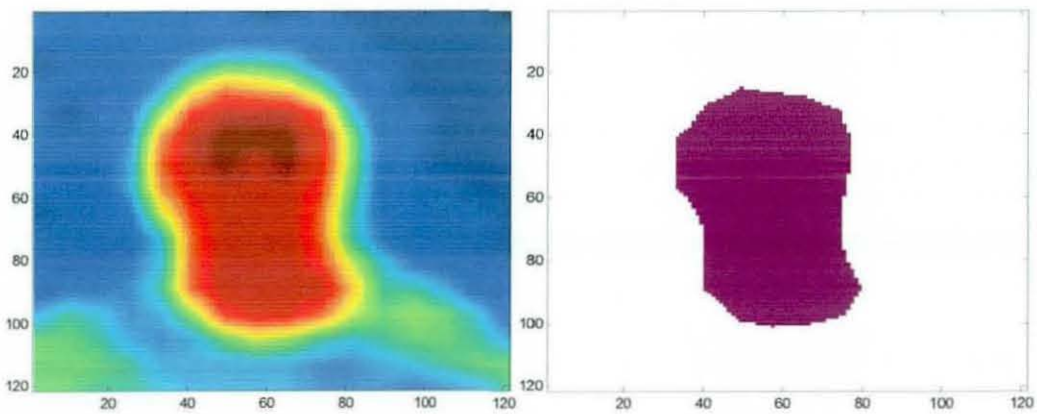

Figure 5-3: Thermal image and threshold image of driver looking straight.

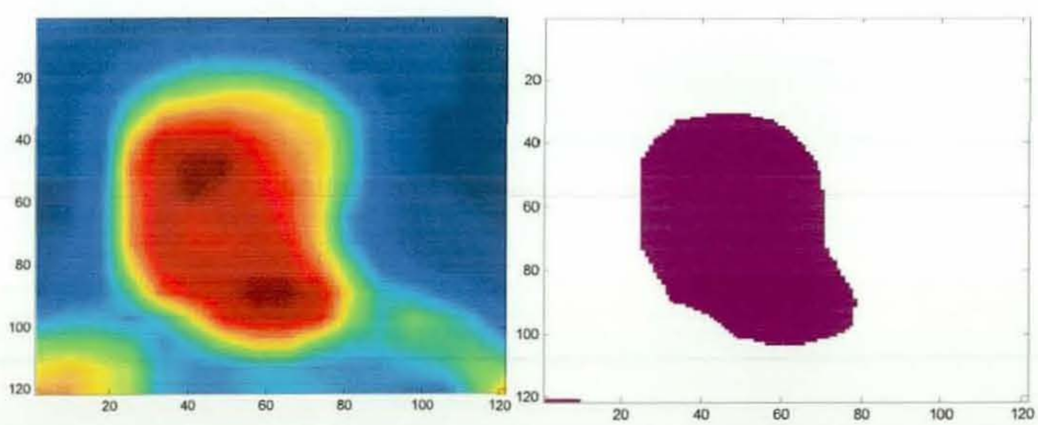

Figure 5-4: Thermal image and threshold image of driver looking right.

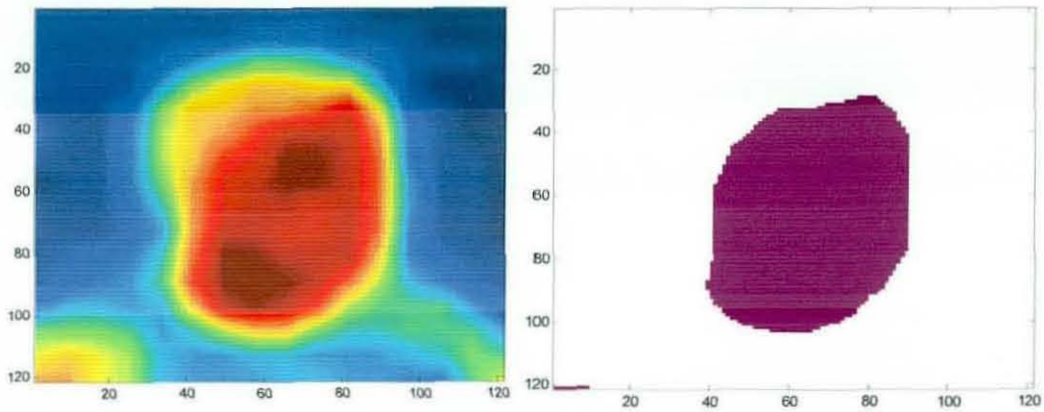

Figure 5-5: Thermal image and threshold image of driver looking left.

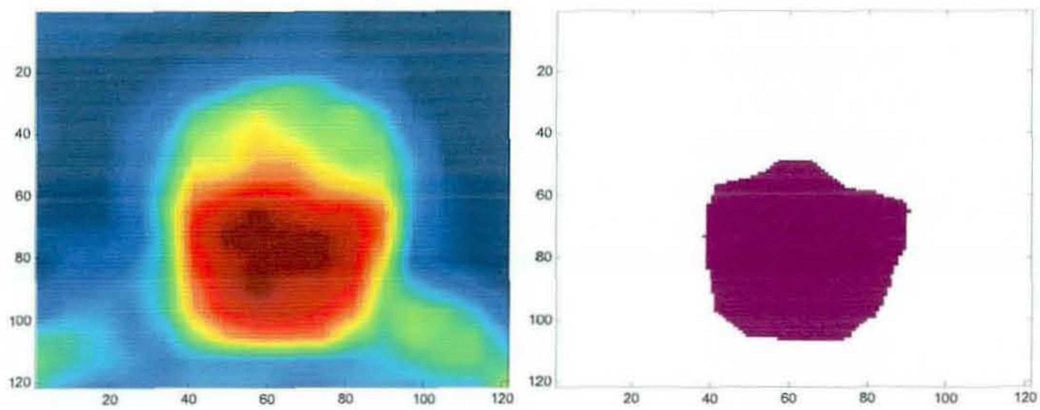

Figure 5-6: Thermal image and threshold image of driver leaning forward

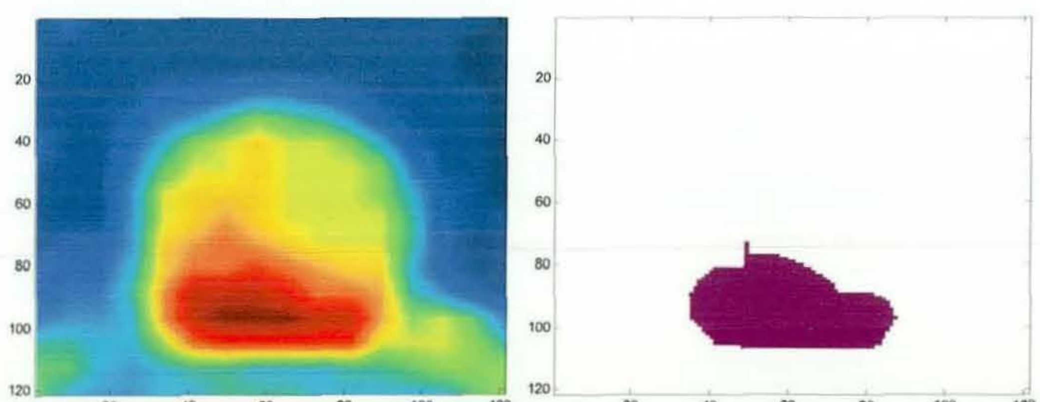

Figure 5-7: Thermal image and threshold image of driver with head on steering wheel.

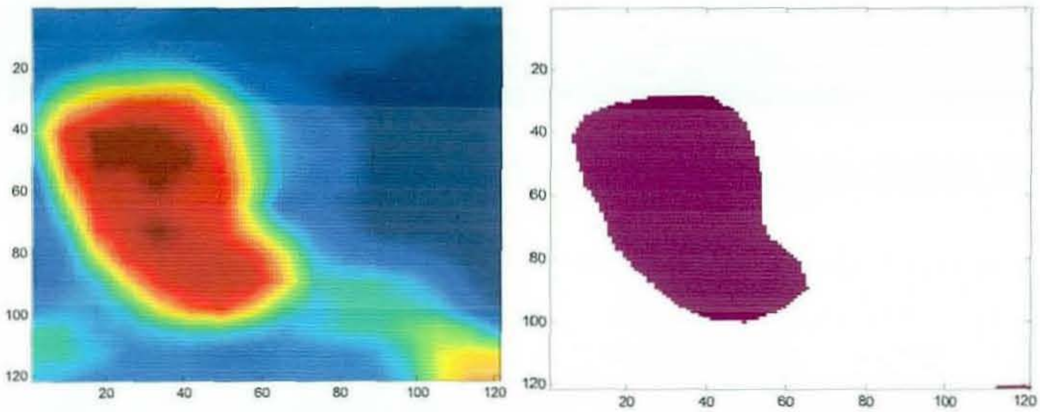

Figure 5-8: Thermal image and threshold image of driver leaning right.

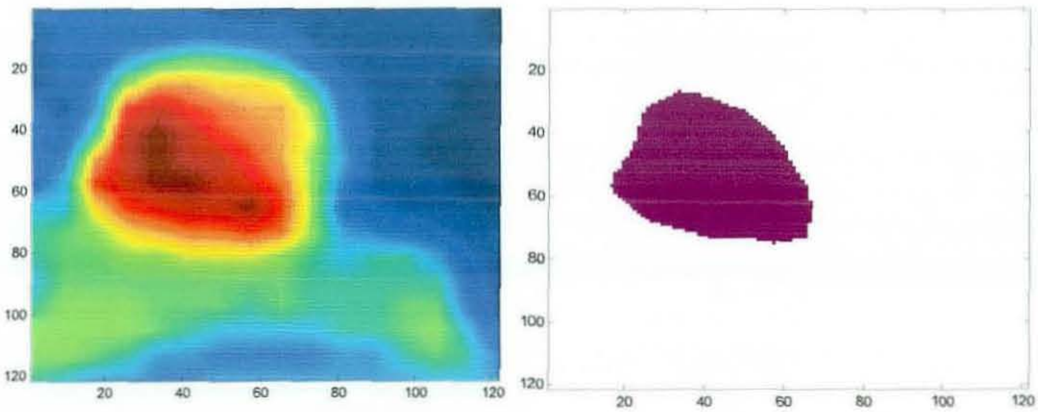

Figure 5-9: Thermal image and threshold image of driver reaching right.

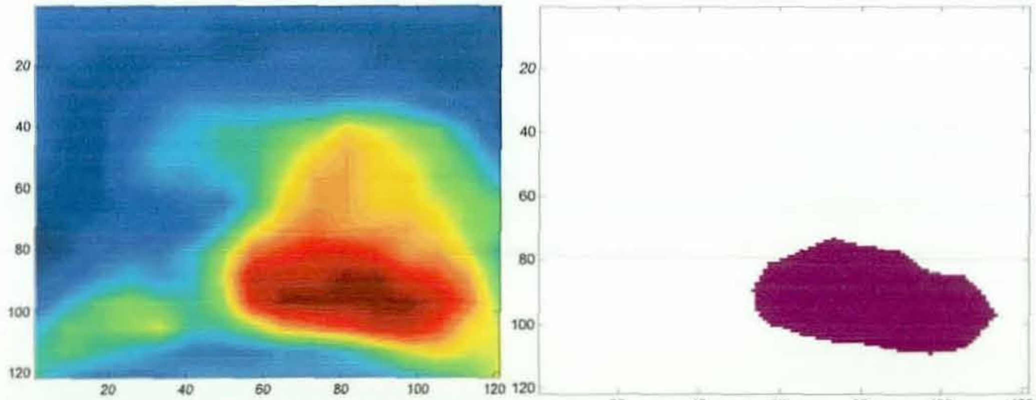

Figure 5-10: Thermal image and threshold image of driver leaning left.

Figures 5-3 to 5-10 show the thermal image and the corresponding threshold image for one of the driver volunteers used in the experiment. The driver in figure 5-3 is 'looking straight ahead', which is the default position for all the drivers. Figure 5-4 shows the same driver when he is 'looking right'. As can be seen from the threshold image, the area of the threshold region has migrated to his right side, when compared with the threshold image shown in figure 5-3.

Figure 5-5 shows the driver as he is 'looking left'. It can be seen that the centroid of mass of the threshold image has moved towards his left side. Although at first glance there may not appear to be much difference between this image and the driver as he is looking straight, it can be proved that there has been head movement. To test this, an imaginary line was drawn down the centre of the image (vertically), and a function was written in Matlab to count the number of 'hot' pixels on the left and the right side of the image. The function would determine which side of the image had the highest number of 'hot' pixels and it could be said that the driver's head had moved to that side of the image. Also, it is noticeable that the width (or minor axis length) of the threshold region is slightly larger compared with the threshold region of the driver 'looking straight ahead', which could also indicate that a head positional change had taken place.

The driver in figure 5-6 is 'leaning forward' towards the steering wheel. Due to the fact that the head is facing downwards, the overall area of the face that can be viewed by the thermal imager has reduced in size, and this is seen in the threshold image in figure 5-6. This is even more pronounced in figure 5-7, which is of the driver with his 'head on the steering wheel'. With the head being in this position, only a small part of the driver's face is visible, and this is shown very clearly by the threshold image. The threshold region is now a flatter shape, and also the centroid of mass of the region has shifted considerably towards the bottom of the image. The contrast between this image and that of the driver whilst in his default position of 'looking straight ahead' is very clear.

Figure 5-8 is the driver whilst he is 'leaning right'. In this position, the centroid of the threshold region has moved significantly towards his right side, and also the major axis is also at an angle, leaning towards the right side. These differences should clearly distinguish it from the image of the driver 'looking straight ahead'.

Figure 5-9 shows the driver whilst he is in the 'reach right' position, i.e. when he has his right arm outstretched out of the window in order to operate a roadside barrier, for example. The threshold region has also moved towards his right side, however, it is different form figure 5-8 in that the area of the threshold region is considerably smaller.

The driver in figure 5-10 is 'leaning left'. In this image, the driver was unbuckling his seatbelt. The threshold region is positioned on the left side of the image (from the driver's view), and also the area of the region is smaller and the shape is flatter.

Once the threshold images were obtained for each of the different driver actions, the mathematical properties of the threshold shape was found using the 'regionprops' command in MatLab. These properties are the mathematical or geometrical properties of the region which is left after the threshold function has operated on the original infrared image. These properties include the x and y coordinates of the centroid of mass of the region (in pixels), area, major axis length, minor axis length.

The data exported into MatLab from the 'compareiq2' GUI enabled images such as the one shown below to be created. As can be seen, the head region is clearly defined from the rest of the background and from his torso as well. Note also how the eye regions show up clearly as cooler areas of the face. This is due to the fact that this volunteer was wearing eye glasses.

5.4 Analysis of Threshold Images

The threshold technique was done for a specific purpose, i.e. to reduce the amount of information (pixels) from the original thermal image down to a more manageable size for both the researcher and the computer to handle. Once this was completed, another MatLab command was used to analyse the resultant head and neck region. This command was called 'regionprops', short for 'region properties'. Using this command enabled the operator to automatically conduct a series of mathematical measurements applied to the threshold region. This provided scope for the researcher to use this data to discern any changes using a more reliable and quantifiable method than the previously used method of visual inspection. The mathematical operators that could be calculated using the 'regionprops' command were as follows:

- Centroid.
- Area.
- Eccentricity.
- Orientation.
- Major Axis Length.
- Minor axis Length.
- Bounding Box.

Although there were other measurements that could have been found, it was felt that these represented the main measurements that were necessary for adequate processing of the images. These variables were decided upon by comparing the values of these variables for different scenarios (e.g. look straight, lean forward, lean right etc). It was found that these variables exhibited significant change when the driver's position or movement changed in the image, and this was important when it came to using this data in the neural network analysis described in chapter 6.

Area, measured in pixels, was a useful measurement as it would provide a measure of the size of the head and neck regions, as indeed would the Major and Minor Axis Lengths. The centroid of the mass of the region was given as an x and y co-ordinate (in pixels) and was useful as it could provide information relating to both driver behaviour and head position.

5.5 MatLab Region Properties of Threshold Images

The threshold regions that resulted from the image processing done were then subjected to mathematical analysis in order to differentiate them from each other. This was done using the 'regionprops' command in MatLab, a tool specifically designed for use on segmented images using the threshold technique. These mathematical properties are presented below, and were determined from a number of sources **[101], [102]**:

Perimeter

The perimeter is the distance in pixels around the circumference of the object. One pixel is given a nominal unit of 1.

Area

The area is the area inside the foreground of the threshold image and the boundary of the object, measured in number of pixels, and this provides a measure of the size of the object.

Major Axis Length

The major axis length is the length of the threshold object measured along the longest or major axis of the object, or is the distance between the major axis endpoints, and can be expressed by the following equation:

Major Axis Length = $\sqrt{(x_2 - x_1)^2 + (y_2 - y_1)^2}$.
Where (x_1,y_1) and (x_2,y_2) are the major axis endpoints.

Minor Axis Length

The minor axis length is the length of the threshold object measured along the shortest or minor axis of the object, or is the distance between the minor axis endpoints, and can be expressed by the following equation:

Minor Axis Length = $\sqrt{(x_2 - x_1)^2 + (y_2 - y_1)^2}$.
Where (x_1,y_1) and (x_2,y_2) are the minor axis endpoints.

The major axis angle is the angle that is made between the major axis of the object and the x-axis of the image, and can range from 0° to 360°. The major axis can be expressed in the form:

Major Axis Angle = $\tan^{-1}[(y^2 - y^1)/(x^2 - x^1)]$.

Centroid

The centroid or the centre of mass of the object is the point of the object where there is an equal mass above, below, left or right of that point. This is expressed as an x and y coordinate.

Eccentricity

Eccentricity is the ratio of the distance between the foci of the ellipse and its major axis length, and is normally given as a value between 0 and 1. An eccentricity of 0 denotes that the ellipse is actually a circle, whilst an eccentricity of 1 denotes that the ellipse is a line segment. In other words, this property approximates the shape in the image to an ellipse.

Orientation

The orientation is the angle in degrees between the x axis and the major axis of the ellipse that has the same second-moments as the region.

EquivDiameter

This is the diameter of a circle which has the same area as the region in question, and is calculated as the square root of the sum of 4 times the area of the region, divided by pi.

5.6 Graphical Treatment of the Images

Once the 'regionprops' command was applied to calculate the various mathematical and graphical properties of the segmented image, the first batch of results were tabulated and are presented in figures 5-11 to 5-17. The data contained in these tables allowed images to be scrutinised to a greater degree than merely by examination by the naked eye.

LOOKING STRAIGHT AHEAD				Centroid						
Name	Test No.	Data from Frame No.	Face threshold value	x co-ordinate	y co-ordnate	Area	Major Axis Length	Minor Axis Length	Eccentricity	Orientation
			degree C	pixel	pixel	pixel	pixel	pixel	pixel	pixel
Amjad	1	1	30	47.8945	58.865	2200	91.6722	37.7847	0.9111	89.7935
Andy	2	1	30	53.7368	53.2115	2052	103.3856	35.9161	0.9377	86.2382
Bilal	3	4	30	55.5731	55.8697	2195	94.3566	39.4544	0.9084	85.5635
Faraz	4	2	30	51.5214	48.2212	4204	112.3702	49.3043	0.8986	-86.9914
Gavin	5	9	30	59.0489	47.7226	3864	110.3529	45.9159	0.9093	-89.3627
Imran	6	85	30	57.4392	63.3274	2639	79.4537	43.6608	0.8355	-83.7612
James	7	34	30	53.9757	66.362	2555	85.2537	41.1153	0.876	-88.6045
Mark H	8	17	30	51.3361	60.8919	3859	94.9595	52.5254	0.8331	-89.5546
Stephen	9	1	30	68.9616	72.9317	2476	72.4965	46.2711	0.7698	-88.6807
Val	10	39	30	50.5772	65.0979	2216	67.557	42.8535	0.7731	-78.8909
Diming	11	22	30	58.0509	55.836	3202	94.3873	44.4771	0.882	82.7666

Figure 5-11: Table of region properties of threshold shape when looking straight.

LOOKING LEFT				Centroid						
Name	Test No.	Data from Frame No.	Face thresholding value	x co-ordinate	y co-ordnate	Area	Major Axis Length	Minor Axis Length	Eccentricity	Orientation
			degree C	pixel	pixel	pixel	pixel	pixel	pixel	pixel
Amjad	1	362	30	52.0194	52.5021	2828	85.3913	45.3385	0.8474	-89.9779
Andy	2	108	30	62.2225	62.1486	2611	90.6026	39.0941	0.9021	72.2398
Bilal	3	115	30	58.0603	52.1173	3001	81.4939	48.7909	0.801	-82.9005
Faraz	4	174	30	64.9553	65.5682	2617	74.8406	46.2823	0.7859	75.0367
Gavin	5	102	30	60.7637	44.4992	4299	104.7962	54.3204	0.8552	-89.283
Imran	6	143	30	64.6652	66.6163	3091	79.5942	51.2345	0.7653	72.5216
James	7	310	30	68.5703	69.7712	2902	82.2892	45.4399	0.8337	63.5403
Mark H	8	402	30	63.6807	58.9905	3883	87.6417	56.5394	0.7641	82.932
Stephen	9	116	30	80.8638	74.8168	3149	73.6749	56.2555	0.6457	67.356
Val	10	110	30	70.7348	62.4321	2002	76.1307	34.9853	0.8882	74.5769
Diming	11	534	30	71.2755	60.008	3252	90.2815	46.7949	0.8552	-88.6403

Figure 5-12: Table of region properties of threshold shape when looking left.

LOOKING RIGHT				Centroid						
Name	Test No.	Data from Frame No.	Face thresholding value	x co-ordinate	y co-ordnate	Area	Major Axis Length	Minor Axis Length	Eccentricity	Orientation
			degree C	pixel	pixel	pixel	pixel	pixel	pixel	pixel
Amjad	1	360	30	40.3246	54.0339	3007	86.8821	45.6376	0.8509	-63.7241
Andy	2	107	30	40.3587	64.7334	2746	88.4693	41.6815	0.8821	-62.6451
Bilal	3	110	30	55.1557	51.5427	3114	82.0083	50.4837	0.7881	-82.2999
Faraz	4	171	30	53.2086	65.7784	2689	78.1023	45.3931	0.8138	-63.7296
Gavin	5	104	30	50.1019	44.3275	4367	102.2713	56.4895	0.8336	-75.2071
Imran	6	139	30	49.8409	67.26	2954	79.3201	50.164	0.7746	-71.9672
James	7	312	30	31.2028	70.385	2974	93.5197	41.8058	0.8945	-54.2463
Mark H	8	400	30	48.6973	61.0795	3822	89.6212	54.9282	0.7902	-68.5276
Stephen	9	22	30	44.8179	75.9285	2756	70.6128	52.1362	0.6744	-33.3023
Val	10	108	30	47.5845	64.7378	2277	82.2829	37.8406	0.888	-68.1437
Diming	11		30	66.1681	58.8258	3289	93.6745	46.177	0.8701	-77.8319

Figure 5-13: Table of region properties of threshold shape when looking right.

LEANING LEFT-SIDE, OUT OF POSITION				Centroid						
Name	Test No.	Data from Frame No.	Face thresholding value	x co-ordinate	y co-ordnate	Area	Major Axis Length	Minor Axis Length	Eccentricity	Orientation
			degree C	pixel	pixel	pixel	pixel	pixel	pixel	pixel
Amjad	1	21	30	104.8466	71.7369	1258	48.926	36.7749	0.6596	-44.0385
Andy	2	25	30	62.4624	74.0827	1717	63.5736	51.3651	0.5892	15.2143
Bilal	3	876	30	97.1483	83.4725	2785	70.3964	56.4364	0.5977	-44.576
Faraz	4	26	30	102.3208	90.8669	1540	61.0977	34.1438	0.8293	-48.5292
Gavin	5									
Imran	6									
James	7									
Mark H	8	27	30	102.5604	81.9053	2566	74.0871	46.6326	0.7771	-85.8957
Stephen	9	28	30	100.705	98.0836	1400	54.7576	35.321	0.7641	-21.2163
Val	10	24	30	119.12	116.46	50	11.8555	5.6797	0.8778	84.9351
Diming	11	21	30	102.5578	87.8149	1669	59.5995	39.0166	0.7559	-50.4952

Figure 5-14: Table of region properties of threshold shape when leaning left.

LEAN RIGHT-SIDE, OUT OF POSITION				Centroid						
Name	Test No.	Data from Frame No.	Face thresholding value	x co-ordinate	y co-ordnate	Area	Major Axis Length	Minor Axis Length	Eccentricity	Orientation
			degree C	pixel	pixel	pixel	pixel	pixel	pixel	pixel
Amjad	1	49	30	24.2638	67.4238	1994	63.6403	42.3719	0.7461	-32.359
Andy	2	41	30	20.0322	85.6014	838	78.3422	34.1969	0.8997	-4.4887
Bilal	3	391	30	35.0221	56.3249	2992	82.7353	52.0841	0.777	-50.9975
Faraz	4		30	45.0948	66.1685	2659	82.2389	42.4363	0.8566	-55.7924
Gavin	5	156	30	28.9904	47.7548	3939	111.3274	46.4136	0.9089	-67.5548
Imran	6	361	30	36.6998	66.3152	2805	83.9656	44.1936	0.8503	-58.4983
James	7	380	30	38.6559	66.1052	2671	92.9771	40.039	0.9025	-65.7803
Mark H	8									
Stephen	9	219	30	49.4569	75.1509	2565	72.1274	47.0693	0.7577	-65.1119
Val	10	159	30	33.3137	62.1865	2611	74.2428	45.9115	0.7859	-72.2457
Diming	11	531	30	66.1681	58.8258	3289	93.6745	46.177	0.8701	-77.8319

Figure 5-15: Table of region properties of threshold shape when leaning right.

LOOK UP TO REAR VIEW MIRROR				Centroid						
Name	Test No.	Data from Frame No.	Face thresholding value	x co-ordinate	y co-ordnate	Area	Major Axis Length	Minor Axis Length	Eccentricity	Orientation
			degree C	pixel	pixel	pixel	pixel	pixel	pixel	pixel
Amjad	1	7	30	45.3032	55.0496	2599	92.7549	42.6856	0.8878	-80.6746
Andy	2									
Bilal	3	695	30	58.5723	54.1946	2076	79.2906	39.4312	0.8676	-79.6376
Faraz	4									
Gavin	5									
Imran	6									
James	7									
Mark H	8	356	30	56.337	55.5354	3442	96.5248	46.2458	0.8778	-81.8453
Stephen	9	12	30	63.5096	71.1215	2651	76.4243	46.0922	0.7977	-87.247
Val	10	383	30	66.2925	61.2369	2537	74.3617	46.9243	0.7758	-89.8159
Diming	11	11	30	60.0979	55.4536	3117	92.1757	44.782	0.8741	80.8574

Figure 5-16: Table of region properties of threshold shape when looking up.

HEAD ON OR NEAR STEERING WHEEL				Centroid						
Name	Test No.	Data from Frame No.	Face thresholding value	x co-ordinate	y co-ordnate	Area	Major Axis Length	Minor Axis Length	Eccentricity	Orientation
			degree C	pixel	pixel	pixel	pixel	pixel	pixel	pixel
Amjad	1	190	30	85.4143	98.1571	70	12.72	7.9722	0.7792	38.0184
Andy	2	347	30	55.7573	85.7791	824	60.1727	21.906	0.9314	-1.863
Bilal	3	850	30	64.7251	85.8827	1986	67.8577	58.6054	0.5041	-10.7388
Faraz	4	781	30	52.3745	92.9236	275	19.0173	18.5585	0.2183	-31.4442
Gavin	5	463	30	40.9928	77.555	555	109.4191	67.2812	0.7886	78.1594
Imran	6	304	30	57.9696	74.4942	2503	62.1275	52.2685	0.5406	-84.3945
James	7	498	30	51.3586	93.8956	1082	58.8136	26.5427	0.8924	-6.5942
Mark H	8	767	30	66.3387	75.1707	3797	74.5907	66.4645	0.4539	-31.3614
Stephen	9	313	30	48.5095	83.896	1894	53.9751	47.4502	0.4766	-4.3186
Val	10	663	30	73	85	9	10.3923	1.1547	0.9938	90
Diming	11	422	30	67.0277	71.6013	3283	73.1241	60.9745	0.552	-80.004

Figure 5-17: Table of region properties of threshold shape when head is on steering wheel.

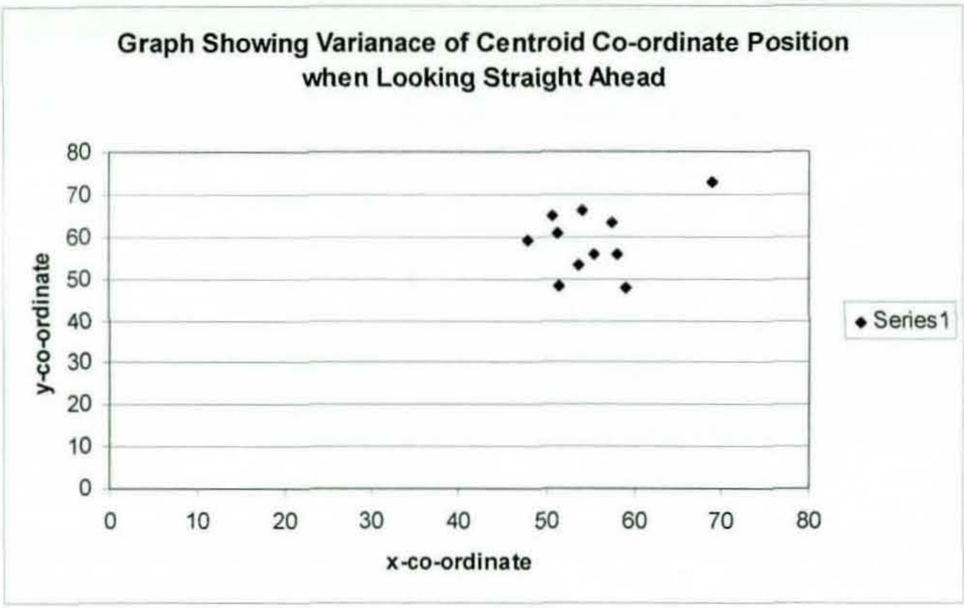

Figure 5-18: Centroid positions when looking straight ahead.

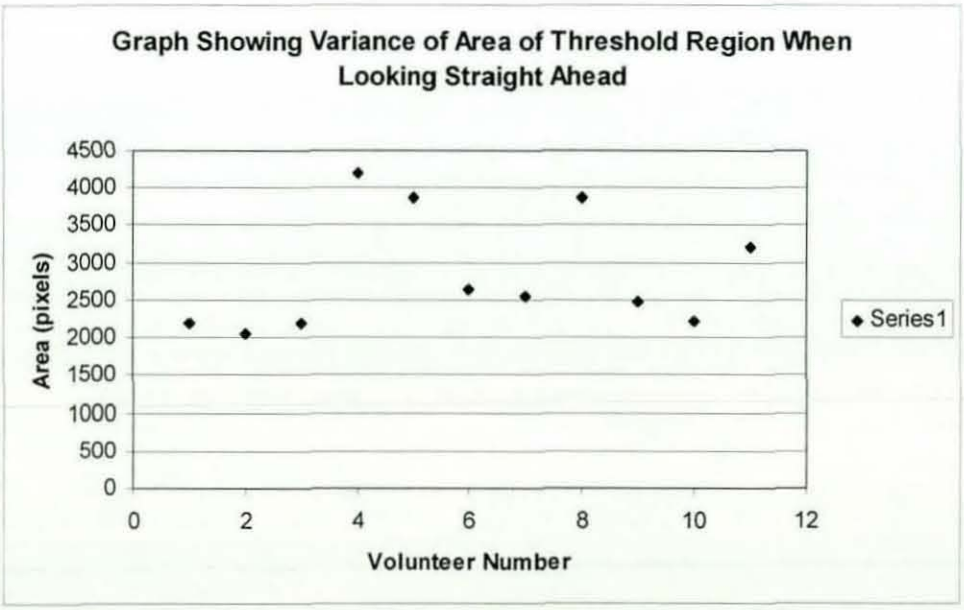

Figure 5-19: Area variation when looking straight ahead.

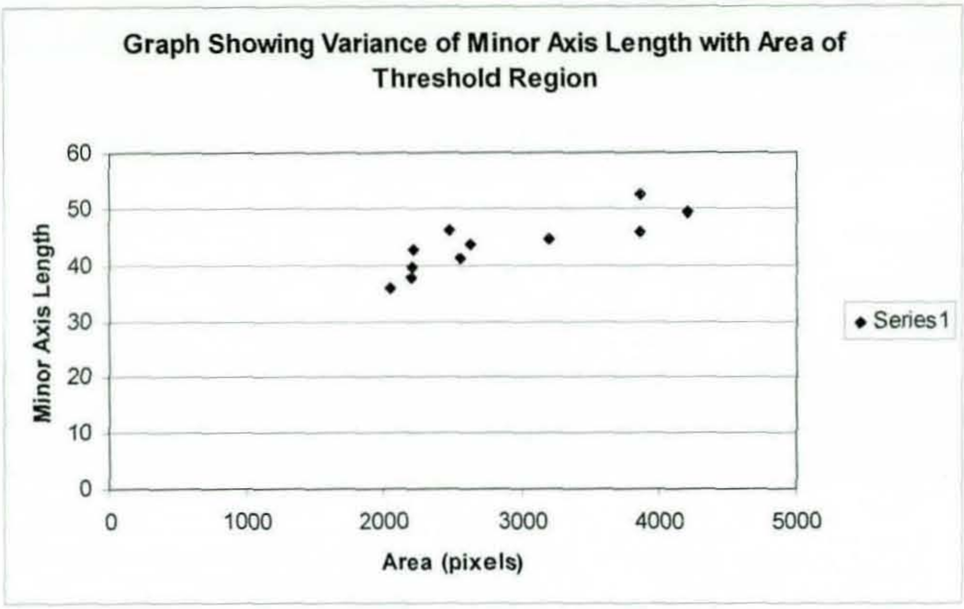

Figure 5-20: Minor axis length variation when looking straight ahead.

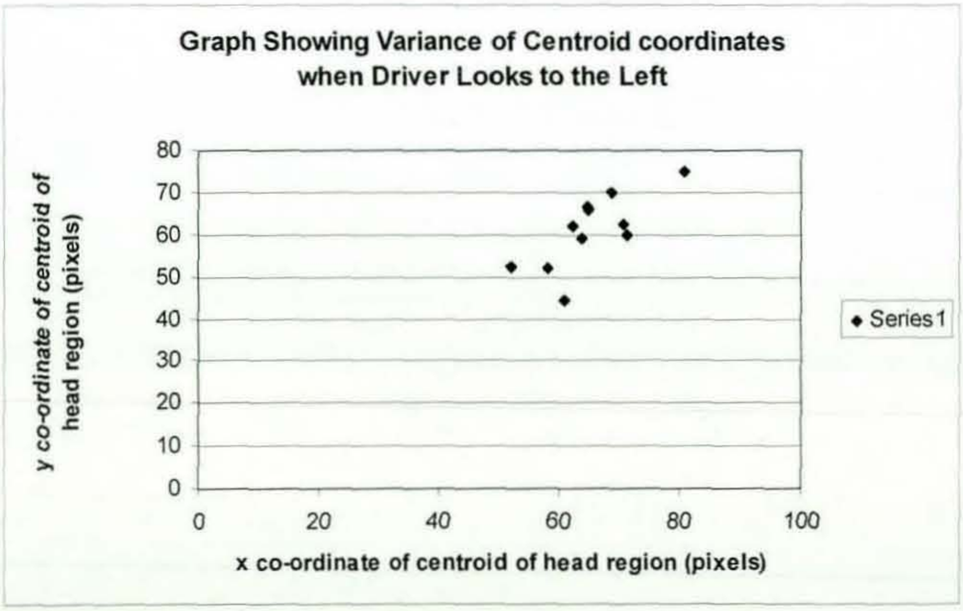

Figure 5-21: Centroid variation when looking to the left.

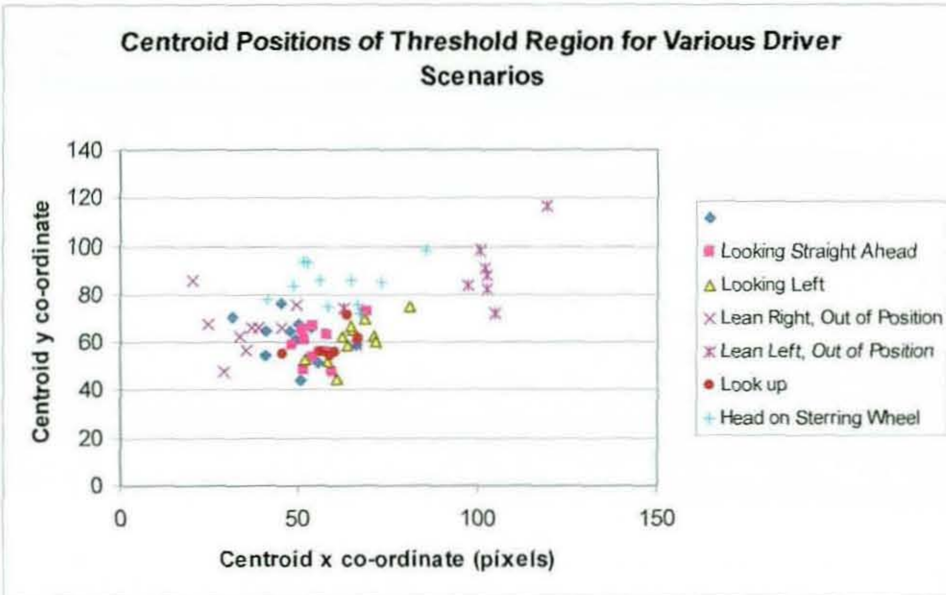

Figure 5-22: Centroid position for multiple driver scenarios.

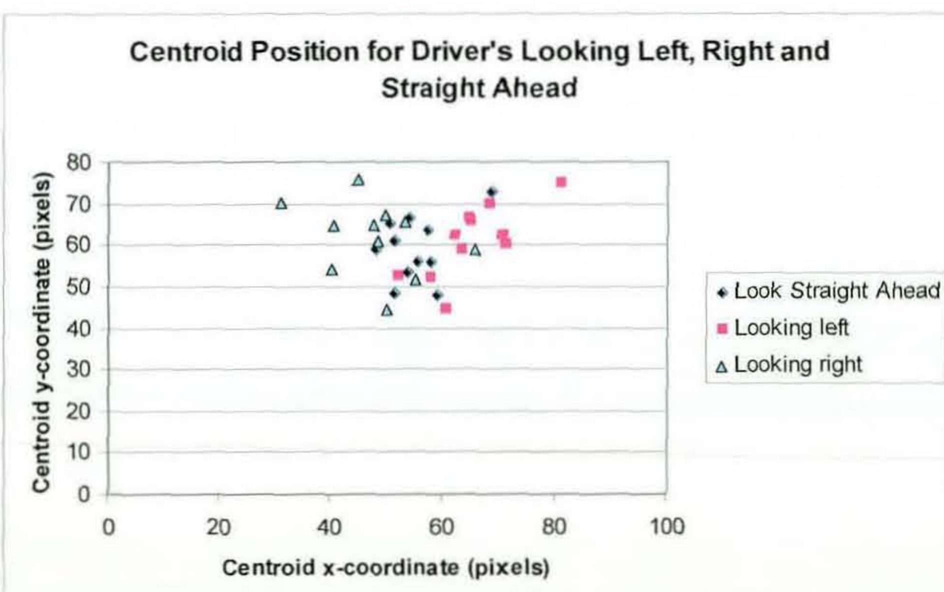

Figure 5-23: Centroid position when looking to the left, right, and straight ahead.

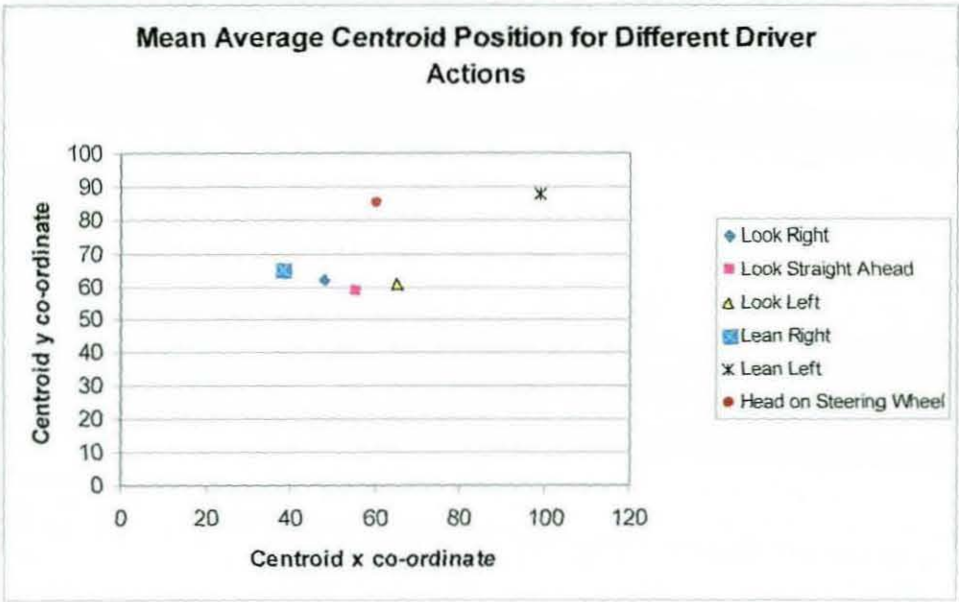

Figure 5-24: Average centroid positions for multiple driver scenarios.

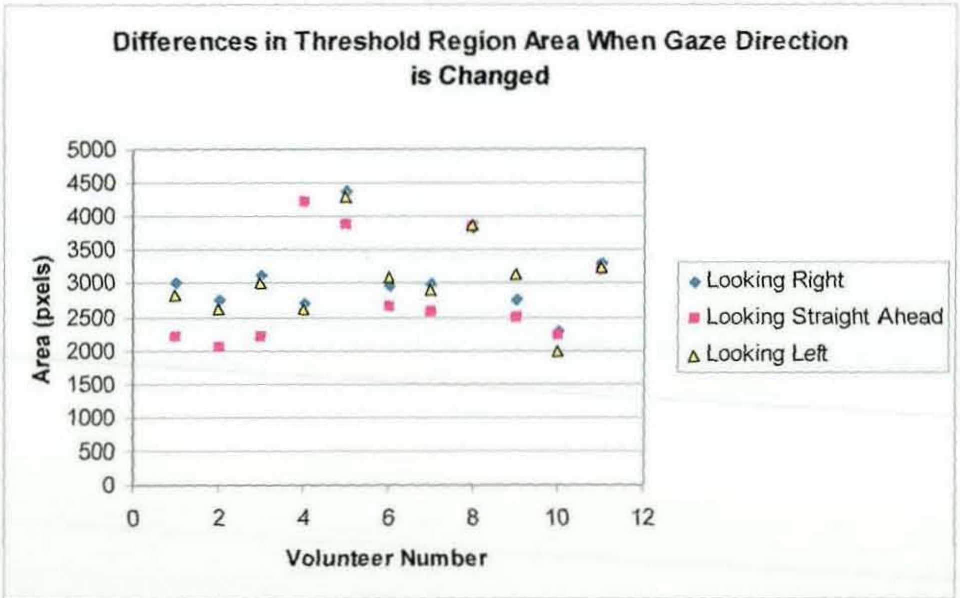

Figure 5-25: Area variation for multiple driver scenarios.

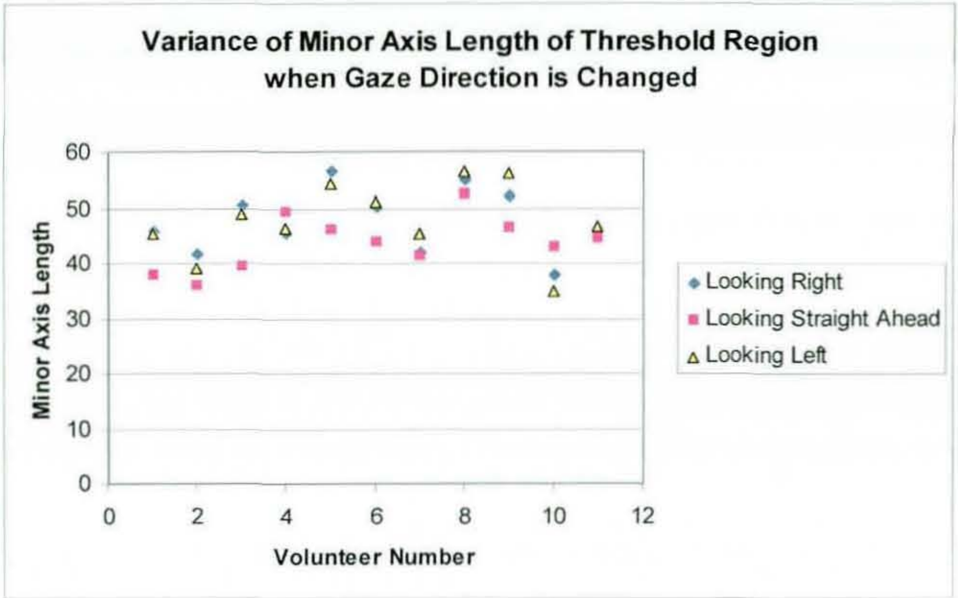

Figure 5-26: Minor axis length variation for multiple driver scenarios

5.7 Discussion of the Graphs

Figure 5-18, showing the centroid position when the volunteer driver was looking straight ahead, illustrates a varied pattern of x and y co-ordinates, but it can be said that they mostly lie within the 50-60 x co-ordinate band, and the 45-70 y co-ordinate range. This concentration of centroid positions within a particularly defined region of the image does indicate that there is a similarity of driver head position and gaze directions for different driver height and build.

Figure 5-19, showing the head area variation throughout the volunteer population, shows a large variation with areas ranging from 2000 to 4000 pixels. This could be the result of the threshold temperature being set at 30 degrees Centigrade and some volunteers having lower facial skin temperature readings than others, thus resulting in an artificially smaller facial area due to the simplicity of the MatLab 'thresh' function.

There is as expected, a clear correlation between the Minor Axis length of the threshold head region and its area, as shown in figure 5-20. Most of the volunteers have a minor axis length, or head width (which is essentially what the minor axis length represents) in the 40 to 50 pixel range.

Figure 5-21, showing the variation of the centroid positions when the volunteer driver's gaze is directed the left, shows a spread of data points within the 60 to 80 x co-ordinate pixel range. This clearly demonstrates that there is correlation between the gaze direction of the volunteer driver and the centroid position of the threshold head region, and that this can be determined from the analysis of the resultant images.

Figure 5-22 and figure 5-23 present the centroid positions of the volunteer drivers when the driver exhibits numerous different eye gaze directions and head positions. In figure 5-23, which shows the centroid positions for the volunteer driver looking left, right and straight ahead, it is evident that the centroid position changes unmistakably as the driver volunteer changes his gaze direction. Therefore, centroid position can be used as a method for determining the driver's gaze direction. Figure 5-23 shows the average centroid position or different gaze directions and head movements and positions. It reveals that the centroid position shifts to the right when the driver looks to the right, to the left when the driver looks to the left and remains in the centre between these two data points when the driver's gaze is towards the road scene ahead. This is illustrated more clearly in figure 5-24, where the mean average centroid position for all the various gaze directions and head positions are presented. The average height of the three different gaze directions (to the left, to the right, and straight ahead) are on the 60 pixel mark which suggests that the head does not move up or down , but the x co-ordinate of the data points of all three gaze directions changes considerably. The average x co-ordinate when looking left is 65 pixels, compared to 55 pixels whilst looking straight ahead and finally the average for when the driver is looking to the right is 48 pixels. If the y co-ordinate had changed significantly, then it could be said that the driver's overall head position was changing, therefore indicating another driver activity or response. However, since the y co-ordinate for all three gaze direction data points is approximately 60 pixels, this does not apply in this case and therefore it can be argued that the this shows that the head has rotated slightly about the major length axis, i.e. turned towards a particular gaze direction.

The x co-ordinate when the driver leaned to the left is 99 pixels, whilst it is approximately 38 pixels when leaning right. This is a significantly large difference between the two and is considerably different the three different gaze direction positions than was mentioned before.

The centroid position for when the driver has brought his head towards the steering wheel seem like an anomaly. The x co-ordinate of 60 pixels is very similar to that of the driver looking straight ahead, but that is where the similarities end because the y co-ordinate of 85 is much higher than the 59 pixels value when the driver is sitting in his normal sitting position and looking straight ahead. This seems puzzling at first, as it would surely be expected that the y co-ordinate of the data points for when the driver has his head near the steering wheel to be less, and not higher than before. Perhaps this can be explained by the fact that as the driver pivots about his waist and brings his head down towards the steering wheel, the head is moved closer towards the thermal imager, thus enlarging the image of the head on the thermal image, and so the centroid will move higher up than when the driver is in his normal sitting position.

Figure 5-25 presents the apparent head area variation when the gaze direction is changed, and shows the areas to vary considerably between the 2000 pixel mark and the 4500 pixels mark. Ideally, the head area should remain the same regardless of whether the driver moves gaze direction or not, but in reality it does change because the rotation of the head to the left or the right exposes the side of the head, neck and other parts of the head, thus increasing the effective skin surface area exposed to the thermal imager, thus increasing the threshold region area. This is borne out by the spread of the data points on the graph. The data points corresponding to the driver looking straight ahead is generally the lowest with most points being between the 2000 and 2500 pixels mark, whilst the left and right side gaze direction data points have higher values and area almost identical to one another.

Figure 5-26 displays how the Minor Axis Length varies for varying driver gaze directions. As can be seen, the data points for the scenario of the driver looking straight ahead have the lowest Minor Axis Lengths of the three.

5.8 MatLab Detection System

Weight, height, and overall size of the volunteer driver are significant factors to investigate in the search for better understanding and solving of airbag related incidents. However, by far the most important factor according to the NHTSA, is the distance between the steering wheel and the driver/occupant measured linearly between the centre of the airbag cover compartment and the breastbone of the occupant. This in turn means that the position of the driver relative to the fixed in – car furniture such as the dashboard, steering wheel and the controls is the most important factor to consider firstly, in the pursuit of a viable airbag safety system. As has already been described by the NHTSA, if the occupant is closer than 10 inches (measured linearly between the steering wheel central console and the breastbone of the driver), then he is at risk of serious injury and even death.

Once the images were captured using the data acquisition software, and stored, the next priority was the examination of the images. Processing of the images was done using the commercially available MatLab version 6.5 software. The data images were stored in a portable external hard disk and transported back to the laboratory for further processing offline.

The rationale behind analysing the image data was to detect the principal information contained within the images themselves. The information to be detected was:

- Linear position.
- Gender.
- Size.
- Driver actions inside the vehicle (e.g. look left, lean forward).

One important point that needs to be made is that the detection of different factors and driver actions inside the vehicle are easily done by human visual inspection and the thought processes of the brain. However, the goal was to automate this process using a stand alone computer based system that would replicate this process to some degree. A human, for example, is able to distinguish whether the occupant driver in the image shown is leaning forwards towards the steering wheel, and is able to perceive that this is different to the image of a driver sitting back against the backrest of the car seat. The human is able to recognise this by relying on past experiences and making appropriate estimates as to the likely position of the driver from viewing a random sample of images. However, this is beyond the scope of a computer as it has not the experiences of the human, and cannot make a judgement as to what one particular image represents and what the response should be to that image. The computer needs to be programmed in order to be able to do this. This is where artificial neural networks become very useful, as thy allow the user to 'train' the network into recognising certain patterns through repeated learning. This will be explained in chapter 6.

For MatLab infrared detection, the variables that could be deduced were:

- Linear longitudinal position between the steering wheel, or the closeness of the driver to the steering wheel.

- Driver's head, body apparent size is larger than when the driver is sitting back onto the backrest.

- Higher average temperature of the image is detected when the driver is leaning forward and thus filling the image with the hotter parts of the face.

- Lower number of 'cold' or background pixels in the image when the driver is close to the steering wheel and the thermal imager.

- Changing position of the 'hot' and 'cold' pixels when the driver moves into a different position in successive images.

- Width of the driver's head increases when the driver leans forward to the steering wheel and the thermal imager.

- Apparent height of the driver increases when the driver is closer to the steering wheel. This is true for cases when the camera is mounted straight ahead, in front of the driver.

5.9 Visual Warning System

The next step after the driver position and behavioural information has been determined from the images is to display the corrective action instructions. In a real car, this would entail the airbag to be switched off by a command from the airbag safety system. However, since this system has not been built yet, other methods had to be employed to do this, and the simplest method to show this was to have an on screen display showing the corrective action required.

5.10 MatLab Functions

Using some simple reasoning, it was possible to write some functions in MatLab that would be able to detect specific characteristics of the occupant within each frame.

The smart airbag system is required to first be able to tell whether there is an occupant present in the driver or front passenger seat or not. To do this, a simple MatLab function was written using an IF argument as the basis of the function. It works by using the assumption that a human occupant will exhibit thermal radiation which can be 'seen' by the thermal imager, whereas an unoccupied seat will exhibit little or no thermal radiation greater than the background level. Therefore, in the function script below, the programme is asked to find a pixel within the centre of the image which is greater than 30°C, the lowest value for skin temperature detected using this thermal imager in the trials. The centre pixel was used as this from experience, this would be located within the facial region of the occupant in the image, the hottest part of the image. This was a reasonable technique to use as the face of every image of the driver looking straight ahead covered the centre pixel of the image, and this was usually the hottest part of the image for a random selection of images which were examined. However, further testing would be needed to establish whether this is the case in all instances.

```
function y = detect(x, t)
% AVERAGE Mean of vector elements.
% AVERAGE(X), where X is a vector, is the mean of vector
elements.
% Non-vector input results in an error.
[m,n] = size(x);
if (m<=1 | n<=1)
    error('Input must be a 2D matrix')
end
y=x;
for i=1:121
    for j=1:121
        if x(60,60)>30;
           disp 'living occupant detected';
        else
            disp 'no occupant detected';
        end
    end
end
```

A similar assumption was used for the following function. This assumed that if the occupant was leaning to one side, either to the left or to the right, this would be shown in the thermal image by high temperature pixels located either at the extreme left or the extreme right of the image, and this would indicate that the driver's upper body position had moved in that frame, thus causing the smart airbag system to recognise that the occupant was in an 'out of position' situation, and so the airbag should not fire. It was felt that this was a reasonable strategy to employ. Taking into account the low resolution of the images, some definite patterns needed to be detected, and a cluster of 'hot' pixels on the extreme right or left of the image would suggest that the driver's position had indeed changed from his default position of sitting in the centre, looking straight ahead. If the images were of a higher resolution (i.e. had more pixels), then a distribution analysis would be more robust perhaps.

```
function y = detect(x, t)
% AVERAGE Mean of vector elements.
% AVERAGE(X), where X is a vector, is the mean of vector
elements.
% Non-vector input results in an error.
[m,n] = size(x);
if (m<=1 | n<=1)
    error('Input must be a 2D matrix')
end

if x(60,60)>30;
            disp ('living occupant detected');
else
             disp ('no occupant detected');
end


if x(60,115)>30;
    disp ('occupant leaning to the left');
if x(60,5)>30;
    disp ('occupant leaning to the right');
else
    ('occupant positioned in centre');
end

end
end
end
```

The function below is slightly more sophisticated as it can detect whether the driver's head is slightly positioned to the left or to the right, i.e. whether the driver is looking to the left or to the right. This is done by assuming that the face of the occupant is normally in the centre of the image, with both left and right halves of the face equally positioned on the left and the right of the imaginary vertical centre line running down the middle of the image, and that there is an equal and opposite area of the facial region on the two sides. Again due to the low number of pixels per image, a simplified approach was best employed. However, it is acknowledged that this approach would have problems dealing wit exceptional circumstances such as if the camera is misaligned and offset, or if the driver had an unusual feature such as the wearing of an eye patch.

From visual inspection of images where the driver is looking to the left or to the right, a slight shift in facial area is visible to the naked eye. For example, when the driver looks to the left, the head turns to the left and the majority of the facial and head region visible in the image has now moved to the left of the imaginary vertical line, or it can be said that the centroid of the facial region has shifted to the left. This principle has been used in the function below. Again using an IF argument, it calculates the mean temperature of the left side and the right sided of the facial region either side of the imaginary line, and whichever side has the highest average temperature, then it concludes that the majority of the facial region resides on that side of the imaginary line and therefore concludes that the driver is looking in that direction. The evidence for this is that this function was tried on a number of different images where it was known that the driver was looking to the left or to the right, and it predicted the correct driver action in the vast majority of cases. However, further work would need to be done in order to 'tune' this function to provide the correct answer in all cases.

```
for i=1:121
    for j=1:121
        if mean(mean(x(:,20:59)))>mean(mean(x(:,61:80)))
            disp('drivers head leaning right')
        else
            disp('drivers head leaning left')
        end
    end
end
```

Below is a short function that is programmed to determine whether the occupant is wearing eyeglasses or not. From viewing many different images of occupants with and without eyeglasses or spectacles, an imaginary bounding box can be drawn onto a random image whose boundaries would encompass the occupant's eyeglasses, should he be wearing them. Also from analysing some of the images, the eyeglasses are shown as circular/elliptical blobs near the top of the face, and the temperature of this region is much lower than the temperature of the rest of the face, approximately in the region of 26°C, plus or minus 1 degree Celsius, compared to the face and the head which is over 30°C for all occupants. Therefore, the function was programmed using a simple IF argument which states that if a pixel within the bounding box region is within a certain temperature range (in this case between 25°C and 27°C), then this would mean that a cooler temperature object was present within this region, with a high probability of this object being a pair of eyeglasses. Therefore, if this was detected, then the output should display that the eyeglasses have been detected, otherwise it should display that there are no eyeglasses present within this region. This is shown in the script below. The function is called 'detect8'. As can be seen, the logic contained within this function is very simple. The 'x' refers to the image as a matrix. Lines 2 to 8 ensure that the input 'x' is given as a 2 dimensional matrix, otherwise the function will give an error message.

```
function y = detect8(x)
% AVERAGE Mean of vector elements.
% AVERAGE(X), where X is a vector, is the mean of vector
elements.
% Non-vector input results in an error.
[m,n] = size(x);
if (m<=1 | n<=1)
    error('Input must be a 2D matrix')
end

if 25<max(max(x(25:45, 30:70)))<27
           disp ('spectacles detected');
       else
            disp ('no spectacles detected');
        end
```

5.11 Summary

These functions would be run on the MatLab programming screen and show the result of the function as a one line sentence on the screen, indicating whether one of the statements about the driver in the image is true or not. For example, in the function labelled 'detect 8', the user will see on the screen of the computer either 'spectacles detected' or 'no spectacles detected'. This is because the function has a statement which 'tells' it to 'disp (spectacles detected')' or to 'disp ('no spectacles detected')' on the command screen.

It was clear, however, that this approach was limited in the sense that it relied too heavily on human visual perception to make the distinctions between the images, and also the scope of what these functions could detect was also limited. This was because it relied on large changes being observed with regards to the distribution of the hot and cold pixels within the image. A more nuanced method was needed in order to detect more scenarios, and also one which was autonomous, as the eventual goal was to have a system that could detect and make decisions without the need for human involvement, and an example of this was required in order for this project to be successfully moving towards that goal.

The reasons why artificial neural networks were used as the main method of analyzing the processed image data is also explained. An explanation is also given as to why neural networks were chosen ahead of other contemporary types of artificial intelligence such as fuzzy logic.

The results of the analysis are presented in chapter 6 and a commentary is given so that the reader is able to understand the importance of the results that he is reading. This leads onto chapter 7, the conclusions of the entire body of the work. The results are stated in clear terms.

Chapter 6 Use of Artificial Neural Networks (ANN)

This chapter will explain the work done on understanding and implementing ANN on aspects of the experimental work done on this project. It will provide background knowledge on ANN, how they came into being, what they can be used for and how they will be applied here. The results of the ANN are presented here in this chapter and discussed at length. (A number of sources were referenced and used for this section **[103 - 105]**.)

6.1 Background

The inspiration behind neural networks and the whole field of artificial intelligence in general was research done in the 1960's and onwards, when researchers and scientists tried to replicate the human brain's neural systems with simple models **[103]**.

The human brain has over 10 billion (10,000,000,000) neurons which are connected together, with each neuron being connected to another by thousands of interconnections.

A neuron can be considered to be a specialised cell which produces an electrochemical signal. The branching output structure of one cell is connected to the dendrites (branching input structures) of another cell via a synapse. An electrochemical signal is transmitted along the axon when a neuron is activated. The signal is transferred along the synapses onto other neurons, which can also transmit an electrochemical signal, if the signal received from the dendrites exceeds the 'firing threshold'. The signal strength received by a neuron, and by implication, its probability of transmitting a signal, is dependent on the efficacy of the synapses. The synapse itself actually contains a gap over which a neurotransmitter sends a signal. It has been considered by others such as Donald Hebb that the act of learning could be achieved by altering the strength of synaptic connections. One such experiment to test this theory was the 'Pavlovian Dog' experiment into conditioning. It basically involved a bell being rung just before the dog was given food every day. This process was continued over a period of time, and so over time, the dog came to realise that the ringing of the bell was a signal that food was about to be served.

It must be stressed that an artificial model of the human biological neural system cannot be reproduced at the present time of writing, nor is it likely in the foreseeable future. Nevertheless, by using a number of simple units which are capable of being programmed to perform a weighted sum of its inputs and then transmitting a binary signal if a certain sum total has been reached, then complex models and accurate results can be accomplished.

6.2 Definition of an Artificial Neuron

A neuron receives a number of inputs, and these inputs can either be from the output of other neurons, or from original data. An input comes from a connection that has a certain 'weight', and this weight represents the synaptic efficacy of a biological neuron. There is only one threshold value per neuron, and 'activation', or 'post-synaptic potential' (PSP), of the neuron is calculated by subtracting the threshold value from the weighted sum of all the inputs. The output of the neuron is produced by passing an activation signal through an 'activation function', otherwise known as a 'transfer function.'

6.3 Why Use ANN?

Neural Networks can accurately model complex functions and systems accurately. They also are non-linear models which are very useful when linear approximations are not valid in certain circumstances. Another reason to use ANN is their ease of use. The usability of a neural network is very high because they 'learn by example'. The user does not need any detailed knowledge to use it, which he would need to do if he were trying to apply linear statistical methods to a problem. The basic requirement for the user to be able to competently apply neural networks is that he should be able to select appropriate data, select a neural network fit for the job, and to be able to interpret the results correctly **[104]**.

The problem solving ability of ANN should not be ignored either. The ANN is able to confront, and in most cases, solve problems without prior knowledge of the probability distribution of the data produced by a process. They learn by example and can recognise these patterns or correlations in other data sets, patterns that are too complex to be recognised by human perception, or indeed other computational techniques. They are commonly used in the following:

- Pattern recognition
- Pattern classification
- Function approximation
- Optimisation

The major advantage is that the ANN has the ability to solve a problem more accurately and faster than human capabilities, and when the data suffers from noise and incompletion. Other types of artificial intelligence (AI) were considered, such as 'Fuzzy Logic' which is becoming an increasingly popular tool amongst researchers. However, a decision was made to use ANN for two reasons. One, ANN has been available for many more years than Fuzzy Logic, and can therefore be said to be a 'tried and tested' tool. ANN has also been used in critical application in the past successfully, for example, they have been used in banking trading systems and also in the computer systems in flight decks within aeroplanes. This track record strongly suggests that ANN is a reliable tool to use, and reliability is thought to be essential for any safety system. The second reason is that it was found that the outputs from both ANN and Fuzzy Logic were similar in that they would ultimately produce a number which would either be very close to the 'target' number, therefore signifying that the AI tool had successfully recognised the pattern and made the correct choice. Conversely, if there was a large difference between the number that the AI tool produced and the target number, it would suggest poor pattern recognition by the AI tool. Since the outputs were similar in format, Fuzzy Logic did not offer any significant advantages over ANN and so ANN was used as the sole AI tool in this project.

6.4 The Backpropagation Neural Network

Literature reviews have shown that the most commonly favoured neural network structure is the so called 'backpropagation' neural network or the 'feed-forward backpropagation' (FFBP) network. Due to their simplicity and their effectiveness, they have been used in a wide range of important applications such as:

- Voice recognition
- Medical diagnosis
- Automatic control
- Image pattern recognition

One slight drawback is that it is also a network which requires supervised 'learning'. It has 'n' number of neurons connected together to form an input layer, a hidden layer and an output layer. An example of a simple feed-forward neural network is shown in figure 6-1, [reproduced from the book 'Artificial Intelligence Illuminated' by Coppin] **[105]**,

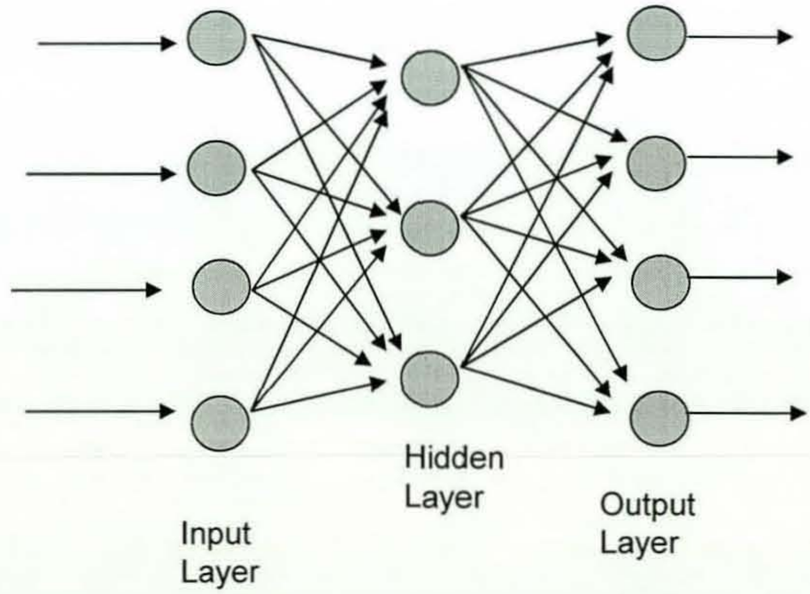

Figure 6-1: Schematic diagram of a feed-forward neural network

Backpropagation is a widely used algorithm for training a 'multi-layer perceptron' (MLP) under supervision. This means that the data inputs need to be trained to find certain user-specified targets in order to be able to create a good correlation between inputs and targets. Backpropagation is a 'gradient descent algorithm' which means that the weights are moved along the negative of the gradient of the performance function. The FFBP network was used in this case because previous work has shown that it produces reasonable results when it is faced with input data that it has never encountered before. It follows that it is possible to train a network on a representative set of input and output target pairs and be able to produce good results without the need for training the network on all the available input/output pairs. In the case of the ANN analysis for this project, where there was a limited supply of data, using the FFBP network was the correct network to select.

For a given problem, it is difficult to determine which of the many training algorithms to use, as deciding which one is best for a particular situation is dependent upon a number of factors, which are:

- the number of data points in the training set.
- the number of weights and biases.
- error goal.
- the purpose of the network – pattern recognition (discriminant analysis) or function approximation (regression).

After some research, a decision was made to use the Levenberg-Marquardt training algorithm, as its main advantage over the other training algorithms that were considered was that the Levenberg-Marquardt algorithm can resolve its training between 10 and 100 times faster than the others. This algorithm is also popular with other researchers in the field of pattern recognition, and with this track record, it was reasonable to use it for the purposes described in this chapter.

6.5 Issues with ANN

According to Zorriassatine **[104]**, there are a number of issues that need to be understood before tackling ANN, and these are:

Data Preparation for Training and Testing of ANN

The data used for training should highlight the patterns that should be detected. The pattern sets should be distinct, which means that they should not overlap one another, although in practice this can prove problematic.

The size of the data set depends on the ANN designer. Some choose to include large data sets or even all of the available data; others choose to use a small representative sample size. Having a large data set for training enables the network to view a large number of different changes, and is able to detect them later. However, this comes at the price of network solving speed, and may bias the network in favour of detecting large process changes, and may have trouble detecting slight but significant changes.

Feature Extraction

The purpose of feature extraction is to obtain characteristics which maximise the similarity of patterns in different classes.

Standardisation or Normalisation of Training and Simulation Data

This is important because it enables all the data to be standardised for data with different ranges and scales. The training and simulation data was standardised between the values 0 and 1.

Number of Layers

A typical ANN will consist of 3 layers, an input layer, a hidden layer and an output layer. Previous literature argues that a classification problem would need only 1 or 2 hidden layers, any more could lead to noise entering the network, requiring the need for a larger training set.

Number of nodes (Neurons)

It has been said by Zorriasatine's thesis review that the number of nodes or neurons that a layer has should be greater than 5 and less than 60.

Transfer Functions

The characteristics of the transfer function are largely responsible for the behaviour of a neural network. A transfer function can be used as a threshold device to limit the output of each processing element to a certain range, and it can also filter out small signals to prevent them from having an effect on the PR. Transfer functions can be linear or non-linear, symmetrical or non-symmetrical. In this project, a linear and symmetrical transfer function was used.

Problems of Training

Underfitting occurs when there is a large error on both the training and simulation data sets. The capacity of the network is too little, and so can only be trained with a small size training set of data.

Overfitting occurs when the capacity is large and performs very well to recognise the training set, but badly when it comes to the simulation set.

6.6 Neural Network Analysis Results – In-Car Driver Activity Detection

One of the goals of the ANN analysis was the detection of different types of driver movement (from which driver activity could be deduced) that a typical driver would conduct during the course of a car journey. The results of the analysis are presented below. However, some brief notes are needed to understand the results. There are 23 different graphs (see Figure 6-15 to Figure 6-37), one for each of the driver volunteers who took part in the experiments. There are two different graph lines shown in each figure. One graph line represents the 'targets' and is shown in **bold**. The targets were assigned to specify a different driver activity. For example, target number 1 would represent the driver 'looking straight ahead'. Target number 2 may be assigned to 'driver looking left', target number 3 may be assigned to 'driver leaning right', and so on. The second graph line represents the neural network simulation. This is from a completely different set of data which was inputted into the same neural network as the first 'training' set of data was inputted into, and the 'goal' of the simulation was determined. The 'goal' is a percentage inputted into the MatLab workspace to determine how close the simulation output had to be to the target. Naturally, it was desirable to ensure that that the simulation output was as close to the target as possible, but this had to be balanced by the need for the network to resolve itself, hence, it was decided to use the MatLab suggested figure of 0.01 as the value of the 'goal'.

If the simulated results match those of the first set of results, then it could be said that the neural network analysis is 100 percent accurate in detecting each type of driver position (hence diver activity) inside the car. It must be noted that the number of different types of driver activity that could be gleaned from the image files of the experimental trials varied for each volunteer. This was due to the fact that although all volunteers performed the same actions, some of the images captured were not of a high enough standard for processing. This occurred when there were only a few images of a particular driver position or activity within the dataset, and when these images did not show fully the head or face of the driver in the image. This meant that there was uncertainty as to what exactly the driver was doing, and so these images had to be discarded.

The MatLab neural network toolbox graphical user interface (GUI) is shown in Figure 6-2. As can be seen, it is very easy for the inputs, targets and network to be created using this GUI, as it saves time spent on writing text in the MatLab command workspace.

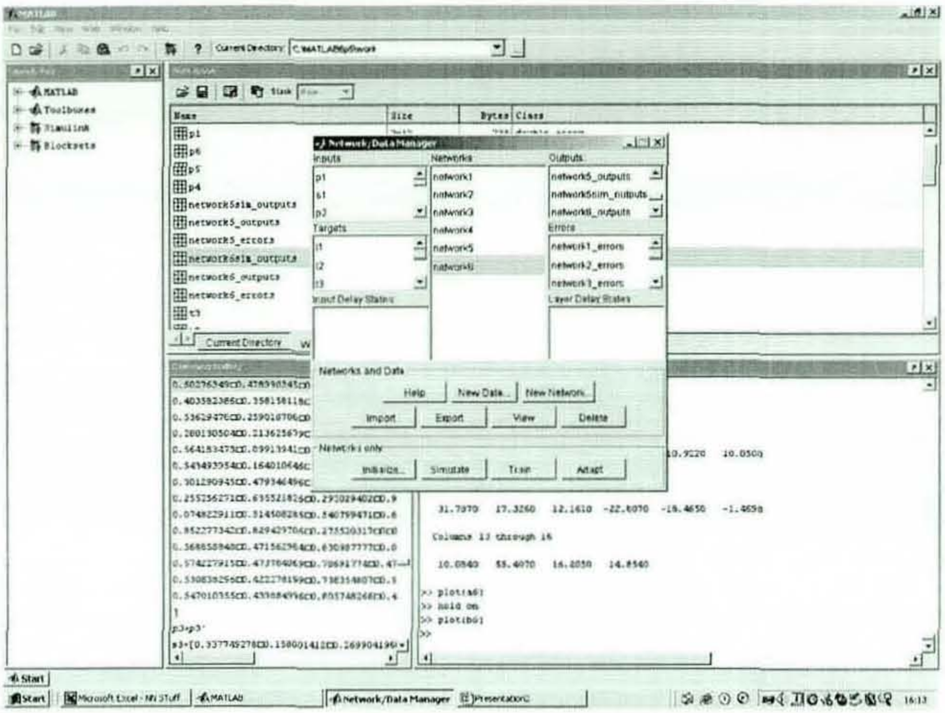

Figure 6-2: GUI of MatLab neural network toolbox being used.

An example of how the network resolves itself is given in figure 6-3. As can be seen, the network resolves itself very quickly at the start and the errors are reduced significantly, before the gradient of the graph flattens out considerably as the goal is slowly reached. In most cases, the training of the ANN was completed within 100 epochs, although this was dependent on the number of neurons, and the number of inputs and targets. A few networks took far longer to resolve themselves and an example of this is shown below:

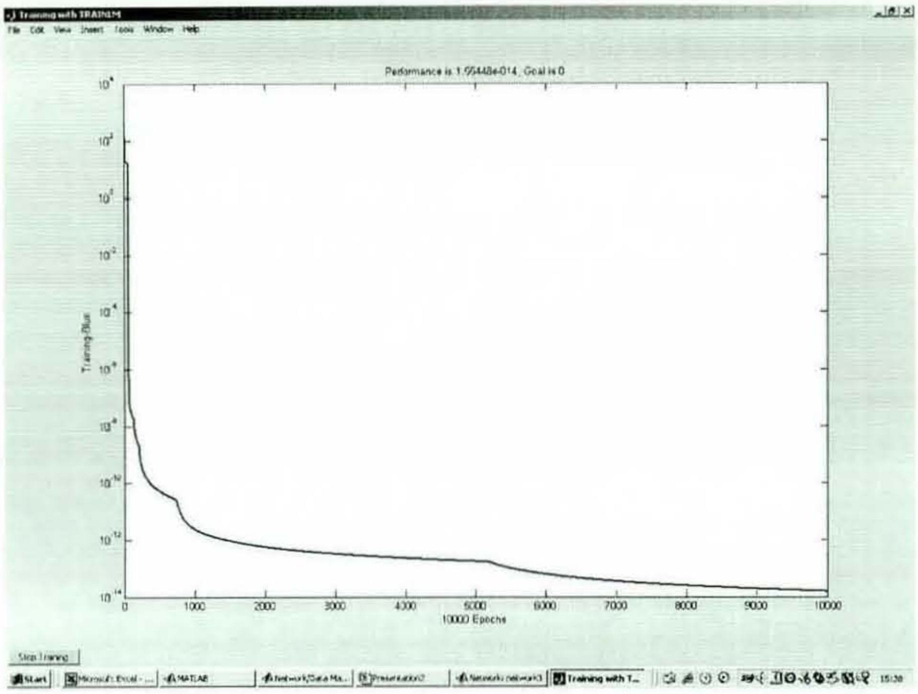

Figure 6-3: MatLab neural network training in progress.

In the following pages, the reader will see graphs (figures 6-4 to 6-14) which represent the ANN analysis work that was done using the 'regionprops' data obtained from the experiments on all the volunteers. This was for the purpose of detecting driver activity inside the car cabin. The y-axis of the graphs show the absolute difference between the target and its corresponding simulated output; and the x-axis shows the number of the volunteer diver. For there to be a good match, the difference should be small, although this was not the case sometimes, thus indicating a poor match.

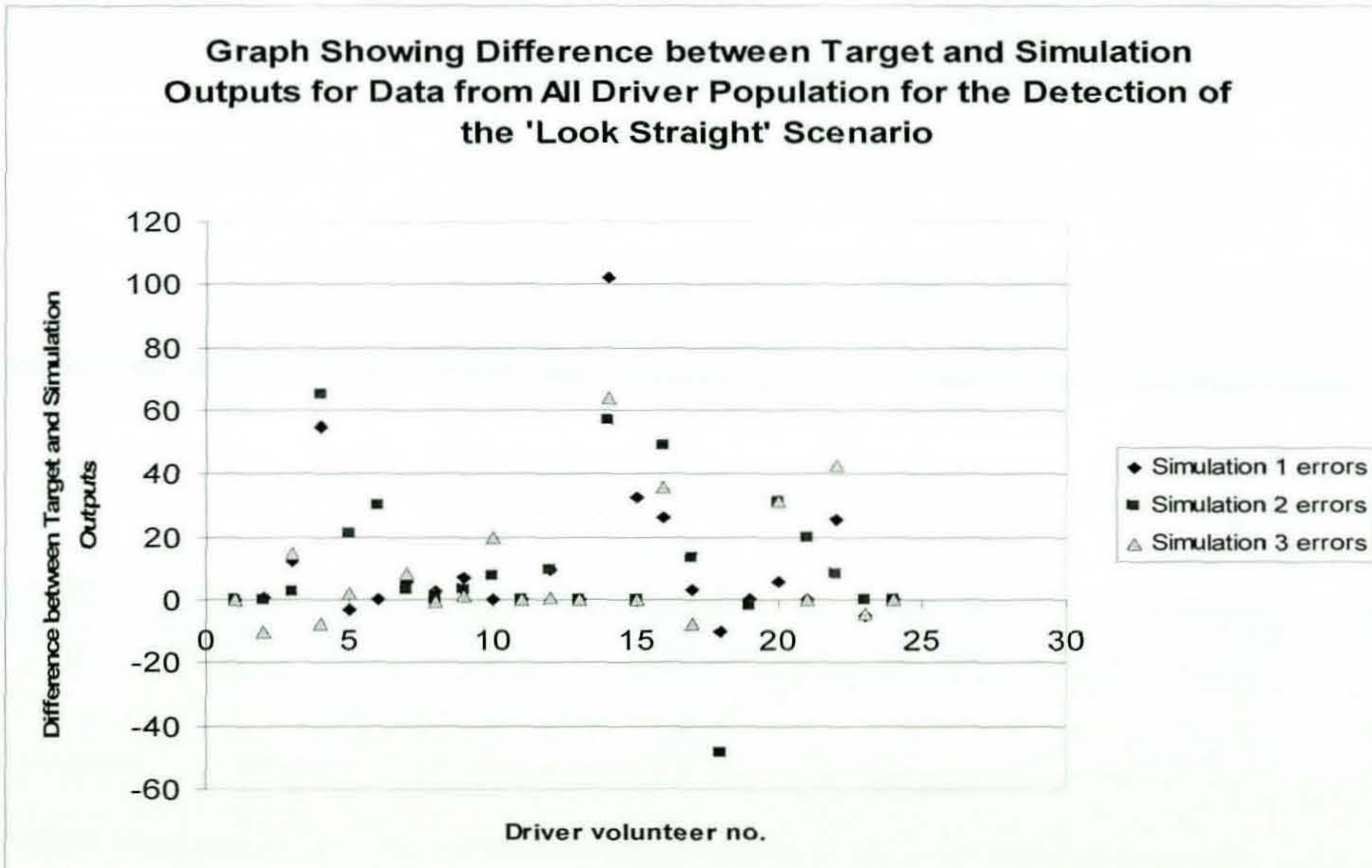

Figure 6-4: ANN Results to Detect 'Look Straight' Scenario

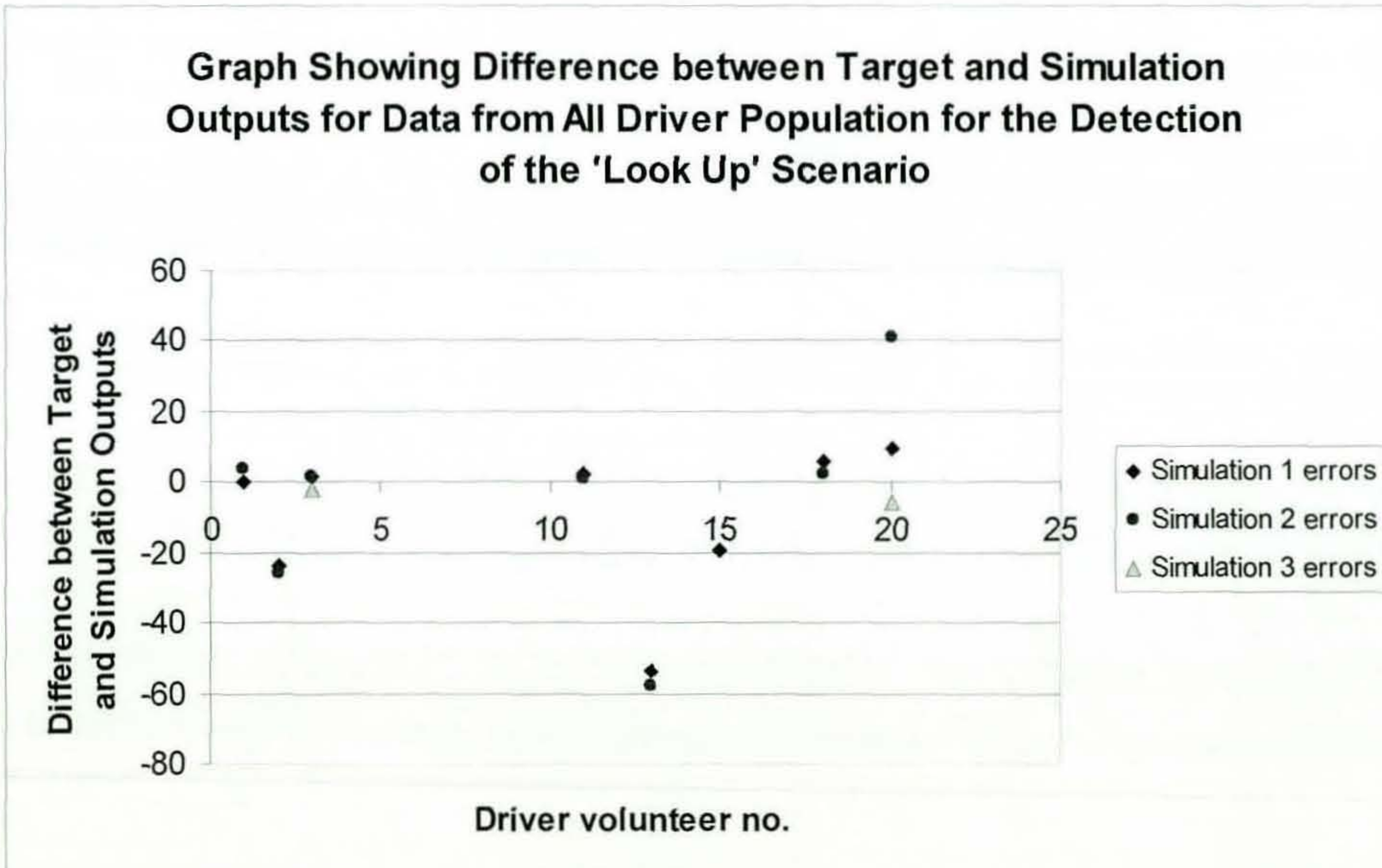

Figure 6-5: ANN Results to Detect 'Look Up' Scenario

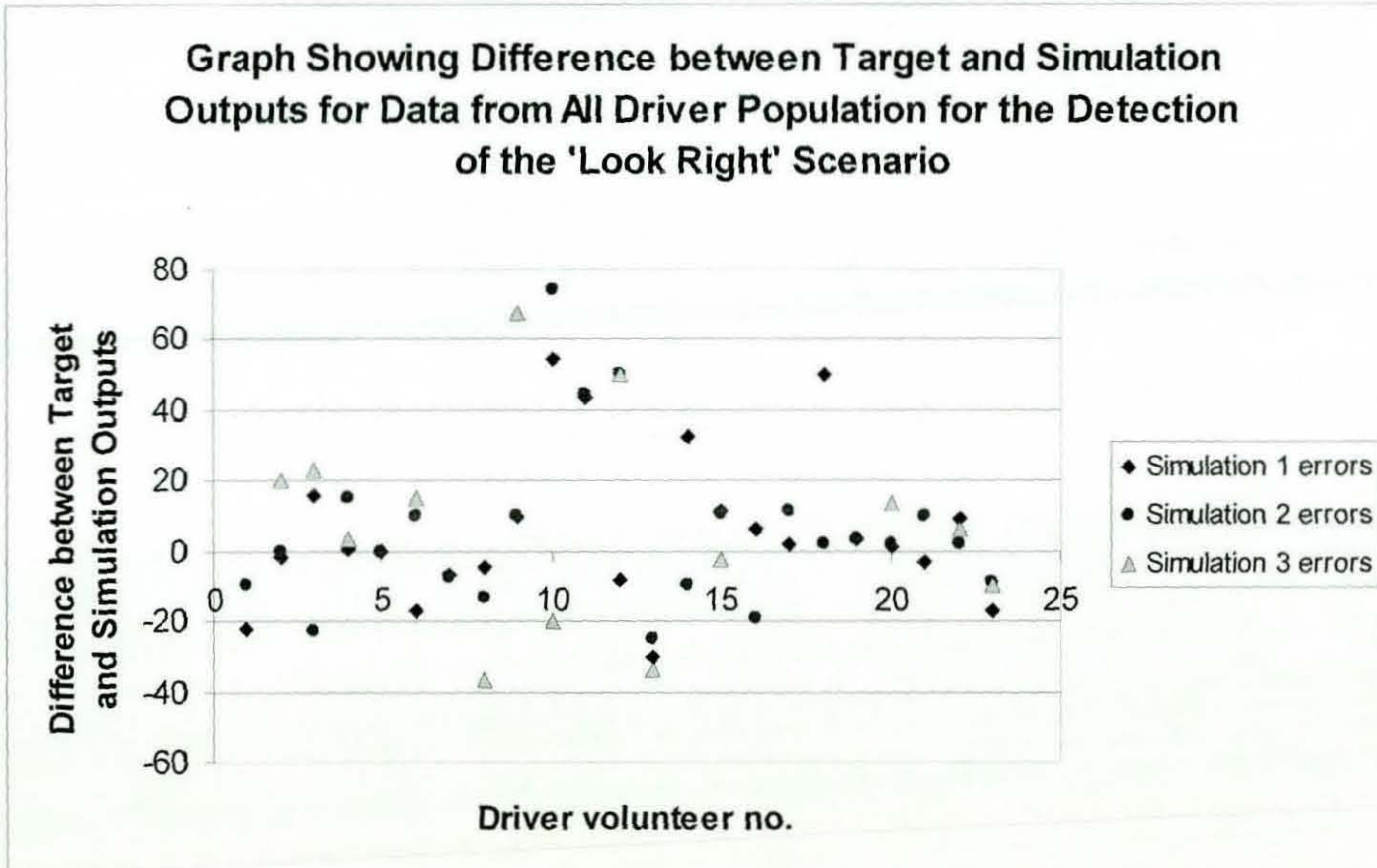

Figure 6-6: ANN Results to Detect 'Look Right' Scenario

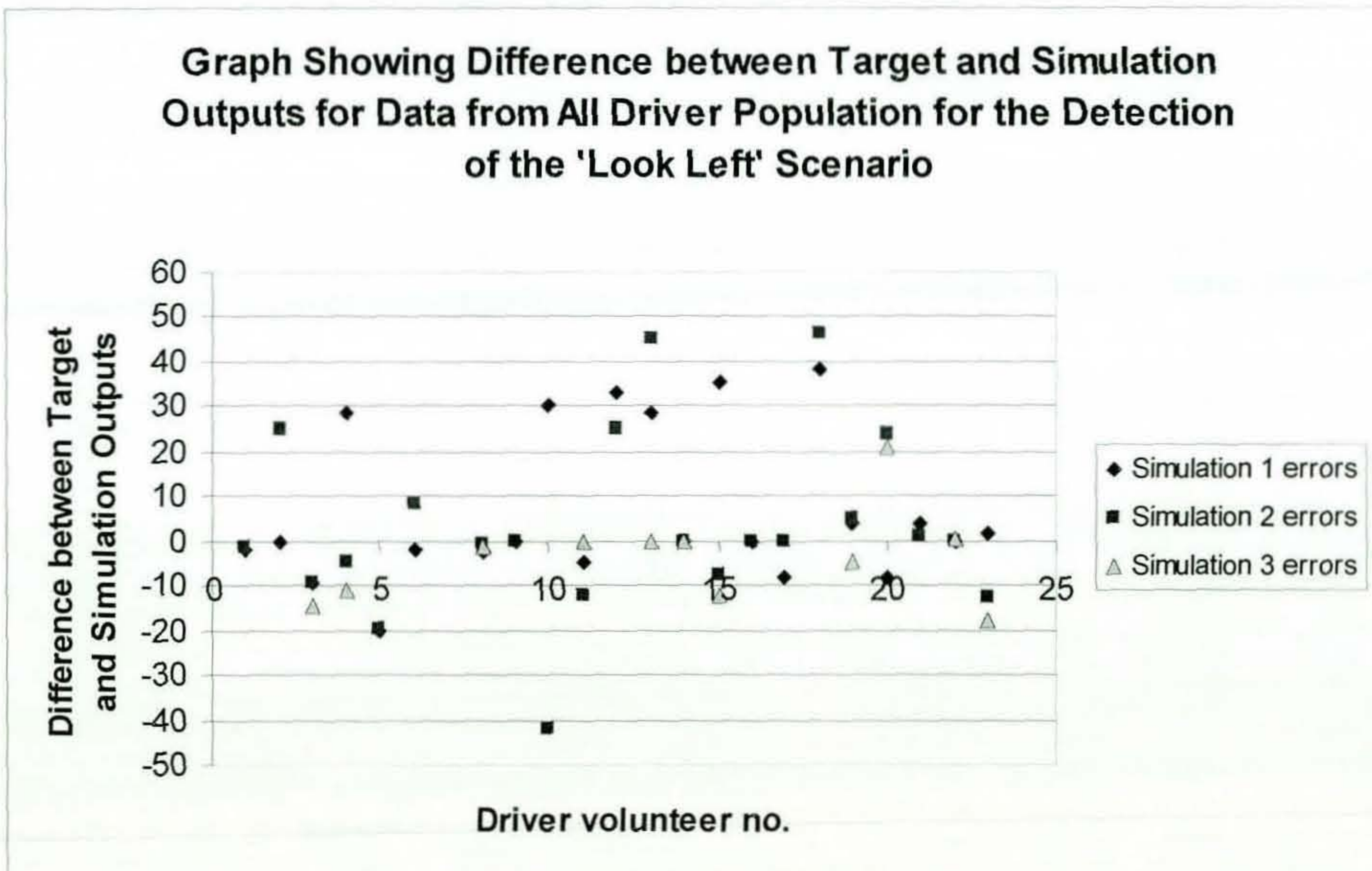

Figure 6-7: ANN Results to Detect 'Look Left' Scenario

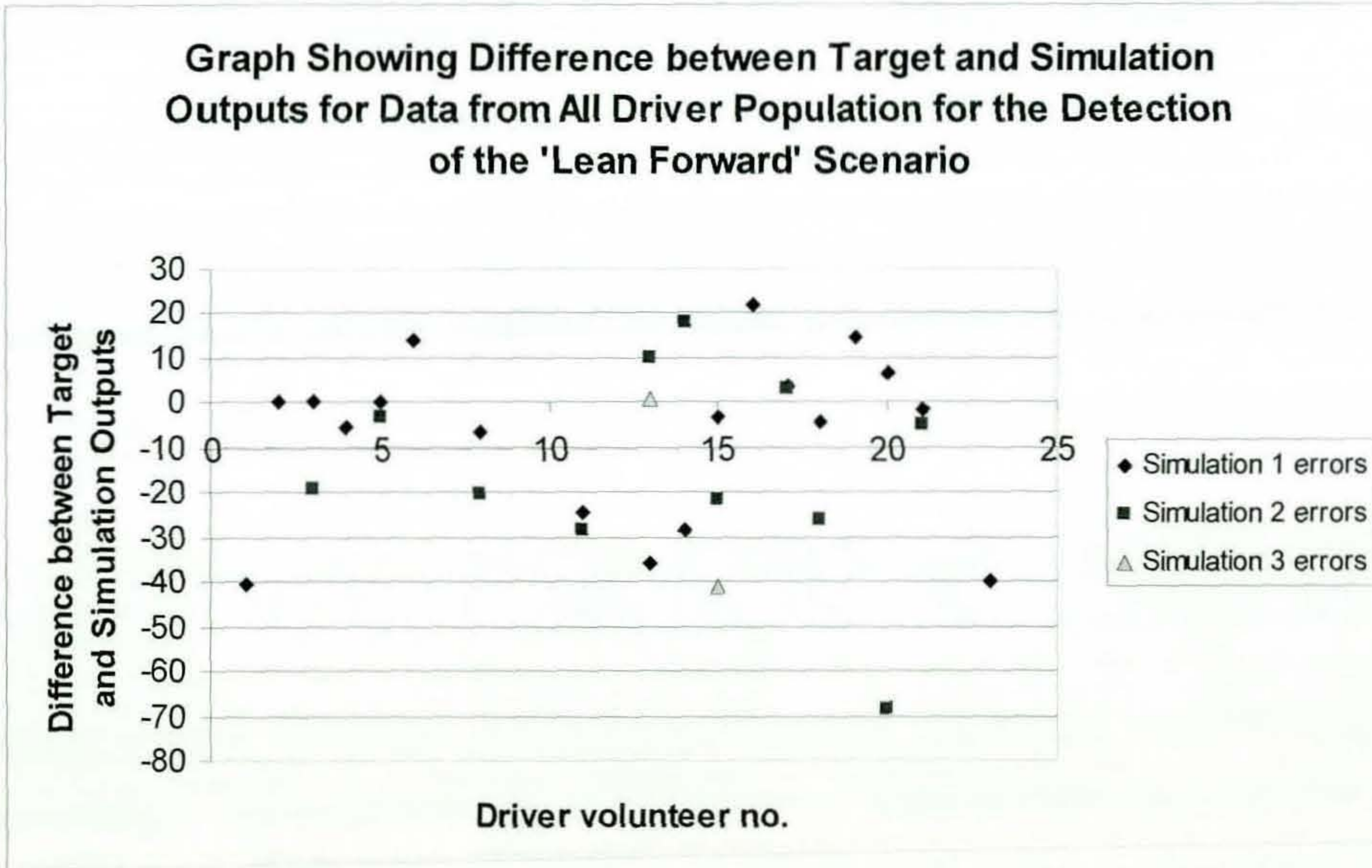

Figure 6-8: ANN Results to Detect 'Lean Forward' Scenario

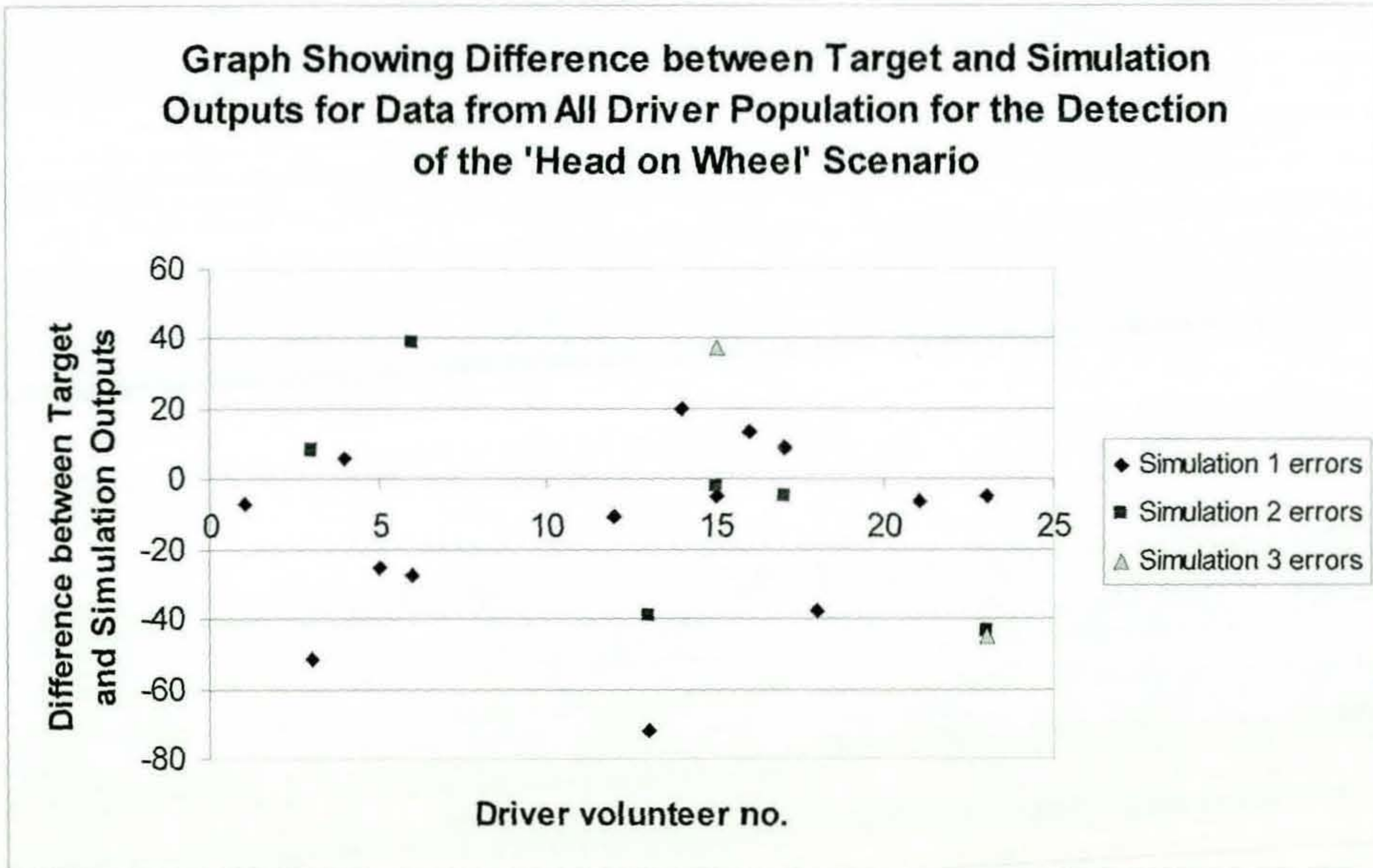

Figure 6-9: ANN Results to Detect 'Head on Wheel' Scenario

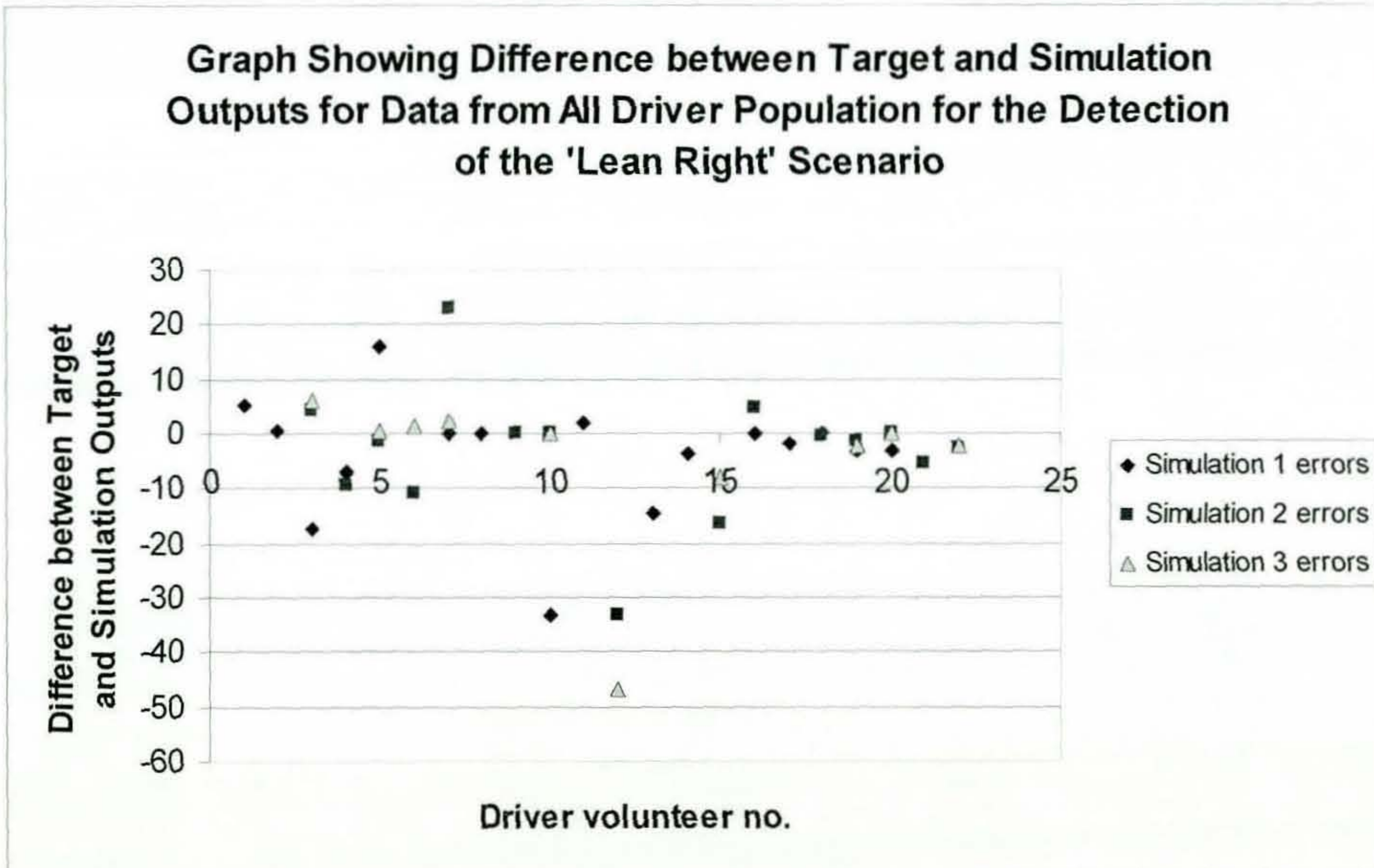

Figure 6-10: ANN Results to Detect 'Lean Right' Scenario

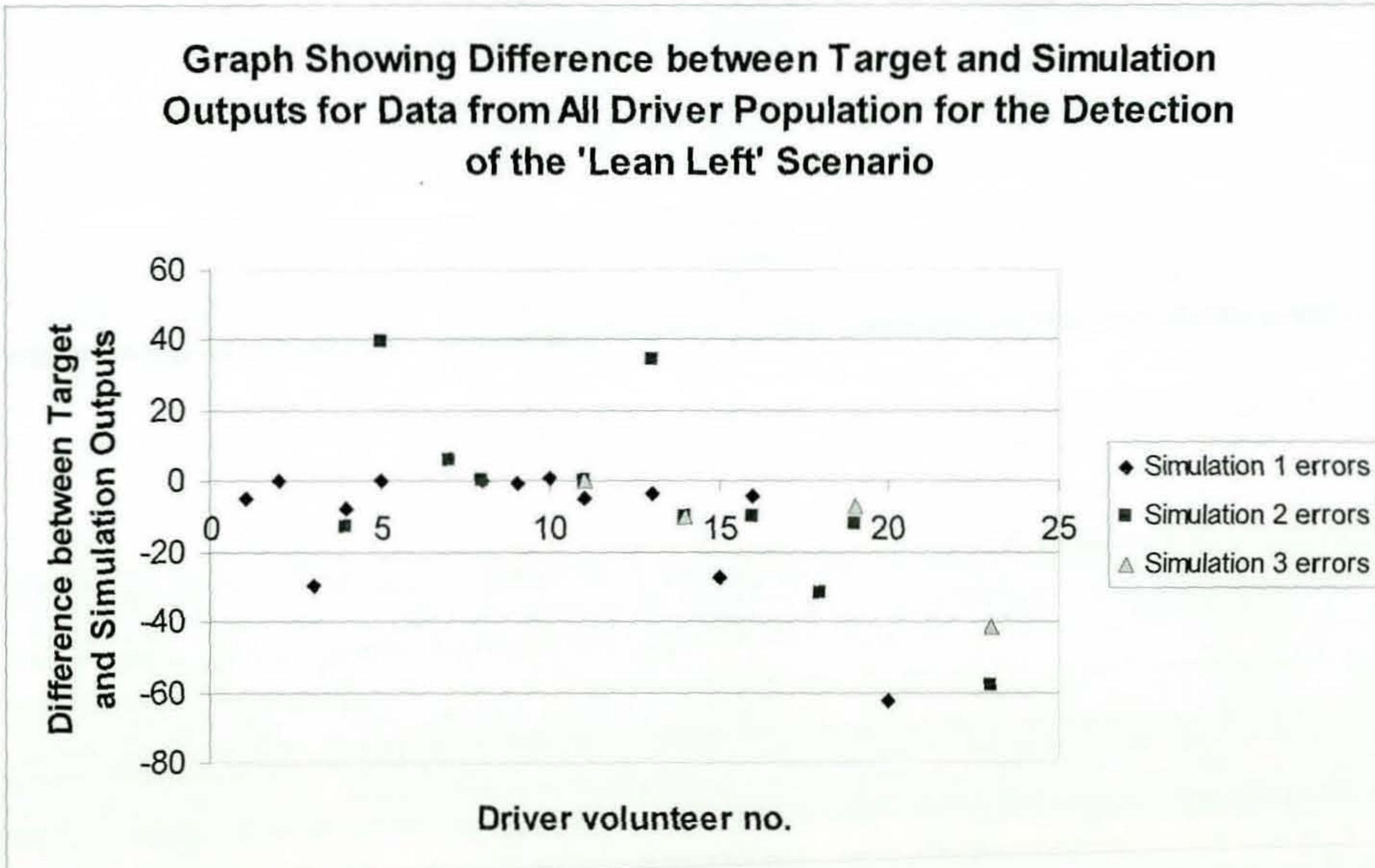

Figure 6-11: ANN Results to Detect 'Lean Left' Scenario

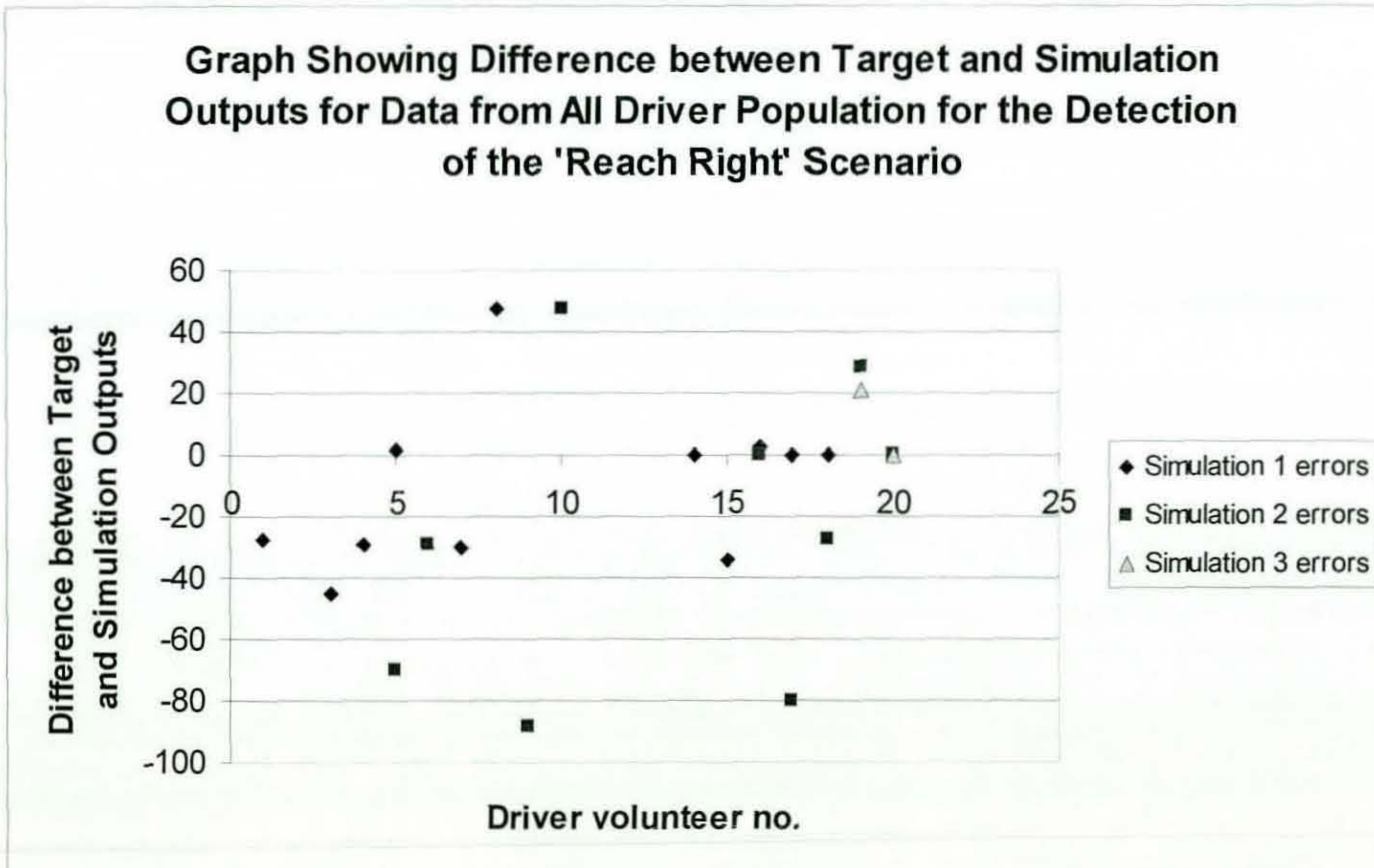

Figure 6-12: ANN Results to Detect 'Reach Right' Scenario

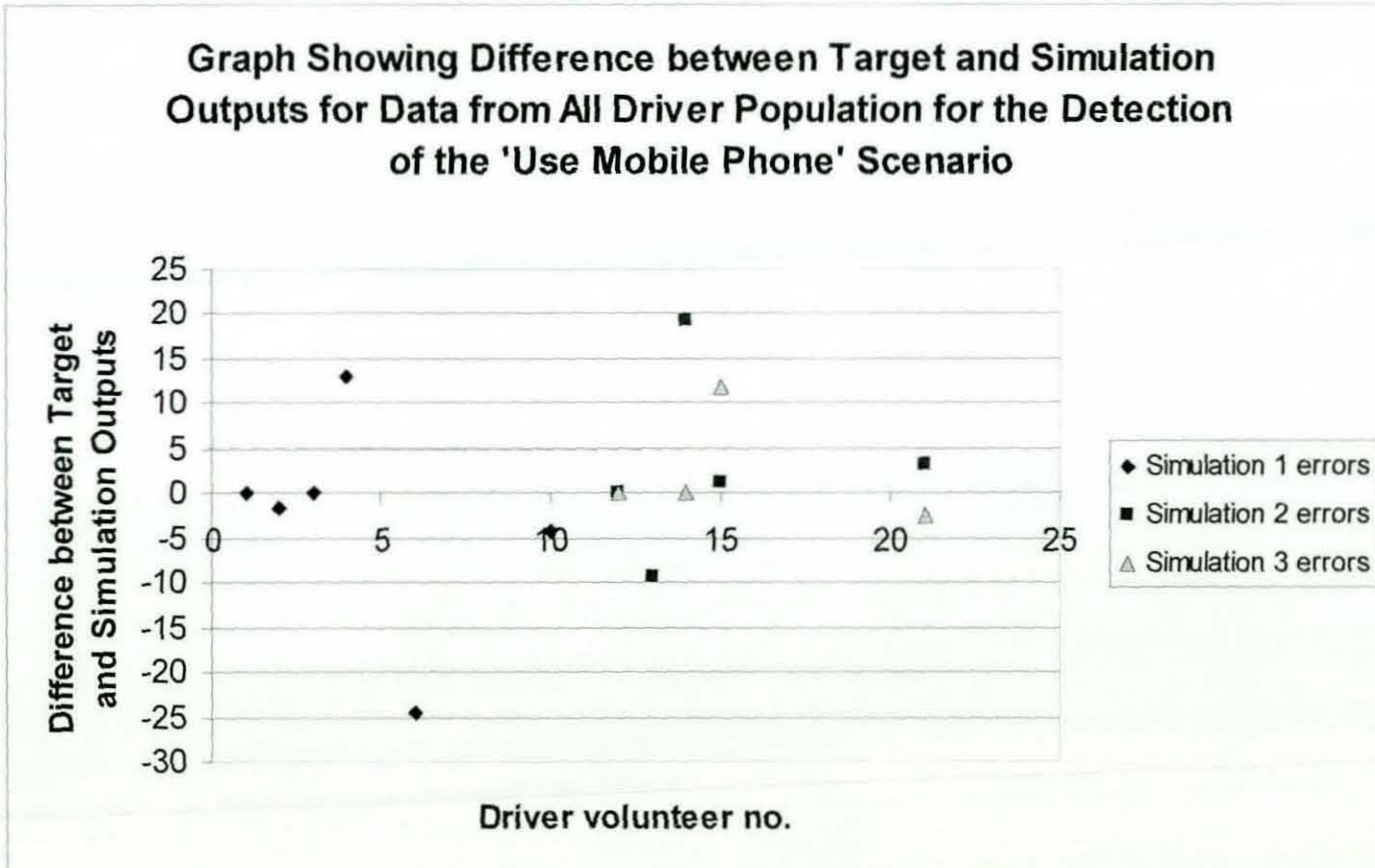

Figure 6-13: ANN Results to Detect 'Use Mobile Phone' Scenario

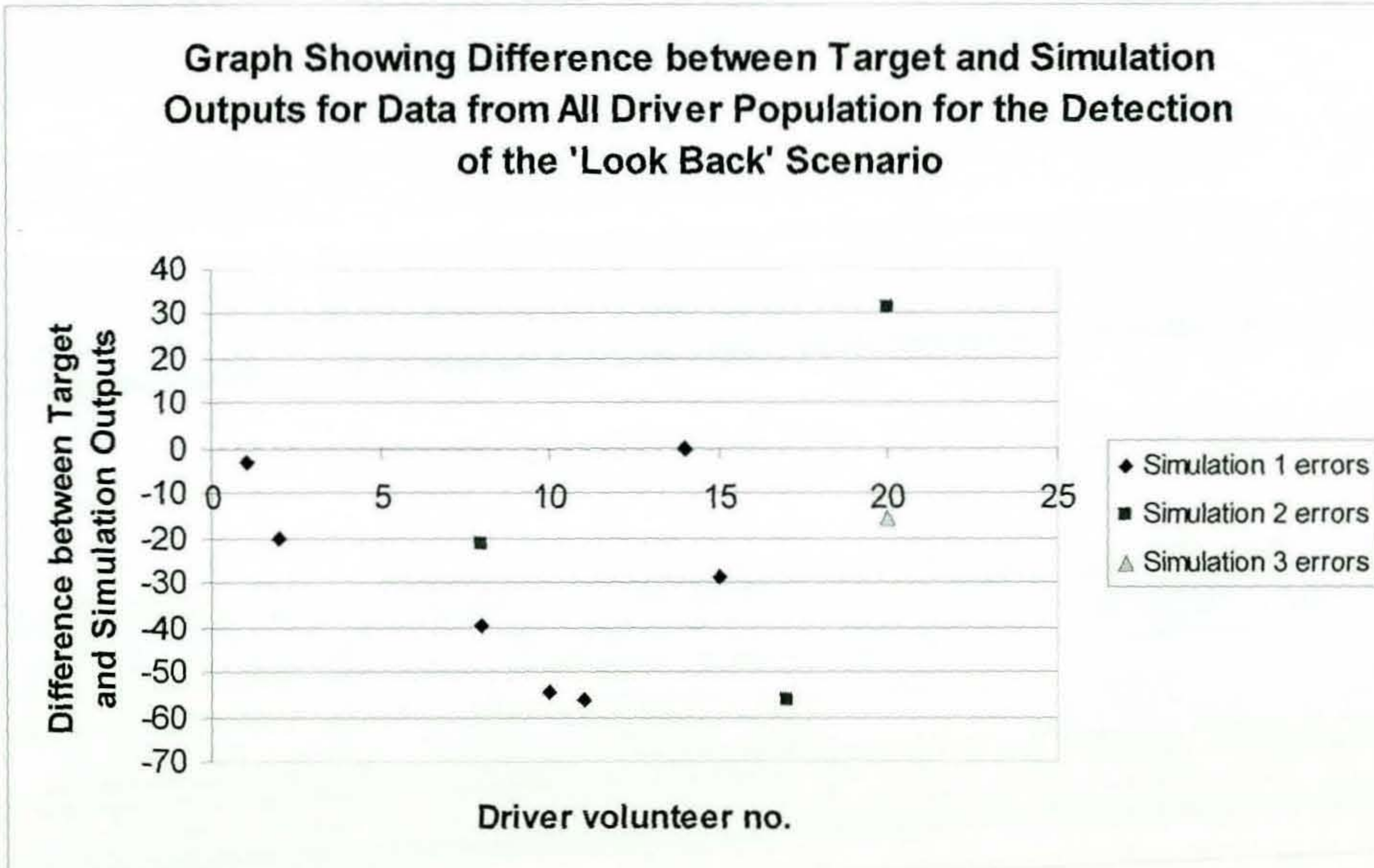

Figure 6-14: ANN Results to Detect 'Look Back' Scenario

Figure 6-4 shows the results of the ANN analysis done when the driver was sitting in his normal driving position and looking 'straight ahead'. The results of all the volunteers are included in these graphs, in order to provide a visual comparison between the results of each of the volunteers. It should be realised that these graphs simply present the results of the analysis done. These graphs show the difference between the target and the related simulation outputs. Ideally, there would be no difference between simulation outputs and the intended targets, but in reality this was not always the case.

From the graph shown in figure 6-4, it can be seen that a large number of simulation outputs are indeed on or very close to their simulation targets. In fact 32 out of 65 simulation outputs 'match' the target, where a 'match' is said to have occurred when the simulation output is within 5 units of the intended target. This value of 65 outputs is more than the 23 volunteers, and may seem incongruous at first, but it must be remembered that some volunteers had more data available for processing than others, and so it was possible for a volunteer to have 2 or even 3 simulation outputs. This 32 out of 65 target match by the simulation outputs represents a success rate of approximately 49 %.

Figure 6-5, the results of the 'look up' detection analysis, shows that 8 out of 17 simulation targets match their intended targets, a success rate of 47 %. In figure 6-6, the results of the 'look right' detection, only 16 out of 59 simulation outputs match the target, giving a low 27% success rate. This could be explained by examining the images of when the drivers are looking either to the left and to the right, and in some of the cases, the image is similar to that of the driver when he is leaning to the left and to the right. This means that some of the 'regionprops' data would have overlapped, and when fed into the neural network, this could have resulted in confusing the ANN into thinking the driver was leaning to the right when in reality he was merely looking to the right.

Figure 6-7 shows the results of the 'look left' detection. The success rate is a reasonable 51 %, where 28 simulation outputs match their intended target. However, the success rate in figure 6-8 ('lean forward' detection) is only 35 %, where only 11 out of 31 simulation targets match. Again this could be because there is some confusion as to whether the driver is leaning forward or has his head on the steering wheel. This is borne out when examining the results of the 'head on wheel' ANN detection shown in figure 6-9. Only 4 out of 22 simulation outputs match their targets, giving a very low 18 % success rate. The results of figure 6-10, the 'lean right' detection, are much more encouraging. Here, 25 out of 41 simulation outputs match their intended targets, giving a relatively high 61 % success rate. Figure 6-11, the results of the 'lean left' detection, show only a 36 % success rate, where 10 out of 28 simulation outputs match their intended targets. This level of accuracy is also shown in figure 6-12 ('reach right' detection) where 8 out of 21 targets are matched by their simulation outputs, giving an accuracy of 38 %. This illustrates the point of the neural network being confused by the overlap of some of the 'regionprops' data, thus giving inaccurate results in some of the graphs. Figure 6-13 shows a much higher success rate of 67 %, however. In this graph, the 'use mobile phone' driver scenario was to be detected, and this was done to a reasonably successful degree with 10 out of 15 simulation outputs matching their intended targets. Figure 6-14, the 'look back' detection, shows again the problem with overlap of data. Here, only 2 out of 11 simulation outputs match, giving a low success rate of 18 %.

However, it is clear that whilst the ANN had some success in identifying the various actions and positions that the driver was undertaking whilst in the car seat, however, this accuracy could be improved. There were many possible reasons why the accuracy of the ANN was not as high as one would have liked. Although it was anticipated that there would be some problems, it was thought that by using many different variables to differentiate the images would have mitigated this problem. One of the main reasons is that there were too many different variables whose patterns or cluster of data points overlapped one another. For example, in order for the ANN to distinguish between an image of the driver 'looking straight' and a driver 'leaning left', for example, data inputs need to have been fed into the GUI of the neural network toolbox in MatLab which highlight these differences. For example, when attempting to distinguish between the 'look straight' and 'lean left' images, some variables proved to be better at making this distinction than other variables.

The x-coordinate of the centroid of mass would change depending on whether the driver had changed his posture from 'looking straight' to 'leaning left', whereas the y-coordinate of the centroid would not have changed by any significant amount. Likewise, the major axis length did not change by much.

Another factor that could explain the relatively low accuracy of the results from the ANN analysis, and perhaps one of the most important, was the sheer number of targets that the ANN was tasked with detecting. The ANN for some of the volunteers had upwards of 9 separate targets to match by the simulated outputs, and clearly this proved to be very challenging for it to do successfully. Therefore, new networks were created using MatLab's toolbox. The number of driver positions or activities to be detected was reduced, and the number of variables used was also reduced in order to improve the accuracy of the neural network analysis results.

The results are shown in figure 6-15 to 6-37. A note to explain the graphs. The targets are assigned values of 10, 20, 30, 0 etc and increases in units of 10, and this was done to provide a large distinction between the targets. The simulation outputs or goals are given as crosses, and should 'match' the target. For there to be a match, the cross has to be within 5 units of its intended target.

Figure 6-15: ANN Results to detect OOP Scenarios for Volunteer 1

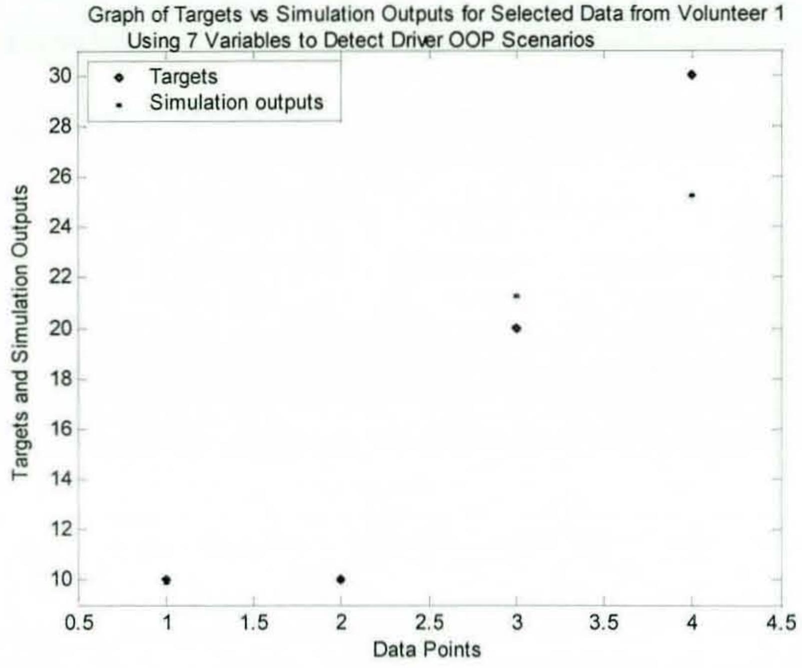

Figure 6-16: ANN Results to detect OOP Scenarios for Volunteer 2

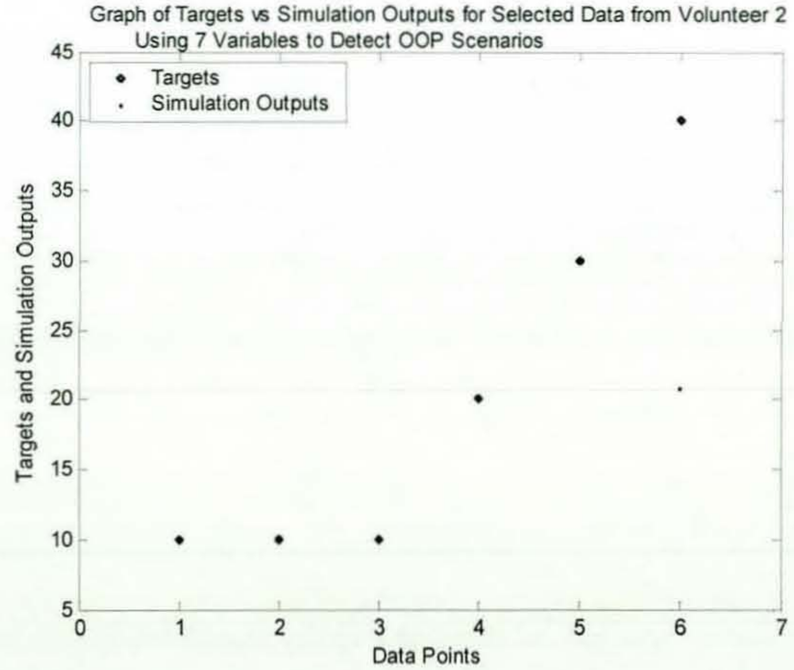

Figure 6-17: ANN Results to detect OOP Scenarios for Volunteer 3

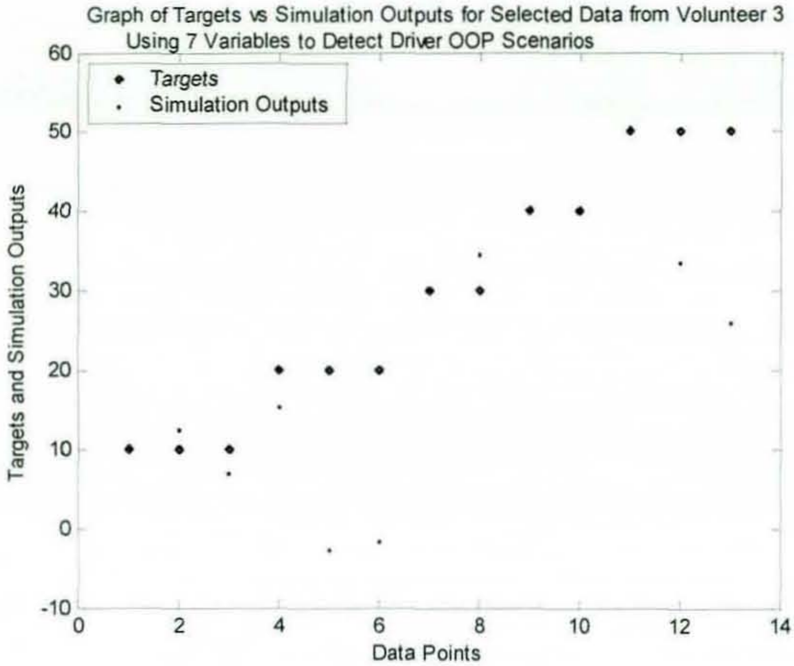

Figure 6-18: ANN Results to detect OOP Scenarios for Volunteer 4

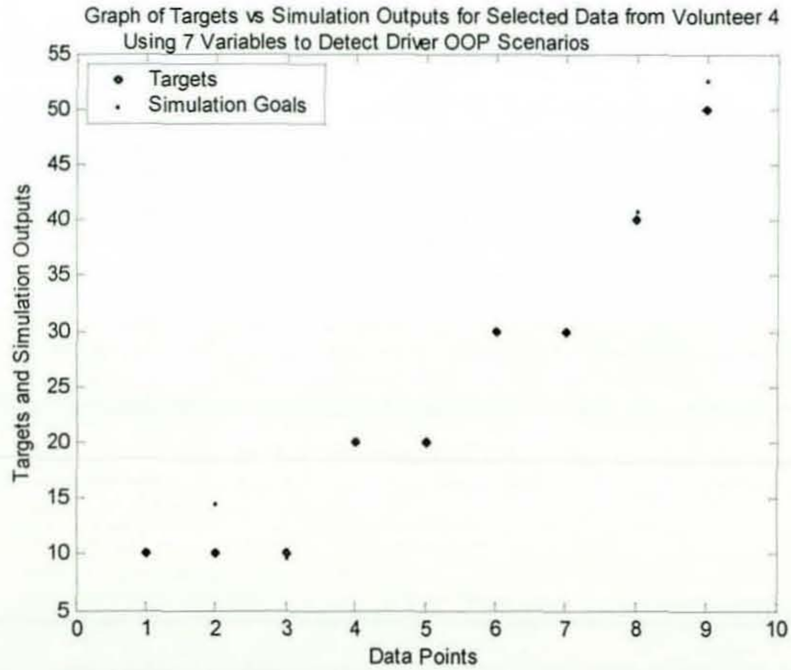

Figure 6-19: ANN Results to detect OOP Scenarios for Volunteer 5

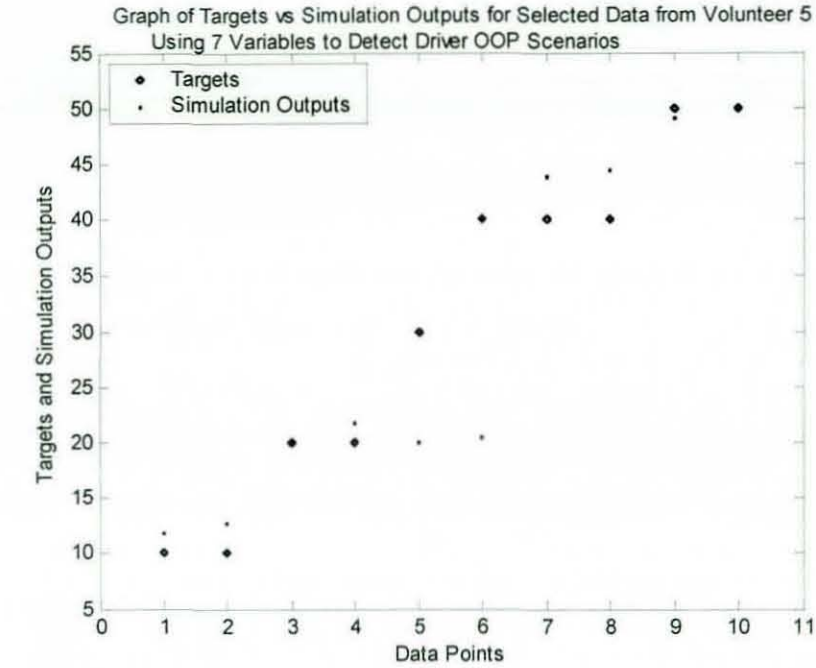

Figure 6-20: ANN Results to detect OOP Scenarios for Volunteer 6

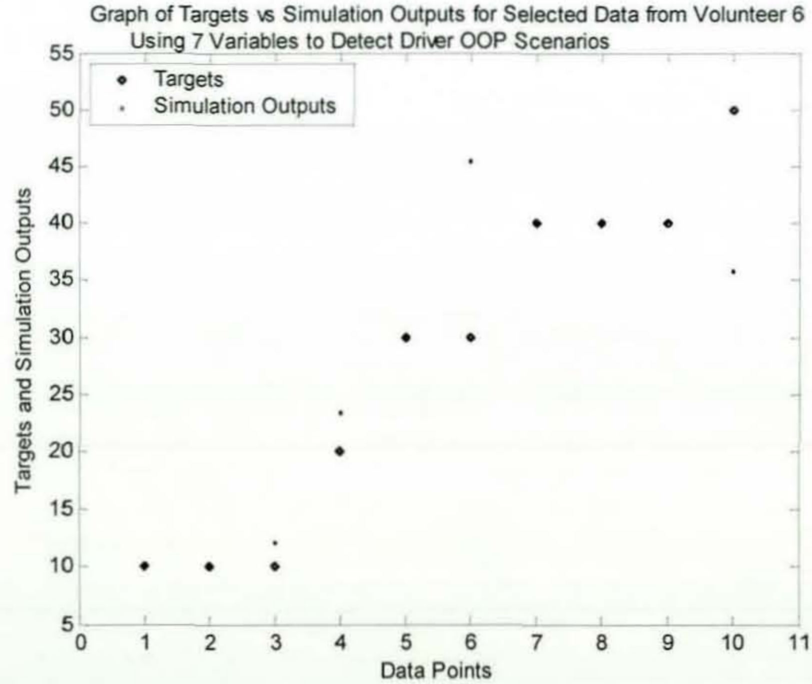

Figure 6-21: ANN Results to detect OOP Scenarios for Volunteer 7

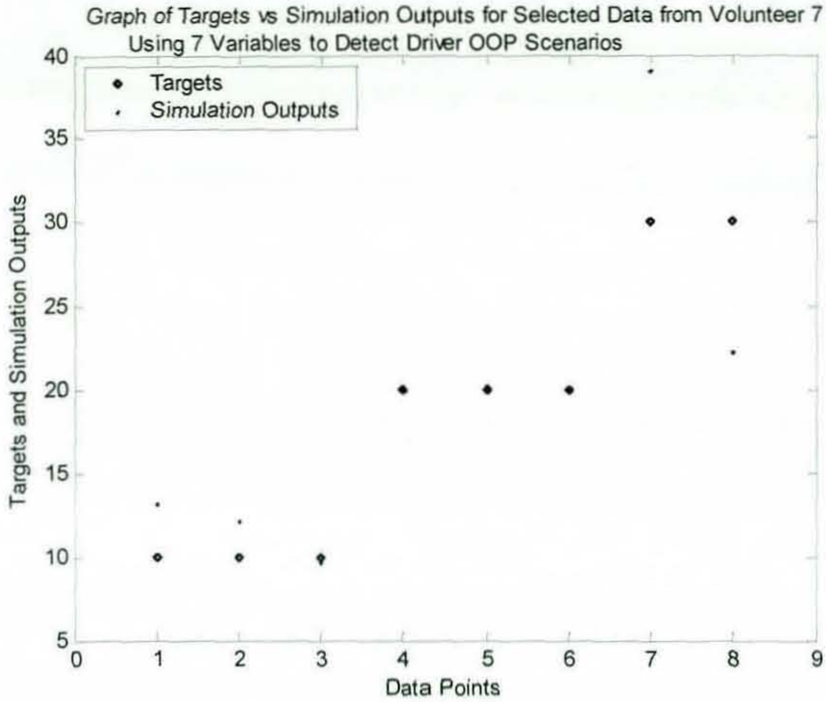

Figure 6-22: ANN Results to detect OOP Scenarios for Volunteer 8

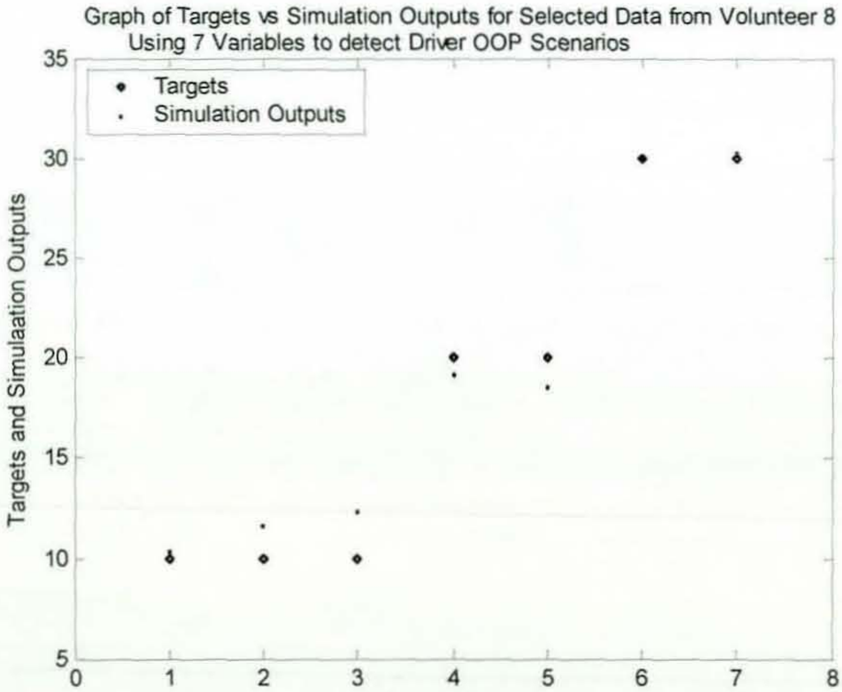

Figure 6-23: ANN Results to detect OOP Scenarios for Volunteer 9

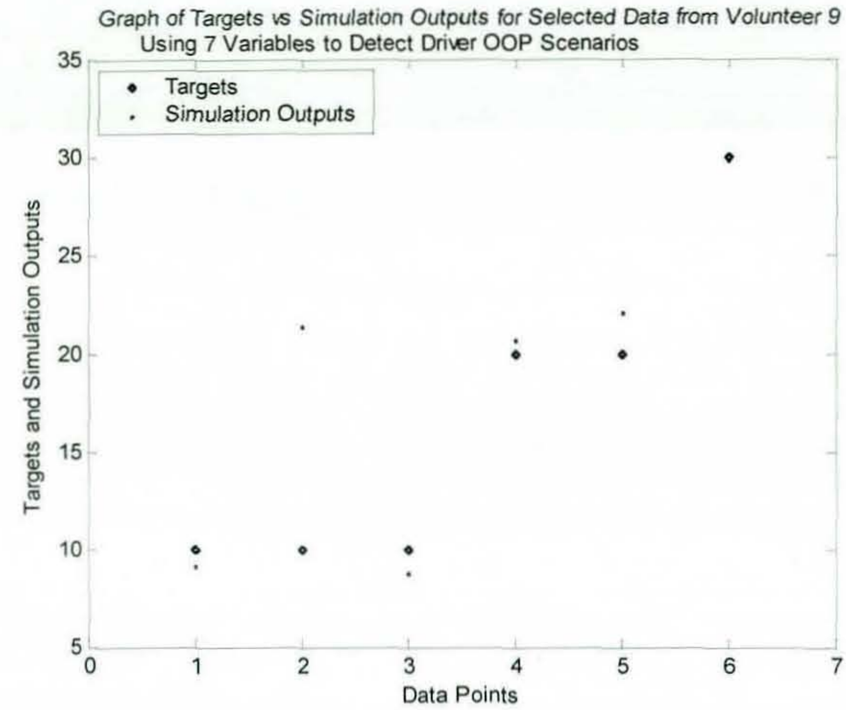

Figure 6-24: ANN Results to detect OOP Scenarios for Volunteer 10

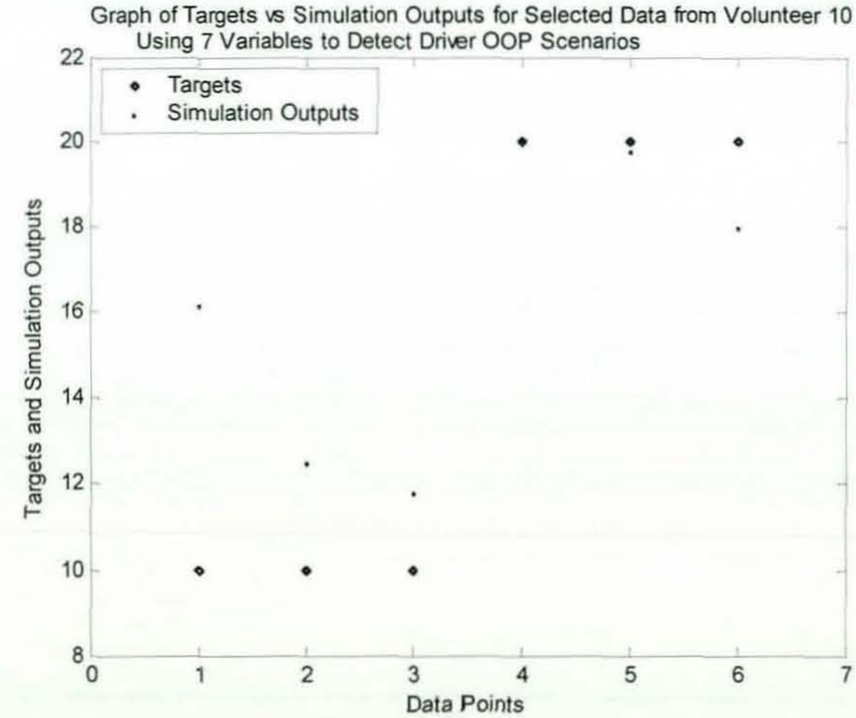

Figure 6-25: ANN Results to detect OOP Scenarios for Volunteer 11

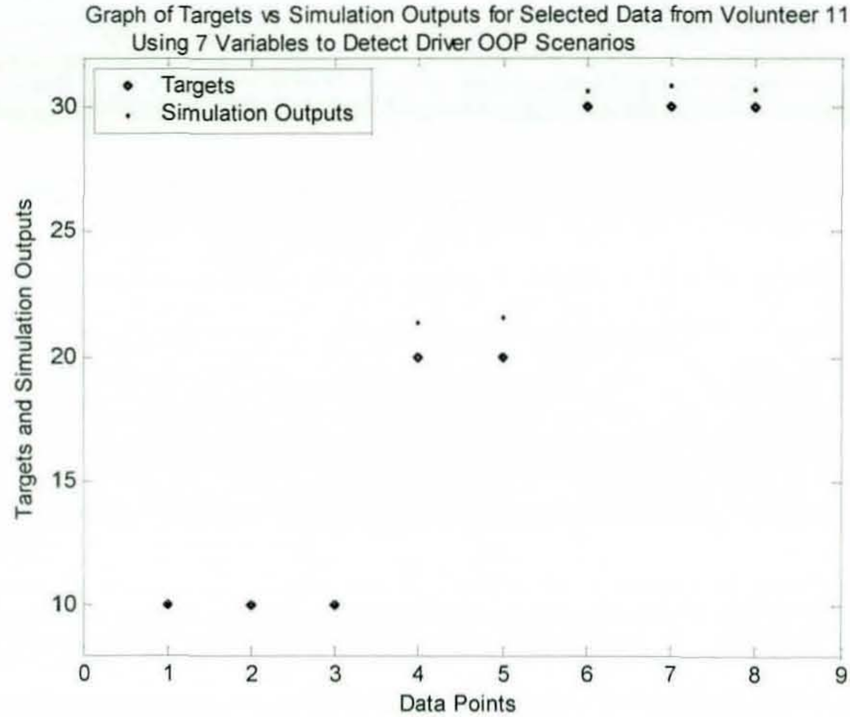

Figure 6-26: ANN Results to detect OOP Scenarios for Volunteer 12

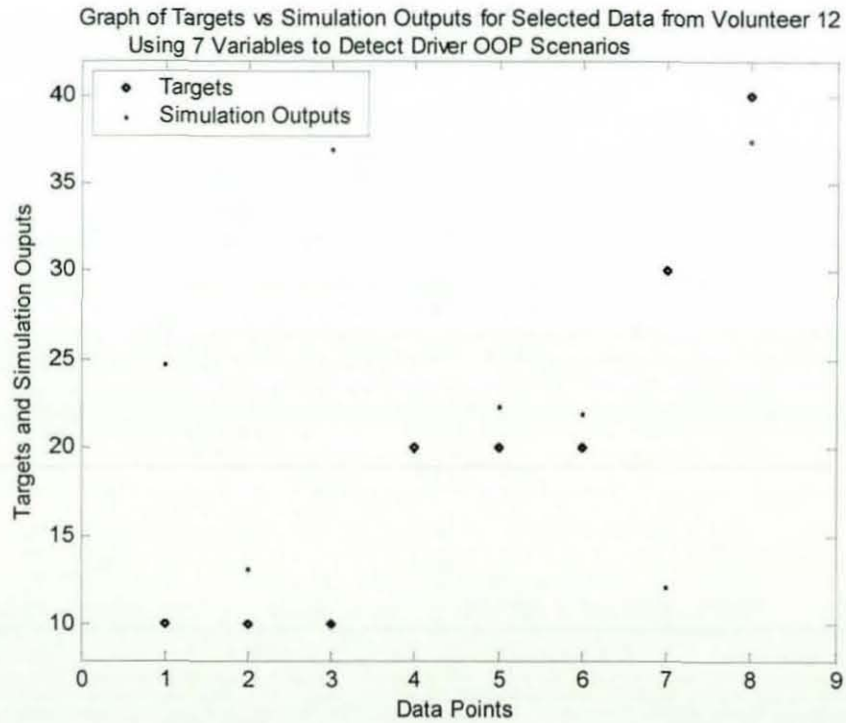

Figure 6-27: ANN Results to detect OOP Scenarios for Volunteer 13

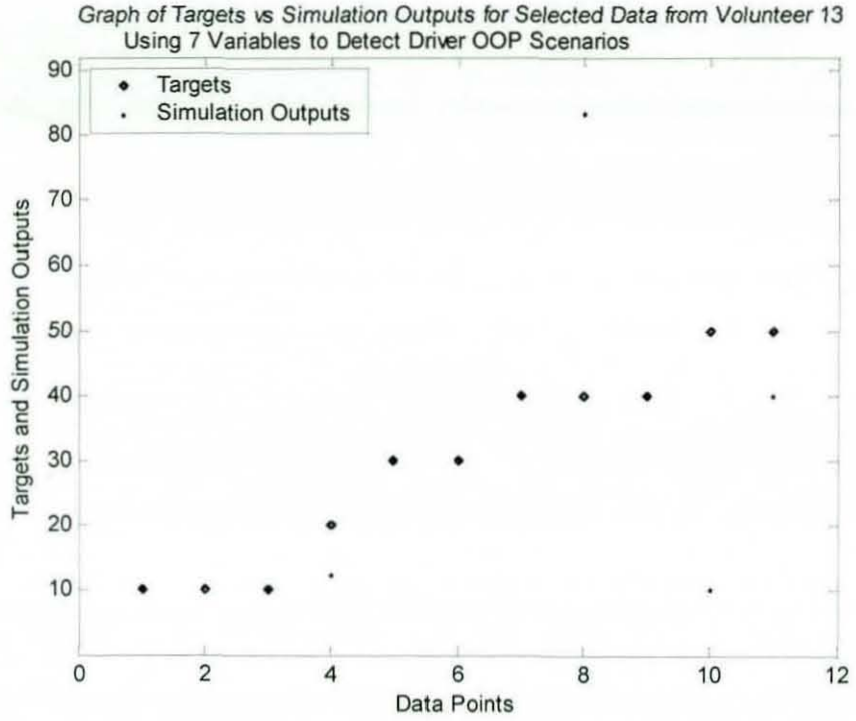

Figure 6-28: ANN Results to detect OOP Scenarios for Volunteer 14

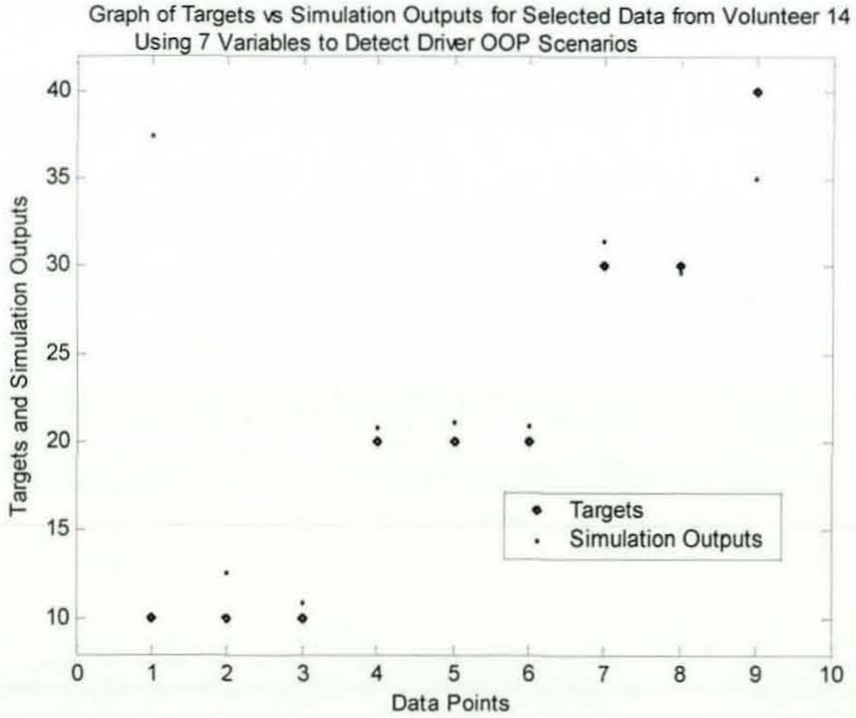

Figure 6-29: ANN Results to detect OOP Scenarios for Volunteer 15

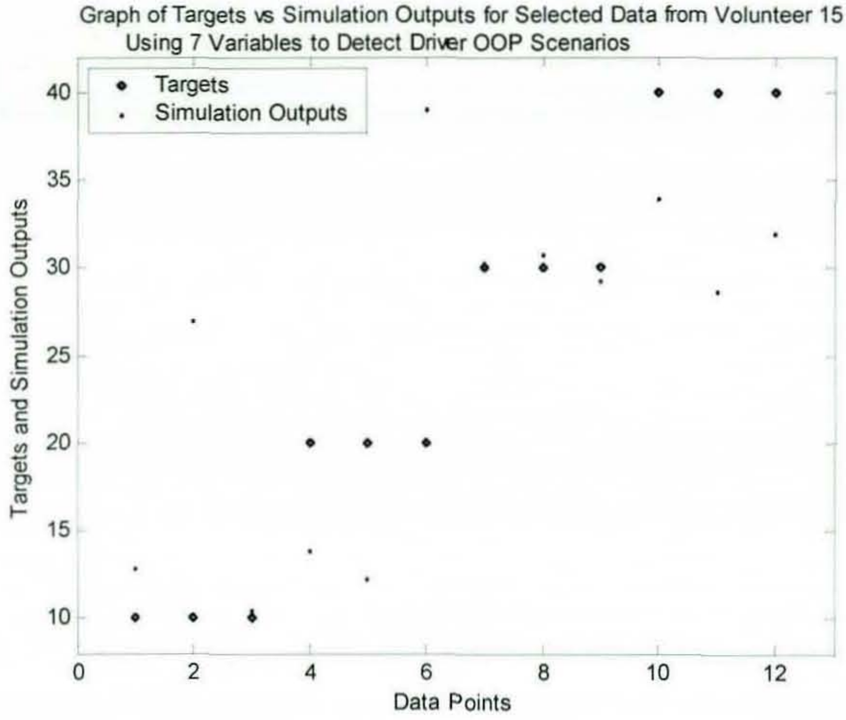

Figure 6-30: ANN Results to detect OOP Scenarios for Volunteer 16

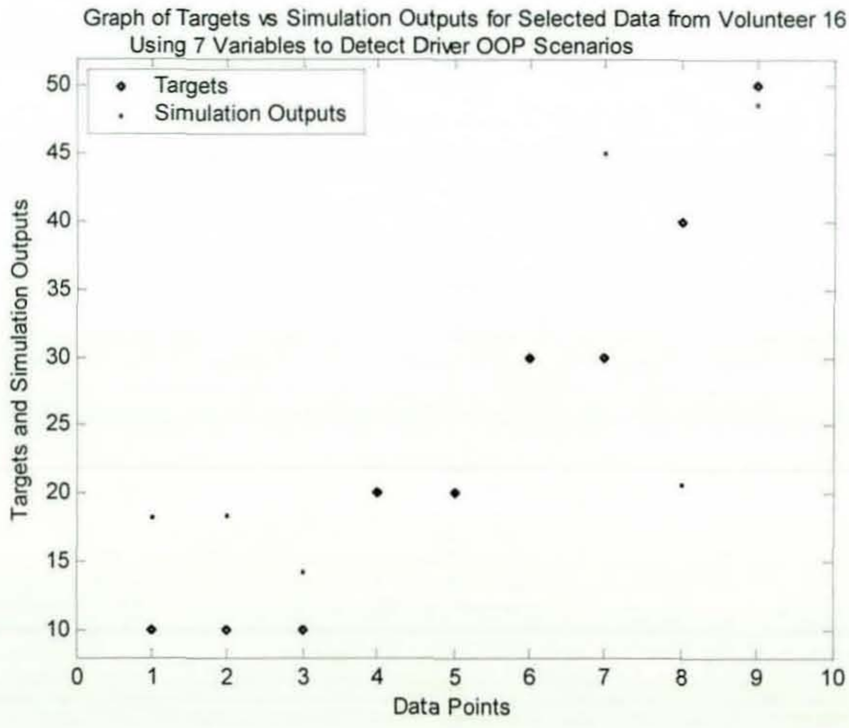

Figure 6-31: ANN Results to detect OOP Scenarios for Volunteer 17

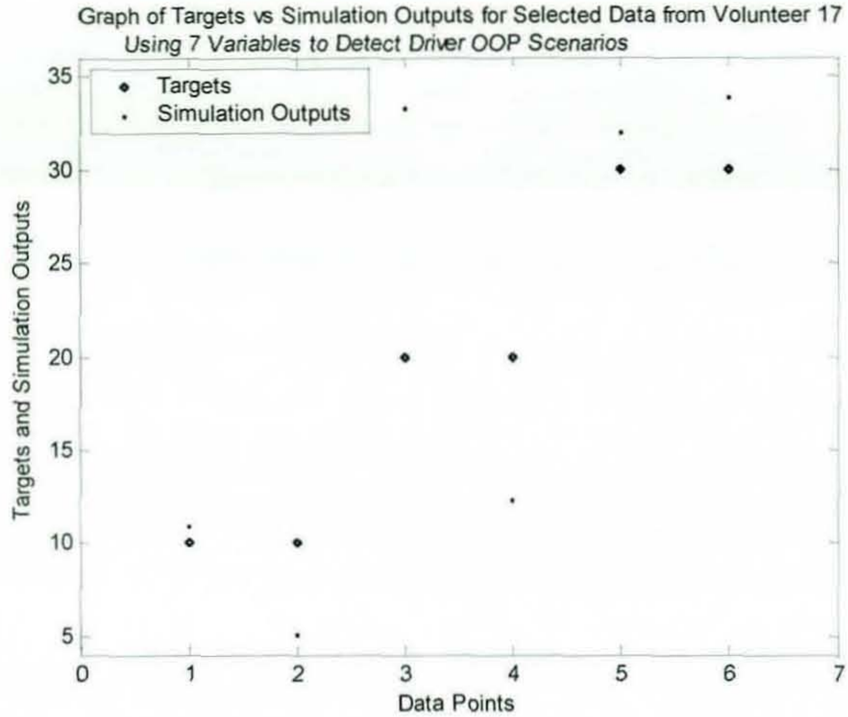

Figure 6-32: ANN Results to detect OOP Scenarios for Volunteer 18

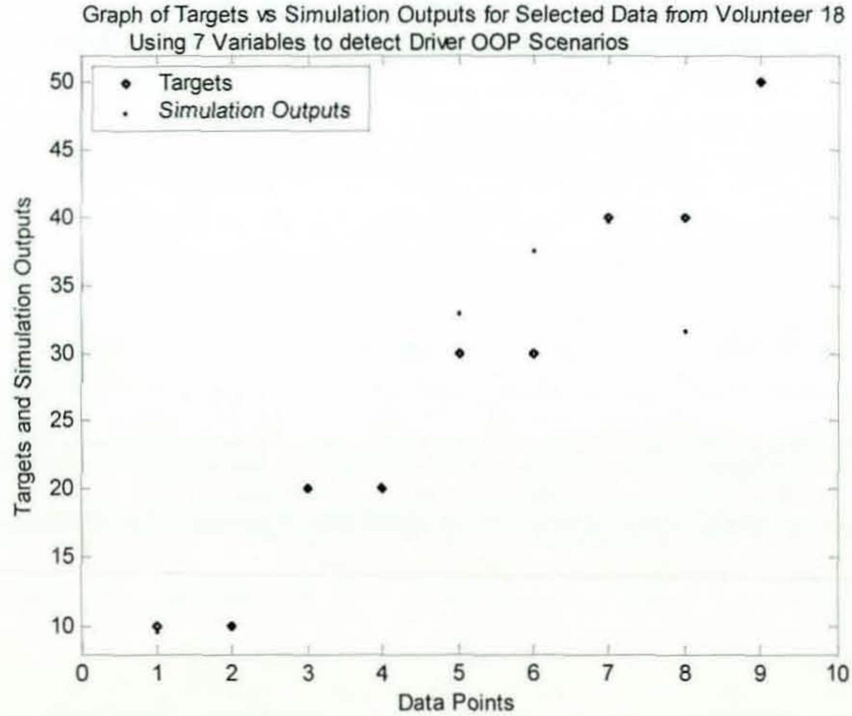

Figure 6-33: ANN Results to detect OOP Scenarios for Volunteer 19

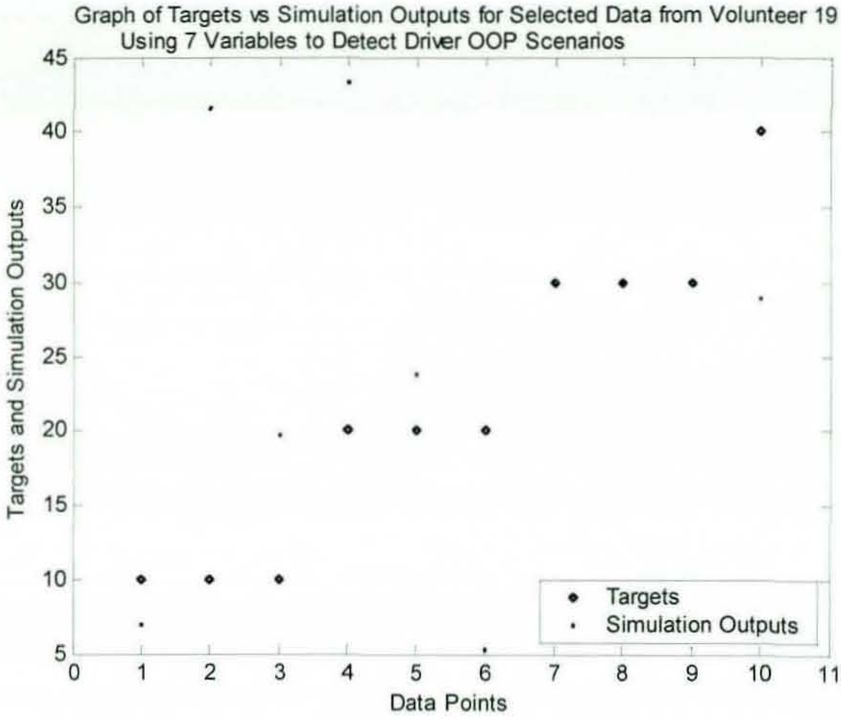

Figure 6-34: ANN Results to detect OOP Scenarios for Volunteer 20

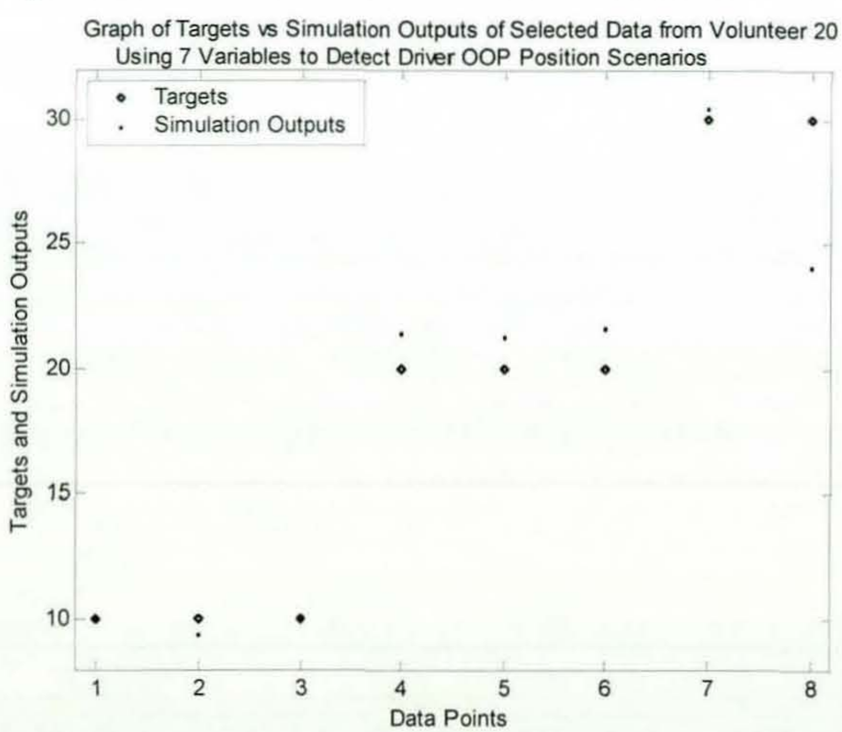

Figure 6-35: ANN Results to detect OOP Scenarios for Volunteer 21

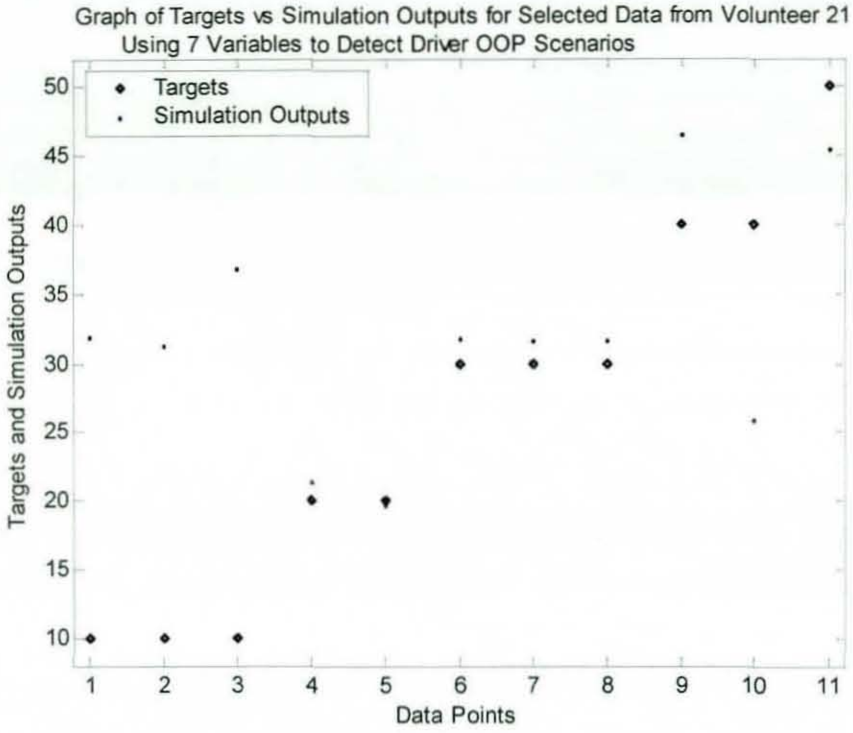

Figure 6-36: ANN Results to detect OOP Scenarios for Volunteer 22

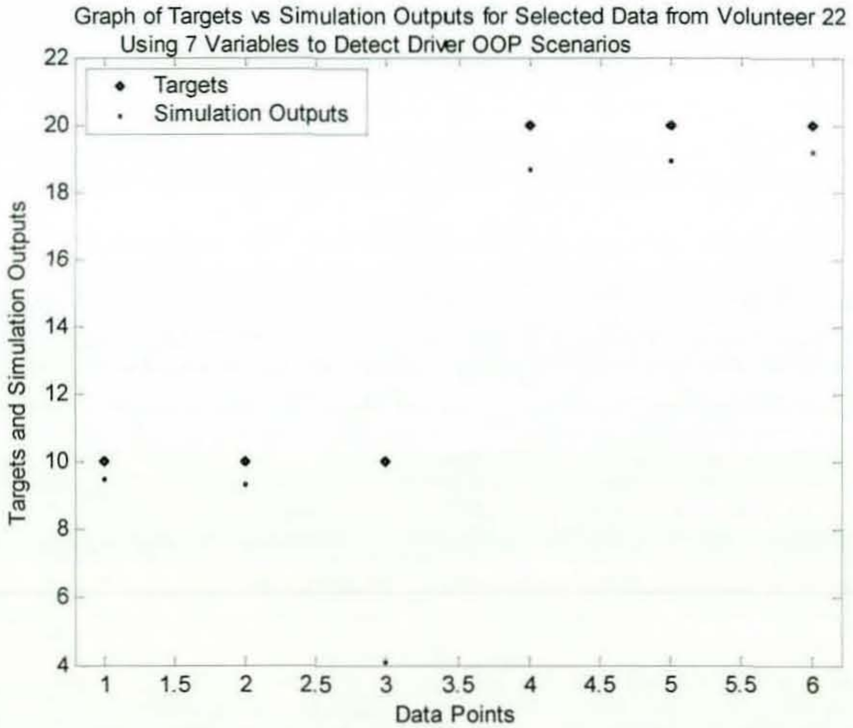

Figure 6-37: ANN Results to detect OOP Scenarios for Volunteer 23

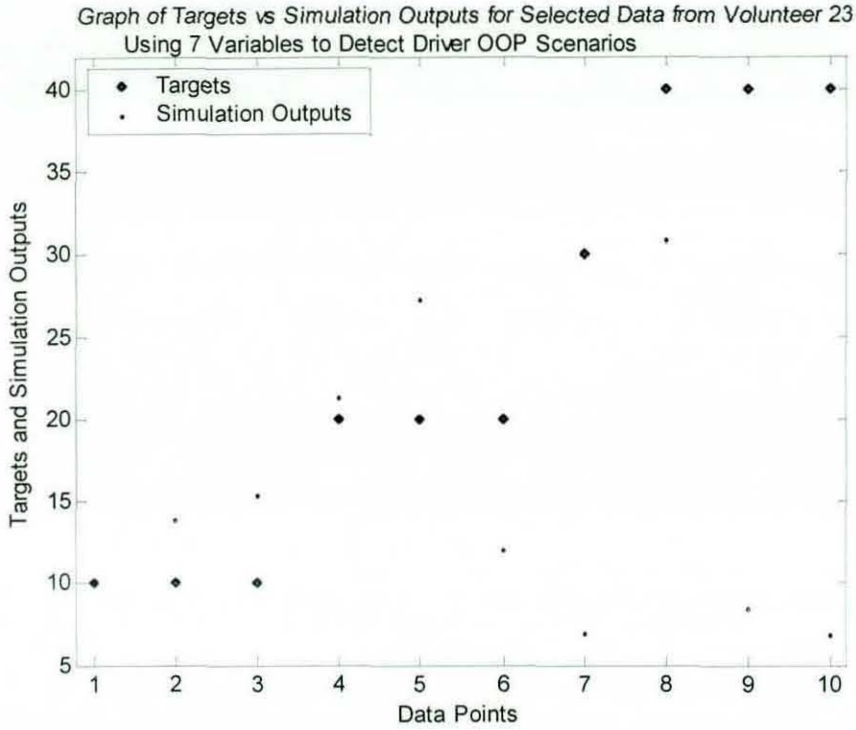

For the purpose of detecting whether the driver was out of position or not, and could therefore be classed as being at risk of airbag induced injuries, not all the scenarios presented earlier need be included. Although the value of detecting whether the occupant was looking to the left or to the right was not questioned, what was questioned was whether it was necessary to be able to detect the driver looking left or right for the purpose of detecting whether the **driver was out of position**. Clearly, only the 'out of position' scenarios need be included because ultimately it was these positions which would determine whether the occupant was at risk of airbag related injury. The most important driver actions to focus on were:

- look straight.
- lean forward.
- head on the wheel.
- lean right.
- lean left.

The 'look straight' position of the driver was the default potion, which would entail the driver being seated with his back set up against the backrest of the seat, and the driver's gaze looking directly at the road ahead. The 'look straight' position was included because it was important to compare the other 'out of position' scenarios with it. If the neural network could distinguish the 'look straight' position from the 'lean forward' or 'lean right' or 'lean left' position, then this would represent success and real progress towards the goal of an occupant detection system for intelligent airbag deployment. The importance of detecting whether the occupant is leaning forward or is leaning so far forward as to have his head resting up against the steering wheel cannot be overstated, as to be in such a position would render the occupant extremely vulnerable to serious injury which would be experienced should the airbag be deployed whilst during these scenarios.

Although it is not commonly thought of as being 'out of position', the 'lean right' and the 'lean left' driver actions were included because it was considered that to be in such a position was to be outside the normal, 'safe' seating position of the driver, and so detecting whether the occupant was in such a position was important.

As can be seen from the graphs shown in figures 6-15 to 6-37, generally, there is a much closer 'match' between the simulation outputs and their respective targets. In a lot of the graphs, the simulation outputs markers are on or very close to their targets. The graph for volunteer 1, for example, shows two different driver actions. There are 4 targets in total, and 3 of which were successfully matched by their corresponding simulation output, giving an accuracy of 75%.

Figure 6-38: Table showing accuracy of revised ANN analysis

Volunteer Number	Number of Scenarios	Number of Targets	Number of Simulation Outputs Match	Percentage Accuracy
1	2	4	3	75
2	4	6	5	83
3	5	13	9	69
4	5	9	8	89
5	5	10	7	70
6	5	10	9	90
7	3	8	6	75
8	3	7	7	100
9	3	6	5	83
10	2	6	5	83
11	3	8	8	100
12	4	8	5	63
13	5	11	7	64
14	4	9	7	78
15	4	12	5	42
16	5	9	5	56
17	3	6	3	50
18	5	9	7	78
19	4	10	5	50
20	3	8	7	88
21	5	11	6	55
22	2	6	5	83
23	4	10	3	30

As can be seen from the table in figure 6-38, the overall accuracy of the ANN analysis has improved considerably up to an overall of 72 %, which is far higher than before. In fact 13 of the 23 volunteers had an accuracy higher than 75 %, and 17 had a success rate of 60 % or higher.

6.7 Discussion of Accuracy of Neural Network Analysis for the Detection of In-Car Driver Activity

As was discussed previously, initial results derived from the neural network analysis conducted for the purpose of detecting different driver actions, gave mixed messages. For the neural network analysis to be considered a perfect success (100% match between simulated output and target), the following conditions should have been met:

- The neural network training process should have resolved itself within the parameters set by the user. These parameters included number of iterations, or 'epochs', and accuracy.
- The outputs produced by the data used in the simulation process should be exactly the same or very similar to the outputs produced by the training set of data.

This would mean that it could be said that the neural network analysis can detect certain in-car driver actions and gaze directions with perfect reliability. The reality is somewhat less clear. There is positive evidence to suggest that artificial intelligence can be trained to recognise driver activity, but not in all cases.

Less than perfect results are to be expected whenever one is using raw experimental data, as was the case in this instance.

6.8 Neural Network Verification

Due to the fact that the initial ANN results were of mixed success, it was thought that perhaps the method of using the neural network toolbox in MatLab was wrongly carried out. So, in order to check whether the neural networks created were functioning correctly, a simple and quick test was done. The data used for the training process of the neural network, p1, was exported from the Microsoft Excel spreadsheet where it was housed and into the MatLab workspace as the matrix, p1. A FFBP network was created, initialised, input ranges reset and trained with inputs p1, to target, t1. However, instead of using a separate training set of data, s1, for the simulation process, the same training set of data, p1, was used in the simulation process instead. The outputs from the simulation process matched the targets with negligible or no errors. This was the result expected if the simulation set of data had numerical values close to the training set of data, and so this confirmed that the neural network was functioning correctly.

This proved that it was not the network or method of conducting the analysis that was at fault, but the data itself which was somewhat varied, and so led to somewhat inaccurate results in some cases. This is the reason why a second neural network analysis was done with fewer variables and fewer targets to match, and the results shown in figure 6-15 to 6-38.

6.9 Discussion of Possible Causes and Solutions of Neural Network Analysis Inaccuracy

In the first instance of using neural network analysis for the sole purpose of in car driver action detection, many different examples of in-car driver activity were selected for targeting. These actions were:

- Look Straight Ahead.
- Look Right.
- Look Left.
- Lean Right.
- Lean Left.
- Lean Forward.
- Position Head onto steering Wheel.
- Look Back over Shoulder (car reversing action).
- Reach with right hand outside driver window (swipe card gate opening action).
- Look up (looking at rear-view mirror).

All these different scenarios entailed the driver having to move his upper body and head position to slightly different positions, to varying extents in order to carry out these instructions. This meant that the images of the head would be in a slightly different position and/or have a different shape when the image was processed with the threshold function. This enabled the user to obtain a large quantity of data for each individual image using the 'regionprops' command in the MatLab software workspace, and could therefore be used, in theory, to differentiate between each image and therefore positively identify what action the driver was doing inside the car cabin. However, to allow the neural network to tell apart different types of driver activity with any great certainty, the regionprops data needed to show distinct patterns. For example, the x-coordinates of the threshold region in the images of the driver looking straight ahead should ideally have been completely dissimilar to the x-coordinates when the driver was leaning to his left. Initial inspection of some of the regionprops data for some of the driver volunteers indicated that there was some overlap of groupings of data points for different driver activity. For example, the y coordinates for one particular driver volunteer did not significantly change when the driver was undertaking the variety of actions when he was driving in the car simulator.

Other possible factors to explain the inaccuracies of the initial ANN analysis include:

- Volunteer driver height and build.
- Variance in interpretation of commands.
- Lack of driver mobility.

The height of the drivers selected varied from short to medium height to tall drivers, and of course, their build and body shape differed as well. Although head length was found not to have varied significantly, the height of the driver determined the position of the head in the image, and so a tall driver's head would be higher up in the image than that of the average height driver. This would mean that different drivers doing the same movement or activity (e.g. look straight) would still have different data values, and would not be as similar as one would have hoped. In this case, the y-coordinate would vary significantly, and so the accuracy of the neural network analysis would be affected.

Perhaps of even greater significance is the tendency for different people to misinterpret the commands during the experiment. The volunteers are human beings after all and are prone to make mistakes and interpret things differently to others. One person may move their head further forward onto the steering wheel than another driver would, for example. Such inconsistency would also lead to varied and dissimilar data values, which would reduce the accuracy of the neural network analysis.

Lack of driver mobility ties in with the point given above. Since some people used in this project's experiment were considerably older than others, it was to be expected that their mobility would not be as great as the younger members of the experimental volunteers used. This is because it is known that as one tends to grow older, the mobility of the joints will tend to decrease, as will reaction times. In terms of the experiment, this could have meant that some of the movements of the drivers may not have been as discernible as others, and hence the images produced would not have been as distinct from one another, which would have made it difficult for the ANN to find some distinct pattern and therefore lead to errors in judgement by the ANN. Although speed of movement did not make a major difference in this experiment as the frame capture rate of the thermal imager was set at 2 frames per second, the thermal imager is capable of 5 frames per second, and speed of body movement would then become an issue at this point.

Another point to be aware of is that the driver, with the best will in the world, was not able to remain positioned in the same position throughout the duration of the experiment, This would have mean that the data for the driver 'looking straight ahead' or for any other driving activity, was not constant for the same volunteer. Even though this error was reduced by ensuring that images were taken from the entirety of the dataset in order to train the ANN with as many different variations of the driver 'looking straight ahead', nevertheless, the reader ought to realise that this would have had an impact on the accuracy of the ANN.

6.10 Detection of Tall and Short Drivers

Since driver 'out of position' had been successfully identified by the ANN, it was thought that the ANN could be used to detect other potentially important factors about the driver. Driver height has been explained previously to be an interesting factor in terms of driver airbag safety, as the upper torso height from the seat will drastically affect the location at which the head will interact with the steering wheel column and or the airbag and/or the dashboard. A tall driver may strike the airbag over the top of the steering wheel, whilst a short driver would have their head pushed underneath the airbag, and such an event would have caused serious injury to the driver concerned, and that is why it is important that any proposed occupant detection and classification system ought to be able to recognise different types of drivers.

Again, ANN analysis was used in the first instance to demonstrate this. Tall and short drivers were selected from the database of volunteers, although since most volunteers were of average height and build, the number of tall and short volunteers was limited. The images from which the data was extracted were the images where the drivers were in the 'look straight' position. This was because this would provide the most accurate representation of the driver's torso height, as they would invariably be sitting upright and in their most natural position. Using other positions such as the 'lean forward' or the 'lean left' position would not be a fair representation of the driver's height, as different people would interpret these commands in different ways and would lean left or lean forward to varying degrees.

Again, the FFBP neural network was selected with 15 neurons in the first layer using a Tansigmoid transfer function, and 1 neuron and a purelinear transfer function in the second layer. The tall drivers were assigned targets of 10, whilst the short drivers were assigned targets of value 20. Training data was used to train the network, which resolved itself within 284 epochs, and the simulation set was used. The results are shown in figure 6-39:

Figure 6-39: ANN Results to detect Tall and Short Drivers

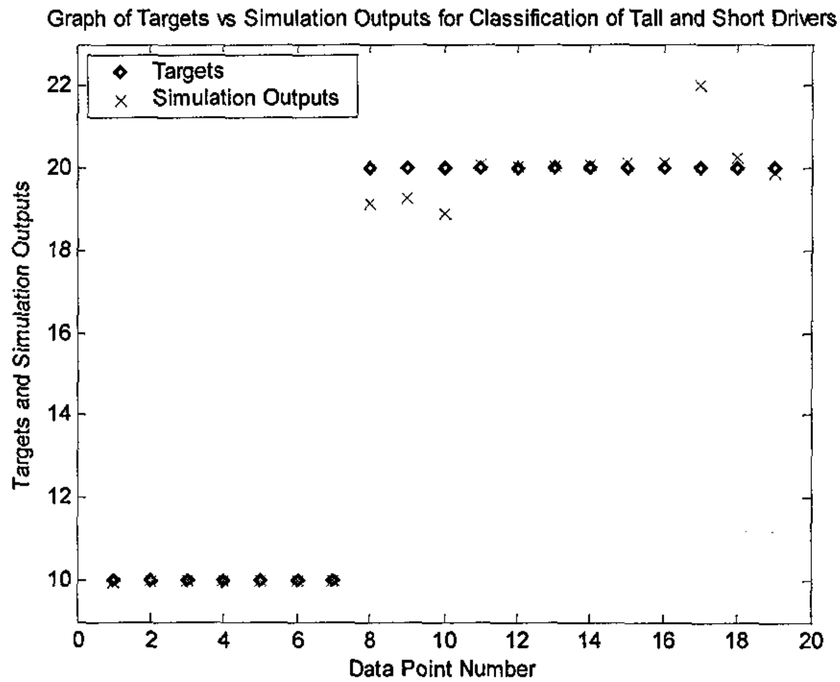

It can be seen that the results are very accurate. All the targets are matched by the simulation output within 2 units. Although the number of data points is relatively low, nevertheless this is clear evidence that it is possible to identify variations in driver sitting height using an automated method, such as ANN. There were 19 targets to match by the simulation outputs, and as can be seen, they were matched by every single simulation output, a perfect success rate.

Chapter 7 Conclusions

The previous chapter has processed the experimental data obtained from the main experimental work that was done in chapter 4, and has successfully used ANN as the basis for a future, fully functioning intelligent airbag deployment system. This chapter will now comment upon the objectives and results obtained from this investigation.

This thesis has given an extensive account of the work done for the purpose of investigating the application of thermography for use in an advanced airbag system. At the beginning of the project, the objectives which were initially formalised were as follows:

1. To detect the presence of a human being on the seat. The detection system must also be intelligent enough to detect whether the thermal profile it detects is that of an animal or another object such as luggage or bags of shopping. In these cases, the airbag should not fire.

2. To measure the occupants height and position inside the car. He could be leaning forward to use the radio or to get something out of the glove compartment or could be leaning to the side for an overtaking manoeuvre. This would be termed 'out of position' (OOP) and the airbag should not activate.

3. To identify the type of occupant i.e. whether it is male or female and whether it is a small child or an elderly person. In some of these cases, the decision to activate the airbag would need careful consideration since it could injure the elderly and child occupants.

4. To identify any other possible factors that may have safety issues.

The first objective has been fulfilled completely. The various tests done have conclusively proved that is possible to differentiate the human occupant from the rest of the background, and to differentiate it from other objects such as an Alsatian dog, a warm car seat etc. The IRISYS thermal imager is also capable of monitoring the human occupant in real-time and show movement and changes of position. This is possible because the thermal imager has a maximum frame rate of 5 frames per second, and is sufficient to detect most of the driver's movements inside the cabin as soon as they happen.

The ANN analysis described in chapter 6 has gone a long way to meeting the second objective. The ANN analysis conducted in chapter 6 proved that it was possible to successfully detect specific and subtle changes in driver position, which manifested itself as the driver was performing certain actions. Detection of the crucial OOP scenarios that the driver experienced, proved to be the most successful of the ANN analyses done (shown in figures 6-15 to 6-38) and it proves that a repeatable and autonomous method of detecting driver behaviour and position is possible with current technology.

The third objective has also been met. The preliminary experiments, which were done in chapter 4 and shown in figures 4-4 to 4-5 and 4-16 to 4-17, have shown clear differences between male and female drivers, as well as even more apparent differences between the head shape of a small 2 year old infant, and a large male adult driver. This work was expanded further by using ANN analysis to distinguish between tall and short drivers, and this was done with a 100 % success rate, as was shown in chapter 6, figure 6-39.

The final objective was also satisfied. It was shown in chapter 4 by the preliminary work that miscellaneous driver actions such as the act of smoking, wearing spectacles, both of which have serious implications for the severity of the injuries which the driver would suffer in the event of an accident, could be detected. Further analysis in chapter 6 showed that the act of using a mobile phone could also be detected.

Other notable discoveries that need to be mentioned are the fact that the IRISYS thermal imager and associated equipment (laptop computers) have proved themselves to be robust enough to withstand the effects of a sudden impact into another vehicle, as was demonstrated by the fact that it survived intact during the crash tests and was able to transmit clear images of the driver inside the car cabin. The importance of this should not be underestimated as the ability of any future airbag deployment system ought to be able to function properly in the event of a crash. Failure to do so would render the system redundant.

In conclusion, the experimental work and analysis of the results has successfully met the objectives set in the beginning. The next chapter will describe what work should be done in order to progress this project towards the ultimate goal of a fully functional, stand alone system incorporated into the cabin of the vehicle.

Chapter 8 Future Work

It was concluded in chapter 7 that most of the objectives which were initially set at the start of the investigation were satisfied as a result of the literature review done in chapter 2 and the experimental work and analysis which was done in chapters 4, 5 and 6. It can therefore be argued that this investigation has been a success in reaching the goals set. Now, the challenge is to build upon the foundations that this thesis has laid down.

It is proposed that the following tasks would need to be done in order to mover further towards realising an intelligent airbag deployment system:

1. The experimental work using the STISIM driving simulator needs to be expanded to encompass drivers of different ages. More elderly (otherwise known as 'third age') drivers and female drivers need to participate in these trials in order to make them more representative of the driver population. This is deemed necessary because it was established earlier in the thesis that 'third age' (otherwise known as elderly) drivers and occupants are one category of people who are particularly at risk of suffering airbag induced injury and death. Therefore, the more information that can be obtained about their reactions and movements inside the car cabin, the easier it would be to understand their needs.

2. Other 'at risk' occupants also need to be tested on this apparatus, such as infants inside a rear facing child safety seat on the front passenger's side. More tests need to be made to confirm the work that children and small infants can indeed be detected by the thermal imager. Although this is affected by the imager mounting position, using a wide angle lens could possibly enable the imager to view both tall drivers and children who are positioned low down on the seat.

3. A robust thermal imager and computer set up needs to be created in order to go to the next step of the testing process – real life in-car trials. This would be

fitted into the dashboard or head lining of the car cabin and images would be produced of the driver as the car was driven around a specified journey. This is important as it would test the capabilities of the thermal imaging system under normal driving conditions, and would be subjected to vibration, shock, and random lighting conditions, and differences in thermal environment.

4. The next step would be to create a real-time thermal imaging tracking system. This project has used 'off line' data, but 'real time' data needs to be used. This would be used to determine whether the car occupant was in the danger zone of airbag deployment during the car journey.

5. Other autonomous techniques need to be explored, other than ANN. Although ANN may be the best method for 'off line' work, it may not be suitable for use on 'real time' imaging.

6. The IRISYS thermal imager's size would need to be reduced somewhat in order to be fully integrated into the car cabin and become unobtrusive. It is thought that this device would need to be built into the dashboard or the ceiling of the car cabin, and in order for this to be safe and practical; the size needs to be reduced into something less bulky. Also, the associated computer required to run the equipment and software needs to be reduced in size and cost for it to be fully integrated into the car cabin. This was not done during this project as this research was primarily concerned with **proving** that such technologies and methods **could** be used for solving this problem.

7. The capabilities of the thermal imager need to be tested under real road conditions, in a real life situation. This would subject the equipment to:

- Varying temperatures, with the air conditioning being used, the windows being opened and closed, and different background temperatures during the daytime and at night.

- Extreme lighting conditions, such as light and dark, during day and night, as well as the less obvious conditions of under bridges, in tunnels, and in heavily forested areas.

- Vibrations and shocks due to uneven road surfaces, as well as the effects of sudden accelerations and braking by the driver. This could affect the performance of the thermal imager, particularly the operation of the moving parts such as the chopper, as well as the computer.

Upon completion of this work, it is anticipated that the goal of achieving a reliable and autonomous airbag deployment system would be achieved, and would be recognised as making a significant contribution to the safety of the vehicle occupant.

References

[1] http://europa.eu.int/comm/dgs/energy_transport/figures/pocketbook/doc/tran_safety_2003.pdf viewed on 31/07/04.

[2] http://www.dft.gov.uk/stellent/groups/dft_rdsafety/documents/pdf/dft_rdsafety_pdf_026183.pdf viewed on 31/07/04.

[3] http://europa.eu.int/comm/transport/care/statistics/most_recent/detailed_breakdown/index_en.htm viewed on 31/07/04.

[4] http://www-nrd.nhtsa.dot.gov/pdf/nrd-30/NCSA/TSF2002/2002ovrfacts.pdf viewed on 31/07/04.

[5] King, P., Jackson, M.R., Galer-Flyte, M.D., Grafton, A.J. **The Smart Seat Approach.** Sensor Review, Volume 16, Number 4, 1996, pp.25-30. ISSN 0260-2288.

[6] Lovsund, P. **Impact Biomechanics and its Importance to reduce Health Losses and Costs from Road Accidents.** (From 1995-1996 Annual Report School of Technology Management and Economics, Chalmers University of Technology, pp55-68, 1996).

[7] Scholz, H.J. **The Daimler-Benz Development of a Final Production Air Bag System for the U.S.A.** Air Bag Development and Performance, pp.251-259. ISBN 0-7680-1119-1.

[8] Fleming, P. **Application of Airbag Technology to Vehicles in the Lower Classes.** Safety and the automobile, pp 55-60. Selected Papers from AUTOTECH '93. Professional Engineering Publishing. ISBN 085298894X.

[9] Hinger, J.E., Clyde, H.E.. **Advanced Air Bag Systems and Occupant Protection: Recent Modifications to FMVSS 208.** Paper No. 2001-01-0157.

2001 Society of Automotive Engineers, Inc. Air Bag Development and Performance, pp.205-210. ISBN 0-7680-1119-1.

[10] **Final Economic Assessment.** FMVSS No.208 Advanced Air Bags. Office of Regulatory Analysis and Evaluation Plans and Policy, May 2000. NHTSA, pp.191-203. 2003, SAE International. ISBN 0-7680-1119-1.

[11] Galer Flyte, M. **Frontal Impact Protection: Tailoring Safety System Performance By The Prediction Of Driver Size And Seated Position.** Paper Number 98-S1-O-09. http://www.nhtsa.dot.gov/esv/16/98S1O09.PDF

[12] Breed, D.S. A **Smart Airbag System.** Automotive Technologies International, Inc. United Sates. Paper No: 98-S5-O-13. http://www.nhtsa.dot.gov/esv/16/98S5O13.PDF

[13] http://www.airbagswitches.com/ (as seen on 26/04/2002).

[14] Evans, L. **Driver Injury and Fatality Risk in Two-Car Crashes Versus Mass Ratio Inferred Using Newtonian Mechanics.** Accident Analysis and Prevention, Volume 26, No.5, pp 609-616, 1994. ISSN 0001-4575.

[15] Mock, C.N., Grossman, D.C., Kaufman, R.P., Mack, C.D., Rivara, F.P. **The Relationship Between Body Weight and Risk of Death and Serious Injury in Motor Vehicle Crashes.** Accident Analysis and Prevention 34 (2002), pp.221-228, Issue 2. ISSN 0001-4575.

[16] Parkin, S., Mackay, G.M., Cooper, A. **How Driver's Sit In Cars.** Accident, Analysis and Prevention, Vol. 27, pp. 777-783, 1995, Paper No. 0001-4575(95)00035-6. ISSN 0001-4575.

[17] Kuner, E.H., Schlickewei,W., Oltmann, D. **Injury reduction by the airbag in accidents.** Injury Vol. 27, No.3, pp.185-188, 1996 Elsevier Science Ltd, Paper No. 0020-1383(95)00211-1. ISSN 0020-1383.

[18] Nirula, R., Mock, C., Kauffman, R., Rivara, F.P., Grossman, D.C. **Correlation of head injury to vehicle contact points using the crash injury research and engineering network data.** Accident Analysis and Prevention 35 (2003), pp.201-210. ISSN 0001-4575.

[19] Fildes, B.N., Cameron, M.H., Vulcan, A.P., Digges, K.H., Taylor, D. **Airbag and Facebag Benefits and Costs.** Accident Analysis and Prevention, Vol. 26, No. 3, pp. 339-346, 1994 Elsevier Science Ltd. ISSN 0001-4575.

[20] Lehto, K.S., Sulander, P.O., Tervo, T.M.T. **Do Motor Vehicle Airbags Increase Risk of Ocular Injuries in Adults?** American Academy of Ophthalmology, Volume 110, No. 6, June 2003, pp.1082-1088, Elsevier Inc 2003. ISSN 0161-6420.

[21] Evans, L. **Restraint Effectiveness, Occupant Ejection From Cars, and Fatality Reductions.** Accident Analysis and Prevention, Vol. 22, No. 2, pp.167-175, 1990 Pergamon Press. ISSN 0001-4575.

[22] Evans, L. **Airbag Effectiveness in Preventing Fatalities Predicted According to Type of Crash, Driver Age, and Blood Alcohol Concentration.** Accident Analysis and Prevention, Vol. 23, No. 6, pp.531-541, 1991. ISSN 0001-4575.

[23] Stefanopoulos, N., Vagianos, C., Stavropoulos, M., Panagiotopoulos, E., Androulakis, J. **Deformations and Intrusions of the Passenger Compartment as Indicators of Injury Severity and Triage in Head-On Collisions of Non-Airbag-Carrying Vehicles.** Injury, International Journal of the Care of the Injured, Volume 34, pp.487-492, 2003. ISSN 0020-1383.

[24] Chidester, A.B., Roston, T.A. **Air Bag Crash Investigations**. National Highway Traffic Safety Administration United States of America. Paper Number 246.

[25] Kang, J., Agaram, V., Nusholtz, G., Kostyniuk, G. **Air Bag Loading on In-Position Hybrid III Dummy Neck**. Paper No. 2001-01-0179, Biomechanics Research and Development, SAE SP-1577, pp.69-84. ISBN 0-7680-0724-0.

[26] Buzeman, D.G., Viano, D.C., Lovsund, P. **Car Occupant Safety In Frontal crashes: A Parameter Study of Vehicle Mass, Impact Speed, and Inherent Vehicle Protection**. Accident Analysis and Prevention, Vol. 30, No. 6, pp. 713-722, 1998 Elsevier Science Ltd. ISSN 0001-4575.

[27] Hobbs, C.A. **Essential Requirements for an Effective Full Scale Frontal Impact Test.** Paper number: 900410. Vehicle Crashworthiness and Occupant Protection in Frontal Collisions, SP-807. ISBN 1-56091-016-X.

[28] **Counts for Air Bag Related Fatalities and Seriously Injured Persons.** http://www-nrd.nhtsa.dot.gov/pdf/nrd30/NCSA/SCI/3Q_2001/ABFSISR.html (as seen on 27/04/2002).

[29] Segui-Gomez. **Driver Air Bag Effectiveness by Severity of the Crash.** American Journal of Public Health, October 2000, Vol. 90, No. 10. http://www.hcra.harvard.edu/pdf/airbags.pdf (viewed on 13th May 2005). ISSN (print) 0090-0036ISSN (electronic) 1541-0048.

[30] Huelke, D.F., Moore, J.L., Compton, T.W., Samuels, J., Levine, R.S. **Upper Extremity Injuries Related to Air Bag Deployments.** Air Bag Development and Performance, pp. 655-664, 2003 SAE International. ISBN 0-7680-1119-1.

[31] Langweider, K., Hummel, T.A., Anselm, D. **The Effect Of Airbags On Injuries and Accident Costs.** Allianz Center for Technology, Germany. Paper Number 98-S1-W-27.

[32] Augenstein, J., Perdeck, E., Stratton, J., Digges, K., Steps, J. **Performance of Depowered Air Bags in Real World Crashes.** Paper No. 2002-01-0186, Air Bag Development and Performance, pp. 801-806, 2003 SAE International. ISBN 0-7680-1119-1.

[33] Miller II, M.P., Phillips, S. **Vehicle Seating – An Overview of How Advanced Airbag Regulations Will Effect Non-FMVSS Test Procedures.** Paper No. 2001-01-0116, Progress in Safety Test Methodology, SP-1596. ISBN 0-7680-0743-7.

[34] http://www.theengineer.co.uk/item.asp?id=36371&pub=&type=News (as seen on 30/04/2002).

[35] Ryan, S. **An Innovative Approach to Adaptive Airbag Modules.** Air Bag Development and Performance, pp.289-293, 2003 SAE International. ISBN 0-7680-1119-1.

[36] Rohr, S.N., Lind, R.C., Myers, R.J., Bauson, W.A., Kosiak, W.K; Yen, H. **An Integrated Approach to Automotive Safety Systems.** SAE 2000 World Congress, Detroit, Michigan. March 6-9, 2000. 2000-01-0346. ISSN 0148-7191.

[37] Hollingum, J. **Vehicle Sensing gets an inflated image.** Sensor Review, Vol. 16, No. 4, pp. 31-36, 1996 MCB University Press. ISSN 0260-2288.

[38] Mackay, M., Hassan, A.M., Hill, J.R., **Observational Studies of Car Occupants' Positions.** Birmingham Accident Research Centre, University of Birmingham. Paper No. 98-S6-W-42.

[39] Galer, M., Jones, S. **Intelligent Occupant Protection Systems.** University of Technology, Loughborough, U.K. Paper No. 98-S3-O-11.

[40] Libertiny, G.Z. **The Effect of Driver Age on Traffic Accidents.** Paper No. 970277. Progress with Human Factors in Automotive Design: Seating Comfort, Visibility, and Safety, SAE SP-1242.
ISBN 1-56091-954-X.

[41] http://www.i-car.com **Developing Smart Airbag Sensors – New Standards Coming.** July-August 1999.

[42] Breed, D.S., Summers, L., Carlson, J., Koyzreff, M. **Development Of An Occupant Position Sensor System To Improve Frontal Crash Protection.** Autoliv, United States, Paper No. 325.

[43] Paula, G. **Sensors help make air bags safer.**
http://www.memagazine.org/backissues/august97/features/airbag/airbag.html.
(as seen on 04/03/2002).

[44] Jinno, K., Ofuji, M., Saito, T., Sekido, S.
Occupant Sensing Utilizing Perturbation of Electric Fields. Anthropomorphic Dummies and Crash Instrumentation Sensors, Paper No. 971501, pp.117-129, SAE SP-1261. ISBN 1-56091-973-6.

[45] Lu, Y., Marschner, C., Eisenmann, L., Sauer, S.
The New Generation of the BMW Child Seat and Occupant Detection System SBE2. International Journal of Automotive Technology, Vol. 3, No.2, pp. 53-56 (2002). 2002 KSAE. ISSN 1229-9138.

[46] Kimberley, W., Editor Automotive Engineer.
http://www.autofieldguide.com/articles/110101.html (as seen on 07/03/2002).

[47] Birch, S. http://www.sae.org/automag/globalvehcles/05-2001/global3.htm (as seen on 07/03/2002).

[48] Kosiak, W.K., Rohr, S.N. **Future Trends in restraint Systems Electronics.** www.delphi.com/pdf/sae/future_trends.pdf- (as seen on 15/11/02).

[49] Henriksson, M., Hallen, A., Howing, M., Lundell, B., Ericson, M., Nilsson, L; Berlin, M. **Passenger AIR-BAG Status Indication Awareness Study.** 1997 Society of Automotive Engineers, Inc. Paper No. 970276. Progress with Human Factors in Automotive Design: Seating Comfort, Visibility, and Safety. SAE SP-1242. ISBN 1-56091-954-X.

[50] Mao, Y., Appel, H. **Influence of Air Bag Folding Pattern on OOP-injury Potential.** Paper No. 2001-01-0164. Air Bag Development and Performance, pp.325-332, 2003 SAE International. ISBN 0-7680-1119-1.

[51] Slazas, P.A. **Non-Contact Optical Displacement Sensing.** Sensor Review, Vol. 16, No.3, pp.33-37, MCB University Press. ISSN 0260-2288.

[52] Ogawa, M., Ochiai, S., Shoji, K., Nishihara, M., Togawa, T. **An attempt of monitoring daily activities at home.** Proceedings of the 22nd Annual EMBS International Conference, July 23-28, 2000, Chicago IL, pp.786-788. 2000 IEEE. ISBN 0-7803-6465-1.

[53] Lambert, D.K. **Direct Thermal Detection for Front Passenger Seat Airbag Suppression.** Air Bag Development and Performance, pp. 315-318, 2003 SAE International. ISBN 0-7680-1119-1.

[54] Teuner, A., Hillebrand, M., Hosticka, B.J., Park, S.B., Santos Conde, J.E., Stevanovis, N. **Surveillance Sensor Systems Using CMOS Imagers.**

10th International Conference on Image Analysis and Processing, 1999 IEEE. ISBN 0-7695-0040-4.

[55] Novotny, P.M., Ferrier, N.J. **Using Infrared Sensors and the Phong Illumination Model to Measure Distances.** Proceedings of the 1999 IEEE International Conference on Robotics and Automation, 1999 IEEE. ISBN 0-7803-5180-0.

[56] Miller, D.P., Wright, A., Sargent, R. **Attitude and Position Control Using Real-Time Colour Tracking.** 1997 American Association for Artificial Intelligence (www.aaai.org). http://www.kipr.org/papers/tracking.pdf (viewed on 14th may 2005).

[57] Fukui, T., Kyota, N., Isonaga, K., Kamiji, K., Ino, T. **Occupant position detection system (OPDS) for side airbag system**. JSAE Review 22 (2001), pp. 69-74, Paper JSAE20014010. ISSN 0389-4304.

[58] Hashimoto, K., Tsuruta, T., Morinaka, K., Yoshiike, N. **High performance human information sensor**. Sensors and Actuators 79, 2000, pp. 46-52, 2000 Elsevier Science S.A. ISSN 0924-4247.

[59] Gitelman, D.R., Parrish, T.B., LaBar, K.S., Mesulam, M.M. **Real-Time Monitoring of Eye Movements Using Infrared Video-Oculography During Functional Magnetic Resonance Imaging of the Frontal Eye Fields**. NeuroImage 11, pp. 58-65 (2000). ISSN 1053-8119.

[60] Wtzel, G., Braunwarth, H., Pulido, F., Reisacher, G. **Occupant Detection Systems.** Paper No. 971047, Anthropomorphic Dummies and Crash Instrumentation Sensors, SAE SP-1261, pp. 55-60. ISBN 1-56091-973-6.

[61] Parenteau, C.S., Shah, M., Desai, T., Frampton, R.
US and UK Belted Driver Injuries with and without Airbag Deployments

– **A Field Data Analysis.** Paper No.1999-01-0633, International Congress and Exposition, Detroit, Michigan. March 1 – 4, 1999. Reprinted from 'Occupant Protection' (SP – 1432). 1999 Society of Automotive Engineers, Inc. ISSN 0148-7191.

[62] Billen, K., Federspiel, P., Schockmel, P., Serban, B., Sherrill, W. **Occupant Classification System for Smart restraint Systems.** Paper No. 1999-01-0761, 2001 Society of Automotive Engineers, Inc.
Air Bag Development and Performance, pp.319-323, 2003 SAE International. ISBN 0-7680-1119-1.

[63] Kuboki, N., Okamura, H., Enomonto, T., Nishimoto, T. Ohue, T., Ando, K. **An Occupant Sensing System for Automobiles Using a Flexible Tactile Force Sensor.** Furukawa Review, No.20, 2001. ISSN 0911-9280.

[64] Chandrasekaran, N., Kumar, P., Joseph, C.S. **A Computer Interfaced Fiber Optic Reflective Displacement Sensor For Weight Measurement.**
International Conference on Fiber Optics and Photonics, 2000, Vol. 2, pp. 569-571. ISBN 817764-1034.

[65] Krumm, J., Kirk, G. **Video Occupant Detection for Airbag Deployment.**
Fourth IEEE Workshop on Applications of Computer Vision, October 1998, pp. 30-35. ISBN 0-8186-8606-5.

[66] Owechko, Y., Srinivasa, N., Medasani, S., Boscolo, R.
Vision-Based Fusion system for Smart Airbag Applications. IEEE Intelligent Vehicle Symposium IV, 2002, Versailles, France, June 2002.
Part 1, pp.245-50. ISBN 0780373464.

[67] Ran, B., Liu, H.X. **Development of A Vision-Based Vehicle Detection and Recognition System For Intelligent Vehicles.**
http://www.topslab.wisc.edu/resources/publications/ran_1999_0226.pdf
(as seen on 14^{th} May 2005).

[68] Victor, T. **A Technical Platform for Driver Inattention Research.** http://www-nrd.nhtsa.dot.gov/departments/nrd-13/driver-distraction/PDF/7.PDF
(as seen on 14th May 2005).

[69] Haro, A., Flickner, M., Essa, I. **Detecting and Tracking Eyes Using Their Physiological Properties, Dynamics, and Appearance.** www.cc.gatech.edu/cpl/projects/pupil/pupil.pdf (as seen on 15/11/02) Appears in IEEE CVPR 2000, pp.163-168.

[70] Russakoff, D.B., Herman, M. **Head Tracking Using Stereo.** Machine Vision and Applications (2002) 13: pp.164-173. Springer-Verlag 2002. ISSN (print) 0932-8092. ISSN (electronic) 1432-1769.

[71] Boverie, S. **A new class of intelligent sensors for the inner space monitoring of the vehicle of the future.** Control Engineering Practice, 10, (2002), pp. 1169-1178. ISSN 0967-0661.

[72] **The Science of Crash Avoidance.** http://detnews.com/AUTOS/1101/lead.htm (as seen on 26/02/2002).

[73] Verwey, W.B., Zaidel, D.M. **Preventing Drowsiness Accidents by an Alertness Maintenance Device.** Accidents Analysis and Prevention, 31, pp. 199-211. 1999. ISSN 0001-4575.

[74] **Big Brother Watches You Drive.** http://news.bbc.co.uk/1/hi/technology/2246115.stm (as seen on 06/11/2002).

[75] Mita, S., Norimatsu, Y., Itou, S., Kozuka, K., Nakano, T., Yamamoto, S. **Detection of the Gaze Direction of a Driver Using the Time-Varying Image Processing.** JSAE Review 24 (2003), pp. 347-353, Paper No. JSAE20034260. ISSN 0389-4304.

[76] Liu, A., Salvucci, D. **Modeling and Prediction of Human Driver Behaviour**. To appear in Proceedings of the 9th International Conference on Human-Computer Interaction, New Orleans, LA, August 2001. http://cog.cs.drexel.edu/publications/ICEPCE01.pdf (viewed on 13th May 2005).

[77] Wouters, P.I.J., Bos, J.M.J. **Traffic Accident Reduction by Monitoring Driver Behaviour With In-Car Data Recorders**. Accident Analysis and Prevention 32 (2000), pp. 643-650. ISSN 0001-4575.

[78] McAllister, G., McKenna, S.J., Ricketts, I.W. **Hand Tracking for Behaviour Understanding**. Image and Vision Computing 20 (2002), pp.827-840. ISSN 0262-8856.

[79] Zhang, H., Gopal, M.M., Sazena, R., Avula, X.J. **An Integrated Optimization System for Airbag Design and Modeling by Finite Element Analysis**. SAE Technical Paper Series 2003-01-0506. Reprinted from Airbags and Safety Test Methodology (SP-1776). ISSN 0148-7191.

[80] Nishimura, K., Takahashi, N., Sasaki, Y. **The Development of New Polyester Fabrics for Attaining Advanced Uncoated Airbags**. Frontal Impact Protection: Seat Belts and Air Bags, SAE SP-947, Paper No. 930649, pp.109-118. ISBN 1-56091-332-0.

[81] Al-Habaibeh, A., Parkin, R.M., Jackson, M.R., Whitby, D.R., Mansi, M., Coy, J. **The Application of an Autonomous Low Cost Infra-red Thermal Imager For Condition Based Maintenance Of Machinery.** Mechatronics Research Centre, Loughborough University, U.K. www.mechatronics.org.uk/alcis

[82] Transactions in Measurement and Control, Volume 1, 3rd Edition. Non Contact Temperature Measurement. 2000 Putnam Publishing Company and

OMEGA Press LLC. www.omega.com

[83] Dereniak, E.L., Boreman. **Infrared Detectors and Systems.** John Wiley and Sons, Inc, 2000. ISBN 0-471-12209-2.

[84] Rogalski, A. **Infrared Detectors.** Overseas Publishers Association, 2000. ISSN 0275-7230.

[85] Porter, S., Mansi, M., Sumpter, N., Galloway, L. **Low Cost Smart Sensors Using Infrared Detector Arrays.** Sensor Review, Vol. 21 – No.4 – 2001, pp. 283 – 287, MCB University Press. ISSN 0260-2288.

[86] Burnay, S.G., Williams, T.L., Jones, C.H. **Applications of Thermal Imaging.** IOP Publishing Ltd 1988. ISBN 0-85274-421-8.

[87] Casiday, R., Frey, R. **Gas Laws Save Lives: The Chemistry Behind Airbags. Stoichiometry and the Gas Constant Experiment.** Department of Chemistry, Washington University St. Louis, MO 63130. http://www.chemistry.wustl.edu/~edudev/LabTutorials/Airbags/airbags.html

[88] Nahum, A.M., Melvin, J.W (Editors). **Accidental Injury, Biomechanics and Prevention.** Springer – Verlag New York Inc, 2nd Edition, 2002, pp.254-273. ISBN 0-387-98820-3.

[89] Halldin, P., Holst, H., Von; E.I. **An Experimental Head Restraint Concept For Primary Prevention Of Head And Neck Injuries In Frontal Collisions.** Accident Analysis And Prevention, Vol. 30, No.4, pp.535-543, 1998. ISSN 0001-4575/98.

[90] Nozumi, S. **Development of Occupant Classification System for Advanced Airbag Requirements**. Mitsubishi Motors Technical Review 2004 No.16. http://www.mitsubishimotors.com/corporate/about_us/technology/review/e/pdf/2004/16E_12.pdf (viewed on 15/01/06).

[91] Bertozzi, M., Broggi, A., Fasciolo, A. **Vision-based intelligent vehicles: State of the art and perspectives**. Robotics and Autonomous Systems, Vol. 32 (2000), pp.1-16. ISSN: 00921-8890/00, Elsevier Science 2000. PII: S0921-8890(99)00125-6.

[92] Morris, C.R., Zuby, D.S., Lund, A.K. **Measuring Airbag Injury Risk To Out-Of-Position Occupants**. Insurance Institute for Highway Safety, United Sates, Paper Number 98-S5-O-08. http://www.nhtsa.dot.gov/esv/16/98S5008.PDF (viewed on 04/01/06).

[93] **Foresight Vehicle Technology Roadmap: Technology and Research Directions for Future Road Vehicles, version 1.0.** http://www.foresightvehicle.org.uk/public/info_/FV/TRM_v1.pdf

[94] Pischinger, S., Sconfelder, C., Ogrzewalla, J. **Analysis of Dynamic Requirements For Fuel Cell Systems For Vehicle Applications.** (Article In Press) Journal of Power Sources. ISSN 0378-7753.

[95] Kato, S., Minobe, N., Tsugawa, S. **Applications of Inter-Vehicle Communications To Driver Assistance System.** JSAE Review 24, Issue 1, January 2003, pp. 9-15. ISSN 0389-4304.

[96] Piechulla, W., Mayser, C., Gehrke, H., Konig, W. **Reducing Drivers' Mental Workload By Means Of An Adaptive Man-Machine Interface.** Transportation Research Part F 6 (2003), pp. 233-248. ISSN 1369-8478.

[97] Butler, R. **Drivers Take A Back Seat.** Professional Engineering, 14th December 2005.

[98] Marchau, V.A.W.J., Van der Heijden, R.E.C.M., Molin, E.J.E. **Desirability of Advanced Driver Assistance From Road Safety Perspective: The Case of ISA.** Safety Science, Vol. 43, 2005, pp.11-27. ISSN 0925-7535.

[99] Garvill, J., Marell, A., Westin, K. **Factors Influencing Drivers' Decision To Install An Electronic Speed Checker In The Car.** Transportation Research Part F 6 (2003), pp. 37-43. ISSN 1369-8478/02.

[100] Burdick, H.E. **Digital Imaging Theory and Applications**. McGraw-Hill, 1997. ISBN 0-07-913059-3.

[101] Awcock, G.J., Thomas, R. **Applied Image Processing**. Macmillan New Electronics, 1995 Edition. ISBN 0-33-58242-X.

[102] Baxes, G.A. **Digital Image Processing, Principles and Applications**. John Wiley and Sons, Inc, 1994 Edition. ISBN 0-471-00949-0.

[103] http://www.statsoftinc.com/textbook/stneunet.html
Electronics Textbook, Statsoft. © Copyright StatSoft, Inc.1984-2003 STATISTICA is a trademark of StatSoft, Inc.

[104] Zorriassatine, F., Tannock, J.D.T. **A review of neural networks for statistical process control**. Journal of Intelligent Manufacturing (1998), 9, pp. 209-224. Kluwer Academic Publishers, 1998. ISSN 0956-5515.

[105] Coppin, B. **Artificial Intelligence Illuminated.** 1st Edition, Jones and Bartlett Publishers, Inc, 2004. ISBN 0-7637-3230-3.

Appendix 1 List of Papers

1. R M Parkin, A F Juna, A Al-Habaibeh, M R Jackson, M Mansi+ **LOW COST INFRA-RED SENSORS FOR INTELLIGENT DEPLOYMENT OF AUTOMOTIVE RESTRAINT SYSTEMS.**

2. A F. Juna, A. Al-Habaibeh, D.R. Whitby, M. Jackson, R.M. Parkin. **Smart Restraint Systems Utilising Low Cost Infra Red Sensors.**

47. Internationales Wissenschaftliches Kolloquium
Technische Universität Ilmenau
23.-26. September 2002

R M Parkin, A F Juna, A Al-Habaibeh, M R Jackson, M Mansi[+]

LOW COST INFRA-RED SENSORS FOR INTELLIGENT DEPLOYMENT OF AUTOMOTIVE RESTRAINT SYSTEMS

ABSTRACT

It is a long accepted fact that the advent of vehicle restraint systems such as seat belts and air bags have reduced injuries during collisions and saved many lives. Despite the acknowledged benefits it is still a matter of concern that there are a small number of cases where death results as a direct consequence of the use of the restraint systems.

In such cases, it is often found that there are contributory factors, which may predispose a seat occupant to belong to a high-risk category. Such factors may be age, gender, body morphology and, possibly, even fitness. There have been many attempts to address some of these (eg, weight detection for babies – smart seats for motorcycles, determination of skeletal bone density) with varying degrees of success. It is felt by the authors that the route to success lies in integrating a range of sensory techniques in order to intelligently assess vehicle occupants for gender, age, height, and fitness. It is believed that simple time-history of occupant motion will enable the determination of head position in 3 dimensions and encumbrances (eg cigarettes, spectacles) at the time of impact. This will enable a truly sensitive deployment of restraints governing seat-belt pre-tensioning and front/side air bag inflatant injection profiles.

The paper describes the current work being undertaken by the Mechatronics Research Centre at Loughborough in conjunction with IRISYS Ltd concerning a low cost infra-red sensor integrated with other sensors in the cabin of a vehicle in order to determine and categorise a range of the above-mentioned parameters identifying occupants as high-risk.

The construction of a static test rig is complete. This allows for the testing of a range of people with age, gender, morphology and fitness differences in order to permit the generation of algorithms on embedded controllers to identify risk parameters and pass deployment parameters to the restraint systems. The embedded controllers communicate via CAN-bus in order to integrate with accepted automotive standards.

Although the experimental programme is at an early stage, it is clear that a wide range of cockpit occupancy situations and driver behaviour patterns can be reliably detected. It is anticipated that the project will provide valuable information and experience in order to seek further commercial partners with a view towards developing a proposal to seek funding for a major research & development programme.

INTRODUCTION

Crash energy absorbing crushable front-end structures combined with active seatbelts and multiple airbags in the vehicle cockpit have improved the safety of automotive vehicle occupants [1].

Although wearing seatbelts reduce death and injury by 50% [2], there is a severe limitation in that there is a need for a zone ahead of the occupant such that he can move forward and be slowed down by the belt. At rapid decelerations from 50 km/hr, the head arcs forwards and down, and thus impacts the steering wheel or dashboard. It was this type of accident that the airbag was designed for.

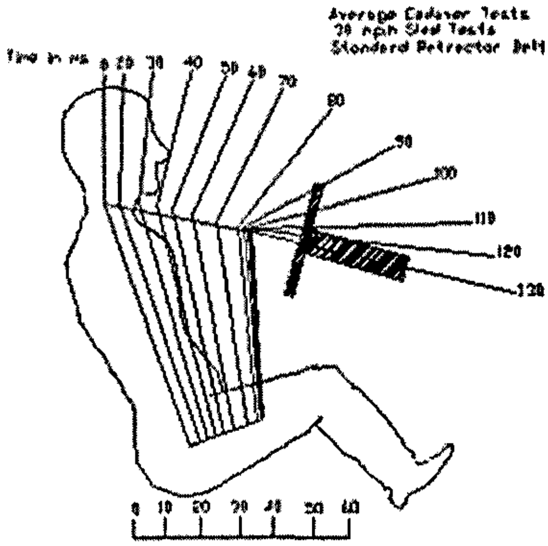

Figure 1 Crash Progress

A head on crash and the deployment of safety restraints is over within one second. Figure 1 (redrawn from Mackay et al [2]) shows that the head of the driver strikes the top of the steering wheel after 90 ms have elapsed.

With the introduction of the airbag in the late 1980's, it seemed that finally a device had been found that would protect the driver from striking the steering block in the event of a front end impact. However, whilst the airbag has been credited with saving thousands of lives over the years, there have been a steady trickle of reports, particularly in the U.S.A, of unwanted side-effects, namely that they have caused injuries (sometimes fatal) to the occupant. The total confirmed airbag related fatalities in the U.S.A, between the period of 1990 to 2001 inclusive was 195. This number includes 119 children, 68 adult drivers and 2 adult passengers [3].

Although it must be stressed that the ratio of people killed by airbags to the number of people saved by airbags is small, nevertheless it is somewhat of an embarrassment to the car industry as a whole to see that a device designed to save lives, can also kill. In fact, such is the concern in the U.S.A about the safety of airbags that the NHTSA has allowed companies to produce and install airbag switches that allow the driver to deactivate the airbag when required i.e. when a child or elderly person is in the passenger seat. However, since this switch is manually operated, there is the potential for the driver to forget to activate or deactivate the airbag, when inflated, could cause injury.

BACKGROUND RESEARCH

Progress is being in developing intelligent methods of activating the safety restraint systems. For example, one idea is that not all crashes require the need for an airbag to deploy – a seatbelt on its own could adequately restrain the driver and secure him to his seat. In order to utilise this method, the on-board processor needs to know if the driver is wearing a seatbelt or not. Such an approach has been adopted by Mercedes-Benz [4].

The problem of accidental or unwanted activation of the airbag is not only a safety issue, but also an economic one. In fact it is estimated that it costs approximately €2000 to replace and reset an airbag [4]. Therefore one of the most important criteria for activating an airbag is that the airbag should not activate if there is no-one in the driver or passenger seat! Although it sounds obvious, there have been occasions in the past where the airbag has fired with no occupants, although this was the result of vandals hitting the front end of the car with baseball bats. To stop unwarranted deployments, Mercedes-Benz have installed a weight sensor into the front seats – if it detects a load of more than 26 pounds, then the airbag will activate [4]. The weight threshold is designed so that if babies are left on the seat, the low weight exerted would mean that the airbag should not fire. However, there is still the problem of heavy luggage or other cargo being left on the seats which would be detected and therefore could cause unnecessary airbag deployment.

Some of the casualties caused by airbag inflation are the result of the driver not seated correctly, when he is said to be 'out of position'. He could be leaning forward or leaning to the side, which would render him too close to the steering wheel at the time of impact. When the airbag inflates at more than 200mph, and is fully inflated less than a second from the initial impact, the high pressure inside the airbag makes it a surprisingly solid object to hit, and a driver who is too close would sustain injury. Methods to overcome this problem are being examined. For example, one method is to have the airbag not so 'hard' or solid when the driver strikes it, by reducing the pressure inside the airbag or having the airbag inflate at slightly slower speeds. This makes sense because the harder or more solid the airbag is, the more it tends to be an elastic collision and so due to Newton's 3rd Law (action and reaction) more of the force is rebounded onto the driver himself, thus causing him his injuries. If the airbag was softer, more of the impact energy would be absorbed by the airbag and the gas inside it as it deforms, thus softening the blow to the driver. Other methods of doing this have been to separate the airbag into different compartments and inflate each of them at different times, although this would make it more expensive and more complex.

Volvo's 'EyeCar' uses a video camera to scan the driver's head and to locate the centre of each eye [5]. This is used by the on-board processor to adjust the driving seat to the optimum height. Volvo's second innovation is its driver height measurement system. It uses a sensor above the driver's head to measure electrical current patterns, which change according to the water content of the body, which in turn depends on the height of the body.

Galer and Jones [1] postulated that having advance warning of an impending accident would allow time for the priming of appropriate secondary safety features, for example to activate seatbelt pre-tensioners or adjust the position of head restraints for rear impacts. In fact, the airbag has inflated and completely deflated within 150ms, which is extremely fast when you consider that it takes 200ms for the human eye to blink![6].

Conventional methods for accident prediction have all involved the use of sensors located on the front of the vehicle to detect objects that are immediately in danger of colliding. Breed [7] also explains how the severity of the crash can also be forecast by using an accelerometer to measure the deceleration that occurs in a crash and so prime the airbag to be inflated to the correct volume.

EXPERIMENTAL PROGRAMME

The work being conducted by the Mechatronics Research Centre at Loughborough University [8] is concerned with the use of low-cost sensing to characterise parameters of individuals in order to more effectively deploy restraint systems. The objectives of the research are to

- Discover whether an individual is present – if a seat is unoccupied, or is occupied by an inanimate object (eg shopping) then air bag or seat belt tensioner deployments are unnecessary and costly to reset.
- Identify the type of person – if the person is a child, then deployments need to be different from those for adults. A person with a large body structure will have different needs form those with a petite structure. Aged females with osteoporosis will require different deployments from fit young males.
- Identify positional factors – is the person facing straight ahead or to the side?

Is the person leaning forwards, or well back in the seat? Is the person reaching down to the radio/cassette or a door storage pocket? Is the person slumped across the steering wheel (fainted or sleepy)?

- Identify other factors which may influence optimal deployments – eg is the person wearing spectacles, or smoking, or drinking? Is the person wearing a thick coat or in shirtsleeves?

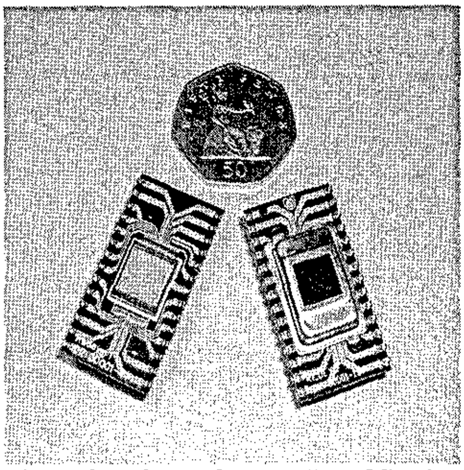

Figure 2 Infra Red Array Based Device

The work centres around sensor fusion, the combination of information from a range of sensors, to provide a broad range of data giving different facets of the cockpit occupancy scenario and enabling cross correlations to enhance confidence levels of predictions. The most important sensor in this work is a low-cost Infra Red Array Based Device (ABD), based on pyro-electric technology, supplied by our collaborator IRISYS Ltd (Figure 2). The array is a 16x16 matrix. It is expected that the sensing system may be reduced in size to fit into the head lining of a vehicle cockpit band thus be unobtrusive. Despite the small number of pixels, useful image data can be extracted. The benefit of IR over conventional imaging techniques is that vehicle users do not feel that their privacy is being invaded.

In order to progress the work at a rapid pace an industrially sized imager is being used for preliminary work (Figure 3). This is set up outside of a static vehicle simulation rig (Figure 4). The simulation rig is an instrumented version of a vehicle cockpit which allows for excessive adjustment of seat height, rake and lateral position. Vehicle height and door width can be adjusted across a range simulating two and four door chassis for sports and small hatchbacks up to large 4x4 vehicles.

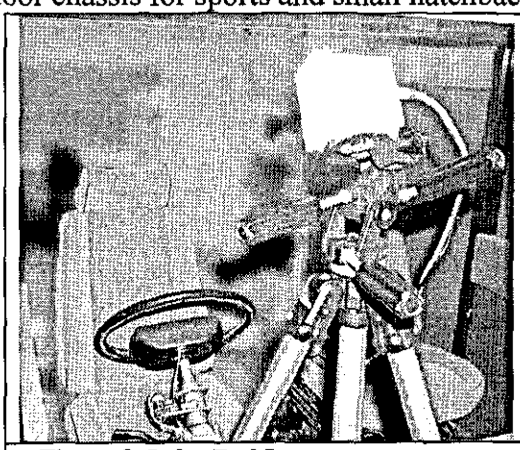

Figure 3 Infra Red Imager

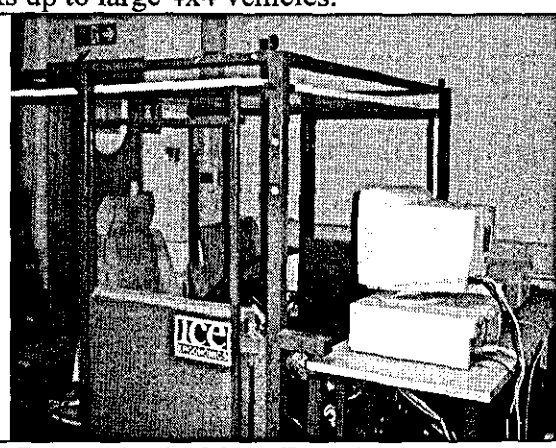

Figure 4 Static Vehicle Test Rig

RESULTS

The driver position and a corresponding infra-red image are shown in figures 5 and 6.

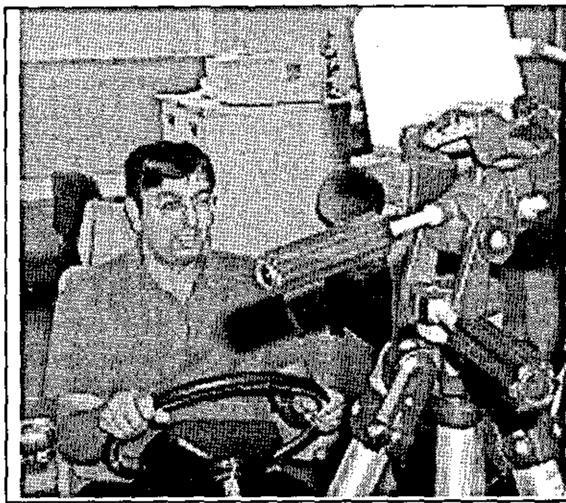

Figure 5 Driver in Position

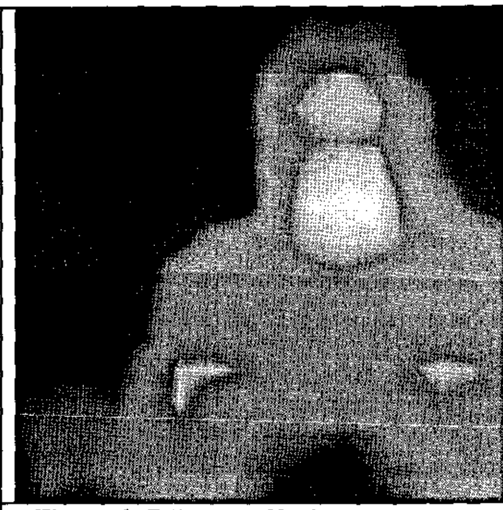

Figure 6 IR Image of Driver

Figure 6 shows the driver (Figure 5) being a tall person. In the lower third of the image, the hands can both clearly be seen in the classic "ten to two" position on the steering wheel rim. The nose and mouth area are well identified (north east of centre). The head position is discernible and the fact that this driver wears spectacles (hence the cooler area around the eyes).

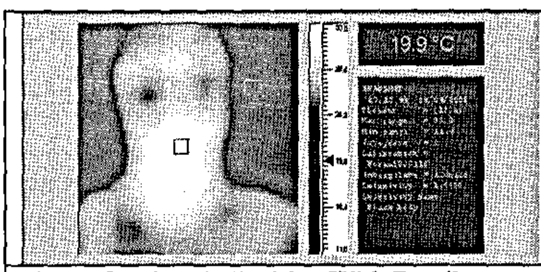

Figure 7 Driver in Position With Detail

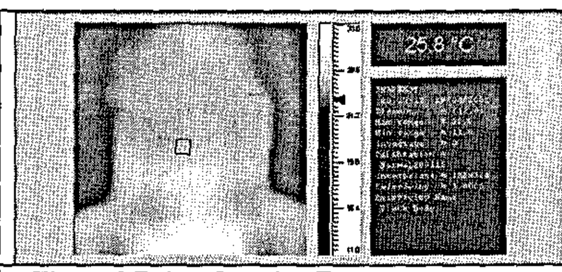

Figure 8 Driver Leaning Forward

Figure 7 depicts a driver in his normal position. The image is embedded in a software display giving various amounts of information including a temperature reading for the pixel identified as (12,4) – ie a horizontal position of 12 and vertical of 4 with the co-ordinate origin (0,0) at the top left of the 16x16 matrix. Figure 8 shows the same driver having leaned forward so as to be closer to the windscreen; the head is depicted to be much larger – as would be expected.

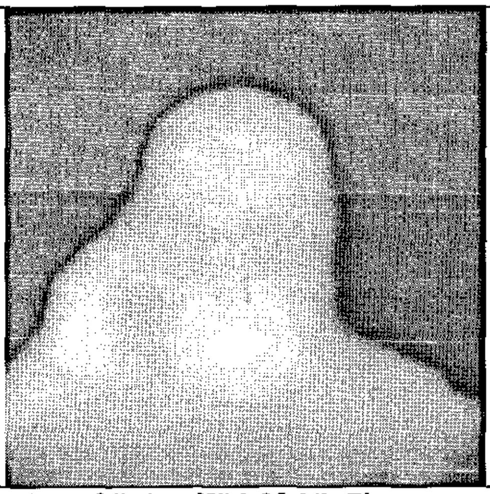

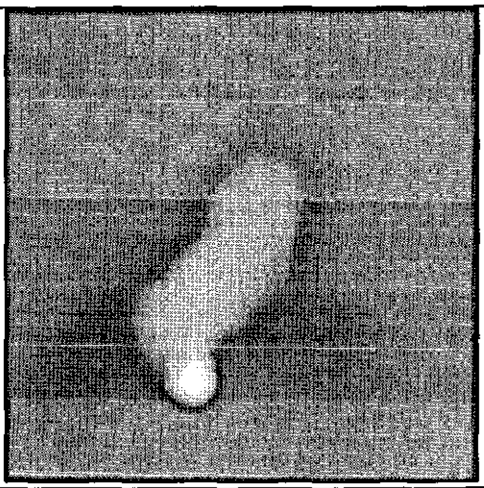

Figure 9 Driver With Mobile Phone	Figure 10 Driver Smoking

Various tests have been carried out with tall and short drivers, with and without spectacles, drinking (hot and cold) and in a range of situations expected in vehicles. Figure 9 shows a driver operating a mobile phone and Figure 10 a driver who is smoking.

DISCUSSION

It should be noted that the IR images obtained are all of a 16x16 pixel resolution. The images shown have been processed by interpolation to a 128x128 pixel size. Any image processing work is carried out on the raw images as no extra data is present from the interpolation, however it aids visualisation for humans.

It is clear from the relatively sparse set of results presented here that we can identify tall and short drivers. We can also see how close a driver is to the windscreen. Of course it could be a person with a large head far back or one with a small head close to, this cannot be differentiated in absolute terms with a "snapshot". If, however, one takes time history of a journey into account, one can determine the full extent or range of forward/reverse head positions. When taken in conjunction with the reasonable range of possible positions (given seat longitudinal position) we can postulate instantaneous head position with some confidence (in three axes).

In addition we can identify other significant factors, eg that a person is wearing spectacles. This may be important as an excessive air bag deployment could cause glass breakage with concomitant risk of eye damage (and perhaps liability claims in litigious environments). Another detection possibility is that of smoking, this may have no direct impact on air bag deployment, but in an intelligent traffic environment this information could prove useful to crash team personnel; the information could be passed by the car communication system to the emergency services warning of potential fire risk. The ability to detect use of a mobile phone may have no direct impact again. However the knowledge may prove useful in determining the level of potential awareness of a driver in assessing blame in accidents and even insurance liabilities.

CONCLUSION

The paper describes work being undertaken by the Mechatronics Research Centre at Loughborough in conjunction with IRISYS Ltd concerning a low cost infra-red sensor integrated with other sensors in the cockpit of a vehicle in order to determine and categorise a range of parameters identifying levels of risk of damage to occupants by crash restraint deployments.

Although the experimental programme is at an early stage, it is clear that a wide range of cockpit occupancy situations and driver behaviour patterns can be reliably detected. It is anticipated that the project will provide valuable information and experience in order to seek further commercial partners with a view towards developing a proposal to seek funding for a major research & development programme.

ACKNOWLEDGEMENT

The work is supported by the Engineering and Physical Sciences Research Council (EPSRC) by a quota PhD studentship administered by the Faraday PRIME partnership. The award is a CASE (Cooperative Award in Science and Engineering) type, which includes a significant industrial contribution from IRISYS Ltd.

References

1. **Galer, M; Jones, S.** "Intelligent Occupant Protection Systems", University of Technology, Loughborough. United Kingdom. 94-S3-O-11.
2. **Mackay, M; Hassan, A.M; Hill, J.R.** "Observational Studies of Car Occupants' Positions", Birmingham Accident Research Centre, University of Birmingham, Birmingham, U.K. Paper Number: 98-S6-W-42.
3. http://www-nrd.nhtsa.dot.gov/pdf/nrd-30/NCSA/SCI/3Q_2001/ABFSISR.html (as viewed on 27/4/02).
4. Paula, G. **"Sensors help make air bags safer". http://www.memagazine.org/backissues/august97/features/airbag/airbag.html (as viewed on 4/3/02).**
5. **http://www.sae.org/automag/globalvehicles/05-2001/global3.htm (as viewed on 7/3/02).**
6. Hollingum, J. **"Vehicle sensing gets an inflated image", Sensor Review, Volume 16, Number 4, 1996, pp.31-36. ISSN 0260-2288.**
7. **Breed, D.S.** "A Smart Airbag System", Automotive Technologies International, Inc. United States. Paper Number: 98-S5-O-13.
8. http://www.mechatronics.org.uk/ (as viewed on 10/5/02).

Authors
Professor Robert M Parkin

Mr Amjad F Juna

Dr Amin Al-Habaibeh

Dr Michael R Jackson

Mr Michael Mansi+

Mechatronics Research Centre, Loughborough University, UK
+IRISYS Ltd, Towcester Mill, Towcester, UK
Tel 01509 227505, Fax 01509 227502
Email: R.M.Parkin@Lboro.ac.uk
Web: www.mechatronics.org.uk

Smart Restraint Systems Utilising Low Cost Infra Red Sensors

A. F. Juna, A. Al-Habaibeh, D.R. Whitby, M. Jackson, R.M. Parkin.
Mechatronics Research Centre, Wolfson School of Mechanical and Manufacturing Engineering, Loughborough University, Loughborough, United Kingdom.
www.mechatronics.org.uk

ABSTRACT

Safety is still the main priority for automobile manufacturers. A novel approach to driver monitoring is being tested at Loughborough University using low cost infrared technology. This is motivated by the significant number of people killed and injured by the activation of airbags that are unsuitable for some drivers and occupants, with particularly severe consequences to the elderly and the young, and small women. An autonomous system is proposed that will be able to detect, track and measure his position in real-time, and also to detect any other safety risks. This system is to be comprised of an infrared thermal imager connected up to a computer system to perform image processing in real-time.

1 INTRODUCTION

The introduction of passive safety systems such as front end deformable crush zones (1), together with seatbelts and multiple airbags seemed to be the final answer in the quest for road safety. Indeed, wearing seatbelts is said to reduce death and injury by 50% compared with not wearing them (2), although its limitation is that it needs a zone ahead of the occupant so that the driver can be decelerated by the belt, which risks contact with the dashboard. At rapid decelerations of 50 km/hr, the head is thrown towards the steering column and it was this type of accident that the airbag was designed for. However, airbags have unwittingly been the cause of some fatalities and injuries, particularly in the U.S. The National Highway Traffic Safety Administration (NHTSA) website (3) reports that the total confirmed airbag related fatalities in the U.S between the period of 1990 to 2001 inclusive was 195, including 119 children. The number of child fatalities is particularly high because the airbag was originally designed for use on an average sized male adult. Figures 3b and 3c compares and adult and child occupant. It is clear that the child's head is approximately the same height up from the seat as the adult's chest. This means that in the event of a front impact crash, the child's head is more likely to hit the edge of the steering wheel or other parts of the dashboard, thus resulting in severe injury or death. It must be stressed that the ratio of people killed by the airbag to the people saved by the airbag is relatively small, nevertheless it concerns the automobile manufacturer because it could leave them exposed to potential legal action from the victims. So concerned are drivers associations in the U.S. that the NHTSA has even allowed companies such as 'The Airbag Switch Company' (4) to fit switches onto cars that deactivate the airbag when required, for example when a child or elderly person is in the passenger seat. There is a risk that the driver may forget to activate the switch, and so the driver monitoring system proposed in this paper would, among other tasks, be able to take this decision automatically and safely.

2 CURRENT TECHNOLOGY

Automobile manufacturers and other researchers have mainly been concentrating on measuring one or two factors such as weight or height. For example, some Mercedes-Benz cars have weight sensors embedded in the front seats so that if a load greater than 26 pounds was measured, then the airbag would activate (5). However, this system is not intelligent enough to recognize other objects such as luggage on the seats, which would exert such a load and so there is the potential for unnecessary airbag activation. Note that unnecessary airbag deployment is also an economic consideration as well, particularly when it costs the motorist approximately US$2000 to replace and reset an airbag (5).

BMW has developed a driver classification system (6). It uses a force-sensitive resistor sensor array within the seat to measure the imprint of the person's buttocks. Then, capacitive plates within the seat generate an electric field around the seat. This electric field changes due to the conductivity of the body, and using these two systems, the system could detect if there is an empty seat, a child in the seat or an adult in the seat.

Volvo's 'EyeCar' system uses a video camera to scan the driver and locate the centre of each eye (7). An on-board processor adjusts the driving seat to the correct height. They have also developed a system to measure driver height. A sensor above the driver's head measures the electrical current patterns emanating from the driver, and this changes according to the water content of the body, which also varies according to the driver's height.

3 INFRARED THERMAL IMAGER

Humans emit infrared radiation that can be detected by an infrared imager. The radiation is converted into an electrical voltage by the imager, and is then read by a computer system for image analysis. The IRISYS low-cost infrared imager used in this research work is an improvement on current infrared thermal imagers because it combines good performance, small size with low cost. The images produced consist of 256 pixels only, but this is enough to provide useful image data.

The reasons why an infrared thermal imager is being used and not a video camera are because:

1. The thermal imager can view the scene during the day and at night. The video camera can only work in good lighting conditions i.e. during the day. If the car was travelling under a bridge or in a tunnel or travelling at night, then it would not be possible to view the scene.
2. The thermal imager only sees the image of the driver and little else. The video camera sees not only the driver but the entire background as well, which is not needed (see figure 1). This extra detail means that the video cameras pictures would take longer to process and require larger and possibly more expensive equipment.
3. The thermal imager respects the privacy of the drivers because it shows an image of the driver that does not closely resemble the driver himself. This may be an issue because some people may not like their behaviour being recorded because in the event of an accident, it may be used to incriminate them.

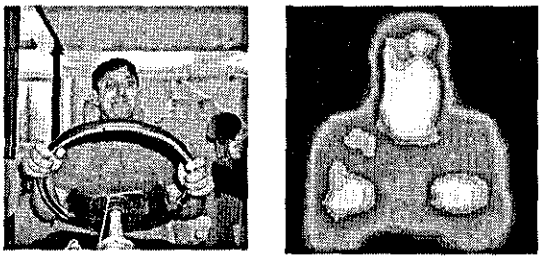

(a) Camera picture (b) Thermal image

Fig. 1 Comparison between camera and thermal imager

4 EXPERIMENTAL WORK

A test rig was built to replicate the layout of a modern car cabin. Only the main pieces of equipment were fitted onto the test rig i.e. the seats, the steering column and steering wheel, the pedals and the gear lever. Figure 2 shows the test rig:

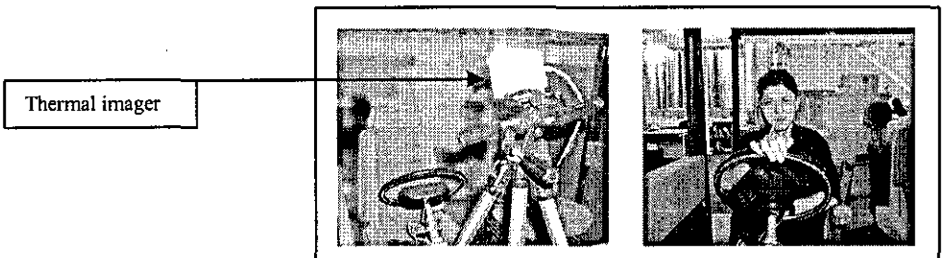

(a) Imager set-up (b) Driver in test rig

Fig. 2 Test rig being used

The seat position could be moved forwards and backwards (relative to the steering wheel) using a remote control. The length of the door and the floor of the test rig could also be adjusted. These adjustments enabled drivers of different heights and shapes to be tested within the test rig. The volunteers were set everyday tasks such as entering and exiting the car, to 'drive' by operating the steering wheel, pedals and gear lever, and to also use a mobile phone and to smoke a cigarette whilst 'driving' the car. Ten people were selected for the initial demonstrative work, with an equal split between male and female. The IRISYS thermal imager was mounted upon a tripod and set into position looking down onto the driver's seat. Each volunteer was asked to perform the same routine of actions and this was captured using the video stream function of the imager. Images were extracted that showed the test subjects to be in approximately the same position inside the car (i.e. sitting up straight, looking directly at the imager).

5 RESULTS

Table 1 below shows the characteristics of each of the volunteers used. The final two columns show torso image height and the head image area measured manually from the hardcopy images.

Table 1. Test subject's data

Subject No.	Gender	Weight Category	Age Category	Torso image height	Head image area
			years	m	m^2
1	Male	Heavy	20-30	0.21	0.0049
2	Male	Heavy	50+	0.19	0.0056
3	Male	Medium	30-40	0.19	0.0051
4	Male	Medium	20-30	0.18	0.0039
5	Male	Light	under 5	0.10	0.0033
6	Female	Medium	20-30	0.17	0.0049
7	Female	Medium	20-30	0.18	0.0044
8	Female	Medium	20-30	0.19	0.0040
9	Female	Medium	20-30	0.18	0.0040
10	Female	Medium	20-30	0.17	0.0042

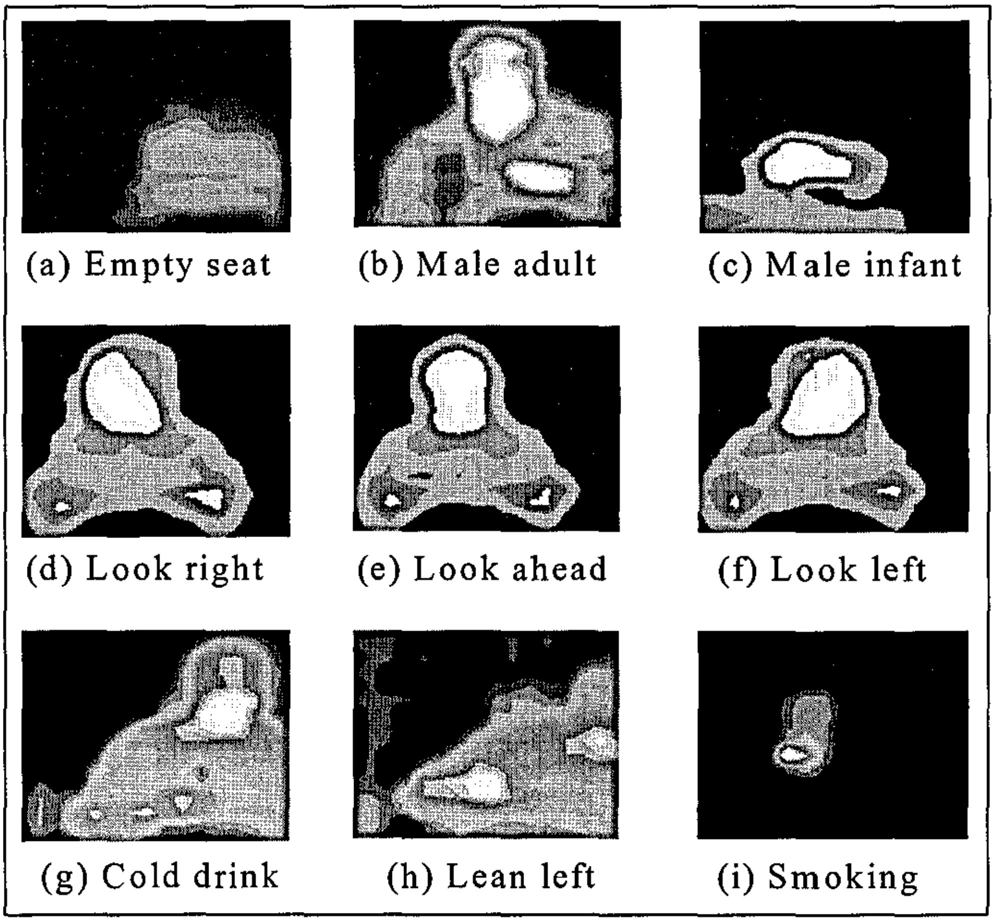

Fig. 3 Thermal images of seat occupants and typical driver behaviour

6 DISCUSSION OF RESULTS

6.1 Occupant detection

Elementary observations have shown that it is possible to detect the presence of a human person in the car seat. When a person sits on the driver's seat, the imager shows a light coloured shape of that person, and so it is clear that the seat is now occupied. The thermal imager's default colour scheme is set so that light colours represent the 'hot areas' (i.e. humans) whilst dark colours represent 'cold' areas (i.e. background). When the driver leaves the seat, a heat pattern on the seat remains due to the heat emitted by the body (figure 3a) but the temperature of this heat pattern is much less than that of the body and there is a clear difference between the images shown in figures 3a and 3b. Hence, the imager can be used for driver detection.

6.2 Occupant type

The risk of airbag-related-injury depends on the type of occupant. For example, the elderly (65+ years) are more likely to be injured by the impact of the airbag than a healthy adult because they tend to have lower bone density making their bones more likely to fracture. Small children and babies are at risk because of their smaller size. The thermal imager is able to distinguish between an adult and a small child because it is easy to tell that the image of the adult's head is oblong shaped (figure 3b) compared to the rounded baby's head seen in figure 3c. Also, it is clear that the adult is taller – the top of the baby's head is approximately at the same height as the chest of an adult. It may also be possible to tell whether the occupant is male or female, and this is important because the typical 'out of position' airbag injury occurs to a female front seat passenger (157cm, 67kg) with her front seat too far forward (8). Table 1 shows that generally men are taller than women and also that they are larger, in this case, the head area viewed by the imager is larger, although further methods to distinguish between men and women would be required.

6.3 Occupant behaviour and activity

Figures 3d, 3e and 3f show typical driver behaviour at a junction. Figure 3d shows him looking to his right, looking straight ahead in figure 3e, and looking to the left in figure 3f. It is clear that the driver is looking either to the left or to the right because of the area of the head and face has moved to the left or to the right, compared with the image of the driver looking straight ahead, whose face is in the centre of the image picture and is not inclined at an angle. Figures 3g, 3h and 3i show a selection of typical in- car driver activities. Figure 3g shows him holding a cold drink, with the cold drink showing up as a dark area against the rest of his body in the centre. Airbag deployment now would cause the cup to strike the face and if he had a hot drink that spilt, this would cause burn injuries. The driver is leaning to one side in figure 3h, possibly to operate the radio. This driver is 'out of position', and the airbag should not fire because this would expose the driver to the effects of the airbag sudden expansion and heat emissions. In fact the NHTSA has recommended being a safe distance of 10 inches away from the steering wheel. The image of the driver in figure 3i has a very high 'hot spot' near the driver's chin, caused by the driver smoking a cigarette. Notice that because the cigarette is so much hotter than the rest of the body, the image of the driver fades into the background. Airbag deployment in this case would be dangerous because of the risk of fire.

7 CONCLUSION AND FUTURE WORK

The problems of current automotive occupant safety work in this field, and the advantages of using infrared technology have been explained in this paper. Initial analysis of the infrared data has shown that an intelligent system capable of detecting a variety of occupant types and behaviour is an attainable goal. Future work will consist of developing a computerised image processing system that will analyse the data in real-time so that it can be implemented into an integrated, automatic occupant safety system.

REFERENCES

1 **Galer Flyte, Margaret.** Frontal Impact Protection: Tailoring Safety System Performance
By The Prediction Of Driver Size And Seated Position. Paper number 98-S1-O-09.

2 **Mackay, M; Hassan, A.M; Hill, J.R.** Observational Studies of Car Occupants' Positions. Birmingham Accident Research Centre, University of Birmingham. Paper number
98-S6-W-42.

3 **http://www-nrd.nhtsa.dot.gov/pdf/nrd30/NCSA/SCI/3Q 2001/ABFSISR.html** (as seen on 27/04/2002).

4 **http://www.airbagswitches.com/** (as seen on 26/04/2002)

5 **Paula, Greg.** Sensors help make air bags safer. **http://www.memagazine.org/backissues/august97/features/airbag/airbag.html.** (as seen on 04/03/2002)

6 **Lu, Yan; Marschner, Christian; Eisenmann, Lutz; Sauer, Sivart.**
The New Generation of the BMW Child Seat and Occupant Detection System SBE2. Seoul 2000 FISITA World Automotive Congress. June 12-15, 2000, Seoul, Korea. Paper number: F2000G379.

7 **Birch, Stuart.** **http://www.sae.org/automag/globalvehcles/05-2001/global3.htm** (as seen on 07/03/2002)

8 **Langweider, Klaus; Hummel, Thomas. A; Anselm, Dieter.** The Effect Of Airbags On Injuries and Accident Costs. Allianz Center for Technology, Germany. Paper number 98-S1-W-27.

Appendix 2 Tables of Image Properties Data

The tables presented here are the 'regionprops' data that was used for the basis of the ANN analysis done:

Driver Volunteer 1
Name: Amjad Juna ALL DATA

Frame number	Frame description	Face threshold value degree C	Centroid position x co-ordinate pixel	y co-ordnate pixel	Area pixel	Major Axis Length pixel	Minor Axis Length pixel	Eccentricity pixel	Equivdiameter pixel
1	Look straight	30	47.8945	58.865	2200	91.6722	37.7847	0.9111	52.9257
482	Look straight	30	47.7816	55.0803	2441	89.7045	41.3338	0.8875	55.7492
7	Look up (rearview mirror)	30	45.3032	55.0496	2599	92.7549	42.6856	0.8878	57.5252
5	Look up (rearview mirror)	30	45.3644	55.1323	2607	92.3286	43.5616	0.8817	57.6137
360	Look right	30	40.3246	54.0339	3007	86.8821	45.6376	0.8509	61.8759
86	Look right	30	49.4792	47.181	3099	96.8347	45.9279	0.8804	62.8154
362	Look left	30	52.0194	52.5021	2828	85.3913	45.3385	0.8474	60.006
90	Look left	30	53.1707	53.8867	2894	83.2339	46.4789	0.8296	60.7022
188	Lean forward	30	57.1345	65.2568	1702	76.9959	45.6831	0.805	46.5516
190	Head on steering wheel	30	85.4143	98.1571	70	12.72	7.9722	0.7792	9.4407
3	Look straight	30	47.8707	58.5195	2227	92.6863	37.9878	0.9122	53.2495
500	Look straight	30	48.8132	54.8402	2441	93.1438	41.1166	0.8973	55.7492
447	Look up (rearview mirror)	30	45.2994	56.5552	2518	90.0479	43.9926	0.8725	56.6217
451	Look up (rearview mirror)	30	45.9461	56.2281	2560	89.4744	44.8986	0.865	57.092
97	Look right	30	46.0582	51.173	2630	86.0584	41.2262	0.8778	57.8673
64	Look right	30	37.2564	53.4255	2691	83.9554	44.9609	0.8445	58.5345
93	Look left	30	55.3626	52.5206	3056	83.9358	48.3017	0.8178	62.378
363	Look left	30	50.9268	53.2113	2731	85.647	44.9443	0.8512	58.9679
192	Lean forward	30	60.5095	68.7281	1048	57.5465	30.5407	0.8476	36.5288
191	Head on steering wheel	30	84.709	98.8881	134	14.3391	12.2038	0.525	13.0619
1	Look straight	30	0.2209	0.225965	0.703202	0.938625	0.739223	0.99715909	0.814711839
482	Look straight	30	0.218556	0.15277	0.782767	0.915232	0.827226	0.93620868	0.867611434
7	Look up (rearview mirror)	30	0.167092	0.152176	0.834929	0.951497	0.860745	0.93698347	0.900885626
5	Look up (rearview mirror)	30	0.168363	0.153776	0.83757	0.946429	0.882466	0.92122934	0.902543715
360	Look right	30	0.063711	0.132533	0.969627	0.881678	0.933942	0.84168388	0.982398028
86	Look right	30	0.253807	0	1	1	0.94114	0.9178719	1
362	Look left	30	0.306554	0.102908	0.910532	0.863955	0.926525	0.83264463	0.947364575
90	Look left	30	0.330461	0.129686	0.932321	0.838307	0.954802	0.78667355	0.960408208
188	Lean forward	30	0.412769	0.349581	0.538792	0.764146	0.93507	0.7231405	0.695290091
190	Head on steering wheel	30	1	0.985863	0	0	0	0.65650826	0
3	Look straight	30	0.220406	0.219283	0.712116	0.950682	0.744259	1	0.820778384
500	Look straight	30	0.239977	0.148127	0.782767	0.956121	0.82184	0.9615186	0.867611434
447	Look up (rearview mirror)	30	0.167013	0.181294	0.808188	0.919315	0.893153	0.89746901	0.88395813
451	Look up (rearview mirror)	30	0.180442	0.174968	0.822053	0.912497	0.915618	0.87809917	0.892769421
97	Look right	30	0.18277	0.077204	0.845163	0.871886	0.824558	0.91115702	0.907295029
64	Look right	30	0	0.120767	0.865302	0.846884	0.917162	0.82515496	0.919795334
93	Look left	30	0.375976	0.103266	0.985804	0.846651	1	0.75619835	0.991805106
363	Look left	30	0.283866	0.116624	0.878508	0.866995	0.916751	0.84245868	0.927915286
192	Lean forward	30	0.482851	0.416715	0.322879	0.532921	0.559603	0.83316116	0.507508239
191	Head on steering wheel	30	0.985354	1	0.021129	0.019249	0.104926	0	0.067844878

Driver Volunteer 1
Name: Amjad Juna OOP DATA

Frame number	Frame description	Face threshold value degree C	Centroid position x co-ordinate pixel	y co-ordnate pixel	Area pixel	Major Axis Length pixel	Minor Axis Length pixel	Eccentricity pixel	Equivdiameter pixel
1	Look straight	30	47.8945	58.865	2200	91.6722	37.7847	0.9111	52.9257
482	Look straight	30	47.7816	55.0803	2441	89.7045	41.3338	0.8875	55.7492
188	Lean forward	30	57.1345	65.2568	1702	76.9959	45.6831	0.805	46.5516
190	Head on steering wheel	30	85.4143	98.1571	70	12.72	7.9722	0.7792	9.4407
3	Look straight	30	47.8707	58.5195	2227	92.6863	37.9878	0.9122	53.2495
500	Look straight	30	48.8132	54.8402	2441	93.1438	41.1166	0.8973	55.7492
192	Lean forward	30	60.5095	68.7281	1048	57.5465	30.5407	0.8476	36.5288
191	Head on steering wheel	30	84.709	98.8881	134	14.3391	12.2038	0.525	13.0619
1	Look straight	30	0.003	0.091373	0.898355	0.981702	0.780564	0.99715909	0.939028472
482	Look straight	30	0	0.005451	1	0.957235	0.884667	0.93620868	1
188	Lean forward	30	0.248531	0.236483	0.688317	0.799215	1	0.7231405	0.801384195
190	Head on steering wheel	30	1	0.983404	0	0	0	0.65850826	0
3	Look straight	30	0.002368	0.08353	0.909743	0.994311	0.79594	1	0.946020709
500	Look straight	30	0.027412	0	1	1	0.878908	0.9615186	1
192	Lean forward	30	0.338214	0.315291	0.412484	0.557379	0.598461	0.83316116	0.584948768
191	Head on steering wheel	30	0.981258	1	0.026993	0.020132	0.112212	0	0.078197307

Driver Volunteer 2
Name: Andy Taylor ALL DATA

Frame number	Frame description	Face threshold value degree C	Centroid position x co-ordinate pixel	y co-ordnate pixel	Area pixel	Major Axis Length pixel	Minor Axis Length pixel	Eccentricity pixel	Equivdiameter pixel
1	Look straight	30	53.7368	53.2115	2052	103.3856	35.9161	0.9377	51.1145
6	Look straight	30	47.4187	60.3985	2763	92.5824	92.5824	0.94011	59.3124
63	Look straight	30	47.9982	55.7539	2166	105.1684	41.2767	0.9198	52.5151
41	Lean extreme right	30	20.0322	85.6014	838	78.3422	34.1969	0.8997	32.6646
37	Look right	30	48.0602	62.9591	2642	92.1772	43.9358	0.8791	57.9991
107	Look right	30	40.3587	64.7334	2746	88.4693	41.6815	0.8821	59.1297
37	Look right	30	48.0602	62.9591	2642	92.1772	43.9358	0.8791	57.9991
108	Look left	30	62.2225	62.1486	2611	90.6026	39.0941	0.9021	57.6579
59	Look left	30	55.7783	53.5726	2246	2.9814	39.3712	0.924	53.4761
224	Look up	30	54.8787	53.1279	2721	102.3299	41.8881	0.9124	58.8599
225	Look up	30	54.702	52.2029	2795	103.4795	41.3257	0.9168	59.6549
574	Lean forward	30	51.6577	57.6005	2781	102.2641	48.676	0.8795	59.5053
284	Lean left	30	71.2268	56.0231	2509	107.7197	39.7872	0.9293	56.5204
64	Look straight	30	47.9927	55.4521	2462	102.5067	42.592	0.9096	55.9885
65	Look straight	30	50.7219	55.5651	2244	105.1322	39.1897	0.9279	53.4523
203	Look straight	30	55.7783	53.5726	2246	102.9814	39.3712	0.924	53.4761
43	Lean extreme right	30	20.8902	85.6217	920	78.9222	32.3279	0.9123	34.2254
56	Look right	30	42.4275	59.33	2627	90.7702	40.1337	0.8969	57.8342
106	Look right	30	47.03	60.3113	2631	90.8187	38.6607	0.9049	57.8783
317	Look right	30	51.5642	56.6655	2834	94.5824	42.0857	0.8955	60.0696
108	Look left	30	62.2225	62.1486	2611	90.6026	39.0941	0.9021	57.6579
319	Look left	30	62.4987	59.8746	2990	100.1411	42.1143	0.9073	61.7008
226	Look up	30	53.4406	50.3178	2508	102.2653	38.33	0.9271	56.5092
227	Look up	30	52.3053	51.8409	2552	103.0649	38.3698	0.9281	57.0027
571	Lean forward	30	51.6577	57.6005	2781	102.2641	48.676	0.8795	59.5053
285	Lean left	30	65.8158	54.8448	2487	108.9359	41.7304	0.9237	56.2721
1	Look straight	30	0.658362	0.081965	0.564126	0.947616	0.059551	0.960498279	0.635410281
6	Look straight	30	0.534949	0.285641	0.894517	0.845655	1	1	0.917744057
63	Look straight	30	0.546269	0.15398	0.6171	0.964442	0.148517	0.667103753	0.68364662
41	Lean extreme right	30	0	0.999425	0	0.711256	0.031018	0.337649566	0
37	Look right	30	0.54748	0.358071	0.83829	0.841831	0.192648	0	0.87251431
107	Look right	30	0.397044	0.408329	0.886617	0.806836	0.155235	0.049172267	0.911451912
37	Look right	30	0.54748	0.358071	0.83829	0.841831	0.192648	0	0.87251431
108	Look left	30	0.824116	0.335113	0.823885	0.82697	0.112294	0.376987379	0.860763461
59	Look left	30	0.69824	0.092194	0.654275	0	0.116893	0.735944927	0.716743238
224	Look up	30	0.680667	0.079597	0.875	0.937652	0.158664	0.545812162	0.902160062
225	Look up	30	0.677216	0.053396	0.909387	0.948502	0.14933	0.617931487	0.929539678
574	Lean forward	30	0.617751	0.206286	0.902881	0.937031	0.271317	0.006556302	0.924387489
284	Lean left	30	1	0.161605	0.776487	0.988521	0.123797	0.822815932	0.821588224
64	Look straight	30	0.546161	0.145432	0.754647	0.939321	0.170346	0.499918046	0.803269712
65	Look straight	30	0.599471	0.148632	0.653346	0.964101	0.11388	0.799868874	0.715923571
203	Look straight	30	0.69824	0.092194	0.654275	0.943801	0.116893	0.735944927	0.716743238
43	Lean extreme right	30	0.01676	1	0.038104	0.71673	0	0.544173086	0.05375359
56	Look right	30	0.437454	0.255275	0.83132	0.828552	0.129547	0.29175545	0.866835192
106	Look right	30	0.527356	0.283071	0.833178	0.82901	0.105101	0.422881495	0.868353986
317	Look right	30	0.615924	0.179802	0.927509	0.864531	0.161943	0.268808392	0.94382185
108	Look left	30	0.824116	0.335113	0.823885	0.82697	0.112294	0.376987379	0.860763461
319	Look left	30	0.829511	0.270701	1	0.916995	0.162418	0.462219308	1
226	Look up	30	0.652577	0	0.776022	0.937043	0.099612	0.786756269	0.821202499
227	Look up	30	0.6304	0.043143	0.796468	0.944589	0.100273	0.803147025	0.838198525
571	Lean forward	30	0.617751	0.206286	0.902881	0.937031	0.271317	0.006556302	0.924387489
285	Lean left	30	0.894305	0.128229	0.766264	1	0.156046	0.7310277	0.81303683

Driver Volunteer 2
Name: Andy Taylor OOP DATA

Frame number	Frame description	Face threshold value degree C	Centroid position x co-ordinate pixel	y co-ordnate pixel	Area pixel	Major Axis Length pixel	Minor Axis Length pixel	Eccentricity pixel	Equivdiameter pixel
1	Look straight	30	53.7368	53.2115	2052	103.3856	35.9161	0.9377	51.1145
6	Look straight	30	47.4187	60.3985	2763	92.5824	92.5824	0.94011	59.3124
63	Look straight	30	47.9982	55.7539	2166	105.1684	41.2767	0.9198	52.5151
41	Lean extreme right	30	20.0322	85.6014	838	78.3422	34.1969	0.8997	32.6646
574	Lean forward	30	51.6577	57.6005	2781	102.2641	48.676	0.8795	59.5053
284	Lean left	30	71.2268	56.0231	2509	107.7197	39.7872	0.9293	56.5204
64	Look straight	30	47.9927	55.4521	2462	102.5067	42.592	0.9096	55.9885
65	Look straight	30	50.7219	55.5651	2244	105.1322	39.1897	0.9279	53.4523
203	Look straight	30	55.7783	53.5726	2246	102.9814	39.3712	0.924	53.4761
43	Lean extreme right	30	20.8902	85.6217	920	78.9222	32.3279	0.9123	34.2254
571	Lean forward	30	51.6577	57.6005	2781	102.2641	48.676	0.8795	59.5053
285	Lean left	30	65.8158	54.8448	2487	108.9359	41.7304	0.9237	56.2721
1	Look straight	30	0.658362	0	0.624807	0.81858	0.059551	0.960237585	0.687385202
6	Look straight	30	0.534949	0.221751	0.990736	0.465462	1	1	0.992813153
63	Look straight	30	0.546269	0.078444	0.683479	0.876854	0.148517	0.664906781	0.73956715
41	Lean extreme right	30	0	0.999374	0	0	0.031018	0.333278337	0
574	Lean forward	30	0.617751	0.13542	1	0.781922	0.271317	0	1
284	Lean left	30	1	0.08675	0.86001	0.960247	0.123797	0.821646593	0.888792021
64	Look straight	30	0.546161	0.069133	0.835821	0.789852	0.170346	0.49661772	0.868975101
65	*Look straight*	*30*	*0.599471*	*0.072619*	*0.723623*	*0.87567*	*0.11388*	*0.798548094*	*0.774484272*
203	Look straight	30	0.69824	0.011142	0.724653	0.805368	0.116893	0.734202277	0.775370985
43	Lean extreme right	30	0.01676	1	0.042203	0.018958	0	0.541164824	0.058150495
571	Lean forward	30	0.617751	0.13542	1	0.781922	0.271317	0	1
285	Lean left	30	0.894305	0.050395	0.848688	1	0.156046	0.729252599	0.879541145

Driver Volunteer 3
Name: Bilal Ashraf ALL DATA

Frame number	Frame description	Face threshold value degree C	Centroid position x co-ordinate pixel	 y co-ordnate pixel	Area pixel	Major Axis Length pixel	Minor Axis Length pixel	Eccentricity pixel	Equivdiameter pixel
4	Look straight	30	55.5731	55.8697	2195	94.3566	39.4544	0.9084	52.8655
5	Look straight	30	55.1989	55.4989	2187	84.6463	39.0655	0.8871	52.7691
41	Look straight	30	59.2609	55.9559	2288	89.4999	42.2817	0.8814	53.9738
110	Look right	30	55.1557	51.5427	3114	82.0083	50.4837	0.7881	62.9672
109	Look right	30	55.57	52.4195	2763	83.327	45.9849	0.8339	59.3124
111	*Look right*	30	*53.4274*	*52.3546*	*3142*	*81.5133*	*51.0255*	*0.7798*	*63.2497*
115	Look left	30	58.0603	52.1173	3001	81.4939	48.7909	0.801	61.8142
114	Look left	30	55.4029	52.2717	2775	82.7023	45.5961	0.8343	59.4411
116	Look left	30	60.6629	51.411	2937	79.1342	48.1861	0.7932	61.1515
391	Lean right, overtaking	30	35.0221	56.3249	2992	82.7353	52.0841	0.777	61.7214
390	Lean right, overtaking	30	41.4841	55.349	2954	82.4323	50.7591	0.7879	61.3282
392	Lean right, overtaking	30	34.5809	56.2395	3002	82.3577	52.3607	0.7719	61.8245
695	Look up	30	58.5723	54.1946	2076	79.2906	39.4312	0.8676	51.4125
176	Look up	30	59.4806	55.8379	2091	79.3637	38.9584	0.8712	51.5979
177	Look up	30	59.3006	54.8158	2009	83.7341	38.4921	0.8881	50.5761
847	Head arcing down	30	53.5628	72.0059	3200	70.1498	58.8134	0.5451	63.8308
874	Head arcing down	30	57.5932	64.1298	2989	69.144	55.4933	0.5966	61.6905
850	Head on steering wheel	30	64.7251	85.8827	1986	67.8577	58.6054	0.5041	50.2857
848	Head on steering wheel	30	60.6081	83.1632	2340	67.5914	60.4978	0.446	54.5837
11	Down left	30	100.4001	70.2175	2777	73.7267	50.8906	0.7236	59.4625
12	Down left	30	99.5637	67.5279	2881	74.7443	50.7281	0.7344	60.5657
13	*Down left*	30	100.1289	61.4798	2676	71.9022	49.0004	0.7318	58.3711
6	Reach right	30	51.6888	38.3446	2095	57.6997	46.9757	0.5807	51.6472
47	Look straight	30	57.0043	54.3667	2116	90.6465	39.6403	0.8993	51.9054
63	Look straight	30	58.0954	55.2457	2108	88.9909	40.1056	0.8927	51.8072
151	look straight	30	58.0599	52.9698	2255	87.4252	40.8441	0.8842	53.5832
112	Look right	30	54.4548	51.7032	2951	83.1934	48.0364	0.8165	61.2971
173	Look right	30	57.0661	52.3644	2662	84.9122	45.6763	0.843	58.2182
303	Look right	30	51.9865	52.6416	2824	81.4641	47.8265	0.8095	59.9636
307	Look left	30	63.1394	50.9772	2855	79.0594	47.6365	0.7981	60.2918
308	Look left	30	63.1394	50.9772	2855	79.0594	47.6365	0.7981	60.2918
690	Look left	30	61.7638	50.8681	2798	79.8219	46.5779	0.8121	59.6869
393	Lean right, overtaking	30	36.1467	55.8929	2754	82.4956	49.9697	0.7957	59.2157
394	Lean right, overtaking	30	39.5924	52.9015	2537	77.8404	46.5848	0.8011	56.8349
395	Lean right, overtaking	30	39.1831	52.8189	2567	78.5897	46.6339	0.8049	57.17
179	Look up	30	59.2506	54.8587	2031	84.6161	38.7496	0.889	50.8522
261	Look up	30	59.2506	54.8587	2031	84.6161	38.7496	0.889	50.8522
836	*Look up*	30	*58.5415*	*53.2521*	*2098*	*79.8231*	*39.153*	*0.8714*	*51.6842*
874	Head arcing down	30	57.5932	64.1298	2989	69.144	55.4933	0.5966	61.6905
873	Head arcing down	30	64.5605	62.7297	3056	72.6929	53.9357	0.6704	62.378
849	Head on steering wheel	30	62.8954	85.4413	2198	70.9216	58.3341	0.5687	52.9016
851	Head on steering wheel	30	66.7114	86.11	2055	68.8303	58.87	0.5181	51.1518
14	Down left	30	103.5017	66.229	2358	74.7083	41.7458	0.8293	54.7932
902	Down left	30	105.2393	55.9629	2344	79.6958	39.1182	0.8712	54.6303
903	Down left	30	108.1226	56.271	1941	79.3588	33.3324	0.9075	49.7128
7	Reach right	30	53.3455	32.8008	1812	52.9305	44.5298	0.5406	48.0324
4	Look straight	30	0.285446	0.432738	0.275937	1	0.22536	1	0.305923385
5	Look straight	30	0.280358	0.425782	0.270173	0.765599	0.211044	0.96393599	0.299821501
41	Look straight	30	0.335592	0.434355	0.342939	0.882762	0.329437	0.941609	0.376076058
110	Look right	30	0.279771	0.35157	0.93804	0.70192	0.631366	0.73983564	0.945336237
109	Look right	30	0.285404	0.368017	0.685159	0.733752	0.465758	0.83888408	0.713996354
111	Look right	30	0.25627	0.3668	0.958213	0.669971	0.65131	0.72188581	0.963217794
115	Look left	30	0.319266	0.362348	0.856628	0.689503	0.569051	0.76773356	0.872354162
114	*Look left*	30	*0.283132*	*0.365245*	*0.693804*	*0.718673*	*0.451446*	*0.83974913*	*0.722142749*
116	Look left	30	0.354656	0.349099	0.810519	0.632541	0.546787	0.75086505	0.830406877
391	Lean right, overtaking	30	0.005999	0.441277	0.850144	0.719469	0.690279	0.71583045	0.86648015
390	Lean right, overtaking	30	0.093868	0.42297	0.822767	0.712155	0.641504	0.73940311	0.841591554
392	Lean right, overtaking	30	0	0.439675	0.857349	0.710354	0.700461	0.70480104	0.873006127
695	Look up	30	0.326229	0.401315	0.190202	0.636316	0.224506	0.91176471	0.213952046
176	Look up	30	0.338579	0.432141	0.201009	0.638081	0.207102	0.91955017	0.226687411
177	Look up	30	0.336132	0.412968	0.141931	0.74358	0.189936	0.95609862	0.161009976
847	Head arcing down	30	0.258111	0.735428	1	0.415663	0.937995	0.21431661	1
874	Head arcing down	30	0.312915	0.587665	0.847983	0.391384	0.815777	0.32569204	0.864524256
850	Head on steering wheel	30	0.409893	0.995736	0.12536	0.360333	0.930338	0.12564879	0.142628367
848	Head on steering wheel	30	0.353911	0.944722	0.380403	0.353905	1	0	0.414681234
11	Down left	30	0.894992	0.701881	0.695245	0.502007	0.646344	0.60034602	0.723497316
12	Down left	30	0.883618	0.651428	0.770173	0.526571	0.640362	0.62370242	0.793327172
13	Down left	30	0.891304	0.537975	0.622478	0.457965	0.576763	0.61807958	0.654414371
6	Reach right	30	0.232629	0.103993	0.20389	0.115125	0.502231	0.29130623	0.228807981
47	*Look straight*	30	*0.304907*	*0.404544*	*0.21902*	*0.910441*	*0.232203*	*0.98032007*	*0.245151408*
63	Look straight	30	0.319744	0.421032	0.213256	0.870475	0.249332	0.96604671	0.238935588
151	look straight	30	0.319261	0.37834	0.319164	0.83268	0.276517	0.94766436	0.351352036
112	Look right	30	0.27024	0.35458	0.820605	0.730527	0.541277	0.80125433	0.839623
173	Look right	30	0.305748	0.366984	0.612392	0.772018	0.454398	0.85856401	0.644736176
303	Look right	30	0.236677	0.372183	0.729107	0.688783	0.53355	0.78611592	0.755215718
307	Look left	30	0.388331	0.340962	0.751441	0.630735	0.526556	0.76146194	0.775989974
308	Look left	30	0.388331	0.340962	0.751441	0.630735	0.526556	0.76146194	0.775989974
690	Look left	30	0.369626	0.338915	0.710375	0.649141	0.487587	0.79173875	0.737701286
393	Lean right, overtaking	30	0.021291	0.433173	0.678674	0.713683	0.612445	0.75627163	0.707875481
394	Lean right, overtaking	30	0.068145	0.377059	0.522334	0.601309	0.487841	0.76794983	0.557176676
395	Lean right, overtaking	30	0.062579	0.375509	0.543948	0.619397	0.489649	0.77616782	0.578387665
179	Look up	30	0.335452	0.413773	0.157781	0.76487	0.199415	0.95804498	0.178486429
261	Look up	30	0.335452	0.413773	0.157781	0.76487	0.199415	0.95804498	0.178486429
836	Look up	30	0.32581	0.383635	0.206052	0.64917	0.214265	0.9199827	0.23114999
874	Head arcing down	30	0.312915	0.587665	0.847983	0.391384	0.815777	0.32569204	0.864524256
873	*Head arcing down*	30	*0.407654*	*0.561421*	*0.896254*	*0.477052*	*0.758439*	*0.48529412*	*0.908041321*
849	Head on steering wheel	30	0.385013	0.987456	0.278098	0.434294	0.920351	0.26535467	0.308208426
851	Head on steering wheel	30	0.436902	1	0.175072	0.383811	0.940078	0.15592561	0.197450375
14	Down left	30	0.937166	0.627062	0.393372	0.525702	0.30971	0.82893599	0.42794207
902	Down left	30	0.960794	0.434486	0.383285	0.646098	0.212984	0.91955017	0.417630899
903	*Down left*	30	1	*0.440265*	*0.092939*	*0.637963*	0	0.99805363	0.106365202
7	Reach right	30	0.255156	0	0	0	0.412193	0.20458478	0

Driver Volunteer 3
Name: Bilal Ashraf OOP DATA

Frame number	Frame description	Face threshold value degree C	Centroid position x co-ordinate pixel	y co-ordnate pixel	Area pixel	Major Axis Length pixel	Minor Axis Length pixel	Eccentricity pixel	Equivdiameter pixel
4	Look straight	30	55.5731	55.8697	2195	94.3566	39.4544	0.9084	52.8655
5	Look straight	30	55.1989	55.4989	2187	84.6463	39.0655	0.8871	52.7691
41	Look straight	30	59.2609	55.9559	2288	89.4999	42.2817	0.8814	53.9738
391	*Lean right, overtaking*	30	35.0221	56.3249	2992	82.7353	52.0841	0.777	61.7214
390	Lean right, overtaking	30	41.4841	55.349	2954	82.4323	50.7591	0.7879	61.3282
392	Lean right, overtaking	30	34.5809	56.2395	3002	82.3577	52.3607	0.7719	61.8245
847	Head arcing down	30	53.5628	72.0059	3200	70.1498	58.8134	0.5451	63.8308
874	Head arcing down	30	57.5932	64.1298	2989	69.144	55.4933	0.5966	61.6905
850	Head on steering wheel	30	64.7251	85.8827	1986	67.8577	58.6054	0.5041	50.2857
848	Head on steering wheel	30	60.6081	83.1632	2340	67.5914	60.4978	0.446	54.5837
11	Down left	30	100.4001	70.2175	2777	73.7267	50.8906	0.7236	59.4625
12	Down left	30	99.5637	67.5279	2881	74.7443	50.7281	0.7344	60.5657
13	*Down left*	30	100.1289	61.4798	2676	71.9022	49.0004	0.7318	58.3711
47	Look straight	30	57.0043	54.3667	2116	90.6465	39.6403	0.8993	51.9054
63	Look straight	30	58.0954	55.2457	2108	88.9909	40.1056	0.8927	51.8072
151	look straight	30	58.0599	52.9698	2255	87.4252	40.8441	0.8842	53.5832
393	Lean right, overtaking	30	36.1467	55.8929	2754	82.4956	49.9697	0.7957	59.2157
394	Lean right, overtaking	30	39.5924	52.9015	2537	77.8404	46.5848	0.8011	56.8349
395	Lean right, overtaking	30	39.1831	52.8189	2567	78.5897	46.6339	0.8049	57.17
874	Head arcing down	30	57.5932	64.1298	2989	69.144	55.4933	0.5966	61.6905
873	Head arcing down	30	64.5605	62.7297	3056	72.6929	53.9357	0.6704	62.378
849	*Head on steering wheel*	*30*	*62.8954*	*85.4413*	*2198*	*70.9216*	*58.3341*	*0.5687*	*52.9016*
851	Head on steering wheel	30	66.7114	86.11	2055	68.8303	58.87	0.5181	51.1518
14	Down left	30	103.5017	66.229	2358	74.7083	41.7458	0.8293	54.7932
902	Down left	30	105.2393	55.9629	2344	79.6958	39.1182	0.8712	54.6303
903	Down left	30	108.1226	56.271	1941	79.3588	33.3324	0.9075	49.7128
4	Look straight	30	0.285446	0.09164	0.201747	1	0.22536	1	0.223310667
5	Look straight	30	0.280358	0.080502	0.195393	0.637204	0.211044	0.95393599	0.216482505
41	Look straight	30	0.335592	0.094229	0.275616	0.818544	0.329437	0.941609	0.301813288
391	Lean right, overtaking	30	0.005999	0.105313	0.83479	0.565806	0.690279	0.71583045	0.850587902
390	*Lean right, overtaking*	*30*	*0.093668*	*0.075999*	*0.804607*	*0.554485*	*0.641504*	*0.73940311*	*0.822736932*
392	Lean right, overtaking	30	0	0.102748	0.842732	0.551698	0.700461	0.70480104	0.857890636
847	Head arcing down	30	0.258111	0.57634	1	0.095587	0.937995	0.21431661	1
874	Head arcing down	30	0.312915	0.339757	0.832407	0.058008	0.815777	0.32569204	0.848399207
850	Head on steering wheel	30	0.409893	0.993172	0.035743	0.009949	0.930338	0.12564879	0.040579402
848	Head on steering wheel	30	0.353911	0.911484	0.316918	0	1	0	0.345013458
11	Down left	30	0.894992	0.52262	0.664019	0.229227	0.646344	0.60034602	0.690586485
12	Down left	30	0.883618	0.44183	0.746624	0.267246	0.640362	0.62370242	0.768727865
13	Down left	30	0.891304	0.260157	0.583797	0.16106	0.576763	0.61807958	0.613280918
47	Look straight	30	0.304907	0.046493	0.138999	0.861383	0.232203	0.98032007	0.155305284
63	Look straight	30	0.319744	0.072896	0.132645	0.799527	0.249332	0.96604671	0.148349625
151	look straight	30	0.319261	0.004533	0.249404	0.741029	0.276517	0.94766436	0.27414648
393	Lean right, overtaking	30	0.021291	0.092337	0.645751	0.55685	0.612445	0.75627163	0.673105256
394	Lean right, overtaking	30	0.068145	0.002481	0.473392	0.382923	0.487841	0.76794983	0.504469472
395	Lean right, overtaking	30	0.062579	0	0.49722	0.410918	0.489649	0.77616782	0.528205128
874	Head arcing down	30	0.312915	0.339757	0.832407	0.058008	0.815777	0.32569204	0.848399207
873	Head arcing down	30	0.407654	0.297701	0.885624	0.190602	0.758439	0.48529412	0.897095906
849	Head on steering wheel	30	0.385013	0.979914	0.20413	0.124423	0.920351	0.26535467	0.225867687
851	Head on steering wheel	30	0.436902	1	0.090548	0.046288	0.940078	0.15592561	0.101926619
14	Down left	30	0.937166	0.402813	0.331215	0.265901	0.30971	0.82893599	0.35985267
902	Down left	30	0.960794	0.09444	0.320095	0.452244	0.212984	0.91955017	0.348314209
903	Down left	30	1	0.103694	0	0.439653	0	0.99805363	0

Driver Volunteer 4

Name: Faraz Junejo ALL DATA

Frame number	Frame description	Face threshold value degree C	Centroid position x co-ordinate pixel	y co-ordnate pixel	Area pixel	Major Axis Length pixel	Minor Axis Length pixel	Eccentricity pixel	Equivdiameter pixel
178	Look straight ahead	30	60.0022	63.4393	2718	79.9174	44.4758	0.8308	58.8274
306	Look straight ahead	30	50.9884	48.0577	4318	113.0485	50.546	0.8945	74.1475
117	Look straight ahead	30	62.5788	47.5091	2797	82.0025	44.4537	0.8403	59.6762
174	Look left	30	64.9553	65.5682	2617	74.8406	46.2823	0.7859	57.7241
173	Look left	30	63.745	64.7329	2726	76.8968	46.922	0.7923	58.9139
193	Look left	30	70.6638	64.2849	2766	79.1759	45.4653	0.8187	59.3446
171	Look right	30	53.2086	65.7784	2689	78.1023	45.3931	0.8138	58.5127
194	Look right	30	55.0432	64.9895	2570	79.6843	42.1263	0.8488	57.2034
196	Look right	30	57.1027	64.6758	2619	79.5099	42.9573	0.8415	57.7461
26	Lean extreme left	30	102.3208	90.8669	1540	61.0977	34.1438	0.8293	44.2808
24	Lean extreme left	30	92.3354	82.7624	2054	59.057	45.6687	0.634	51.1394
316	Lean to right, overtaking	30	45.0948	66.1685	2659	82.2389	42.4363	0.8566	58.1854
318	Lean to right, overtaking	30	41.8343	66.0476	2860	85.398	44.0598	0.8566	60.3446
779	Lean forward	30	55.8294	72.0202	2327	66.5172	45.5707	0.7285	54.4319
781	Head on steering wheel	30	52.3745	92.9236	275	19.0173	18.5585	0.2183	18.7121
256	Look straight ahead	30	62.7202	63.7728	2588	83.487	46.8644	0.8276	57.4033
442	Look straight ahead	30	56.6605	62.4239	2536	79.1855	41.3779	0.8526	56.8237
748	Look straight ahead	30	69.2376	62.2853	2597	76.0706	43.8011	0.8176	57.5031
276	*Look left*	*30*	*74.6066*	*66.2934*	*2618*	*77.4899*	*50.4143*	*0.7594*	*57.7351*
204	Look left	30	72.6445	66.7697	2605	77.4163	43.9898	0.8229	57.5916
385	Look left	30	71.6098	64.85	2627	79.1509	42.9263	0.8402	57.8342
244	Look right	30	57.345	65.012	2504	77.8542	42.3149	0.8394	56.4641
409	Look right	30	47.2879	66.2844	2584	76.6673	44.7833	0.8117	57.359
681	Look right	30	52.4809	65.4158	2489	77.2411	42.2171	0.8374	56.2947
25	Lean extreme left	30	99.948	90.0299	1806	62.1199	38.9041	0.7796	47.9528
27	Lean extreme left	30	105.5348	93.3068	1092	60.6582	25.0127	0.911	37.2878
320	Lean to right, overtaking	30	41.189	66.3812	2878	84.9078	44.3509	0.8527	60.5342
327	Lean to right, overtaking	30	45.5322	63.8384	2685	83.3079	43.5397	0.8526	58.4692
19	Lean forward	30	55.4257	69.9514	2119	62.5608	44.1979	0.7077	51.9422
780	Head on steering wheel	30	53.2199	81.9897	291	26.282	14.4593	0.8351	19.2487
178	Look straight ahead	30	0.292377	0.347638	0.604254	0.647658	0.831768	0.884221164	0.72364049
306	Look straight ahead	30	0.152293	0.011979	1	1	1	0.976180165	1
117	Look straight ahead	30	0.33242	0	0.623794	0.669833	0.831176	0.897935614	0.738952005
174	Look left	30	0.369353	0.394323	0.579273	0.593668	0.881848	0.819402339	0.703738045
173	Look left	30	0.350543	0.376084	0.606233	0.615535	0.899575	0.828641546	0.725200864
193	Look left	30	0.458069	0.366302	0.616127	0.639773	0.859209	0.866753284	0.732970268
171	Look right	30	0.186797	0.398913	0.597081	0.628355	0.857208	0.859679515	0.717963612
194	Look right	30	0.215309	0.381687	0.567648	0.645179	0.766681	0.910206439	0.69434513
196	Look right	30	0.247315	0.374838	0.579767	0.643325	0.789709	0.899667966	0.704134903
26	Lean extreme left	30	0.950051	0.946724	0.312886	0.447515	0.545478	0.882055724	0.461234157
24	Lean extreme left	30	0.794868	0.769761	0.44002	0.425813	0.864845	0.60011549	0.584956544
316	Lean to right, overtaking	30	0.0607	0.407431	0.589661	0.672347	0.775272	0.921466724	0.712059442
318	Lean to right, overtaking	30	0.010029	0.404791	0.639377	0.705943	0.820261	0.921466724	0.751009283
779	Lean forward	30	0.227527	0.535204	0.507544	0.50515	0.862129	0.736538184	0.64435
781	Head on steering wheel	30	0.173834	0.991633	0	0	0.113593	0	0
256	Look straight ahead	30	0.334617	0.35512	0.5721	0.68562	0.897979	0.879601559	0.697951129
442	Look straight ahead	30	0.240443	0.325667	0.559238	0.639875	0.745942	0.915692219	0.687495716
748	Look straight ahead	30	0.435904	0.322641	0.574326	0.606749	0.813092	0.865165295	0.699751422
276	Look left	30	0.519344	0.410158	0.57952	0.621843	0.99635	0.781146239	0.703936474
204	Look left	30	0.488851	0.420558	0.576305	0.62106	0.818321	0.872816515	0.701347875
385	Look left	30	0.472771	0.378641	0.581746	0.639507	0.78885	0.897791252	0.70572414
244	Look right	30	0.251081	0.382179	0.551323	0.625717	0.771908	0.896636351	0.681008886
409	Look right	30	0.094783	0.409962	0.571111	0.613094	0.84031	0.8566479	0.697152
681	Look right	30	0.175488	0.390996	0.547613	0.619197	0.769198	0.893749098	0.677953077
25	Lean extreme left	30	0.913175	0.928448	0.378679	0.458386	0.677391	0.810307492	0.52747342
27	Lean extreme left	30	1	1	0.202078	0.442841	0.292446	1	0.335087327
320	Lean to right, overtaking	30	0	0.412075	0.643829	0.70073	0.828327	0.915836581	0.75442948
327	Lean to right, overtaking	30	0.067498	0.356553	0.596092	0.683716	0.805848	0.915692219	0.717178915
19	Lean forward	30	0.221253	0.490031	0.456097	0.463075	0.824088	0.706510755	0.599438265
780	Head on steering wheel	30	0.186973	0.752889	0.003957	0.077258	0	0.890428757	0.009679735

Driver Volunteer 4 OOP DATA

Name: Faraz Junejo

Frame number	Frame description	Face threshold value *degree C*	Centroid position x co-ordinate *pixel*	y co-ordinate *pixel*	Area *pixel*	Major Axis Length *pixel*	Minor Axis Length *pixel*	Eccentricity *pixel*	Equivdiameter *pixel*
178	Look straight ahead	30	60.0022	63.4393	2718	79.9174	44.4758	0.8308	58.8274
306	Look straight ahead	30	50.9884	48.0577	4318	113.0485	50.546	0.8945	74.1475
117	Look straight ahead	30	62.5788	47.5091	2797	82.0025	44.4537	0.8403	59.6762
26	Lean extreme left	30	102.3208	90.8669	1540	61.0977	34.1438	0.8293	44.2808
24	Lean extreme left	30	92.3354	82.7624	2054	59.057	45.6687	0.634	51.1394
316	Lean to right, overtaking	30	45.0948	66.1685	2659	82.2389	42.4363	0.8566	58.1854
318	*Lean to right, overtaking*	*30*	*41.8343*	*66.0476*	*2860*	*85.398*	*44.0598*	*0.8566*	*60.3446*
779	Lean forward	30	55.8294	72.0202	2327	66.5172	45.5707	0.7285	54.4319
781	Head on steering wheel	30	52.3745	92.9236	275	19.0173	18.5585	0.2183	18.7121
256	Look straight ahead	30	62.7202	63.7728	2588	83.487	46.8644	0.8276	57.4033
442	Look straight ahead	30	56.6605	62.4239	2536	79.1855	41.3779	0.8526	56.8237
748	Look straight ahead	30	69.2376	62.2853	2597	76.0706	43.8011	0.8176	57.5031
25	Lean extreme left	30	99.948	90.0299	1806	62.1199	38.9041	0.7796	47.9528
27	*Lean extreme left*	*30*	*105.5348*	*93.3068*	*1092*	*60.6582*	*25.0127*	*0.911*	*37.2878*
320	Lean to right, overtaking	30	41.189	66.3812	2878	84.9078	44.3509	0.8527	60.5342
327	Lean to right, overtaking	30	45.5322	63.8384	2685	83.3079	43.5397	0.8526	58.4692
19	Lean forward	30	55.4257	69.9514	2119	62.5608	44.1979	0.7077	51.9422
780	Head on steering wheel	30	53.2199	81.9897	291	26.282	14.4593	0.8351	19.2487
178	Look straight ahead	30	0.292377	0.347838	0.604254	0.647658	0.831788	0.884221164	0.72364049
306	Look straight ahead	30	0.152293	0.011979	1	1	1	0.976180165	1
117	Look straight ahead	30	0.33242	0	0.623794	0.669833	0.831176	0.897935614	0.738952005
26	Lean extreme left	30	0.950051	0.946724	0.312886	0.447515	0.545478	0.882055724	0.461234157
24	Lean extreme left	30	0.794868	0.769761	0.44002	0.425813	0.864845	0.60011549	0.584956544
316	Lean to right, overtaking	30	0.0607	0.407431	0.589661	0.672347	0.775272	0.921466724	0.712059442
318	Lean to right, overtaking	30	0.010029	0.404791	0.639377	0.705943	0.820261	0.921466724	0.751009283
779	Lean forward	30	0.227527	0.535204	0.507544	0.50515	0.862129	0.736538184	0.64435
781	Head on steering wheel	30	0.173834	0.991633	0	0	0.113593	0	0
256	Look straight ahead	30	0.334617	0.35512	0.5721	0.68562	0.897979	0.879601559	0.697951129
442	Look straight ahead	30	0.240443	0.325667	0.559238	0.639875	0.745942	0.915692219	0.687495716
748	Look straight ahead	30	0.435904	0.322641	0.574326	0.606749	0.813092	0.865165295	0.699751422
25	Lean extreme left	30	0.913175	0.928448	0.378679	0.458386	0.677391	0.810307492	0.52747342
27	Lean extreme left	30	1	1	0.202078	0.442841	0.292446	1	0.335087327
320	Lean to right, overtaking	30	0	0.412075	0.643829	0.70073	0.828327	0.915836581	0.75442948
327	*Lean to right, overtaking*	30	*0.067498*	*0.356553*	*0.596092*	*0.683716*	*0.805848*	*0.915692219*	*0.717178915*
19	Lean forward	30	0.221253	0.490031	0.456097	0.463075	0.824088	0.706510755	0.599438265
780	Head on steering wheel	30	0.186973	0.752889	0.003957	0.077258	0	0.890428757	0.009679735

Driver Volunteer 5
Name: Gavin Walker

ALL DATA

Frame number	Frame description	Face threshold value degree C	Centroid position x co-ordinate pixel	y co-ordnate pixel	Area pixel	Major Axis Length pixel	Minor Axis Length pixel	Eccentricity pixel	Equivdiameter pixel
51	Look straight	30	54.6153	45.9487	3683	108.28	44.7914	0.9104	68.4788
112	Look straight	30	56.5354	45.6779	3670	108.6373	44.7401	0.9113	68.3578
102	Look left	30	60.7637	44.4992	4299	104.7962	54.3204	0.8552	73.9842
349	Look left	30	61.9301	46.1855	4350	106.9522	53.6817	0.8649	74.4217
352	Look right	30	46.905	45.7741	4410	108.8272	53.0851	0.873	74.9332
353	Look right	30	45.2555	45.7176	4490	106.5603	55.1401	0.8557	75.6098
460	Lean forward, before crash	30	56.3027	49.5501	4110	107.8246	49.5607	0.8881	72.3396
96	Lean forward	30	55.46	53.443	3833	97.227	51.5531	0.8479	69.8593
463	Head on steering wheel	30	40.9928	77.555	555	109.4191	67.2812	0.7886	26.5829
156	Lean right, overtaking	30	28.9904	47.7548	3939	111.3274	46.4136	0.9089	70.8187
186	Lean right, overtaking	30	38.029	46.0622	3891	115.1304	47.0867	0.9125	70.3859
286	Lean right, overtaking	30	50.2809	54.8493	4261	157.1958	54.0646	0.939	73.6565
17	Lean left	30	95.736	69.0088	2379	66.2996	47.5463	0.6969	55.0367
18	Lean left	30	98.8269	65.0292	2496	63.5859	54.9344	0.5036	56.3738
37	Reach right	30	36.5091	48.7434	4333	101.3271	56.6703	0.829	74.2762
38	Reach right	30	29.0896	50.0421	4343	104.2763	55.7396	0.8451	74.3618
361	Look straight	30	58.1637	46.729	3727	109.6181	44.9814	0.9119	68.8866
588	Look straight	30	53.7854	46.9632	3780	110.7842	45.2485	0.9128	69.3747
350	Look left	30	63.0257	46.0705	4324	105.2685	53.7673	0.8597	74.199
351	Look left	30	60.1069	45.3224	4181	106.2003	51.9876	0.872	72.9617
354	Look right	30	44.9844	45.6663	4423	106.6199	54.3856	0.8601	75.0436
105	Look right	30	49.7117	44.4816	4221	104.0134	53.3576	0.8584	73.3099
460	Lean forward	30	56.3027	49.5501	4110	107.8246	49.5607	0.8881	72.3396
724	Lean forward	30	53.5288	51.1849	4359	110.0488	51.7317	0.8826	74.4987
462	Head on steering wheel	30	42.4041	70.8363	782	104.461	56.5756	0.8406	31.5543
529	Lean right, overtaking	30	40.7331	46.343	3848	112.8062	45.169	0.9163	69.9959
642	Lean right, overtaking	30	33.78	52.0778	3972	139.3627	52.7558	0.9256	71.1147
643	Lean right, overtaking	30	29.3181	53.8541	3687	121.8278	51.2381	0.9073	68.5159
20	Lean left	30	93.0326	60.0033	2761	65.5224	56.0672	0.5175	59.2909
23	Lean left	30	95.1017	62.212	2694	60.5216	58.4198	0.2613	58.5671
39	Reach right	30	45.4041	46.1022	3992	106.1051	49.1187	0.8864	71.2936
40	Reach right	30	54.9727	43.9117	3815	103.5474	48.5581	0.8832	69.6951
51	Look straight	30	0.366927	0.060547	0.794917	0.494014	0.002276	0.95779844	0.854549237
112	Look straight	30	0.394421	0.052498	0.791614	0.49771	0	0.95912646	0.852081204
102	Look left	30	0.454967	0.017463	0.951461	0.457977	0.425015	0.87634647	0.966842692
349	Look left	30	0.471669	0.067586	0.964422	0.480279	0.39668	0.89065958	0.975766365
352	Look right	30	0.256522	0.055357	0.97967	0.499674	0.370213	0.90261178	0.986199413
353	Look right	30	0.232903	0.053678	1	0.476225	0.461379	0.87708428	1
460	Lean forward, before crash	30	0.391089	0.167594	0.903431	0.489303	0.213858	0.92489302	0.933297843
96	Lean forward	30	0.379022	0.283305	0.833037	0.379681	0.302248	0.86557474	0.882707248
463	Head on steering wheel	30	0.171864	1	0	0.505797	1	0.77807289	0
156	Lean right, overtaking	30	0	0.114231	0.859975	0.525536	0.074242	0.95558507	0.902276097
186	Lean right, overtaking	30	0.129425	0.063921	0.847776	0.564875	0.104103	0.96089715	0.893448291
286	Lean right, overtaking	30	0.304862	0.325105	0.941804	1	0.413667	1	0.960158607
17	Lean left	30	0.955741	0.745976	0.463532	0.059768	0.124493	0.64276228	0.580371184
18	Lean left	30	1	0.627688	0.493266	0.031697	0.452254	0.35753283	0.607643967
37	Reach right	30	0.107661	0.143616	0.960102	0.422093	0.529264	0.83768629	0.972798606
38	Reach right	30	0.00142	0.182218	0.962643	0.4526	0.487975	0.86144312	0.974644587
361	Look straight	30	0.417737	0.08374	0.806099	0.507855	0.010705	0.9600118	0.86286712
588	Look straight	30	0.355044	0.090702	0.819568	0.519917	0.022554	0.96133983	0.872822879
350	Look left	30	0.487357	0.064167	0.957814	0.462863	0.400477	0.88298657	0.971223961
351	Look left	30	0.445562	0.041931	0.921474	0.472501	0.321524	0.9011362	0.945986795
354	Look right	30	0.229021	0.052153	0.982973	0.476842	0.427907	0.8835768	0.988451238
105	Look right	30	0.296712	0.016939	0.931639	0.44988	0.382302	0.88106832	0.953089018
460	Lean forward	30	0.391089	0.167594	0.903431	0.489303	0.213858	0.92489302	0.933297843
724	Lean forward	30	0.351369	0.216186	0.966709	0.51231	0.310171	0.91677734	0.977336931
462	Head on steering wheel	30	0.192073	0.800296	0.057687	0.45451	0.525063	0.85480301	0.101401476
529	Lean right, overtaking	30	0.168146	0.072267	0.836849	0.540833	0.019027	0.96650435	0.885493474
642	Lean right, overtaking	30	0.068583	0.242726	0.868361	0.815534	0.355604	0.98022724	0.908313599
643	Lean right, overtaking	30	0.004692	0.295524	0.795934	0.634153	0.288273	0.95322414	0.855305965
20	Lean left	30	0.91703	0.4783	0.56061	0.051728	0.502509	0.37804338	0.667143956
23	Lean left	30	0.946658	0.543951	0.543583	0	0.606878	0	0.652380632
39	Reach right	30	0.23503	0.06511	0.873443	0.471517	0.19425	0.92238454	0.911962616
40	Reach right	30	0.372045	0	0.828463	0.44506	0.169379	0.91766268	0.879358067

Driver Volunteer 5 OOP DATA

Name: Gavin Walker

Frame number	Frame description	Face threshold value degree C	Centroid position x co-ordinate pixel	Centroid position y co-ordnate pixel	Area pixel	Major Axis Length pixel	Minor Axis Length pixel	Eccentricity pixel	Equivdiameter pixel
51	Look straight	30	54.6153	45.9487	3683	108.28	44.7914	0.9104	68.4788
112	Look straight	30	56.5354	45.6779	3670	108.6373	44.7401	0.9113	68.3578
460	Lean forward, before crash	30	56.3027	49.5501	4110	107.8246	49.5607	0.8881	72.3396
96	Lean forward	30	55.46	53.443	3833	97.227	51.5531	0.8479	69.8593
463	Head on steering wheel	30	40.9928	77.555	555	109.4191	67.2812	0.7886	26.5829
156	Lean right, overtaking	30	28.9904	47.7548	3939	111.3274	46.4136	0.9089	70.8187
186	Lean right, overtaking	30	38.029	46.0622	3891	115.1304	47.0867	0.9125	70.3859
286	Lean right, overtaking	30	50.2809	54.8493	4261	157.1958	54.0646	0.939	73.6565
17	Lean left	30	95.736	69.0088	2379	66.2996	47.5463	0.6969	55.0367
18	Lean left	30	98.8269	65.0292	2496	63.5859	54.9344	0.5036	56.3738
361	Look straight	30	58.1637	46.729	3727	109.6181	44.9814	0.9119	68.8866
588	Look straight	30	53.7854	46.9632	3780	110.7842	45.2485	0.9128	69.3747
460	Lean forward	30	56.3027	49.5501	4110	107.8246	49.5607	0.8881	72.3396
724	Lean forward	30	53.5288	51.1849	4359	110.0488	51.7317	0.8826	74.4987
462	Head on steering wheel	30	42.4041	70.8363	782	104.461	56.5756	0.8406	31.5543
529	Lean right, overtaking	30	40.7331	46.343	3848	112.8062	45.169	0.9163	69.9959
642	Lean right, overtaking	30	33.78	52.0778	3972	139.3627	52.7558	0.9256	71.1147
643	Lean right, overtaking	30	29.3181	53.8541	3687	121.8278	51.2381	0.9073	68.5159
20	Lean left	30	93.0326	60.0033	2761	65.5224	56.0672	0.5175	59.2909
23	Lean left	30	95.1017	62.212	2694	60.5216	58.4198	0.2613	58.5671
51	Look straight	30	0.366927	0.008495	0.822292	0.494014	0.002276	0.95779844	0.874365032
112	Look straight	30	0.394421	0	0.818875	0.49771	0	0.95912646	0.871839769
460	Lean forward, before crash	30	0.391089	0.121473	0.934543	0.489303	0.213858	0.92489302	0.954939707
96	Lean forward	30	0.379022	0.243595	0.861725	0.379681	0.302248	0.86557474	0.903175988
463	Head on steering wheel	30	0.171864	1	0	0.505797	1	0.77807289	0
156	Lean right, overtaking	30	0	0.065153	0.88959	0.525536	0.074242	0.95558507	0.923198611
186	Lean right, overtaking	30	0.129425	0.012056	0.876972	0.564875	0.104103	0.96089715	0.9141661
286	Lean right, overtaking	30	0.304862	0.287711	0.974238	1	0.413667	1	0.982423334
17	Lean left	30	0.955741	0.731902	0.479495	0.059768	0.124493	0.64276228	0.593829175
18	Lean left	30	1	0.60706	0.510252	0.031697	0.452254	0.35753283	0.621734376
361	Look straight	30	0.417737	0.032974	0.833859	0.507855	0.010705	0.9600118	0.882875795
588	Look straight	30	0.355044	0.04032	0.847792	0.519917	0.022554	0.96133983	0.893062414
460	Lean forward	30	0.391089	0.121473	0.934543	0.489303	0.213858	0.92489302	0.954939707
724	Lean forward	30	0.351369	0.172757	1	0.51231	0.310171	0.91677734	1
462	Head on steering wheel	30	0.192073	0.789231	0.059674	0.45451	0.525063	0.85480301	0.103752833
529	Lean right, overtaking	30	0.168146	0.020865	0.865668	0.540833	0.019027	0.96650435	0.906026822
642	Lean right, overtaking	30	0.068583	0.200768	0.898265	0.815534	0.355604	0.98022724	0.929376114
643	Lean right, overtaking	30	0.004692	0.256491	0.823344	0.634153	0.288273	0.95322414	0.875139307
20	Lean left	30	0.91703	0.449395	0.579916	0.051728	0.502509	0.37804338	0.682614086
23	Lean left	30	0.946658	0.518683	0.562303	0	0.606878	0	0.667508421

Driver Volunteer 6
Name: Imran Amin

ALL DATA

Frame number	Frame description	Face threshold value degree C	Centroid position x co-ordinate pixel	y co-ordnate pixel	Area pixel	Major Axis Length pixel	Minor Axis Length pixel	Eccentricity pixel	Equivdiameter pixel
85	Look straight ahead	30	57.4392	63.3274	2639	79.4537	43.6608	0.8355	57.9662
82	Look straight ahead	30	58.2237	62.0882	2597	79.8338	42.7401	0.8446	57.5031
129	Look straight ahead	30	61.7305	61.803	2731	80.1607	44.6596	0.8304	58.9679
143	Look left	30	64.6652	66.6163	3091	79.5942	51.2345	0.7653	62.7342
339	Look left	30	62.6142	63.9173	2973	79.6017	48.2251	0.7956	61.5251
139	Look right	30	49.8409	67.26	2954	79.3201	50.164	0.7746	61.3282
69	Look right	30	49.9015	64.0134	2528	75.9487	43.3429	0.8212	56.734
140	Look right	30	49.9296	67.0553	2927	79.1915	48.365	0.7918	61.0473
182	Lean forward	30	62.6163	78.3859	2361	58.1898	52.4502	0.4331	54.8281
183	*Head on steering wheel*	30	58.9471	93.6351	1173	53.8518	28.9021	0.8438	38.646
187	Head on steering wheel	30	63.9681	96.5664	1190	70.8004	22.3416	0.9489	38.925
361	Lean right, overtaking	30	36.6998	66.3152	2805	83.9656	44.1936	0.8503	59.7615
217	Lean right, overtaking	30	36.9744	63.396	2770	82.5635	44.3483	0.8435	59.3875
224	Lean right, overtaking	30	35.0669	63.0557	2782	83.7265	46.1597	0.8343	59.516
53	Lean left	30	94.8932	99.0945	1227	67.5287	24.6211	0.9312	39.5255
72	Reach right	30	36.8968	65.9562	2646	69.4129	49.0857	0.7071	58.043
657	Reach right	30	34.6003	75.1072	2602	62.4661	54.0382	0.5016	57.5584
264	Look straight ahead	30	52.673	60.3482	2771	81.3781	44.5981	0.8365	59.3982
529	Look straight ahead	30	54.2782	60.0957	2768	82.3987	44.0303	0.8453	59.366
627	*Look straight ahead*	30	50.1433	62.0245	2812	81.9147	44.8279	0.837	59.836
144	Look left	30	64.6582	66.955	3087	79.8862	50.9535	0.7702	62.6936
676	Look left	30	62.4835	63.8174	2459	68.6527	46.503	0.7356	55.9544
337	Look right	30	55.8951	63.4951	2773	79.4838	45.5764	0.8193	59.4196
654	Look right	30	45.5938	66.7963	2474	72.5597	44.5795	0.789	56.1246
682	Look right	30	51.0251	66.1427	2754	74.1079	48.0006	0.7619	59.2157
304	Lean forward, towards steering whe	30	57.9696	74.4942	2503	62.1275	52.2685	0.5406	56.4528
188	Head on steering wheel	30	62.5946	88.7823	2205	70.8171	40.839	0.817	52.9858
512	Head on steering wheel	30	57.7037	99.1074	540	57.7121	16.0328	0.9606	26.2212
363	Lean right, overtaking manouvre	30	39.9164	65.2522	2728	81.7013	44.1591	0.8413	58.9355
428	*Lean right, overtaking manouvre*	30	40.7999	64.3527	2784	82.3396	44.6157	0.8405	59.5374
476	Lean right, overtaking manouvre	30	36.6126	64.1812	2803	84.3843	43.9891	0.8534	59.7402
54	Lean left	30	72.9366	95.1045	1120	62.3537	23.6145	0.9255	37.7628
688	Reach right	30	33.71	76.1663	3445	82.7354	55.0929	0.746	66.2292
689	Reach right	30	28.1707	78.6229	2941	72.0964	53.8267	0.6653	61.1931
85	Look straight ahead	30	0.43866	0.062839	0.722547	0.838513	0.70732	0.762843602	0.793466307
82	Look straight ahead	30	0.450418	0.051074	0.70809	0.850962	0.683749	0.780094787	0.781891122
129	Look straight ahead	30	0.502976	0.043764	0.754217	0.861669	0.732891	0.753175355	0.818503799
143	Look left	30	0.546959	0.167145	0.878141	0.843115	0.901219	0.629763033	0.912642472
339	Look left	30	0.51622	0.09795	0.837522	0.84336	0.824174	0.687203791	0.882421016
139	Look right	30	0.324781	0.183645	0.830981	0.834137	0.873812	0.647393365	0.8774995
69	Look right	30	0.325689	0.100424	0.684337	0.723717	0.699182	0.735734597	0.762667467
140	Look right	30	0.32611	0.178398	0.821687	0.829925	0.827755	0.68	0.870478404
182	*Lean forward*	30	0.516252	0.468839	0.62685	0.142078	0.932343	0	0.715029494
183	Head on steering wheel	30	0.46126	0.859727	0.2179	0	0.329474	0.778578199	0.310557888
187	Head on steering wheel	30	0.536512	0.934866	0.223752	0.5551	0.161515	0.977819905	0.317531494
361	*Lean right, overtaking*	30	0.127829	0.159427	0.77969	0.986287	0.720961	0.790900474	0.838339832
217	Lean right, overtaking	30	0.131945	0.084598	0.767642	0.940365	0.724921	0.778009479	0.828991702
224	Lean right, overtaking	30	0.103356	0.075875	0.771773	0.978456	0.771296	0.76056872	0.832203559
53	Lean left	30	1	0.999669	0.236489	0.447946	0.219874	0.944265403	0.332540992
72	Reach right	30	0.130782	0.150224	0.724957	0.509657	0.846206	0.51943128	0.795386923
657	Reach right	30	0.096363	0.384796	0.709811	0.282135	0.972998	0.12985782	0.783273345
264	Look straight ahead	30	0.367227	0.006472	0.767986	0.901541	0.731317	0.764739336	0.829259148
529	Look straight ahead	30	0.391285	0	0.766954	0.934968	0.71678	0.781421801	0.828454309
627	Look straight ahead	30	0.329313	0.049442	0.7821	0.919116	0.7372	0.765687204	0.84020196
144	Look left	30	0.546855	0.175827	0.876764	0.852678	0.894025	0.639052133	0.911627674
676	Look left	30	0.514261	0.0954	0.660585	0.484759	0.780065	0.573459716	0.743181364
337	Look right	30	0.415518	0.087138	0.768675	0.839499	0.756363	0.732132701	0.829794041
654	Look right	30	0.261128	0.171759	0.665749	0.612721	0.73084	0.674691943	0.747440512
682	Look right	30	0.342529	0.155005	0.762134	0.663427	0.818426	0.623317536	0.82469756
304	Lean forward, towards steering whe	30	0.446609	0.369082	0.675731	0.271046	0.927691	0.203791469	0.755638872
188	Head on steering wheel	30	0.515926	0.735333	0.57315	0.555647	0.635078	0.727772512	0.668981204
512	*Head on steering wheel*	30	0.442624	1	0	0.126432	0	1	0
363	Lean right, overtaking manouvre	30	0.176038	0.132178	0.753184	0.912126	0.720078	0.773838863	0.817693961
428	Lean right, overtaking manouvre	30	0.189279	0.109121	0.772461	0.933032	0.731767	0.772322275	0.832738452
476	*Lean right, overtaking manouvre*	30	0.126523	0.104725	0.779002	1	0.715725	0.796777251	0.837807439
54	Lean left	30	0.670927	0.897392	0.199656	0.278454	0.194103	0.933459716	0.288482304
688	Reach right	30	0.08302	0.411943	1	0.945995	1	0.593175355	1
689	*Reach right*	30	0	0.474914	0.826506	0.597547	0.967583	0.440189573	0.874122675

Driver Volunteer 6 OOP DATA
Name: Imran Amin

Frame number	Frame description	Face threshold value degree C	Centroid position x co-ordinate pixel	y co-ordnate pixel	Area pixel	Major Axis Length pixel	Minor Axis Length pixel	Eccentricity pixel	Equivdiameter pixel
85	Look straight ahead	30	57.4392	63.3274	2639	79.4537	43.6608	0.8355	57.9662
82	Look straight ahead	30	58.2237	62.0882	2597	79.8338	42.7401	0.8446	57.5031
129	Look straight ahead	30	61.7305	61.803	2731	80.1607	44.6596	0.8304	58.9679
182	Lean forward	30	62.6163	78.3859	2361	58.1898	52.4502	0.4331	54.8281
183	*Head on steering* wheel	30	58.9471	93.6351	1173	53.8518	28.9021	0.8438	38.646
187	Head on steering wheel	30	63.9681	96.5664	1190	70.8004	22.3416	0.9489	38.925
361	Lean right, overtaking	30	36.6998	66.3152	2805	83.9656	44.1936	0.8503	59.7615
217	*Lean right, overtaking*	30	36.9744	63.396	2770	82.5635	44.3483	0.8435	59.3875
224	Lean right, overtaking	30	35.0669	63.0557	2782	83.7265	46.1597	0.8343	59.516
53	Lean left	30	94.8932	99.0945	1227	67.5287	24.6211	0.9312	39.5255
264	*Look straight ahead*	30	52.673	60.3482	2771	81.3781	44.5981	0.8365	59.3982
529	Look straight ahead	30	54.2782	60.0957	2768	82.3987	44.0303	0.8453	59.366
627	Look straight ahead	30	50.1433	62.0245	2812	81.9147	44.8279	0.837	59.836
304	*Lean forward, towards steering whi*	30	57.9696	74.4942	2503	62.1275	52.2685	0.5406	56.4528
188	Head on steering wheel	30	62.5946	88.7823	2205	70.8171	40.839	0.817	52.9858
512	Head on steering wheel	30	57.7037	99.1074	540	57.7121	16.0328	0.9606	26.2212
363	*Lean right, overtaking manouvre*	30	39.9164	65.2522	2728	81.7013	44.1591	0.8413	58.9355
428	Lean right, overtaking manouvre	30	40.7999	64.3527	2784	82.3396	44.6157	0.8405	59.5374
476	Lean right, overtaking manouvre	30	36.6126	64.1812	2803	84.3843	43.9891	0.8534	59.7402
54	*Lean left*	30	72.9366	95.1045	1120	62.3537	23.6145	0.9255	37.7628
85	Look straight ahead	30	0.373954	0.082839	0.923856	0.838513	0.758648	0.762843602	0.944375692
82	Look straight ahead	30	0.387067	0.051074	0.90537	0.850962	0.733366	0.780094787	0.930599022
129	Look straight ahead	*30*	*0.445684*	*0.043764*	0.964349	*0.861669*	*0.786075*	*0.753175355*	0.974175066
182	Lean forward	30	0.46049	0.468839	0.801496	0.142078	1	0	0.851020979
183	Head on steering wheel	30	0.399159	0.859727	0.278609	0	0.353383	0.778578199	0.369622904
187	Head on steering wheel	30	0.483085	0.934866	0.286092	0.5551	0.173236	0.977819905	0.37792282
361	Lean right, overtaking	30	0.027294	0.159427	0.996919	0.986287	0.773279	0.790900474	0.997783714
217	Lean right, overtaking	30	0.031864	0.084598	0.981514	0.940365	0.777527	0.778009479	0.986657663
224	Lean right, overtaking	30	0	0.075875	0.986796	0.978456	0.827267	0.76056872	0.990480384
53	Lean left	30	1	0.999669	0.302377	0.447946	0.23583	0.944265403	0.395786975
264	Look straight ahead	30	0.294287	0.006472	0.981954	0.901541	0.784386	0.764739336	0.986975975
529	Look straight ahead	30	0.321118	0	0.980634	0.934968	0.768795	0.781421801	0.986018063
627	Look straight ahead	30	0.252003	0.049442	1	0.919116	0.790696	0.765687204	1
304	*Lean forward, towards steering whi*	30	0.38282	0.369082	0.863996	0.271046	0.995011	0.203791469	0.899353856
188	Head on steering wheel	30	0.460127	0.735333	0.732835	0.555647	0.681163	0.727772512	0.796214763
512	Head on steering wheel	30	0.378375	1	0	0.126432	0	1	0
363	Lean right, overtaking manouvre	*30*	*0.08106*	*0.132178*	*0.963028*	*0.912126*	*0.772331*	0.773838863	0.973211205
428	Lean right, overtaking manouvre	30	0.095827	0.109121	0.987676	0.933032	0.784869	0.772322275	0.991117008
476	Lean right, overtaking manouvre	30	0.025836	0.104725	0.996039	1	0.767663	0.796777251	0.997150065
54	Lean left	30	0.632994	0.697392	*0.255282*	*0.278454*	*0.208189*	*0.933459716*	*0.343348763*

Driver Volunteer 7
Name: James

ALL DATA

Frame number	Frame description	Face threshold value degree C	Centroid position x co-ordinate pixel	y co-ordnate pixel	Area pixel	Major Axis Length pixel	Minor Axis Length pixel	Eccentricity pixel	Equivdiameter pixel
34	Look straight ahead	30	53.9757	66.362	2555	85.2537	41.1153	0.876	57.0362
86	Look straight ahead	30	46.4574	66.0321	2678	86.6618	86.6618	0.8735	58.3929
207	Look straight ahead	30	48.8344	67.7413	2717	85.0954	43.4124	0.8601	58.8166
312	Look right	30	31.2028	70.385	2974	93.5197	41.8058	0.8945	61.5355
382	Look right	30	35.6021	69.434	2825	90.1647	41.6811	0.8867	59.9742
380	Lean right, overtaking	30	38.6559	66.1052	2671	92.9771	40.039	0.9025	58.3166
546	Lean right, overtaking	30	26.7519	72.0449	2696	91.3823	40.1708	0.8982	58.5889
548	Lean right, overtaking	30	24.1635	69.6456	2844	93.7021	41.113	0.8986	60.1755
42	Lean left	30	107.7031	101.6278	677	43.8681	20.9719	0.8783	29.3595
43	Lean left	30	115.0634	109.1604	268	25.2408	13.8593	0.8358	18.4724
26	Reach right	30	21.7637	69.8467	1494	54.9909	36.2613	0.7518	43.6144
35	Look back	30	30.3286	80.9699	2124	67.7723	40.9243	0.7971	52.0035
362	Look straight ahead	30	49.2322	66.117	2683	87.4132	41.6292	0.8793	58.4474
366	Look straight ahead	30	47.8527	66.6265	2742	87.5268	43.0063	0.871	59.0866
545	Look straight ahead	30	53.313	64.6811	2709	87.6961	41.9557	0.8781	58.7299
723	Look right	30	32.5804	69.5975	2872	88.3059	43.274	0.8717	60.471
3	Look right	30	42.8843	72.6473	2835	82.4462	45.6439	0.8328	60.0802
549	*Lean right, overtaking*	*30*	*24.8689*	*69.1828*	*2807*	*93.423*	*40.72*	*0.9*	*59.7828*
550	Lean right, overtaking	30	25.8467	69.0076	2752	93.979	40.0247	0.9048	59.1942
552	Lean right, overtaking	30	27.3332	67.6928	2878	93.4143	41.4766	0.896	60.5342
44	Lean left	30	117.7256	108.3537	164	26.0243	8.7985	0.9411	14.4503
45	Lean left	30	110.7363	103.478	546	36.1623	19.9322	0.8344	26.3664
27	Reach right	30	22.5992	71.1738	1582	58.6834	36.4108	0.7842	44.8806
37	Look back	30	29.037	70.9494	2214	72.8952	41.0725	0.8262	53.0938
34	Look straight ahead	30	0.335675	0.037791	0.85089	0.873065	0.415045	0.656101426	0.904443434
86	Look straight ahead	30	0.257328	0.030374	0.894662	0.89355	1	0.642894876	0.933257159
207	Look straight ahead	30	0.282098	0.068801	0.908541	0.870762	0.444547	0.572107765	0.942255741
312	Look right	30	0.098363	0.128237	1	0.993318	0.423913	0.7538299	1
382	Look right	30	0.144207	0.106856	0.946975	0.94451	0.422312	0.712625462	0.966840961
380	Lean right, overtaking	30	0.17603	0.032017	0.892171	0.985424	0.401222	0.796090861	0.931636693
546	Lean right, overtaking	30	0.051981	0.165556	0.901068	0.962223	0.402915	0.773375594	0.937419826
548	Lean right, overtaking	30	0.025008	0.111614	0.953737	0.995972	0.415016	0.775488642	0.971116189
42	*Lean left*	*30*	*0.895558*	*0.830649*	*0.182562*	*0.270989*	*0.156343*	*0.668251453*	*0.316643022*
43	Lean left	30	0.972258	1	0.037011	0	0.064996	0.443740095	0.085421746
26	Reach right	30	0	0.116135	0.47331	0.432803	0.352705	0	0.619389957
35	Look back	30	0.089253	0.366211	0.697509	0.618746	0.412592	0.239302694	0.797558468
362	Look straight ahead	30	0.286244	0.032282	0.896441	0.904481	0.421645	0.673534073	0.934414636
366	Look straight ahead	30	0.271868	0.043737	0.917438	0.906134	0.439331	0.629688325	0.947990027
545	Look straight ahead	30	0.328769	0	0.905694	0.908597	0.425839	0.667194929	0.940414398
723	Look right	30	0.112719	0.110532	0.963701	0.917468	0.44277	0.63338616	0.977392047
3	Look right	30	0.220094	0.179099	0.950534	0.832221	0.473206	0.427892235	0.969092199
549	Lean right, overtaking	30	0.032359	0.101209	0.940569	0.991911	0.409968	0.782884311	0.962775989
550	Lean right, overtaking	30	0.042548	0.09727	0.920996	1	0.401039	0.808240887	0.950275246
552	Lean right, overtaking	30	0.058039	0.06771	0.965836	0.991785	0.419686	0.76175383	0.978734294
44	Lean left	30	1	0.981863	0	0.011398	0	1	0
45	Lean left	30	0.927166	0.872246	0.135943	0.158885	0.14299	0.436344427	0.253075276
27	Reach right	30	0.008707	0.145971	0.504626	0.486521	0.354625	0.171156894	0.646281634
37	Look back	30	0.075794	0.140926	0.729537	0.693274	0.414496	0.393026941	0.820714365

Driver Volunteer 7
Name: James

OOP DATA

Frame number	Frame description	Face threshold value degree C	Centroid position x co-ordinate pixel	y co-ordnate pixel	Area pixel	Major Axis Length pixel	Minor Axis Length pixel	Eccentricity pixel	Equivdiameter pixel
34	Look straight ahead	30	53.9757	66.362	2555	85.2537	41.1153	0.876	57.0362
86	Look straight ahead	30	46.4574	66.0321	2678	86.6618	86.6618	0.8735	58.3929
207	Look straight ahead	30	48.8344	67.7413	2717	85.0954	43.4124	0.8601	58.8166
380	Lean right, overtaking	30	38.6559	66.1052	2671	92.9771	40.039	0.9025	58.3166
546	Lean right, overtaking	30	26.7519	72.0449	2696	91.3823	40.1708	0.8982	58.5889
548	Lean right, overtaking	30	24.1635	69.6456	2844	93.7021	41.113	0.8986	60.1755
42	Lean left	30	107.7031	101.6278	677	43.8681	20.9719	0.8783	29.3595
43	Lean left	30	115.0634	109.1604	268	25.2408	13.8593	0.8358	18.4724
362	Look straight ahead	30	49.2322	66.117	2683	87.4132	41.6292	0.8793	58.4474
366	Look straight ahead	30	47.8527	66.6265	2742	87.5268	43.0063	0.871	59.0866
545	Look straight ahead	30	53.313	64.6811	2709	87.6961	41.9557	0.8781	58.7299
549	*Lean right, overtaking*	*30*	*24.8689*	*69.1828*	*2807*	*93.423*	*40.72*	*0.9*	*59.7828*
550	Lean right, overtaking	30	25.8467	69.0076	2752	93.979	40.0247	0.9048	59.1942
552	Lean right, overtaking	30	27.3332	67.6928	2878	93.4143	41.4766	0.896	60.5342
44	Lean left	30	117.7256	108.3537	164	26.0243	8.7985	0.9411	14.4503
45	Lean left	30	110.7363	103.478	546	36.1623	19.9322	0.8344	26.3664
34	Look straight ahead	30	0.318635	0.037791	0.880987	0.873065	0.415045	0.389878163	0.924094966
86	Look straight ahead	30	0.238279	0.030374	0.926308	0.89355	1	0.366447985	0.953534749
207	Look straight ahead	30	0.263685	0.068801	0.940678	0.870762	0.444547	0.240862231	0.962728849
380	Lean right, overtaking	30	0.154896	0.032017	0.923729	0.985424	0.401222	0.638238051	0.951879073
546	Lean right, overtaking	30	0.027665	0.165556	0.93294	0.962223	0.402915	0.597938144	0.957787861
548	Lean right, overtaking	30	0	0.111614	0.987472	0.995972	0.415016	0.601686973	0.992216371
42	Lean left	30	0.892879	0.830649	0.15902	0.270989	0.156343	0.411433927	0.323522966
43	Lean left	30	0.971546	1	0.03832	0	0.064996	0.0131209	0.087277769
362	Look straight ahead	30	0.267936	0.032282	0.92815	0.904481	0.421645	0.420805998	0.954717374
366	Look straight ahead	30	0.253192	0.043737	0.949889	0.906134	0.439331	0.343017807	0.968587728
545	Look straight ahead	30	0.311552	0	0.93773	0.908597	0.425839	0.409559513	0.960847498
549	Lean right, overtaking	30	0.007539	0.101209	0.973839	0.991911	0.409968	0.614807873	0.983684956
550	Lean right, overtaking	30	0.01799	0.09727	0.953574	1	0.401039	0.659793814	0.9709226
552	Lean right, overtaking	30	0.033878	0.06771	1	0.991785	0.419686	0.577319588	1
44	Lean left	30	1	0.981863	0	0.011398	0	1	0
45	Lean left	30	0.925298	0.872246	0.140752	0.158885	0.14299	0	0.258574036

Driver Volunteer 8
Name: Mark Harriman

ALL DATA

Frame number	Frame description	Face threshold value degree C	Centroid position x co-ordinate pixel	y co-ordnate pixel	Area pixel	Major Axis Length pixel	Minor Axis Length pixel	Eccentricity pixel	Equivdiameter pixel
13	Look straight ahead	30	51.3361	60.8919	3859	94.9595	52.5254	0.8331	70.0959
14	Look straight ahead	30	51.6706	60.7519	3813	94.5304	52.1971	0.8337	69.6768
66	Look straight ahead	30	60.0193	57.8716	3630	94.3831	50.0238	0.848	67.9843
402	Look left	30	63.6807	58.9905	3883	87.6417	56.5394	0.7641	70.3135
21	Look left	30	78.1619	65.2183	4699	92.0781	67.0974	0.6848	77.3495
22	Look left	30	76.7875	64.4559	4330	88.0825	63.1969	0.6966	74.2504
400	Look right	30	48.6973	61.0795	3822	89.6212	54.9282	0.7902	69.759
25	Look right	30	62.4819	57.8787	4549	90.1378	64.523	0.6983	76.105
106	Look right	30	45.9507	63.0696	3939	89.4066	57.1389	0.7691	70.8187
767	Head near steering wheel	30	66.3387	75.1707	3797	74.5907	66.4645	0.4539	69.5305
768	Head near steering wheel	30	64.7782	72.6392	4049	76.0194	68.9988	0.4197	71.8007
42	Lean extreme left	30	116.3325	96.1765	391	44.1378	12.1491	0.9614	22.3123
43	Lean extreme left	30	117.2353	97.4923	323	45.1715	10.0841	0.9748	20.2795
17	Look back	30	56.4647	50.9062	3112	74.9848	54.0548	0.6931	62.947
18	Look back	30	67.4231	50.6608	2730	70.6164	50.8634	0.6937	58.9571
232	Look straight ahead	30	62.8874	55.9058	3632	93.119	50.3517	0.8412	68.003
491	Look straight ahead	30	61.4291	58.5112	3470	90.0723	49.8319	0.833	66.4691
714	Look straight ahead	30	62.9017	59.6507	3561	91.1937	50.545	0.8323	67.335
24	Look left	30	75.1736	61.2559	4119	87.8114	60.8035	0.7215	72.4187
117	Look left	30	63.817	58.6945	3885	88.9525	55.8091	0.7787	70.3316
118	Look left	30	62.37	58.7616	3670	88.1794	53.2283	0.7973	68.3578
115	Look right	30	49.146	60.3224	3766	91.4612	53.3155	0.8125	69.2461
100	Look right	30	54.4761	58.7666	3621	92.0098	51.0467	0.832	67.8999
794	Look right	30	53.3291	70.3336	4385	132.3776	71.8519	0.8399	74.7205
769	Head near steering wheel	30	62.3845	68.6058	4211	81.4905	66.91	0.5708	73.223
785	Head near steering wheel	30	70.0489	62.0546	3679	82.0075	57.8837	0.7084	68.4416
43	Lean extreme left	30	117.2353	97.4923	323	45.1715	10.0841	0.9748	20.2795
50	Lean extreme left	30	118.3556	100.3013	239	42.0723	7.9257	0.9821	17.4443
19	Look back	30	97.6787	54.6651	2275	60.6263	50.5731	0.5515	53.8203
20	Look back	30	92.5068	55.4035	2865	68.9646	54.9913	0.6035	60.3973
13	Look straight ahead	30	0.074379	0.206104	0.811659	0.585649	0.697675	0.73506401	0.878915353
14	Look straight ahead	30	0.078999	0.203284	0.801345	0.580897	0.692539	0.73613087	0.871919299
66	Look straight ahead	30	0.194305	0.14526	0.760314	0.579266	0.658542	0.76155761	0.843666326
402	Look left	30	0.244873	0.1678	0.81704	0.504615	0.760466	0.61237553	0.882547759
21	Look left	30	0.444876	0.293259	1	0.553742	0.925625	0.47137269	1
22	Look left	30	0.425894	0.2779	0.917265	0.509496	0.86461	0.4923542	0.948266595
400	Look right	30	0.037934	0.209883	0.803363	0.526535	0.735262	0.65878378	0.873291467
25	Look right	30	0.228316	0.145403	0.966368	0.532256	0.885354	0.49537696	0.97922551
106	Look right	30	0	0.249973	0.829596	0.524159	0.769844	0.621266	0.890981083
767	Head near steering wheel	30	0.281583	0.493748	0.797758	0.360094	0.915725	0.06081081	0.869477107
768	Head near steering wheel	30	0.260031	0.442751	0.85426	0.375915	0.955369	0	0.90737365
42	Lean extreme left	30	0.972059	0.916907	0.034081	0.022872	0.066067	0.96319346	0.081261727
43	Lean extreme left	30	0.984527	0.943413	0.018834	0.034319	0.033764	0.98701991	0.047328112
17	Look back	30	0.145211	0.004944	0.64417	0.364458	0.721599	0.48613087	0.759578467
18	Look back	30	0.29656	0	0.55852	0.316084	0.671676	0.48719772	0.6929749
232	Look straight ahead	30	0.233916	0.10566	0.760762	0.565268	0.663672	0.74946657	0.843978486
491	Look straight ahead	30	0.213776	0.158145	0.724439	0.53153	0.65554	0.7348862	0.818373029
714	Look straight ahead	30	0.234114	0.1811	0.744843	0.543948	0.666695	0.73364154	0.832827534
24	Look left	30	0.403604	0.213437	0.869955	0.506494	0.827169	0.53662873	0.91768995
117	Look left	30	0.246755	0.161838	0.817489	0.51913	0.749042	0.6383357	0.882849903
118	Look left	30	0.226771	0.163189	0.769283	0.510569	0.70867	0.67140825	0.849901177
115	Look right	30	0.044131	0.194631	0.790807	0.54691	0.710034	0.69843528	0.864729606
100	Look right	30	0.117746	0.16329	0.758296	0.552985	0.674543	0.73310811	0.842257433
794	Look right	30	0.101905	0.396305	0.929596	1	1	0.74715505	0.956113993
769	Head near steering wheel	30	0.226971	0.361499	0.890583	0.436499	0.922694	0.26866999	0.931116164
785	Head near steering wheel	30	0.332826	0.229526	0.7713	0.442224	0.781495	0.5133357	0.851300054
43	Lean extreme left	30	0.984527	0.943413	0.018834	0.034319	0.033764	0.98701991	0.047328112
50	Lean extreme left	30	1	1	0	0	0	1	0
19	Look back	30	0.714427	0.080666	0.456502	0.205459	0.667135	0.23435277	0.607226084
20	Look back	30	0.642997	0.095541	0.588789	0.297793	0.736249	0.32681366	0.717016219

Driver Volunteer 8
Name: Mark Harriman OOP DATA

Frame number	Frame description	Face threshold value degree C	Centroid position x co-ordinate pixel	y co-ordnate pixel	Area pixel	Major Axis Length pixel	Minor Axis Length pixel	Eccentricity pixel	Equivdiameter pixel
13	Look straight ahead	30	51.3361	60.8919	3859	94.9595	52.5254	0.8331	70.0959
14	Look straight ahead	30	51.6706	60.7519	3813	94.5304	52.1971	0.8337	69.6768
66	Look straight ahead	30	60.0193	57.8716	3630	94.3831	50.0238	0.848	67.9843
767	Head near steering wheel	30	66.3387	75.1707	3797	74.5907	66.4645	0.4539	69.5305
768	Head near steering wheel	30	64.7782	72.6392	4049	76.0194	68.9988	0.4197	71.8007
42	Lean extreme left	30	116.3325	96.1765	391	44.1378	12.1491	0.9614	22.3123
43	Lean extreme left	30	117.2353	97.4923	323	45.1715	10.0841	0.9748	20.2795
232	Look straight ahead	30	62.8874	55.9058	3632	93.119	50.3517	0.8412	68.003
491	Look straight ahead	30	61.4291	58.5112	3470	90.0723	49.8319	0.833	66.4691
714	Look straight ahead	30	62.9017	59.6507	3561	91.1937	50.545	0.8323	67.335
769	Head near steering wheel	30	62.3845	68.6058	4211	81.4905	66.91	0.5708	73.223
785	Head near steering wheel	30	70.0489	62.0546	3679	82.0075	57.8837	0.7084	68.4416
43	Lean extreme left	30	117.2353	97.4923	323	45.1715	10.0841	0.9748	20.2795
50	Lean extreme left	30	118.3556	100.3013	239	42.0723	7.9257	0.9821	17.4443
13	Look straight ahead	30	0	0.112311	0.91138	1	0.730267	0.73506401	0.943937381
14	Look straight ahead	30	0.004991	0.109157	0.899799	0.991887	0.724892	0.73613087	0.93642376
66	Look straight ahead	30	0.129562	0.044279	0.853726	0.989101	0.689307	0.76155761	0.906080637
767	Head near steering wheel	30	0.223854	0.433938	0.89577	0.614863	0.958504	0.06081081	0.933800895
768	Head near steering wheel	30	0.20057	0.376917	0.959215	0.641877	1	0	0.974501019
42	Lean extreme left	30	0.969813	0.90709	0.038268	0.039055	0.069153	0.96319346	0.087273457
43	Lean extreme left	30	0.983284	0.936728	0.021148	0.0586	0.035341	0.98701991	0.050829438
232	Look straight ahead	30	0.172357	0	0.85423	0.9652	0.694676	0.74946657	0.90641589
491	Look straight ahead	30	0.150598	0.058686	0.813444	0.907592	0.686165	0.7348862	0.878916145
714	Look straight ahead	30	0.172571	0.084353	0.836354	0.928796	0.697841	0.73364154	0.894439992
769	Head near steering wheel	30	0.164854	0.286065	1	0.745326	0.965798	0.26866999	1
785	Head near steering wheel	30	0.279214	0.138501	0.866062	0.755101	0.818003	0.5133357	0.914279107
43	Lean extreme left	30	0.983284	0.936728	0.021148	0.0586	0.035341	0.98701991	0.050829438
50	Lean extreme left	30	1	1	0	0	0	1	0

Driver Volunteer 9
Name: Stephen ALL DATA

Frame number	Frame description	Face threshold value degree C	Centroid position x co-ordinate pixel	y co-ordnate pixel	Area pixel	Major Axis Length pixel	Minor Axis Length pixel	Eccentricity pixel	Equivdiameter pixel
1	Look straight ahead	30	68.9616	72.9317	2476	72.4965	46.2711	0.7698	56.1475
4	Look straight ahead	30	67.7112	72.798	2441	71.2852	46.3544	0.7597	55.7492
91	Look straight ahead	30	61.2002	72.5263	2512	72.3477	46.8754	0.7617	56.5542
116	Look left	30	80.8638	74.8168	3149	73.6749	56.2555	0.6457	63.3201
117	Look left	30	86.5951	75.2383	3156	74.8359	55.2522	0.6745	63.3904
22	Look right	30	44.8179	75.9285	2756	70.6128	52.1362	0.6744	59.2372
197	Look right	30	67.923	72.2029	2947	78.1348	49.315	0.7757	61.2555
330	Look right	30	43.3108	76.3422	3118	74.4339	55.0193	0.6735	63.0076
219	Lean right, overtaking	30	49.4569	75.1509	2565	72.1274	47.0693	0.7577	57.1477
223	Lean right, overtaking	30	40.3409	74.9825	2740	75.8437	47.7302	0.7771	59.065
26	Lean extreme right	30	98.9214	95.6064	1603	58.5218	37.5275	0.7673	45.1775
20	Reach right	30	56.6055	75.5297	3115	72.914	55.9877	0.6406	62.9773
21	Reach right	30	49.8772	70.5849	2638	70.2587	50.3775	0.697	57.9552
133	Look straight ahead	30	62.3649	71.7537	2546	73.4739	46.6916	0.7721	56.9356
256	Look straight ahead	30	60.336	73.4827	2482	69.7432	47.6274	0.7305	56.2155
421	Look straight ahead	30	65.0331	71.3999	2806	77.455	48.5056	0.7796	59.7722
194	Look left	30	81.2863	73.6098	3273	76.0317	56.3423	0.6715	64.5547
408	Look left	30	81.6921	74.9253	3401	76.9018	58.7046	0.646	65.8049
331	Look right	30	44.921	75.4663	3090	76.3799	53.0935	0.7189	62.7241
409	Look right	30	64.9581	74.8057	3171	74.6808	56.0119	0.6614	63.5409
118	Look right	30	71.3546	76.873	2843	69.1007	53.8499	0.6267	60.1649
226	Lean right, overtaking	30	40.6809	74.0913	2739	75.3834	47.9475	0.7716	59.0542
227	Lean right, overtaking	30	41.6478	74.0247	2757	74.8286	48.4917	0.7616	59.248
27	Lean extreme right	30	99.7673	96.7903	1521	56.5575	37.3851	0.7504	44.0068
22	Reach right	30	44.8179	75.9285	2756	70.6128	52.1362	0.6744	59.2372
39	Reach right	30	35.295	85.38	2664	70.1164	51.4118	0.68	58.2401
1	Look straight ahead	30	0.522187	0.089554	0.507979	0.738693	0.416802	0.93590582	0.556961387
4	Look straight ahead	30	0.502793	0.064452	0.489362	0.682555	0.420709	0.86984957	0.538689152
91	Look straight ahead	30	0.401804	0.074084	0.527128	0.731797	0.445146	0.88293002	0.575618976
116	Look left	30	0.706797	0.16149	0.865957	0.793306	0.885124	0.12426422	0.866008414
117	Look left	30	0.795692	0.177574	0.869681	0.847112	0.838064	0.31262263	0.889233465
22	Look right	30	0.147705	0.203912	0.656915	0.651393	0.691906	0.31196861	0.698703098
197	Look right	30	0.506078	0.061743	0.758511	1	0.559577	0.97449313	0.791293737
330	Look right	30	0.124329	0.219699	0.849468	0.826482	0.827139	0.30608241	0.871672302
219	Lean right, overtaking	30	0.219659	0.174239	0.555319	0.721587	0.454241	0.85676913	0.60264612
223	Lean right, overtaking	30	0.078265	0.167813	0.648404	0.893819	0.485241	0.98364944	0.690803327
26	Lean extreme right	30	0.98688	0.954822	0.043617	0.091035	0.006679	0.91955526	0.053706516
20	Reach right	30	0.333639	0.188694	0.847872	0.758042	0.872563	0.09090909	0.870282272
21	Reach right	30	0.226178	0	0.594149	0.634982	0.609414	0.45977763	0.839890633
133	Look straight ahead	30	0.419869	0.044601	0.545213	0.783991	0.436525	0.95094833	0.593115914
256	Look straight ahead	30	0.388399	0.11058	0.51117	0.611091	0.480419	0.67887508	0.560080924
421	Look straight ahead	30	0.461254	0.0311	0.683511	0.968495	0.521612	1	0.723246521
194	Look left	30	0.71335	0.11543	0.931915	0.902532	0.889195	0.29300196	0.942646377
408	Look left	30	0.719644	0.16563	1	0.942857	1	0.12622629	1
331	Look right	30	0.149304	0.186275	0.834574	0.918669	0.736809	0.6030085	0.858666581
409	Look right	30	0.460091	0.161066	0.87766	0.839924	0.873698	0.22694572	0.896137737
118	Look right	30	0.559304	0.239954	0.703191	0.581315	0.772288	0	0.741261853
226	Lean right, overtaking	30	0.083538	0.133804	0.647872	0.872486	0.495434	0.94767822	0.690307871
227	Lean right, overtaking	30	0.098535	0.131263	0.657447	0.846774	0.52096	0.882276	0.699198554
27	Lean extreme right	30	1	1	0	0	0	0.80902551	0
22	Reach right	30	0.147705	0.203912	0.656915	0.651393	0.691906	0.31196861	0.698703098
39	Reach right	30	0	0.563619	0.607979	0.628387	0.657928	0.34859385	0.652960579

Driver Volunteer 9
Name: Stephen — OOP DATA

Frame number	Frame description	Face threshold value degree C	Centroid position x co-ordinate pixel	y co-ordnate pixel	Area pixel	Major Axis Length pixel	Minor Axis Length pixel	Eccentricity pixel	Equivdiameter pixel
1	Look straight ahead	30	68.9616	72.9317	2476	72.4965	46.2711	0.7698	56.1475
4	Look straight ahead	30	67.7112	72.798	2441	71.2852	46.3544	0.7597	55.7492
91	Look straight ahead	30	61.2002	72.5283	2512	72.3477	46.8754	0.7617	56.5542
219	Lean right, overtaking	30	49.4569	75.1509	2565	72.1274	47.0693	0.7577	57.1477
223	Lean right, overtaking	30	40.3409	74.9825	2740	75.8437	47.7302	0.7771	59.065
26	Lean extreme right	30	98.9214	95.6064	1603	58.5218	37.5275	0.7673	45.1775
133	Look straight ahead	30	62.3649	71.7537	2546	73.4739	46.6916	0.7721	56.9356
256	Look straight ahead	30	60.336	73.4827	2482	69.7432	47.6274	0.7305	56.2155
421	Look straight ahead	30	65.0331	71.3999	2806	77.455	48.5056	0.7796	59.7722
226	Lean right, overtaking	30	40.6809	74.0913	2739	75.3834	47.9475	0.7716	59.0542
227	Lean right, overtaking	30	41.6478	74.0247	2757	74.8286	48.4917	0.7616	59.248
27	Lean extreme right	30	99.7673	96.7903	1521	56.5575	37.3851	0.7504	44.0068
1	Look straight ahead	30	0.481616	0.06033	0.743191	0.762723	0.799065	0.80040733	0.770085123
4	Look straight ahead	30	0.460575	0.055064	0.715953	0.704759	0.806555	0.59470468	0.744820937
91	Look straight ahead	30	0.351011	0.044363	0.771206	0.755602	0.853406	0.63543788	0.795882122
219	Lean right, overtaking	30	0.1534	0.147733	0.812451	0.74506	0.870842	0.55397149	0.833527852
223	Lean right, overtaking	30	0	0.141101	0.948638	0.922895	0.930273	0.9490835	0.955142274
26	Lean extreme right	30	0.985766	0.953372	0.063813	0.093997	0.012805	0.74949084	0.074257551
133	Look straight ahead	30	0.37061	0.013934	0.797665	0.809494	0.836878	0.84725051	0.82007434
256	Look straight ahead	30	0.336468	0.082031	0.74786	0.63097	0.921029	0	0.774398366
421	Look straight ahead	30	0.415509	0	1	1	1	1	1
226	Lean right, overtaking	30	0.005721	0.106001	0.94786	0.900869	0.949813	0.83706721	0.954457229
227	Lean right, overtaking	30	0.021992	0.103378	0.961868	0.87432	0.99875	0.63340122	0.966749871
27	Lean extreme right	30	1	1	0	0	0	0.40529532	0

Driver Volunteer 10
Name: Valerie ALL DATA

Frame number	Frame description	Face threshold value degree C	Centroid position x co-ordinate pixel	y co-ordnate pixel	Area pixel	Major Axis Length pixel	Minor Axis Length pixel	Eccentricity pixel	Equivdiameter pixel
39	Look straight ahead	30	50.5772	65.0979	2216	67.557	42.8535	0.7731	53.1178
90	Look straight ahead	30	56.3668	62.8552	2383	71.184	43.5685	0.7908	55.0829
304	Look straight ahead	30	66.9809	61.428	2411	71.1784	44.349	0.7822	55.4056
110	Look left	30	70.7348	62.4321	2002	76.1307	34.9853	0.8882	50.4879
111	Look left	30	78.9923	64.8788	1692	74.9412	31.65	0.9064	46.4147
108	Look right	30	47.5845	64.7378	2277	82.2829	37.8406	0.888	53.8439
3	Look right	30	47.3223	72.3941	1936	73.8151	42.0115	0.8222	49.6487
40	Look right	30	46.7283	65.341	2135	71.2498	39.9526	0.828	52.138
159	Lean right, overtaking	30	33.3137	62.1865	2611	74.2428	45.9115	0.7859	57.6579
168	Lean right, overtaking	30	31.8127	63.705	2590	73.1228	46.4949	0.7718	57.4255
170	Lean right, overtaking	30	24.1045	65.4029	2363	68.0443	45.2237	0.7472	54.8513
5	Reach right	30	32.3159	51.3205	1298	46.1705	36.6014	0.6096	40.653
11	Reach right	30	36.9213	69.0674	89	27.7669	9.7997	0.9357	10.6451
423	Look straight ahead	30	56.1478	61.0376	2503	75.9094	49.6075	0.7569	56.4528
500	Look straight ahead	30	56.6863	61.8005	2426	70.7768	44.6942	0.7754	55.5777
98	Look straight ahead	30	57.783	62.771	2341	69.2937	44.1028	0.7713	54.5954
331	Look left	30	73.5092	66.9522	1799	73.8213	32.9662	0.8947	47.8598
744	Look left	30	73.8674	70.1378	1734	87.6104	58.307	0.7464	46.9872
328	Look right	30	53.1839	63.0949	2170	78.4886	36.9969	0.8819	52.5636
666	Look right	30	40.7709	64.5607	1960	68.6006	38.0199	0.8324	49.9555
743	Look right	30	47.0795	68.2888	2012	115.3947	42.4499	0.9299	50.6138
173	Lean right, overtaking	30	27.238	64.709	2567	69.8598	48.2497	0.7232	57.17
176	Lean right, overtaking	30	30.6155	64.7118	2429	69.1034	46.3252	0.742	55.612
237	Lean right, overtaking	30	23.4261	64.6537	2342	69.4707	43.8766	0.7753	54.607
42	Reach right	30	47.0497	65.629	1830	73.0452	34.2908	0.883	48.2704
44	Reach right	30	32.6554	70.4167	1512	70.1867	31.4621	0.8939	43.8764
39	Look straight ahead	30	0.488626	0.653775	0.843378	0.454081	0.681419	0.50137994	0.903428428
90	Look straight ahead	30	0.592819	0.547353	0.909596	0.495472	0.696159	0.55565777	0.945227683
304	Look straight ahead	30	0.783836	0.479629	0.920698	0.495408	0.712249	0.5292855	0.952091771
110	Look left	30	0.851393	0.527276	0.758525	0.551923	0.519213	0.85433916	0.847488344
111	Look left	30	1	0.643378	0.635607	0.538349	0.450454	0.91015026	0.760848109
108	Look right	30	0.434768	0.636688	0.867565	0.622131	0.578076	0.85372585	0.918873158
3	Look right	30	0.430049	1	0.732355	0.525498	0.664061	0.65194726	0.829637886
40	Look right	30	0.419359	0.665311	0.811261	0.496223	0.621616	0.66973321	0.882587295
159	Lean right, overtaking	30	0.177943	0.515621	1	0.530378	0.744461	0.54063171	1
168	Lean right, overtaking	30	0.15093	0.587678	0.991673	0.517597	0.756488	0.49739344	0.995056665
170	Lean right, overtaking	30	0.012209	0.668248	0.901665	0.459642	0.730282	0.42195646	0.940301365
5	Reach right	30	0.159986	0	0.479381	0.21002	0.552529	0	0.638292125
11	Reach right	30	0.242867	0.842139	0	0	0	1	0
423	Look straight ahead	30	0.588878	0.461103	0.957177	0.549398	0.820656	0.45170193	0.974366555
500	Look straight ahead	30	0.598569	0.497305	0.926646	0.490825	0.719366	0.508433	0.955752476
98	Look straight ahead	30	0.618306	0.543358	0.892942	0.4739	0.707174	0.49586017	0.934858166
331	Look left	30	0.901323	0.741767	0.678033	0.525568	0.477588	0.8742717	0.791586547
744	Look left	30	0.907769	0.892932	0.65226	0.682928	1	0.41950322	0.773025644
328	Look right	30	0.535538	0.558728	0.825139	0.578831	0.560683	0.83501993	0.891640149
666	Look right	30	0.312147	0.628284	0.741872	0.46599	0.581772	0.683226	0.836163768
743	Look right	30	0.42568	0.805192	0.76249	1	0.673099	0.98221404	0.850166338
173	Lean right, overtaking	30	0.068601	0.635321	0.982554	0.48036	0.792664	0.3483594	0.989621975
176	Lean right, overtaking	30	0.129384	0.635454	0.927835	0.471728	0.75299	0.40601043	0.956482064
237	Lean right, overtaking	30	0	0.632697	0.893339	0.47592	0.702511	0.50812634	0.935104908
42	Reach right	30	0.425143	0.678977	0.690325	0.516712	0.504895	0.83839313	0.800320338
44	Reach right	30	0.166096	0.906167	0.564235	0.484091	0.44658	0.87181846	0.706856431

Driver Volunteer 10
Name: Valerie

OOP DATA

Frame number	Frame description	Face threshold value degree C	Centroid position x co-ordinate pixel	y co-ordnate pixel	Area pixel	Major Axis Length pixel	Minor Axis Length pixel	Eccentricity pixel	Equivdiameter pixel
39	Look straight ahead	30	50.5772	65.0979	2216	67.557	42.8535	0.7731	53.1178
90	Look straight ahead	30	56.3668	62.8552	2383	71.184	43.5685	0.7908	55.0829
304	Look straight ahead	30	66.9809	61.428	2411	71.1784	44.349	0.7822	55.4056
159	Lean right, overtaking	30	33.3137	62.1865	2611	74.2428	45.9115	0.7859	57.6579
168	Lean right, overtaking	30	31.8127	63.705	2590	73.1228	46.4949	0.7718	57.4255
170	Lean right, overtaking	30	24.1045	65.4029	2363	68.0443	45.2237	0.7472	54.8513
423	Look straight ahead	30	56.1478	61.0376	2503	75.9094	49.6075	0.7569	56.4528
500	Look straight ahead	30	56.6863	61.8005	2426	70.7768	44.6942	0.7754	55.5777
98	Look straight ahead	30	57.783	62.771	2341	69.2937	44.1028	0.7713	54.5954
173	Lean right, overtaking	30	27.238	64.709	2567	69.8598	48.2497	0.7232	57.17
176	Lean right, overtaking	30	30.6155	64.7118	2429	69.1034	46.3252	0.742	55.612
237	Lean right, overtaking	30	23.4261	64.6537	2342	69.4707	43.8766	0.7753	54.607
39	Look straight ahead	30	0.623378	0.930131	0	0	0	0.73816568	0
90	Look straight ahead	30	0.756305	0.416375	0.422785	0.434246	0.105863	1	0.432831876
304	Look straight ahead	30	1	0.089433	0.493671	0.433576	0.221424	0.87278107	0.503909606
159	Lean right, overtaking	30	0.227015	0.263189	1	0.800465	0.452769	0.92751479	1
168	Lean right, overtaking	30	0.192553	0.611046	0.946835	0.686371	0.539147	0.71893491	0.9488117
170	Lean right, overtaking	30	0.015576	1	0.372152	0.058343	0.350933	0.35502959	0.381819784
423	Look straight ahead	30	0.751277	0	0.726582	1	1	0.49852071	0.734565318
500	Look straight ahead	30	0.76364	0.174765	0.531646	0.385494	0.272535	0.77218935	0.54181626
98	Look straight ahead	30	0.78882	0.397086	0.316456	0.207928	0.184972	0.71153846	0.325455386
173	Lean right, overtaking	30	0.08752	0.841042	0.888608	0.275705	0.798964	0	0.892535407
176	Lean right, overtaking	30	0.165066	0.841683	0.539241	0.185144	0.514021	0.27810651	0.549371159
237	Lean right, overtaking	30	0	0.828374	0.318987	0.22912	0.151481	0.77071006	0.328010396

Driver Volunteer 11
Name: Diming

ALL DATA

Frame number	Frame description	Face threshold value degree C	Centroid position x co-ordinate pixel	y co-ordnate pixel	Area pixel	Major Axis Length pixel	Minor Axis Length pixel	Eccentricity pixel	Equivdiameter pixel
22	Look straight ahead	30	58.0509	55.836	3202	94.3873	44.4771	0.882	63.8507
101	Look straight ahead	30	64.9264	57.132	3219	92.3526	45.6885	0.8691	64.02
207	Look straight ahead	30	67.9918	56.3925	3292	93.7775	46.3256	0.8695	64.7418
534	Look left	30	71.2755	60.008	3252	90.2815	46.7949	0.8552	64.3473
4	Look left	30	62.2236	67.7231	3081	81.2564	49.957	0.7887	62.6327
5	Look left	30	64.9197	66.9346	3150	83.5916	49.7935	0.8032	63.3301
81	Look right, arm out of window	30	45.9738	53.0801	3396	87.2546	51.5765	0.8066	65.7565
19	Look right, arm out of window	30	41.6188	53	2324	68.3087	44.1557	0.763	54.3968
422	Lean forward, near wheel	30	67.0277	71.6013	3283	73.1241	60.9745	0.552	64.6533
158	Lean forward, near wheel	30	56.0362	63.3217	4252	95.5654	58.5939	0.79	73.5786
41	Lean left, extreme	30	102.5578	87.8149	1669	59.5995	39.0166	0.7559	46.0981
36	Lean left, extreme	30	91.9208	78.0973	2549	73.3406	51.0761	0.7176	56.9692
38	Lean left, extreme	30	99.7831	86.4038	1798	61.5144	39.6656	0.7643	47.8465
11	Look up	30	60.0979	55.4536	3117	92.1757	44.782	0.8741	62.9975
9	Look up	30	57.0348	57.1773	3215	93.4903	45.6122	0.8729	63.9802
315	Look straight ahead	30	71.9934	56.2032	3174	92.8653	45.1369	0.8739	63.5709
415	Look straight ahead	30	72.9223	55.3853	3190	93.694	45.2117	0.8759	63.731
612	Look straight ahead	30	70.6196	57.7438	3333	96.9205	45.7698	0.8815	65.1437
6	Look left	30	66.4167	63.1881	3249	86.6144	48.9849	0.8247	64.3176
475	Look left	30	67.846	59.4322	3512	94.5809	48.3738	0.8593	66.8702
534	Look left	30	71.2755	60.008	3252	90.2815	46.7949	0.8552	64.3473
80	Look right, arm out of window	30	45.5751	57.9389	3255	82.5154	51.9894	0.7765	64.377
82	Look right, arm out of window	30	58.5484	53.2734	3138	83.3037	48.9195	0.8094	63.2094
418	Lean forward, near wheel	30	71.8565	65.1867	3797	87.3581	57.6479	0.7514	69.5305
423	Lean forward, near wheel	30	69.8466	65.3718	3911	87.2332	60.0553	0.7253	70.5666
40	Lean left, extreme	30	101.4891	87.1913	1793	60.427	40.6094	0.7405	47.7799
42	Lean left, extreme	30	101.5618	86.5718	1796	59.3414	41.6523	0.7123	47.8199
43	Lean left, extreme	30	99.599	85.2407	1853	60.1049	41.4428	0.7243	48.5728
10	Look up	30	59.8607	55.8922	3172	93.1088	45.2558	0.8739	63.5509
12	Look up	30	60.1421	55.5808	3139	92.3521	44.969	0.8734	63.2195
22	Look straight ahead	30	0.269648	0.081459	0.593496	0.93259	0.24868	1	0.646007169
101	Look straight ahead	30	0.382474	0.118685	0.600077	0.878446	0.30385	0.96090909	0.652167901
207	Look straight ahead	30	0.432777	0.097444	0.628339	0.916363	0.332864	0.96212121	0.678433799
534	Look left	30	0.486662	0.201293	0.612853	0.823333	0.354237	0.91878788	0.664078165
4	Look left	30	0.338122	0.422897	0.546651	0.58317	0.498244	0.71727273	0.601684831
5	Look left	30	0.382364	0.400248	0.573364	0.645311	0.490798	0.76121212	0.627062826
81	Look right, arm out of window	30	0.071465	0.002301	0.668602	0.742785	0.571999	0.77151515	0.715358163
19	Look right, arm out of window	30	0	0	0.253581	0.238625	0.234043	0.63939394	0.301985044
422	Lean forward, near wheel	30	0.416956	0.534291	0.624855	0.366765	1	0	0.675213333
158	Lean forward, near wheel	30	0.236587	0.296474	1	0.96394	0.891583	0.72121212	1
41	Lean left, extreme	30	1	1	0	0.006868	0	0.61787879	0
36	Lean left, extreme	30	0.825448	0.720878	0.340689	0.372526	0.54921	0.50181818	0.395593239
38	Lean left, extreme	30	0.954468	0.959469	0.049942	0.057825	0.029557	0.64333333	0.063623297
11	Look up	30	0.303239	0.070476	0.560588	0.873738	0.262566	0.97606061	0.614959699
9	Look up	30	0.252974	0.119986	0.598529	0.908721	0.300375	0.97242424	0.650719601
315	Look straight ahead	30	0.498443	0.092007	0.582656	0.892089	0.278729	0.97545455	0.635825403
415	Look straight ahead	30	0.513686	0.068514	0.58885	0.914141	0.282135	0.98151515	0.641651353
612	Look straight ahead	30	0.475899	0.136258	0.644212	1	0.307652	0.99848485	0.693058714
6	Look left	30	0.40693	0.292636	0.611692	0.725749	0.453973	0.82636364	0.662997398
475	Look left	30	0.430384	0.184754	0.713511	0.937742	0.426143	0.93121212	0.755885082
534	Look left	30	0.486662	0.201293	0.612853	0.823333	0.354237	0.91878788	0.664078165
80	Look right, arm out of window	30	0.064922	0.141862	0.614015	0.616673	0.590803	0.68030303	0.665158931
82	Look right, arm out of window	30	0.277812	0.007853	0.568719	0.63765	0.450995	0.78	0.622670621
418	Lean forward, near wheel	30	0.496196	0.350043	0.823848	0.745539	0.848501	0.60424242	0.852691909
423	Lean forward, near wheel	30	0.463214	0.355359	0.867983	0.742216	0.958138	0.52515152	0.890395007
40	Lean left, extreme	30	0.982463	0.982088	0.048006	0.028888	0.072539	0.57121212	0.06119976
42	Lean left, extreme	30	0.983656	0.984294	0.049168	0	0.120034	0.48575758	0.062655337
43	Lean left, extreme	30	0.951447	0.92606	0.071235	0.020317	0.110493	0.52212121	0.090052947
10	Look up	30	0.299347	0.083074	0.581882	0.898569	0.284144	0.97545455	0.635097615
12	Look up	30	0.303965	0.074129	0.569106	0.878432	0.271082	0.97393939	0.623038154

Driver Volunteer 11
Name: Diming

OOP DATA

Frame number	Frame description	Face threshold value degree C	Centroid position x co-ordinate pixel	y co-ordnate pixel	Area pixel	Major Axis Length pixel	Minor Axis Length pixel	Eccentricity pixel	Equivdiameter pixel
22	Look straight ahead	30	58.0509	55.836	3202	94.3873	44.4771	0.882	63.8507
101	Look straight ahead	30	64.9264	57.132	3219	92.3526	45.6885	0.8691	64.02
207	Look straight ahead	30	67.9918	56.3925	3292	93.7775	46.3256	0.8695	64.7418
422	Lean forward, near wheel	30	67.0277	71.6013	3283	73.1241	60.9745	0.552	64.6533
158	Lean forward, near wheel	30	56.0362	63.3217	4252	95.5654	58.5939	0.79	73.5786
41	Lean left, extreme	30	102.5578	87.8149	1669	59.5995	39.0166	0.7559	46.0981
36	Lean left, extreme	30	91.9208	78.0973	2549	73.3406	51.0761	0.7176	56.9692
38	Lean left, extreme	30	99.7831	86.4038	1798	61.5144	39.6656	0.7643	47.8465
315	Look straight ahead	30	71.9934	56.2032	3174	92.8653	45.1369	0.8739	63.5709
415	Look straight ahead	30	72.9223	55.3853	3190	93.694	45.2117	0.8759	63.731
612	Look straight ahead	30	70.6196	57.7438	3333	96.9205	45.7698	0.8815	65.1437
418	Lean forward, near wheel	30	71.8565	65.1867	3797	87.3581	57.6479	0.7514	69.5305
423	Lean forward, near wheel	30	69.8466	65.3718	3911	87.2332	60.0553	0.7253	70.5666
40	Lean left, extreme	30	101.4891	87.1913	1793	60.427	40.6094	0.7405	47.7799
42	Lean left, extreme	30	101.5618	86.5718	1796	59.3414	41.6523	0.7123	47.8199
43	Lean left, extreme	30	99.599	85.2407	1853	60.1049	41.4428	0.7243	48.5728
22	Look straight ahead	30	0.043307	0.013898	0.593496	0.93259	0.24868	1	0.646007169
101	Look straight ahead	30	0.191098	0.053861	0.600077	0.878446	0.30385	0.96090909	0.652167901
207	Look straight ahead	30	0.25699	0.031058	0.628339	0.916363	0.332864	0.96212121	0.678433799
422	Lean forward, near wheel	30	0.236267	0.500037	0.624855	0.366765	1	0	0.675213333
158	Lean forward, near wheel	30	0	0.244727	1	0.96394	0.891583	0.72121212	1
41	Lean left, extreme	30	1	1	0	0.006868	0	0.61787879	0
36	Lean left, extreme	30	0.771354	0.700348	0.340689	0.372526	0.54921	0.50181818	0.395593239
38	Lean left, extreme	30	0.940357	0.956487	0.049942	0.057825	0.029557	0.64333333	0.063623297
315	Look straight ahead	30	0.343006	0.025221	0.582656	0.892089	0.278729	0.97545455	0.635825403
415	Look straight ahead	30	0.362973	0	0.58885	0.914141	0.282135	0.98151515	0.641651353
612	Look straight ahead	30	0.313476	0.072727	0.644212	1	0.307552	0.99848485	0.693058714
418	Lean forward, near wheel	30	0.340064	0.302236	0.823848	0.745539	0.848501	0.60424242	0.852691909
423	Lean forward, near wheel	30	0.29686	0.307944	0.867983	0.742216	0.958138	0.52515152	0.890395007
40	Lean left, extreme	30	0.977028	0.980771	0.048006	0.028888	0.072539	0.57121212	0.06119976
42	Lean left, extreme	30	0.978591	0.961668	0.049168	0	0.120034	0.48575758	0.062655337
43	Lean left, extreme	30	0.936399	0.920622	0.071235	0.020317	0.110493	0.52212121	0.090052947

Driver Volunteer: Terry Harrison No.12 ALL DATA

Frame number	Frame description	Face thresholding value degree C	Centroid position x co-ordinate pixel	y co-ordnate pixel	Area pixel	Major Axis Length pixel	Minor Axis Length pixel	Eccentricity pixel	Equivdiameter pixel
9	Look straight ahead	30	49.4023	75.1706	5745	118.6555	95.3804	0.5948	85.5264
13	Look straight ahead	30	48.5216	75.0477	5824	120.8945	93.7412	0.6315	86.1124
77	Look straight ahead	30	53.9021	76.4767	6908	134.9282	94.8381	0.7113	93.7845
18	Look right	30	50.3849	74.6107	6697	121.8105	98.0017	0.5939	92.3411
19	*Look right*	*30*	*55.0912*	*73.0797*	*6811*	*116.7523*	*99.524*	*0.5228*	*93.1238*
25	Look right	30	46.007	72.3787	7101	117.5011	95.3442	0.5844	95.0856
102	Look left	30	56.0802	70.6107	6872	120.545	95.702	0.608	93.5398
103	Look left	30	55.3465	71.6125	6888	120.4603	99.0974	0.5685	93.6487
32	Lean right	30	46.7574	76.4822	6590	143.7153	78.4318	0.838	91.6005
34	Lean right	30	45.1249	78.894	6151	142.2389	75.6436	0.8469	88.4969
158	Lean right	30	38.7263	77.0252	6901	133.2657	84.3006	0.7745	93.737
29	Lean left	30	66.2967	81.8885	6098	112.8204	92.718	0.5697	88.1148
219	Head on steering wheel	30	56.246	76.362	7174	113.036	99.2576	0.4785	95.5731
182	Use mobile phone	30	56.4364	76.3963	7646	127.6183	101.472	0.6065	98.6671
183	Use mobile phone	30	54.8977	75.6009	7499	128.4986	99.4768	0.633	97.714
184	Use mobile phone	30	55.4712	75.8728	7703	127.3339	100.1805	0.6173	99.0342
90	*Look straight ahead*	*30*	*48.0503*	*71.5197*	*6081*	*118.6311*	*92.5926*	*0.6251*	*87.9919*
262	Look straight ahead	30	54.4986	74.0392	7268	131.1048	102.7303	0.6213	96.1972
413	Look straight ahead	30	45.5122	71.5912	6382	119.1261	89.7172	0.6579	90.1433
104	Look right	30	41.901	69.0797	7103	119.4349	92.5466	0.6321	95.099
289	Look right	30	50.5533	73.4407	8291	132.3316	102.9317	0.6285	102.7445
476	Look right	30	61.522	78.7503	7238	122.947	101.8373	0.5603	95.9985
174	Look left	30	50.4376	75.5001	6833	119.382	92.4661	0.6325	93.274
472	Look left	30	58.3875	74.9017	7009	123.3437	104.3186	0.5336	94.4676
160	Lean right	30	36.0729	77.0277	6389	128.7311	82.6357	0.7668	90.1927
162	Lean right	30	37.5427	75.3736	6727	127.4145	86.9017	0.7313	92.5477
163	Lean right	30	38.2343	76.377	6812	128.6258	85.0976	0.7499	93.1306
30	Lean left	30	71.5353	84.5226	5264	115.1489	83.7878	0.686	81.8678
287	*Head on steering wheel*	*30*	*52.5026*	*82.6292*	*6798*	*115.6001*	*97.1626*	*0.5418*	*93.0348*
185	Use mobile phone	30	56.4938	74.7792	7631	126.6795	102.1246	0.5917	98.5702
186	Use mobile phone	30	56.5818	75.7995	7675	127.122	101.6352	0.6007	98.854
187	Use mobile phone	30	55.0376	75.4996	7350	126.3041	99.3461	0.6175	96.7384
9	Look straight ahead	30	0.37587	0.39441	0.158903	0.188869	0.688293	0.31568947	0.175248004
13	Look straight ahead	30	0.35104	0.38646	0.185002	0.261341	0.631128	0.41530945	0.203317574
77	Look straight ahead	30	0.50276	0.47899	0.543112	0.715581	0.669381	0.63192182	0.570813395
18	Look right	30	0.40358	0.35816	0.473406	0.29099	0.779707	0.31324647	0.501674115
19	Look right	30	0.53629	0.25902	0.511067	0.127267	0.832795	0.12024973	0.539165673
25	Look right	30	0.28013	0.21363	0.606871	0.151504	0.687031	0.28745928	0.633136463
102	Look left	30	0.56418	0.09914	0.531219	0.250028	0.699508	0.35152009	0.559092194
103	Look left	30	0.54349	0.16401	0.536505	0.247287	0.817918	0.24429967	0.564308535
32	*Lean right*	*30*	*0.30129*	*0.47935*	*0.438057*	*1*	*0.097235*	*0.97584148*	*0.46619916*
34	Lean right	30	0.25526	0.63552	0.293029	0.952212	0	1	0.317535817
158	Lean right	30	0.07482	0.51451	0.540799	0.661769	0.301901	0.80347448	0.568538131
29	Lean left	30	0.85228	0.82943	0.27552	0	0.595446	0.247557	0.299233116
219	Head on steering wheel	30	0.56886	0.47156	0.630988	0.006978	0.823505	0	0.656487855
182	Use mobile phone	30	0.57423	0.47378	0.786918	0.478975	0.900729	0.34744843	0.804691354
183	Use mobile phone	30	0.53084	0.42228	0.738355	0.507469	0.831149	0.41938111	0.759037587
184	Use mobile phone	30	0.54701	0.43988	0.805748	0.46977	0.85569	0.37676439	0.822275551
90	Look straight ahead	30	0.33775	0.158	0.269904	0.18808	0.591072	0.39793702	0.293346171
262	Look straight ahead	30	0.51958	0.32115	0.662042	0.591826	0.94461	0.38762215	0.686382426
413	Look straight ahead	30	0.26618	0.16263	0.369343	0.204102	0.490797	0.48697068	0.396398856
104	Look right	30	0.16435	0	0.607532	0.214097	0.589468	0.41693811	0.633778327
289	*Look right*	*30*	*0.40833*	*0.2624*	*1*	*0.631535*	*0.951634*	*0.40716612*	*1*
476	Look right	30	0.71764	0.62622	0.652131	0.327776	0.913468	0.22204126	0.676864639
174	Look left	30	0.40507	0.41575	0.518335	0.212385	0.586661	0.41802389	0.546360296
472	Look left	30	0.62925	0.377	0.576478	0.340616	1	0.14956569	0.603534083
160	Lean right	30	0	0.51467	0.371655	0.514994	0.24384	0.78257329	0.398765131
162	Lean right	30	0.04145	0.40756	0.483317	0.472379	0.39261	0.68621064	0.511570315
163	Lean right	30	0.06095	0.47253	0.511397	0.511586	0.329695	0.73669924	0.539491395
30	Lean left	30	1	1	0	0.075368	0.284017	0.56324647	0
287	Head on steering wheel	30	0.4633	0.87739	0.506772	0.089973	0.750445	0.1718241	0.534902547
185	Use mobile phone	30	0.57585	0.36907	0.781962	0.448589	0.923487	0.3072747	0.800049816
186	Use mobile phone	30	0.57833	0.43514	0.796498	0.462911	0.90642	0.33170467	0.813643919
187	Use mobile phone	30	0.53478	0.41572	0.689131	0.436438	0.826591	0.37730727	0.712306064

Driver Volunteer: Terry Harrison No.12 OOP DATA

Frame number	Frame description	Face thresholding value degree C	Centroid position x co-ordinate pixel	y co-ordnate pixel	Area pixel	Major Axis Length pixel	Minor Axis Length pixel	Eccentricity pixel	Equivdiameter pixel
9	Look straight ahead	30	49.4023	75.1706	5745	118.6555	95.3804	0.5948	85.5264
13	Look straight ahead	30	48.5216	75.0477	5824	120.8945	93.7412	0.6315	86.1124
77	Look straight ahead	30	53.9021	76.4767	6908	134.9282	94.8381	0.7113	93.7845
32	Lean right	30	46.7574	76.4822	6590	143.7153	78.4318	0.838	91.6005
34	Lean right	30	45.1249	78.894	6151	142.2389	75.6436	0.8469	88.4969
158	Lean right	30	38.7263	77.0252	6901	133.2657	84.3006	0.7745	93.737
29	Lean left	30	66.2967	81.8885	6098	112.8204	92.718	0.5697	88.1148
219	Head on steering wheel	30	56.246	76.362	7174	113.036	99.2576	0.4785	95.5731
90	Look straight ahead	30	48.0503	71.5197	6081	118.6311	92.5926	0.6251	87.9919
262	Look straight ahead	30	54.4986	74.0392	7268	131.1048	102.7303	0.6213	96.1972
413	Look straight ahead	30	45.5122	71.5912	6382	119.1261	89.7172	0.6579	90.1433
160	Lean right	30	36.0729	77.0277	6389	128.7311	82.6357	0.7668	90.1927
162	Lean right	30	37.5427	75.3736	6727	127.4145	86.9017	0.7313	92.5477
163	Lean right	30	38.2343	76.377	6812	128.6258	85.0976	0.7499	93.1306
30	Lean left	30	71.5353	84.5226	5264	115.1489	83.7878	0.686	81.8678
287	Head on steering wheel	30	52.5026	82.6292	6798	115.6001	97.1626	0.5418	93.0348
9	Look straight ahead	30	0.37587	0.28078	0.24002	0.188869	0.728653	0.31568947	0.255321228
13	Look straight ahead	30	0.35104	0.27132	0.279441	0.261341	0.668136	0.41530945	0.296216171
77	Look straight ahead	30	0.50276	0.38122	0.820359	0.715581	0.708632	0.63192182	0.831625888
32	Lean right	30	0.30129	0.38165	0.661677	1	0.102936	0.97584148	0.67921197
34	Lean right	30	0.25526	0.56713	0.442615	0.952212	0	1	0.462622301
158	Lean right	30	0.07482	0.42341	0.816866	0.661769	0.319603	0.80347448	0.828311025
29	Lean left	30	0.85228	0.79742	0.416168	0	0.630361	0.247557	0.435956844
219	Head on steering wheel	30	0.56886	0.3724	0.953094	0.006978	0.871793	0	0.956446188
90	Look straight ahead	30	0.33775	0	0.407685	0.18808	0.625731	0.39793702	0.427380072
262	Look straight ahead	30	0.51958	0.19376	1	0.591826	1	0.38762215	1
413	Look straight ahead	30	0.26618	0.0055	0.557884	0.204102	0.519576	0.48697068	0.577518947
160	Lean right	30	0	0.4236	0.561377	0.514994	0.258138	0.78257329	0.580966405
162	Lean right	30	0.04145	0.29639	0.73004	0.472379	0.415632	0.68621064	0.74531383
163	Lean right	30	0.06095	0.37356	0.772455	0.511586	0.349027	0.73669924	0.785992435
30	Lean left	30	1	1	0	0.075368	0.300672	0.56324647	0
287	Head on steering wheel	30	0.4633	0.85439	0.765469	0.089973	0.794449	0.1718241	0.77930688

Test Volunteer number 13
Name: Trevor OOP DATA

Frame number	Frame description	Face thresholding value degree C	Centroid position x co-ordinate pixel	y co-ordnate pixel	Area pixel	Major Axis Length pixel	Minor Axis Length pixel	Eccentricity pixel	Equivdiameter pixel
39	Look straight ahead	30	61.9435	75.9692	5749	114.7054	99.9229	0.4911	85.5561
60	Look straight ahead	30	70.5247	74.616	5542	114.4059	87.2291	0.647	84.0017
63	Look straight ahead	30	66.6774	80.0494	6556	119.1469	98.0888	0.5677	91.3639
499	Lean right	30	42.0736	75.6644	6684	128.07	92.2323	0.6938	92.2515
16	Lean left	30	63.4054	90.1168	5599	151.6812	60.5471	0.9169	84.4326
18	Lean left	30	64.6126	86.77	4786	134.4215	51.3694	0.9241	78.0623
70	Lean forward	30	69.1942	82.0685	6428	117.5598	92.5262	0.6169	90.4676
164	Lean forward	30	64.6829	75.2727	7348	126.2075	95.9934	0.6492	96.7252
209	Lean forward	30	68.064	74.1094	7177	119.7699	101.7044	0.5281	95.5931
212	Head on steering wheel	30	80.7278	76.0531	7230	131.2153	90.4192	0.7247	95.9454
213	Head on steering wheel	30	78.9686	78.2431	6935	117.668	90.3869	0.6403	93.9676
183	Look straight ahead	30	69.7157	78.3995	6300	120.086	98.3544	0.5737	89.5623
208	Look straight ahead	30	69.483	77.1447	5979	117.5148	98.6074	0.544	87.2508
307	Look straight ahead	30	68.7354	77.879	6040	115.8311	98.4591	0.5267	87.6947
500	Lean right	30	41.7984	76.1834	6648	128.9151	91.5383	0.7041	92.0027
20	Lean left	30	64.4874	93.4809	5076	150.0431	52.6758	0.9363	80.3926
19	Lean left	30	65.7667	85.8339	4557	134.6802	47.9575	0.9345	76.1719
211	Lean forward	30	61.5535	74.3824	7221	119.6399	101.9804	0.5229	95.8857
266	Lean forward	30	78.5275	77.4665	7164	136.3973	87.0003	0.7702	95.5065
367	Lean forward	30	69.1678	73.2327	6846	124.3373	95.4484	0.6409	93.3627
295	Head on steering wheel	30	68.2843	82.5634	6391	107.0427	92.9787	0.4955	90.2068
368	Head on steering wheel	30	68.1186	73.6777	6636	107.5372	97.1686	0.4284	91.9196
39	Look straight ahead	30	0.517478	0.135148	0.427087	0.171661	0.961914	0.1234495	0.456578749
60	Look straight ahead	30	0.737908	0.068317	0.35292	0.164952	0.726944	0.43039968	0.380950991
63	Look straight ahead	30	0.63908	0.336657	0.716231	0.271161	0.927964	0.27426659	0.739151377
499	Lean right	30	0.007069	0.120095	0.762092	0.471057	0.819556	0.52254381	0.782336656
16	Lean left	30	0.55503	0.833857	0.373343	1	0.233042	0.9618035	0.401915994
18	Lean left	30	0.58604	0.666568	0.082049	0.613345	0.063157	0.97597952	0.091975498
70	Lean forward	30	0.70373	0.436375	0.670369	0.235606	0.824996	0.37113605	0.695542808
164	Lean forward	30	0.587846	0.10075	1	0.429333	0.889177	0.43473125	1
209	Lean forward	30	0.674698	0.043298	0.938732	0.285117	0.994891	0.19629848	0.944918821
212	Head on steering wheel	30	1	0.139291	0.957721	0.541519	0.785994	0.58338256	0.962059621
213	Head on steering wheel	30	0.954811	0.247449	0.852024	0.23803	0.785397	0.41720811	0.865831764
183	Look straight ahead	30	0.717126	0.255173	0.624507	0.292198	0.93288	0.28607994	0.651496353
208	Look straight ahead	30	0.711149	0.193202	0.509495	0.234598	0.937564	0.22760386	0.539032661
307	Look straight ahead	30	0.691945	0.229467	0.531351	0.196879	0.934818	0.19354204	0.560630166
500	Lean right	30	0	0.145727	0.749194	0.48999	0.80671	0.54282339	0.770231544
20	Lean left	30	0.582824	1	0.185955	0.963303	0.087339	1	0.205353885
19	Lean left	30	0.615686	0.622337	0	0.61914	0	0.996456	0
211	Lean forward	30	0.50746	0.05678	0.954497	0.282205	1	0.18606025	0.959154978
266	Lean forward	30	0.94348	0.209095	0.934074	0.657607	0.722708	0.67296712	0.940705386
367	Lean forward	30	0.703052	0	0.820136	0.387437	0.879088	0.41838945	0.836400967
295	Head on steering wheel	30	0.680357	0.460816	0.657112	0	0.833373	0.13211262	0.682853848
368	Head on steering wheel	30	0.676101	0.021977	0.744894	0.011078	0.91093	0	0.766188398

Test Volunteer number 14
Name: Mary Treasure ALL DATA

Frame number	Frame description	Face thresholding value degree C	Centroid position x co-ordinate pixel	y co-ordnate pixel	Area pixel	Major Axis Length pixel	Minor Axis Length pixel	Eccentricity pixel	Equivdiameter pixel
75	Look straight ahead	30	50.3912	75.983	4992	109.7717	84.5181	0.6381	79.7246
150	Look straight ahead	30	50.7845	75.3797	5212	111.2846	87.4577	0.6184	81.4624
230	Look straight ahead	30	53.3307	75.6881	5056	110.2665	87.2086	0.612	80.234
15	Look right	30	56.9565	75.7584	5634	107.9553	89.1044	0.5646	84.6961
178	Look right	30	50.1646	73.6586	5808	117.1417	89.5631	0.6445	85.994
8	Look left	30	52.2292	75.9641	4734	104.996	81.1083	0.635	77.6371
9	Look left	30	54.1849	76.4283	4847	107.1366	83.4221	0.6275	78.5582
10	Look left	30	54.0676	76.7241	4835	105.8906	83.5519	0.6143	78.4609
27	Lean left	30	89.4339	83.1287	4367	109.4621	79.0095	0.6921	74.567
28	Lean left	30	90.5585	84.8547	3909	110.5607	79.2414	0.6974	70.5485
29	Lean left	30	92.1957	84.8867	3654	104.5977	75.5603	0.6915	68.2086
314	Lean forward	30	49.3826	73.0848	6638	121.0233	94.8564	0.621	91.9335
315	Lean forward	30	48.0714	72.5039	6777	121.3929	92.6589	0.646	92.891
316	Head on steering whe	30	41.9877	73.6216	6659	119.6909	89.2407	0.6664	92.0788
53	Look back	30	79.911	84.7685	3382	110.7055	71.9752	0.7598	65.6209
267	Use mobile phone	30	56.7569	75.0825	5865	104.9129	89.1317	0.5275	86.415
268	Use mobile phone	30	55.7362	75.8826	5962	106.5797	90.3188	0.5309	87.1267
269	Use mobile phone	30	55.4941	74.9333	5865	107.5883	88.6337	0.5668	86.415
382	Look straight ahead	30	54.1814	75.233	5871	121.6676	86.198	0.7057	86.4592
452	Look straight ahead	30	51.0512	75.8238	5427	112.9108	89.1908	0.6132	83.1256
570	Look straight ahead	30	50.8853	75.734	5041	108.6986	86.7013	0.6031	80.1149
179	Look right	30	48.7959	72.7896	5604	115.2468	86.2428	0.6633	84.4703
180	Look right	30	50.345	76.0316	5444	112.4554	88.5234	0.6167	83.2557
11	Look left	30	53.7755	76.5179	4704	104.6987	82.2297	0.619	77.3907
12	Look left	30	53.4697	76.8235	4941	106.0932	84.4647	0.6051	79.3163
13	Look left	30	53.5699	77.2076	4759	104.8567	83.5379	0.6044	77.8418
30	Lean left	30	91.6847	85.6904	3701	108.4927	77.0776	0.7038	68.6459
31	Lean left	30	91.6408	87.3901	3486	106.3756	76.8591	0.6913	66.6222
32	Lean left	30	92.6833	87.9088	3628	104.1774	75.4399	0.6896	64.5054
318	Lean forward	30	48.1327	75.7509	6081	114.6817	91.3816	0.6042	87.9919
334	Lean forward	30	53.1805	74.7415	6151	116.3083	95.9108	0.5657	88.4969
340	Head on steering whe	30	42.5258	74.1607	7083	119.9264	92.2644	0.6388	94.965
54	Look back	30	79.7216	84.5275	3689	109.2152	77.5911	0.7038	68.5345
270	Use mobile phone	30	55.6381	75.1439	5874	107.5992	89.1064	0.5605	86.4813
271	Use mobile phone	30	56.633	75.3823	5537	103.5429	87.6796	0.5319	83.9638
272	Use mobile phone	30	55.818	75.5879	5933	108.1544	89.9142	0.5557	86.9145
75	Look straight ahead	30	0.165764	0.225844	0.435018	0.343664	0.524027	0.47610848	0.499651998
150	Look straight ahead	30	0.173522	0.186681	0.494461	0.427135	0.64684	0.39130435	0.556704619
230	Look straight ahead	30	0.223747	0.2067	0.45231	0.370963	0.636433	0.36375377	0.51637579
15	Look right	30	0.295268	0.211264	0.608484	0.243447	0.715637	0.15970728	0.662868193
178	Look right	30	0.161294	0.074957	0.655499	0.750291	0.734801	0.50365906	0.705478732
8	Look left	30	0.20202	0.224617	0.365307	0.080172	0.38157	0.46276367	0.431118596
9	Look left	30	0.240597	0.25475	0.395839	0.198276	0.478237	0.43047783	0.461358652
10	Look left	30	0.238283	0.273952	0.392597	0.12953	0.48366	0.37365476	0.458164257
27	Lean left	30	0.935904	0.689703	0.266144	0.326582	0.293884	0.70856651	0.330326071
28	Lean left	30	0.958087	0.801745	0.142394	0.387195	0.303573	0.73138183	0.198397221
29	Lean left	30	0.990382	0.803822	0.073494	0.058197	0.149781	0.70598364	0.121577434
314	Lean forward	30	0.145869	0.037709	0.879762	0.964452	0.956032	0.40249677	0.900474727
315	Lean forward	30	0.120004	0	0.91732	0.984844	0.86414	0.51011623	0.931909808
316	Head on steering whe	30	0	0.072555	0.885436	0.890939	0.721331	0.59793371	0.90524498
53	Look back	30	0.748059	0.796149	0	0.395184	0	1	0.03662228
267	Use mobile phone	30	0.291331	0.167388	0.6709	0.075587	0.716778	0	0.719300319
268	Use mobile phone	30	0.271197	0.219326	0.697109	0.16755	0.766373	0.01463625	0.742665695
269	Use mobile phone	30	0.266422	0.157703	0.6709	0.223198	0.695972	0.16917779	0.719300319
382	Look straight ahead	30	0.240528	0.177158	0.672521	1	0.594211	0.76711149	0.720751422
452	Look straight ahead	30	0.178783	0.215509	0.552553	0.516858	0.719247	0.3689195	0.611308093
570	Look straight ahead	30	0.17551	0.20968	0.448257	0.284457	0.615238	0.32544124	0.512465692
179	Look right	30	0.134296	0.018546	0.600378	0.645743	0.596083	0.58456889	0.655455095
180	Look right	30	0.164853	0.228999	0.557147	0.491732	0.691363	0.38398622	0.615579325
11	Look left	30	0.232521	0.260566	0.357201	0.063769	0.42842	0.39388721	0.423029193
12	Look left	30	0.226489	0.280404	0.421238	0.140709	0.521796	0.3340508	0.486247357
13	Look left	30	0.228466	0.305338	0.372062	0.072487	0.483075	0.33103745	0.437838974
30	Lean left	30	0.980302	0.855994	0.086193	0.273097	0.213172	0.75893241	0.135934155
31	Lean left	30	0.979436	0.966329	0.028101	0.156289	0.204043	0.70512269	0.069495332
32	Lean left	30	1	1	0.066469	0.035007	0.144751	0.69780456	0
318	Lean forward	30	0.121214	0.210777	0.729262	0.614565	0.810776	0.3301765	0.771070533
334	Lean forward	30	0.220784	0.145252	0.748176	0.70431	1	0.16444253	0.787649871
340	Head on steering whe	30	0.010614	0.10755	1	0.903932	0.847658	0.47912183	1
54	Look back	30	0.744323	0.780505	0.082951	0.31296	0.234625	0.75893241	0.132276852
270	Use mobile phone	30	0.269262	0.171374	0.673332	0.2238	0.715721	0.14205768	0.721476973
271	Use mobile phone	30	0.286887	0.18685	0.582275	0	0.656111	0.01894102	0.638826511
272	Use mobile phone	30	0.272811	0.200196	0.689273	0.254432	0.749469	0.12139475	0.73569909

Test Volunteer number 14
Name: Mary Treasure OOP DATA

Frame number	Frame description	Face thresholding value degree C	Centroid position x co-ordinate pixel	y co-ordnate pixel	Area pixel	Major Axis Length pixel	Minor Axis Length pixel	Eccentricity pixel	Equivdiameter pixel
75	Look straight ahead	30	50.3912	75.983	4992	109.7717	84.5181	0.6381	79.7246
150	Look straight ahead	30	50.7845	75.3797	5212	111.2846	87.4577	0.6184	81.4624
230	Look straight ahead	30	53.3307	75.6881	5056	110.2665	87.2086	0.612	80.234
27	Lean left	30	89.4339	83.1287	4367	109.4621	79.0095	0.6921	74.567
28	Lean left	30	90.5585	84.8547	3909	110.5607	79.2414	0.6974	70.5485
29	Lean left	30	92.1957	84.8867	3654	104.5977	75.5603	0.6915	68.2086
314	Lean forward	30	49.3826	73.0848	6638	121.0233	94.8584	0.621	91.9335
315	Lean forward	30	48.0714	72.5039	6777	121.3929	92.6589	0.646	92.891
316	Head on steering whe	30	41.9877	73.6216	6659	119.6909	89.2407	0.6664	92.0788
382	Look straight ahead	30	54.1814	75.233	5871	121.6676	86.198	0.7057	86.4592
452	Look straight ahead	30	51.0512	75.8238	5427	112.9108	89.1908	0.6132	83.1256
570	Look straight ahead	30	50.8853	75.734	5041	108.6986	86.7013	0.6031	80.1149
30	Lean left	30	91.6847	85.6904	3701	108.4927	77.0776	0.7038	68.6459
31	Lean left	30	91.6408	87.3901	3486	106.3756	76.8591	0.6913	66.6222
32	Lean left	30	92.6833	87.9088	3628	104.1774	75.4399	0.6896	64.5054
318	Lean forward	30	48.1327	75.7509	6081	114.6817	91.3816	0.6042	87.9919
334	Lean forward	30	53.1805	74.7415	6151	116.3083	95.9108	0.5657	88.4969
340	Head on steering whe	30	42.5258	74.1607	7083	119.9264	92.2644	0.6388	94.965
75	Look straight ahead	30	0.165764	0.225844	0.418682	0.319853	0.443469	0.51714286	0.499651998
150	Look straight ahead	30	0.173522	0.186681	0.479844	0.406353	0.587067	0.37642857	0.556704619
230	Look straight ahead	30	0.223747	0.2067	0.436475	0.348144	0.574899	0.33071429	0.51637579
27	Lean left	30	0.935904	0.689703	0.244926	0.302152	0.174374	0.90285714	0.330326071
28	Lean left	30	0.958087	0.801745	0.117598	0.364964	0.185703	0.94071429	0.198397221
29	Lean left	30	0.990382	0.803822	0.046706	0.024031	0.005882	0.89857143	0.121577434
314	Lean forward	30	0.145869	0.037709	0.876286	0.963162	0.94859	0.395	0.900474727
315	Lean forward	30	0.120004	0	0.914929	0.984294	0.841145	0.57357143	0.931909808
316	Head on steering whe	30	0	0.072555	0.882124	0.886982	0.674167	0.71928571	0.90524498
382	Look straight ahead	30	0.240528	0.177158	0.663053	1	0.525531	1	0.720751422
452	Look straight ahead	30	0.178783	0.215509	0.539616	0.499331	0.671729	0.33928571	0.611308093
570	Look straight ahead	30	0.17551	0.20968	0.432305	0.258499	0.550117	0.26714286	0.512465692
30	Lean left	30	0.980302	0.855994	0.059772	0.246727	0.080001	0.98642857	0.135934155
31	Lean left	30	0.979436	0.966329	0	0.125682	0.069328	0.89714286	0.069495332
32	Lean left	30	1	1	0.039477	0	0	0.885	0
318	Lean forward	30	0.121214	0.210777	0.721435	0.600582	0.778749	0.275	0.771070533
334	Lean forward	30	0.220784	0.145252	0.740895	0.693583	1	0	0.787649871
340	Head on steering whe	30	0.010614	0.10755	1	0.900447	0.821874	0.52214286	1

Test Volunteer number 15
Name: Cathy Turner ALL DATA

Frame number	Frame description	Face thresholding value degree C	Centroid position x co-ordinate pixel	y co-ordnate pixel	Area pixel	Major Axis Length pixel	Minor Axis Length pixel	Eccentricity pixel	Equivdiameter pixel
65	Look straight ahead	30	49.9773	75.1015	5153	122.4309	73.8288	0.7977	81
70	Look straight ahead	30	52.4786	75.0558	5201	126.252	72.9213	0.8163	81.3764
182	Look straight ahead	30	51.222	74.5195	5513	119.4436	86.3093	0.6913	83.7817
489	Look right	30	43.749	76.6623	5315	119.7544	82.3144	0.7263	82.2634
490	Look right	30	43.3058	76.7341	5419	123.1429	80.7577	0.7549	83.0643
491	Look right	30	43.323	76.5982	5849	127.2177	82.8479	0.7589	86.297
15	Look left	30	55.145	79.2393	5483	110.0972	97.4124	0.466	83.5534
16	Look left	30	50.6355	77.9624	5314	109.9815	92.4823	0.5412	82.2557
17	Look left	30	48.0089	78.4553	5188	112.4336	88.5758	0.6159	81.2746
310	Lean right	30	44.4521	75.7474	5585	123.767	82.6186	0.7446	84.327
311	Lean right	30	44.6669	75.9737	5590	124.0641	82.5656	0.7464	84.3647
312	Lean right	30	44.4834	75.354	5559	124.2443	82.2617	0.7494	84.1305
24	Lean forward	30	55.3237	77.7275	5864	107.8127	93.5392	0.4972	86.4076
25	Lean forward	30	53.4314	78.4435	5533	112.0291	95.0223	0.5297	83.9335
154	Lean forward	30	44.0655	73.489	5798	118.5967	80.4877	0.7344	85.92
159	Head on steering wheel	30	39.1277	74.2787	5934	94.4106	82.7569	0.4813	86.9218
160	Head on steering wheel	30	37.8264	75.5059	6284	115.2627	85.7086	0.6686	89.4485
161	Head on steering wheel	30	35.6494	77.5501	5930	123.3465	80.607	0.7569	86.8925
10	Look up	30	46.9021	76.857	5524	114.472	86.6634	0.6533	83.8652
223	Use mobile phone	30	47.2342	75.2913	6115	120.3522	84.6617	0.7107	88.2375
224	Use mobile phone	30	45.2988	75.4731	6147	120.9949	82.3471	0.7327	88.4681
225	Use mobile phone	30	45.8202	75.774	5740	118.8803	79.0299	0.747	85.4892
258	Look straight ahead	30	48.464	74.9646	5560	116.5408	88.0341	0.6553	84.1381
300	Look straight ahead	30	48.6913	77.4033	5666	119.857	89.0951	0.6689	84.9363
353	Look straight ahead	30	46.7089	75.3233	5534	119.0712	86.7027	0.6854	83.9411
492	Look right	30	43.9168	76.2201	5519	123.9853	82.4983	0.7465	83.8273
493	Look right	30	43.6651	75.7162	5419	122.193	82.2417	0.7396	83.0643
335	Look right	30	43.0564	76.419	5642	127.3744	81.4901	0.7686	84.7562
18	Look left	30	49.9419	79.27	5437	114.0396	92.207	0.5884	83.2022
187	Look left	30	50.2758	76.6115	5493	119.2827	87.0594	0.6836	83.6296
463	Look left	30	49.3482	77.9252	4986	109.3579	88.7942	0.5837	79.6767
313	Lean right	30	44.1054	75.2924	5380	121.7688	81.5973	0.7423	82.7649
314	Lean right	30	43.3274	75.3911	5324	120.1831	81.9611	0.7314	82.333
318	Lean right	30	42.0558	77.1119	5933	129.6099	79.069	0.7924	86.9145
155	Lean forward	30	42.8355	73.138	5775	118.516	79.4311	0.7422	85.7494
156	Lean forward	30	47.792	71.6622	6009	119.6229	78.7838	0.7525	87.4694
163	Lean forward	30	40.0043	71.7176	6087	126.1842	80.8752	0.7676	88.0353
162	Head on steering wheel	30	35.9438	75.9943	5920	119.8118	82.6993	0.7236	86.8192
273	Head on steering wheel	30	42.8303	78.7496	4968	90.0524	80.9403	0.4383	79.5327
274	Head on steering wheel	30	44.0339	77.3473	5601	110.5152	83.5417	0.6547	84.4477
11	Look up	30	47.5729	77.6455	5577	120.9344	89.4762	0.6727	84.2666
226	Use mobile phone	30	47.0785	76.312	6163	120.3685	83.5739	0.7197	88.5832
227	Use mobile phone	30	46.4008	75.4509	5873	119.2363	81.0002	0.7338	86.4739
228	Use mobile phone	30	45.9106	76.1199	6028	119.547	82.3504	0.7249	87.6076
65	Look straight ahead	30	0.728255	0.452076	0.140578	0.818517	0.037054	0.95079365	0.147975958
70	Look straight ahead	30	0.85539	0.446069	0.177052	0.915113	0	1	0.185935578
182	Look straight ahead	30	0.79152	0.375576	0.414134	0.742999	0.546648	0.66931217	0.428508038
489	Look right	30	0.411684	0.657233	0.263678	0.750856	0.363531	0.76190476	0.275388773
490	Look right	30	0.389157	0.666671	0.342705	0.836616	0.319969	0.83756614	0.356158858
491	Look right	30	0.390032	0.648808	0.669453	0.939526	0.405315	0.84814815	0.682173904
15	Look left	30	0.990917	0.995965	0.391337	0.506726	1	0.07328042	0.405484177
16	Look left	30	0.771875	0.828124	0.262918	0.503801	0.798698	0.27222222	0.274612236
17	Look left	30	0.628205	0.892913	0.167173	0.565789	0.639191	0.46984127	0.175669134
310	Lean right	30	0.447421	0.536975	0.468845	0.852293	0.395952	0.81031746	0.483501079
311	Lean right	30	0.458339	0.566721	0.472644	0.859804	0.393788	0.81507937	0.487303092
312	Lean right	30	0.449012	0.485265	0.449088	0.864359	0.381379	0.82301587	0.463684221
24	Lean forward	30	1	0.797248	0.680851	0.448974	0.841853	0.15582011	0.69332782
25	Lean forward	30	0.903819	0.891361	0.429331	0.555563	0.902409	0.24179894	0.443816939
154	Lean forward	30	0.427771	0.240122	0.630699	0.72159	0.308945	0.78333333	0.644153775
159	Head on steering wheel	30	0.176794	0.343923	0.734043	0.110174	0.401599	0.11375661	0.745184453
160	Head on steering wheel	30	0.110552	0.505231	1	0.637308	0.52212	0.60925926	1
161	Head on steering wheel	30	0	0.773929	0.731003	0.841663	0.313816	0.84285714	0.74222957
10	Look up	30	0.571949	0.682826	0.422492	0.617319	0.561106	0.56878307	0.436928942
223	Use mobile phone	30	0.588829	0.477024	0.871581	0.765969	0.479374	0.72063492	0.87787168
224	Use mobile phone	30	0.490457	0.50092	0.895897	0.782216	0.384866	0.77883598	0.901127493
225	Use mobile phone	30	0.516959	0.540472	0.586626	0.728759	0.249421	0.81666667	0.600707961
258	Look straight ahead	30	0.651337	0.420936	0.449848	0.669618	0.617073	0.57407407	0.464450675
300	Look straight ahead	30	0.66289	0.754633	0.530395	0.75345	0.660395	0.61005291	0.544948466
353	Look straight ahead	30	0.562129	0.48123	0.430091	0.733586	0.562711	0.6537037	0.444563392
492	Look right	30	0.420213	0.599109	0.418693	0.857812	0.39104	0.81534392	0.433106759
493	Look right	30	0.40742	0.532874	0.342705	0.812503	0.380563	0.79708995	0.356158858
335	Look right	30	0.376481	0.625253	0.512158	0.943487	0.349874	0.87380952	0.526785534
18	Look left	30	0.726455	1	0.356383	0.606393	0.787457	0.39708995	0.370065955
187	Look left	30	0.743427	0.650556	0.398936	0.738932	0.577275	0.6489418	0.413168882
463	Look left	30	0.696279	0.823234	0.013678	0.488036	0.648109	0.38465608	0.014522278
313	Lean right	30	0.429799	0.477168	0.31307	0.80178	0.354251	0.8042328	0.325964622
314	Lean right	30	0.390255	0.490142	0.270517	0.761694	0.369106	0.77539683	0.282407874
318	Lean right	30	0.325623	0.716331	0.733283	1	0.251018	0.93677249	0.744448254
155	Lean forward	30	0.365253	0.193985	0.613222	0.71955	0.265803	0.80396825	0.62694691
156	Lean forward	30	0.617181	0	0.791033	0.747532	0.239373	0.83121693	0.800409448
163	Lean forward	30	0.22135	0.007282	0.850304	0.913399	0.324767	0.87116402	0.857479981
162	Head on steering wheel	30	0.014964	0.569429	0.723404	0.752307	0.399247	0.7547619	0.73483733
273	Head on steering wheel	30	0.364989	0.931597	0	0	0.327425	0	0
274	Head on steering wheel	30	0.426165	0.747273	0.481003	0.517293	0.433643	0.57248677	0.495673571
11	Look up	30	0.606044	0.786469	0.462766	0.780686	0.675956	0.62010582	0.47740979
226	Use mobile phone	30	0.580915	0.611169	0.908055	0.766381	0.434958	0.74444444	0.912735231
227	Use mobile phone	30	0.546469	0.498002	0.68769	0.737759	0.329871	0.78174603	0.700014119
228	Use mobile phone	30	0.521553	0.585938	0.805471	0.745613	0.385001	0.75820106	0.8143468

Test Volunteer number 15
Name: Cathy Turner OOP DATA

Frame number	Frame description	Face thresholding value degree C	Centroid position x co-ordinate pixel	y co-ordnate pixel	Area pixel	Major Axis Length pixel	Minor Axis Length pixel	Eccentricity pixel	Equivdiameter pixel
65	Look straight ahead	30	49.9773	75.1015	5153	122.4309	73.8288	0.7977	81
70	Look straight ahead	30	52.4786	75.0558	5201	126.252	72.9213	0.8163	81.3764
182	Look straight ahead	30	51.222	74.5195	5513	119.4436	86.3093	0.6913	83.7817
310	Lean right	30	44.4521	75.7474	5585	123.767	82.6186	0.7446	84.327
311	Lean right	30	44.6669	75.9737	5590	124.0641	82.5656	0.7464	84.3647
312	Lean right	30	44.4834	75.354	5559	124.2443	82.2617	0.7494	84.1305
24	Lean forward	30	55.3237	77.7275	5864	107.8127	93.5392	0.4972	86.4076
25	*Lean forward*	*30*	*53.4314*	*78.4435*	*5533*	*112.0291*	*95.0223*	*0.5297*	*83.9335*
154	Lean forward	30	44.0655	73.489	5798	118.5967	80.4877	0.7344	85.92
159	Head on steering wheel	30	39.1277	74.2787	5934	94.4106	82.7569	0.4813	86.9218
160	Head on steering wheel	30	37.8264	75.5059	6284	115.2627	85.7086	0.6686	89.4485
161	Head on steering wheel	30	35.6494	77.5501	5930	123.3465	80.607	0.7569	86.8925
258	Look straight ahead	30	48.464	74.8646	5560	116.5408	88.0341	0.6553	84.1381
300	Look straight ahead	30	48.6913	77.4033	5666	119.857	89.0951	0.6689	84.9363
353	Look straight ahead	30	46.7089	75.3233	5534	119.0712	86.7027	0.6854	83.9411
313	Lean right	30	44.1054	75.2924	5380	121.7688	81.5973	0.7423	82.7649
314	Lean right	30	43.3274	75.3911	5324	120.1831	81.9611	0.7314	82.333
318	Lean right	30	42.0558	77.1119	5933	129.6099	79.069	0.7924	86.9145
155	Lean forward	30	42.8355	73.138	5775	118.516	79.4311	0.7422	85.7494
156	Lean forward	30	47.792	71.6622	6009	119.6229	78.7838	0.7525	87.4694
163	Lean forward	30	40.0043	71.7176	6087	126.1842	80.8752	0.7676	88.0353
162	Head on steering wheel	30	35.9438	75.9943	5920	119.8118	82.6993	0.7236	86.8192
273	Head on steering wheel	30	42.8303	78.7496	4968	90.0524	80.9403	0.4383	79.5327
274	Head on steering wheel	30	44.0339	77.3473	5601	110.5152	83.5417	0.6547	84.4477
65	Look straight ahead	30	0.728255	0.48527	0.140578	0.818517	0.041061	0.95079365	0.147975958
70	Look straight ahead	30	0.85539	0.478822	0.177052	0.915113	0	1	0.185935578
182	Look straight ahead	30	0.79152	0.403152	0.414134	0.742999	0.605764	0.66931217	0.428508038
310	Lean right	30	0.447421	0.576403	0.468845	0.852293	0.438772	0.81031746	0.483501079
311	Lean right	30	0.458339	0.608333	0.472644	0.859804	0.436374	0.81507937	0.487303092
312	Lean right	30	0.449012	0.520896	0.449088	0.864359	0.422623	0.82301587	0.463684221
24	Lean forward	30	1	0.855786	0.680851	0.448974	0.932894	0.15582011	0.69332782
25	Lean forward	30	0.903819	0.956811	0.429331	0.555563	1	0.24179894	0.443816939
154	Lean forward	30	0.427771	0.257753	0.630699	0.72159	0.342356	0.78333333	0.644153775
159	Head on steering wheel	30	0.176794	0.369176	0.734043	0.110174	0.44503	0.11375661	0.745184453
160	Head on steering wheel	30	0.110652	0.542329	1	0.637308	0.578585	0.60925926	1
161	Head on steering wheel	30	0	0.830756	0.731003	0.841663	0.347753	0.84285714	0.742229573
258	Look straight ahead	30	0.651337	0.451844	0.449848	0.669618	0.683806	0.57407407	0.464450675
300	Look straight ahead	30	0.66289	0.810043	0.530395	0.75345	0.731813	0.61005291	0.544948466
353	Look straight ahead	30	0.562129	0.516565	0.430091	0.733585	0.623565	0.6537037	0.444583392
313	Lean right	30	0.429799	0.512205	0.31307	0.80178	0.392561	0.8042328	0.325964622
314	Lean right	30	0.390255	0.526131	0.270517	0.761694	0.409022	0.77539683	0.282407874
318	Lean right	30	0.325623	0.768928	0.733283	1	0.278164	0.93677249	0.744448254
155	*Lean forward*	*30*	*0.365253*	*0.208229*	*0.613222*	*0.71955*	*0.294548*	*0.80396825*	*0.62694891*
156	Lean forward	30	0.617181	0	0.791033	0.747532	0.265259	0.83121693	0.800409448
163	Lean forward	30	0.22135	0.007817	0.850304	0.913399	0.359889	0.87116402	0.857479981
162	Head on steering wheel	30	0.014964	0.61124	0.723404	0.752307	0.442423	0.7547619	0.73483733
273	Head on steering wheel	30	0.364989	1	0	0	0.362834	0	0
274	Head on steering wheel	30	0.426165	0.802142	0.481003	0.517293	0.480539	0.57248677	0.495673571

Driver Volunteer 16
Name: Volkan ALL DATA

Frame number	Frame description	Face thresholding value degree C	Centroid position x co-ordinate pixel	y co-ordnate pixel	Area pixel	Major Axis Length pixel	Minor Axis Length pixel	Eccentricity pixel	Equivdiameter pixel
93	Look straight ahead	30	54.498	48.2776	1488	75.0969	42.7014	0.8226	43.5268
137	Look straight ahead	30	55.1714	49.6626	1488	78.8233	41.8911	0.8471	43.5268
261	Look straight ahead	30	56.7031	51.1112	1502	78.5645	42.4071	0.8418	43.7311
274	Look right	30	43.5684	51.6059	1761	72.5396	43.5035	0.8002	47.3516
384	Look right	30	48.0509	52.088	1944	72.6395	43.3703	0.8022	49.7512
152	Look left	30	65.6344	52.4352	2013	68.1027	41.2649	0.7955	50.6264
388	Look left	30	63.129	51.285	2077	70.904	42.0917	0.8047	51.4249
300	Lean right	30	42.3402	51.4917	1802	71.5486	43.4033	0.795	47.8997
303	Lean right	30	38.8409	52.9306	1816	71.9417	43.258	0.799	48.0854
31	Lean left	30	99.7135	87.4803	1295	45.9876	37.5701	0.5767	40.606
33	Lean left	30	99.4294	89.5557	1148	46.2711	33.0263	0.7004	38.2319
551	Lean forward	30	50.9426	64.3277	1410	76.1836	39.9094	0.8518	42.3706
767	Head on steering wheel	30	52.6282	90.7991	1498	64.5136	33.9933	0.8499	43.6728
49	Look back	30	93.1588	61.0678	1077	42.7587	36.1471	0.5342	37.0308
55	Reach right	30	19.6045	56.1207	1947	58.5027	44.4535	0.6501	49.7895
56	Reach right	30	23.8027	54.7834	1911	55.5463	46.6568	0.5426	49.3271
449	Look straight ahead	30	58.7252	50.1453	1714	77.1399	44.9617	0.8126	46.7154
466	Look straight ahead	30	56.5967	50.3176	1738	78.3625	43.865	0.8287	47.0414
468	Look straight ahead	30	57.7868	50.0345	1651	78.2925	42.9549	0.8361	45.8489
390	Look right	30	49.9478	51.6462	2032	71.1591	43.226	0.7944	50.8647
385	Look right	30	47.5411	51.4897	1752	74.8471	44.2262	0.8068	47.2305
393	Look left	30	62.9047	53.9745	2192	70.3874	43.1519	0.79	52.8294
394	Look left	30	68.5656	53.4402	2049	71.7318	42.746	0.803	51.0771
301	Lean right	30	42.4684	51.574	1817	71.6548	43.3506	0.7962	48.0986
304	Lean right	30	39.0449	52.5468	1847	72.266	43.9395	0.7939	48.4941
32	Lean left	30	101.2003	88.164	1268	44.7067	37.9194	0.5297	40.1804
34	Lean left	30	97.4137	89.2556	1107	50.1652	30.2804	0.7973	37.543
560	Lean forward	30	51.3819	59.6485	1744	73.8455	46.3478	0.7785	47.1225
769	Head on steering wheel	30	49.4644	81.8285	1096	53.7274	27.1305	0.8631	37.356
50	Look back	30	113.3765	58.8704	409	29.5789	20.7341	0.7132	22.8201
57	Reach right	30	24.8591	54.2122	1852	56.3842	44.2036	0.6208	48.5597
58	Reach right	30	24.9632	54.0368	1765	55.7825	42.7634	0.6421	47.4054
93	Look straight ahead	30	0.37211	0	0.60516	0.924328	0.847416	0.8785243	0.69000943
137	Look straight ahead	30	0.379291	0.032572	0.60516	1	0.816157	0.9520096	0.69000943
261	Look straight ahead	30	0.395626	0.066639	0.613012	0.994745	0.836063	0.93611278	0.69681732
274	Look right	30	0.255555	0.078273	0.758273	0.872398	0.878358	0.81133773	0.817463253
384	Look right	30	0.303357	0.089611	0.860909	0.874426	0.873219	0.81733653	0.897425132
152	Look left	30	0.49087	0.097776	0.899607	0.782298	0.792001	0.79724055	0.926589424
388	Look left	30	0.464152	0.070727	0.935502	0.839184	0.823896	0.82483503	0.953197842
300	Lean right	30	0.242457	0.075588	0.781266	0.852274	0.874492	0.79574085	0.835727591
303	Lean right	30	0.20514	0.109427	0.789119	0.860256	0.868887	0.80773845	0.841915673
31	Lean left	30	0.854296	0.92195	0.496915	0.333209	0.649469	0.14097181	0.592679603
33	Lean left	30	0.851266	0.970758	0.41447	0.338966	0.474187	0.5119976	0.513567461
551	Lean forward	30	0.334195	0.377458	0.561413	0.946396	0.739711	0.96610678	0.651481374
767	Head on steering wheel	30	0.35217	1	0.610768	0.709415	0.51149	0.96040792	0.694874589
49	Look back	30	0.784395	0.300794	0.374649	0.267641	0.594575	0.0134973	0.473543202
55	Reach right	30	0	0.18445	0.862591	0.587352	0.915005	0.36112777	0.898701403
56	Reach right	30	0.04477	0.153	0.8424	0.527317	1	0.03869226	0.883292846
449	Look straight ahead	30	0.41719	0.043924	0.731913	0.965815	0.934609	0.84853029	0.796263158
466	Look straight ahead	30	0.394491	0.047976	0.745373	0.991049	0.892303	0.89682064	0.807126457
468	Look straight ahead	30	0.407182	0.041318	0.696579	0.989221	0.857195	0.9190162	0.767388776
390	Look right	30	0.323586	0.079221	0.910264	0.844364	0.867653	0.79394121	0.934530296
385	Look right	30	0.29792	0.075541	0.753225	0.919256	0.906237	0.83113377	0.813427837
393	Look left	30	0.46176	0.133977	1	0.828693	0.864794	0.78074385	1
394	Look left	30	0.522129	0.121412	0.919798	0.855994	0.849136	0.81973605	0.941608101
301	Lean right	30	0.243824	0.077523	0.78968	0.85443	0.872459	0.79934013	0.842355536
304	Lean right	30	0.207316	0.100401	0.806506	0.866842	0.895177	0.79244151	0.855534784
32	Lean left	30	0.870151	0.938029	0.481772	0.307198	0.662944	0	0.578497332
34	Lean left	30	0.82977	0.963701	0.391475	0.418043	0.36826	0.80263947	0.490611244
560	Lean forward	30	0.338879	0.267415	0.748738	0.898916	0.98808	0.74625075	0.809828953
769	Head on steering wheel	30	0.318431	0.789034	0.385306	0.490381	0.246749	1	0.484379842
50	Look back	30	1	0.249116	0	0	0	0.55038992	0
57	Reach right	30	0.056036	0.139567	0.80931	0.544332	0.905365	0.27324535	0.857720773
58	Reach right	30	0.057146	0.135442	0.760516	0.532113	0.849807	0.33713257	0.819256031

Driver Volunteer 16
Name: Volkan OOP DATA

Frame number	Frame description	Face thresholding value degree C	Centroid position x co-ordinate pixel	y co-ordnate pixel	Area pixel	Major Axis Length pixel	Minor Axis Length pixel	Eccentricity pixel	Equivdiameter pixel
93	Look straight ahead	30	54.498	48.2776	1488	75.0969	42.7014	0.8226	43.5268
137	Look straight ahead	30	55.1714	49.6626	1488	78.8233	41.8911	0.8471	43.5268
261	Look straight ahead	30	56.7031	51.1112	1502	78.5645	42.4071	0.8418	43.7311
300	Lean right	30	42.3402	51.4917	1802	71.5486	43.4033	0.795	47.8997
303	Lean right	30	38.8409	52.9306	1816	71.9417	43.258	0.799	48.0854
31	Lean left	30	99.7135	87.4803	1295	45.9876	37.5701	0.5767	40.606
33	Lean left	30	99.4294	89.5557	1148	46.2711	33.0263	0.7004	38.2319
551	Lean forward	30	50.9426	64.3277	1410	76.1636	39.9094	0.8518	42.3706
767	Head on steering wheel	30	52.6282	90.7991	1498	64.5136	33.9933	0.8499	43.6728
449	Look straight ahead	30	58.7252	50.1453	1714	77.1399	44.9617	0.8126	46.7154
466	Look straight ahead	30	56.5967	50.3176	1738	78.3825	43.865	0.8287	47.0414
468	Look straight ahead	30	57.7868	50.0345	1651	78.2925	42.9549	0.8361	45.8489
301	*Lean right*	30	42.4684	51.574	1817	71.6548	43.3506	0.7962	48.0986
304	Lean right	30	39.0449	52.5468	1847	72.266	43.9395	0.7939	48.4941
32	Lean left	30	101.2003	88.164	1268	44.7067	37.9194	0.5297	40.1804
34	Lean left	30	97.4137	89.2556	1107	50.1652	30.2804	0.7973	37.543
560	Lean forward	30	51.3819	59.6485	1744	73.8455	46.3478	0.7785	47.1225
769	Head on steering wheel	30	49.4644	81.8285	1096	53.7274	27.1305	0.8631	37.356
93	Look straight ahead	30	0.251078	0	0.521971	0.890775	0.810254	0.8765243	0.55402627
137	Look straight ahead	30	0.261877	0.032572	0.521971	1	0.768089	0.9520096	0.55402627
261	Look straight ahead	30	0.28644	0.066639	0.540613	0.992414	0.79494	0.93611278	0.572368716
300	Lean right	30	0.056115	0.075588	0.94008	0.786769	0.846779	0.79574085	0.946633627
303	Lean right	30	0	0.109427	0.958722	0.798292	0.839218	0.80773845	0.963306129
31	Lean left	30	0.976158	0.92195	0.26498	0.037545	0.54324	0.14097181	0.291791239
33	Lean left	30	0.971602	0.970758	0.069241	0.045855	0.306796	0.5119976	0.078639983
551	Lean forward	30	0.194064	0.377458	0.418109	0.922627	0.664969	0.96610678	0.450220415
767	Head on steering wheel	30	0.221094	1	0.535286	0.580565	0.357116	0.96040792	0.56713443
449	Look straight ahead	30	0.318866	0.043924	0.822903	0.950657	0.927872	0.84853029	0.840304899
466	Look straight ahead	30	0.284733	0.047976	0.85486	0.98708	0.870804	0.89682064	0.869573805
468	Look straight ahead	30	0.303818	0.041318	0.739015	0.984442	0.823446	0.9190162	0.762508866
301	Lean right	30	0.058171	0.077523	0.960053	0.789882	0.844036	0.79934013	0.964491251
304	Lean right	30	0.003271	0.100401	1	0.807797	0.874681	0.79244151	1
32	Lean left	30	1	0.938029	0.229028	0	0.561416	0	0.253580054
34	Lean left	30	0.939278	0.963701	0.014647	0.159995	0.16391	0.80263947	0.016789219
560	Lean forward	30	0.201108	0.267415	0.86285	0.854094	1	0.74625075	0.876855119
769	Head on steering wheel	30	0.170359	0.789034	0	0.264408	0	1	0

Driver Volunteer 17
Name: Yasar Ozkaya ALL DATA

Frame number	Frame description	Face threshold value degree C	Centroid position x co-ordinate pixel	y co-ordnate pixel	Area pixel	Major Axis Length pixel	Minor Axis Length pixel	Eccentricity pixel	Equivdiameter pixel
74	Look straight ahead	30	58.3491	77.2186	6513	123.479	99.2197	0.5953	91.0638
152	Look straight ahead	30	58.8739	74.0105	6592	120.4642	104.0271	0.5043	91.6144
226	Look right	30	51.211	73.9073	5987	118.8937	92.0718	0.6327	87.3091
390	Look right	30	48.7187	75.2797	6858	128.5856	90.0995	0.7135	93.4445
130	Look left	30	78.0253	70.5613	7824	129.8594	96.4917	0.6692	99.8089
301	Look left	30	55.9791	79.6175	6946	117.1212	99.8754	0.5223	94.0421
122	Lean forward	30	76.55	78.9008	6642	118.1874	92.8649	0.6186	91.9612
196	Lean forward	30	53.1579	75.2511	7309	120.3042	97.7073	0.5834	96.4682
199	Head on steering wheel	30	49.5091	75.2706	7783	125.4917	97.3808	0.6307	99.5471
292	Head on steering wheel	30	54.5425	84.0566	7349	119.7446	92.6412	0.6336	96.7318
35	Look back	30	73.615	81.1562	6704	125.2555	78.9909	0.7761	92.3894
47	Look back	30	80.4729	80.0394	6010	114.45	76.3998	0.7446	87.4767
252	Use mobile phone	30	58.1055	77.5346	6979	114.8909	101.1688	0.4739	94.2653
253	Use mobile phone	30	61.6752	77.3231	7026	117.6832	99.8938	0.5287	94.5821
11	Reach right	30	47.0877	74.1789	6751	109.1845	97.577	0.4487	92.7127
153	Look straight ahead	30	58.4729	73.9177	6672	122.3683	103.1762	0.5377	92.1686
168	Look straight ahead	30	58.2094	71.5149	6562	126.4172	100.0897	0.6109	91.4057
228	Look right	30	50.7854	74.1648	5861	118.0618	90.0375	0.6468	86.3855
391	Look right	30	49.5826	77.0452	6788	126.8604	90.329	0.7021	92.9664
132	Look left	30	79.5422	71.3152	7136	133.5541	91.5858	0.7278	95.3197
302	Look left	30	55.9176	78.5979	6538	114.556	99.3729	0.4975	91.2384
327	Lean forward	30	56.2885	79.2983	7630	127.5564	90.5536	0.7043	98.5638
425	Lean forward	30	58.6025	85.6238	6164	113.6943	98.669	0.4968	88.5903
293	Head on steering wheel	30	53.1036	81.7079	7642	120.6699	95.0847	0.6157	98.6413
322	Head on steering wheel	30	53.268	79.8116	7652	129.2987	91.0327	0.7102	98.7058
36	Look back	30	76.0501	84.4703	5371	132.494	72.1883	0.8385	82.6956
37	Look back	30	74.2031	83.4103	5298	132.8239	66.9598	0.8636	82.1317
252	Use mobile phone	30	58.1055	77.5346	6979	114.8909	101.1688	0.4739	94.2653
253	Use mobile phone	30	61.6752	77.3231	7026	117.6832	99.8938	0.5287	94.5821
12	Reach right	30	50.3882	76.4915	6731	112.8108	93.5684	0.5586	92.5752
74	Look straight ahead	30	0.337	0.442	0.481	0.587	0.870	0.353	0.505
152	Look straight ahead	30	0.353	0.229	0.512	0.463	1.000	0.134	0.536
226	Look right	30	0.124	0.222	0.273	0.398	0.677	0.443	0.293
390	Look right	30	0.049	0.313	0.618	0.796	0.624	0.638	0.640
130	Look left	30	0.927	0.000	1.000	0.848	0.797	0.531	1.000
301	Look left	30	0.266	0.601	0.652	0.326	0.888	0.177	0.674
122	Lean forward	30	0.882	0.554	0.532	0.369	0.699	0.409	0.556
196	Lean forward	30	0.182	0.311	0.796	0.456	0.830	0.325	0.811
199	Head on steering wheel	30	0.073	0.313	0.984	0.669	0.821	0.439	0.985
292	Head on steering wheel	30	0.223	0.896	0.812	0.433	0.693	0.446	0.826
35	Look back	30	0.795	0.703	0.557	0.659	0.325	0.789	0.580
47	Look back	30	1.000	0.629	0.282	0.216	0.255	0.713	0.302
252	Use mobile phone	30	0.330	0.463	0.665	0.234	0.923	0.061	0.686
253	Use mobile phone	30	0.437	0.449	0.684	0.349	0.888	0.193	0.704
11	Reach right	30	0.000	0.240	0.575	0.000	0.826	0.000	0.599
153	Look straight ahead	30	0.341	0.223	0.544	0.541	0.977	0.215	0.568
168	Look straight ahead	30	0.333	0.063	0.500	0.707	0.894	0.391	0.525
228	Look right	30	0.111	0.239	0.223	0.364	0.623	0.477	0.241
391	Look right	30	0.075	0.430	0.590	0.725	0.630	0.611	0.613
132	Look left	30	0.972	0.050	0.728	1.000	0.664	0.673	0.746
302	Look left	30	0.264	0.534	0.491	0.220	0.874	0.118	0.515
327	Lean forward	30	0.276	0.580	0.923	0.754	0.637	0.616	0.930
425	Lean forward	30	0.345	1.000	0.343	0.185	0.855	0.116	0.365
293	Head on steering wheel	30	0.180	0.740	0.928	0.471	0.759	0.403	0.934
322	Head on steering wheel	30	0.185	0.614	0.932	0.825	0.649	0.630	0.938
36	Look back	30	0.868	0.923	0.029	0.956	0.141	0.940	0.032
37	Look back	30	0.812	0.853	0.000	0.970	0.000	1.000	0.000
252	Use mobile phone	30	0.330	0.463	0.665	0.234	0.923	0.061	0.686
253	Use mobile phone	30	0.437	0.449	0.684	0.349	0.888	0.193	0.704
12	Reach right	30	0.099	0.394	0.567	0.149	0.718	0.265	0.591

Driver Volunteer 17
Name: Yasar Ozkaya OOP DATA

Frame number	Frame description	Face threshold value degree C	Centroid position x co-ordinate pixel	y co-ordnate pixel	Area pixel	Major Axis Length pixel	Minor Axis Length pixel	Eccentricity pixel	Equivdiameter pixel
74	*Look straight ahead*	30	58.3491	77.2186	6513	123.479	99.2197	0.5953	91.0638
152	Look straight ahead	30	58.8739	74.0105	6592	120.4642	104.0271	0.5043	91.6144
122	Lean forward	30	76.55	78.9008	6642	118.1874	92.8649	0.6186	91.9612
196	Lean forward	30	53.1579	*75.2511*	7309	120.3042	97.7073	*0.5834*	*96.4682*
199	Head on steering wheel	30	49.5091	75.2706	7783	125.4917	97.3808	0.6307	99.5471
292	Head on steering wheel	30	54.5425	84.0566	7349	119.7446	92.6412	0.6336	96.7318
153	Look straight ahead	30	58.4729	73.9177	6672	122.3683	103.1762	0.5377	92.1686
168	Look straight ahead	30	58.2094	71.5149	6562	126.4172	100.0897	0.6109	91.4057
327	Lean forward	30	56.2885	*79.2983*	*7630*	*127.5564*	*90.5536*	*0.7043*	*98.5638*
425	Lean forward	30	58.6025	85.6238	6164	113.6943	98.669	0.4968	88.5903
293	Head on steering wheel	30	53.1036	81.7079	7642	120.6699	95.0847	0.6157	98.6413
322	Head on steering wheel	30	53.268	79.8116	7652	129.2987	91.0327	0.7102	98.7058
74	Look straight ahead	30	0.327	0.404	0.216	0.627	0.643	0.462	0.226
152	Look straight ahead	30	0.346	*0.177*	*0.264*	*0.434*	*1.000*	*0.035*	*0.276*
122	Lean forward	30	1.000	0.523	0.295	0.288	0.172	0.571	0.308
196	Lean forward	30	0.135	0.265	0.707	0.424	0.531	0.406	0.719
199	Head on steering wheel	30	0.000	0.266	1.000	0.756	0.507	0.627	1.000
292	Head on steering wheel	30	0.186	0.889	0.732	0.388	0.155	0.641	0.743
153	Look straight ahead	30	*0.331*	*0.170*	*0.314*	*0.556*	*0.937*	*0.192*	0.327
168	Look straight ahead	30	0.322	0.000	0.246	0.815	0.708	0.535	0.257
327	Lean forward	30	0.251	0.552	0.905	0.888	0.000	0.972	0.910
425	Lean forward	30	0.336	1.000	0.000	0.000	0.602	0.000	0.000
293	Head on steering wheel	30	0.133	0.722	0.913	0.447	0.336	0.557	0.917
322	*Head on steering wheel*	30	*0.139*	*0.588*	0.919	1.000	0.036	1.000	0.923

Driver Volunteer 18
Name: Berna ALL DATA

Frame number	Frame description	Face threshold value degree C	Centroid position x co-ordinate pixel	y co-ordnate pixel	Area pixel	Major Axis Length pixel	Minor Axis Length pixel	Eccentricity pixel	Equivdiameter pixel
86	Look straight ahead	30	57.851	69.9149	2127	70.9866	39.3443	0.8324	52.0402
144	Look straight ahead	30	61.6116	70.2482	2196	73.1908	39.848	0.8388	52.8775
62	Look right	30	50.5605	71.8829	2041	69.5114	38.2032	0.8354	50.9773
140	Look right	30	52.002	71.1564	2021	72.1132	36.3832	0.8634	50.7269
401	Look left	30	73.8654	72.396	2177	71.5818	39.4974	0.834	52.6483
63	Look left	30	60.5497	73.9665	1790	69.1582	33.6104	0.874	47.7399
402	Lean right	30	27.9805	75.288	2104	69.7902	39.5997	0.8234	51.7581
403	Lean right	30	26.2417	75.7093	2081	69.6494	39.2171	0.8264	51.4744
27	Lean left	30	78.7818	86.9542	1265	58.9544	30.1623	0.8592	40.1329
28	Lean left	30	83.9469	87.951	1244	59.9792	29.435	0.8713	39.7984
39	Lean forward	30	64.6495	78.6975	1689	54.0668	41.4342	0.6424	46.3735
40	Lean forward	30	62.2507	79.5333	1699	55.393	41.3103	0.6662	46.5106
20	Head on steering wheel	30	55.8794	91.5317	1277	51.1278	32.3242	0.7748	40.3228
127	Look up	30	63.4297	69.2032	2141	76.2445	37.8104	0.8684	52.2112
128	Look up	30	62.8742	68.8263	2067	76.5603	36.7488	0.8773	51.3009
68	Reach right	30	48.7834	74.4748	1967	70.5502	35.9562	0.8604	50.0446
69	Reach right	30	48.6577	74.7754	1937	70.2708	35.586	0.8623	49.6615
145	Look straight ahead	30	62.0776	70.4011	2164	72.9608	39.4822	0.8409	52.4909
147	Look straight ahead	30	62.7552	71.4936	2030	70.0964	38.4342	0.8363	50.8397
139	Look right	30	49.5842	73.6318	1972	70.6844	35.8415	0.8619	50.1082
387	Look right	30	51.5572	71.318	2107	70.6099	39.0101	0.8335	51.7949
162	Look left	30	66.4286	72.4582	1997	71.3704	36.281	0.8612	50.4248
386	Look left	30	65.4488	73.2981	2070	72.7486	36.8314	0.8624	51.3382
404	Lean right	30	27.7891	75.6842	2172	71.2793	39.5245	0.8322	52.5878
405	Lean right	30	25.6804	76.8581	2043	68.5615	38.7849	0.8246	51.0022
29	Lean left	30	81.9108	89.1502	1132	56.9497	28.4869	0.8659	37.9646
30	Lean left	30	77.7274	88.3575	1119	53.8252	28.7127	0.8458	37.7459
41	Lean forward	30	54.8088	79.5211	1710	56.6826	41.1286	0.6881	46.6609
42	Lean forward	30	60.6773	77.1304	1856	60.7688	42.3584	0.717	48.6121
720	Head on steering wheel	30	50.1853	93.1098	1020	47.1194	28.2281	0.8007	36.0375
129	Look up	30	62.428	68.899	2138	76.8475	37.4999	0.8729	52.1746
130	Look up	30	62.4191	69.0193	2121	76.2545	37.4727	0.8709	51.9667
70	Reach right	30	48.8374	74.7106	1949	70.378	35.7527	0.8614	49.8151
71	Reach right	30	48.7947	75.3341	1856	68.698	34.8618	0.8617	48.6121
86	Look straight ahead	30	0.552129	0.044829	0.941327	0.80285	0.786692	0.808854832	0.950279097
144	Look straight ahead	30	0.61667	0.058554	1	0.876995	0.822339	0.836100468	1
62	Look right	30	0.427005	0.125871	0.888197	0.753227	0.705937	0.821626224	0.88716152
140	Look right	30	0.451745	0.095954	0.85119	0.840747	0.577136	0.940825883	0.872292162
401	Look left	30	0.826976	0.147001	0.983844	0.822871	0.797527	0.815666241	0.986389549
63	Look left	30	0.598445	0.211675	0.654762	0.741346	0.380905	0.985951469	0.694916865
402	Lean right	30	0.039476	0.266094	0.921769	0.762605	0.804767	0.770540656	0.933527316
403	Lean right	30	0.009633	0.283443	0.902211	0.757869	0.77769	0.783312048	0.916680523
27	Lean left	30	0.911354	0.746511	0.208333	0.398108	0.136883	0.922945934	0.243194774
28	Lean left	30	1	0.787559	0.190476	0.432581	0.085412	0.974457216	0.223331354
39	Lean forward	30	0.668808	0.406498	0.568878	0.233698	0.934594	0	0.613776722
40	Lean forward	30	0.627639	0.440917	0.577381	0.278309	0.925826	0.101319711	0.621918052
20	Head on steering wheel	30	0.518291	0.935013	0.218537	0.134835	0.289881	0.563644104	0.254471496
127	Look up	30	0.647873	0.015521	0.953231	0.979716	0.678138	0.962111537	0.960433492
128	Look up	30	0.638339	0	0.890306	0.990339	0.603009	1	0.906377672
68	Reach right	30	0.396506	0.232607	0.805272	0.78817	0.546917	0.928054491	0.831775534
69	Reach right	30	0.394346	0.244985	0.779762	0.778772	0.520718	0.93614304	0.809026128
145	Look straight ahead	30	0.624668	0.064851	0.972789	0.869258	0.796452	0.845040443	0.977042755
147	Look straight ahead	30	0.636297	0.10984	0.858844	0.772905	0.722285	0.825457642	0.878990499
139	*Look right*	30	*0.410249*	*0.197892*	*0.809524*	*0.792684*	*0.5388*	*0.934440187*	*0.835552257*
387	Look right	30	0.444111	0.102609	0.92432	0.790178	0.763041	0.813537676	0.935712589
162	Look left	30	0.699342	0.149562	0.830782	0.81576	0.569903	0.931460196	0.854352732
386	Look left	30	0.682526	0.18415	0.892857	0.86212	0.608855	0.936568753	0.908592637
404	Lean right	30	0.036191	0.28241	0.979592	0.812696	0.799445	0.808003406	0.982796912
405	Lean right	30	0	0.330751	0.869898	0.721274	0.747104	0.775649212	0.888640143
29	Lean left	30	0.965055	0.836943	0.095238	0.330674	0.018315	0.95146871	0.114435867
30	Lean left	30	0.893258	0.804299	0.084184	0.225571	0.034295	0.865900383	0.101448931
41	Lean forward	30	0.499917	0.440414	0.586735	0.321689	0.912967	0.194550873	0.63084323
42	Lean forward	30	0.600635	0.341965	0.710884	0.459141	1	0.31758195	0.746710214
720	Head on steering wheel	30	0.420566	1	0	0	0	0.673903789	0
129	Look up	30	0.630681	0.002994	0.95068	1	0.656164	0.981268625	0.958260095
130	Look up	30	0.630529	0.007948	0.936224	0.980053	0.654239	0.972754364	0.945914489
70	Reach right	30	0.397432	0.242317	0.789966	0.782378	0.532515	0.932311622	0.818147268
71	Reach right	30	0.3967	0.267993	0.710884	0.725865	0.469466	0.933588761	0.746710214

Driver Volunteer 18
Name: Berna OOP DATA

Frame number	Frame description	Face threshold value degree C	Centroid position x co-ordinate pixel	y co-ordnate pixel	Area pixel	Major Axis Length pixel	Minor Axis Length pixel	Eccentricity pixel	Equivdiameter pixel
86	Look straight ahead	30	57.851	69.9149	2127	70.9866	39.3443	0.8324	52.0402
144	Look straight ahead	30	61.6116	70.2482	2196	73.1908	39.848	0.8388	52.8775
402	Lean right	30	27.9805	75.288	2104	69.7902	39.5997	0.8234	51.7581
403	Lean right	30	26.2417	75.7093	2081	69.6494	39.2171	0.8264	51.4744
27	Lean left	30	78.7818	86.9542	1265	58.9544	30.1623	0.8592	40.1329
28	Lean left	30	63.9469	87.951	1244	59.9792	29.435	0.8713	39.7984
39	Lean forward	30	64.6495	78.6975	1689	54.0668	41.4342	0.6424	46.3735
40	Lean forward	30	62.2507	79.5333	1699	55.393	41.3103	0.6662	46.5106
20	Head on steering wheel	30	55.8794	91.5317	1277	51.1278	32.3242	0.7748	40.3228
145	Look straight ahead	30	62.0776	70.4011	2164	72.9608	39.4822	0.8409	52.4909
147	Look straight ahead	30	62.7552	71.4936	2030	70.0964	38.4342	0.8363	50.8397
404	Lean right	30	27.7891	75.6842	2172	71.2793	39.5245	0.8322	52.5878
405	Lean right	30	25.6804	76.8581	2043	68.5615	38.7849	0.8246	51.0022
29	Lean left	30	81.9108	89.1502	1132	56.9497	28.4869	0.8659	37.9646
30	Lean left	30	77.7274	88.3575	1119	53.8252	28.7127	0.8458	37.7459
41	Lean forward	30	54.8088	79.5211	1710	56.6826	41.1286	0.6881	46.6609
42	Lean forward	30	60.6773	77.1304	1856	60.7688	42.3584	0.717	48.6121
720	Head on steering wheel	30	50.1853	93.1098	1020	47.1194	28.2281	0.8007	36.0375
86	Look straight ahead	30	0.552129	0	0.941327	0.915455	0.786692	0.830056793	0.950279097
144	Look straight ahead	30	0.61667	0.01437	1	1	0.822339	0.858016601	1
402	Lean right	30	0.039476	0.23165	0.921769	0.869566	0.804767	0.790738314	0.933527316
403	Lean right	30	0.009633	0.249814	0.902211	0.864165	0.77769	0.803844474	0.916680523
27	Lean left	30	0.911354	0.734614	0.208333	0.453946	0.136683	0.947138488	0.243194774
28	Lean left	30	1	0.777589	0.190476	0.493253	0.085412	1	0.223331354
39	Lean forward	30	0.668808	0.378644	0.568878	0.266476	0.934594	0	0.613776722
40	Lean forward	30	0.627639	0.414677	0.577381	0.317344	0.925826	0.103975535	0.621918052
20	Head on steering wheel	30	0.518291	0.931963	0.218537	0.153747	0.289881	0.578418523	0.254471496
145	Look straight ahead	30	0.624668	0.020962	0.972789	0.991178	0.796452	0.867190913	0.977042755
147	Look straight ahead	30	0.636297	0.068062	0.858844	0.881311	0.722285	0.847094801	0.878990499
404	Lean right	30	0.036191	0.248731	0.979592	0.926682	0.799445	0.829183049	0.982796912
405	Lean right	30	0	0.299342	0.869898	0.822438	0.747104	0.795980778	0.888640143
29	Lean left	30	0.965055	0.82929	0.095238	0.377053	0.018315	0.976408912	0.114435867
30	Lean left	30	0.893258	0.795114	0.084184	0.257209	0.034295	0.888597641	0.101448931
41	Lean forward	30	0.499917	0.414151	0.566735	0.366808	0.912967	0.199650502	0.63084323
42	Lean forward	30	0.600635	0.311081	0.710884	0.523539	1	0.325906509	0.746710214
720	Head on steering wheel	30	0.420566	1	0	0	0	0.69156837	0

Driver Volunteer 19
Name: Leo ALL DATA

Frame number	Frame description	Face threshold value degree C	Centroid position x co-ordinate pixel	y co-ordnate pixel	Area pixel	Major Axis Length pixel	Minor Axis Length pixel	Eccentricity pixel	Equivdiameter pixel
74	Look straight ahead	30	54.1655	44.8048	3571	100.7068	47.814	0.8801	67.4295
75	Look straight ahead	30	54.3614	45.6542	3586	102.0448	47.512	0.885	67.571
126	Look straight ahead	30	53.8446	44.8535	3461	98.8415	47.2742	0.8782	66.3828
97	Look right	30	53.7818	43.5162	3396	97.7705	46.7708	0.8782	65.7565
522	Look right	30	53.8992	43.3012	3343	97.8038	46.0177	0.8824	65.2414
637	Look left	30	59.8924	40.743	3160	91.8936	45.7916	0.867	63.4306
698	Look left	30	56.8995	44.9732	3352	95.6524	48.9764	0.859	65.3292
697	Look left	30	56.8745	45.4349	3410	96.9594	49.7422	0.8584	65.8919
107	Lean right	30	40.6568	47.6004	3599	102.2337	47.1823	0.8871	67.6933
108	Lean right	30	43.3625	45.3052	3476	99.2222	47.0278	0.8805	66.5265
109	Lean right	30	43.2306	45.9697	3665	98.525	49.4115	0.8652	68.3112
285	Lean left	30	69.7533	44.3171	3393	96.7241	47.4319	0.8716	65.7275
286	Lean left	30	73.9715	44.5226	3542	98.1176	48.7383	0.8679	67.1552
287	Lean left	30	79.5218	45.7448	3530	95.4157	49.8202	0.8529	67.0413
394	Lean forward	30	47.0794	60.5017	4335	89.1385	64.1578	0.6942	74.2933
12	Reach right	30	53.0659	71.687	2048	66.2362	40.5716	0.7904	51.0646
13	Reach right	30	55.9272	75.4005	2170	72.281	40.9163	0.8244	52.5636
14	Reach right	30	53.0828	71.5617	2391	73.5041	44.1493	0.7995	55.1753
28	Look down	30	73.5666	71.3586	1659	54.8917	39.1861	0.7003	45.9598
29	Look down	30	72.7861	74.9153	1571	58.0531	35.5738	0.7903	44.7243
30	Look down	30	73.9834	75.796	1745	66.9931	37.2647	0.831	47.136
127	Look straight ahead	30	54.2326	44.6679	3397	98.6047	46.3332	0.8827	65.7662
422	Look straight ahead	30	49.1211	42.2809	3353	96.2671	46.9585	0.873	65.3389
424	*Look straight ahead*	*30*	*48.1505*	*42.8787*	*3455*	*97.1725*	*47.7834*	*0.8707*	*66.3253*
628	Look right	30	53.7422	42.4426	3378	97.9236	47.5728	0.8741	65.582
629	Look right	30	53.0918	42.2984	3422	96.7059	48.624	0.8644	66.0078
696	Look left	30	57.2256	45.479	3436	96.4843	50.1169	0.8545	66.1427
695	Look left	30	57.4698	46.1381	3374	95.6243	49.7155	0.8542	65.5432
694	Look left	30	55.99	44.3495	3388	96.3539	49.297	0.8592	65.679
321	Lean right	30	44.4023	45.4701	3463	96.2363	48.4275	0.8642	66.402
338	Lean right	30	45.9278	43.5669	3489	97.0609	48.1042	0.8685	66.6508
339	Lean right	30	46.6681	43.9997	3603	99.2761	49.587	0.8663	67.731
288	Lean left	30	78.6243	45.344	3593	95.1352	50.2172	0.8493	67.6369
289	Lean left	30	78.7254	45.7034	3675	97.7849	50.2019	0.8582	68.4044
290	Lean left	30	74.99	46.3358	3586	97.9651	48.7048	0.8677	67.571
395	Lean forward	30	47.7939	48.6331	4036	95.5129	56.3902	0.8071	71.6854
15	Reach right	30	52.8416	69.4804	2121	67.487	41.2186	0.7918	51.9667
16	Reach right	30	57.5746	64.2442	2400	66.6499	48.0222	0.6934	55.2791
17	Reach right	30	57.8701	60.3742	2595	68.6783	52.8368	0.6388	57.4809
31	Look down	30	71.3281	76.6942	1393	58.1661	31.1411	0.8446	42.1144
32	Look down	30	67.1506	78.7817	1182	53.3546	29.7638	0.8299	38.7939
33	Look down	30	67.4932	78.1281	1249	53.3177	31.2071	0.8108	39.8783
74	Look straight ahead	30	0.34758	0.106781	0.757691	0.968785	0.524807	0.971808296	0.806650253
75	Look straight ahead	30	0.362621	0.129111	0.762448	0.996138	0.516026	0.991542489	0.810636236
126	Look straight ahead	30	0.339323	0.108061	0.722804	0.930653	0.509112	0.964156263	0.777165248
97	Look right	30	0.337707	0.072905	0.702188	0.908758	0.494476	0.964156263	0.759522696
522	Look right	30	0.340728	0.067253	0.685379	0.909439	0.47258	0.981071265	0.745012592
637	Look left	30	0.494934	0	0.627339	0.788615	0.466006	0.919049537	0.694003279
698	Look left	30	0.417926	0.111208	0.688233	0.865457	0.558603	0.886830447	0.747465873
697	Look left	30	0.417283	0.123345	0.706629	0.892176	0.580869	0.884414015	0.763336845
107	Lean right	30	0	0.180274	0.766572	1	0.50644	1	0.814081365
108	Lean right	30	0.069618	0.119936	0.727561	0.938435	0.501948	0.973419251	0.781213204
109	Lean right	30	0.066224	0.137405	0.787604	0.924182	0.571254	0.911800242	0.831487293
285	Lean left	30	0.748656	0.09396	0.701237	0.887366	0.513697	0.937172775	0.758705781
286	Lean left	30	0.85719	0.099362	0.748493	0.915854	0.551681	0.922874184	0.798923362
287	Lean left	30	1	0.131492	0.744688	0.860618	0.583137	0.862263391	0.795714657
394	Lean forward	30	0.165254	0.519437	1	0.732292	1	0.223117197	1
12	Reach right	30	0.319287	0.813487	0.274659	0.264096	0.314235	0.610551752	0.345659363
13	Reach right	30	0.392909	0.911112	0.313352	0.387671	0.324267	0.747482884	0.387885429
14	Reach right	30	0.319722	0.810193	0.383444	0.412675	0.418256	0.647200967	0.461455687
28	Look down	30	0.846772	0.804854	0.151284	0.032178	0.273952	0.247684253	0.20185975
29	Look down	30	0.82669	0.898356	0.123375	0.096807	0.168925	0.610149013	0.167056345
30	Look down	30	0.857496	0.921509	0.17856	0.279569	0.218087	0.774063633	0.234992704
127	Look straight ahead	30	0.349307	0.103182	0.702506	0.925812	0.481753	0.982279501	0.75979594
422	Look straight ahead	30	0.217787	0.04043	0.688551	0.878024	0.499933	0.943213854	0.747759117
424	Look straight ahead	30	0.192814	0.056145	0.720901	0.896533	0.523917	0.933950866	0.775545502
628	Look right	30	0.336689	0.044681	0.69648	0.911888	0.517794	0.947643979	0.75460712
629	Look right	30	0.319954	0.04089	0.710435	0.886994	0.548357	0.908578333	0.766601689
696	Look left	30	0.426317	0.124505	0.714875	0.882464	0.591763	0.868707209	0.770401753
695	*Look left*	*30*	*0.4328*	*0.141832*	*0.695211*	*0.864883*	*0.580092*	*0.867498993*	*0.753514144*
694	Look left	30	0.394525	0.094811	0.699651	0.879798	0.567925	0.887635924	0.757339561
321	Lean right	30	0.096372	0.124271	0.723438	0.877394	0.542644	0.907772855	0.777706102
338	Lean right	30	0.135623	0.074238	0.731684	0.894251	0.533244	0.925090616	0.784714671
339	Lean right	30	0.154671	0.085615	0.76784	0.939537	0.576356	0.916230366	0.815143355
288	Lean left	30	0.976907	0.120956	0.764669	0.854884	0.594679	0.847764801	0.812492606
289	Lean left	30	0.928048	0.130404	0.790676	0.909052	0.594234	0.883608538	0.834112689
290	Lean left	30	0.883396	0.147029	0.762448	0.912736	0.550707	0.921868707	0.810636236
395	Lean forward	30	0.183636	0.207423	0.90517	0.862605	0.774158	0.677609102	0.926536787
15	Reach right	30	0.313516	0.755478	0.297812	0.289666	0.333046	0.616190093	0.37107106
16	Reach right	30	0.435297	0.617823	0.386299	0.272553	0.53086	0.219895288	0.46437968
17	Reach right	30	0.4429	0.516085	0.448145	0.31402	0.670844	0	0.526403263
31	Look down	30	0.789175	0.945122	0.06692	0.099117	0.040045	0.828836085	0.093536792
32	Look down	30	0.681688	1	0	0.000754	0	0.769633508	0
33	Look down	30	0.690503	0.982817	0.02125	0	0.041964	0.692710431	0.030546995

Driver Volunteer 19
Name: Leo

OOP DATA

Frame number	Frame description	Face threshold value degree C	Centroid position x co-ordinate pixel	y co-ordnate pixel	Area pixel	Major Axis Length pixel	Minor Axis Length pixel	Eccentricity pixel	Equivdiameter pixel
74	Look straight ahead	30	54.1655	44.8048	3571	100.7068	47.814	0.8801	67.4295
75	Look straight ahead	30	54.3614	45.6542	3586	102.0448	47.512	0.885	67.571
126	Look straight ahead	30	53.8446	44.8535	3461	98.8415	47.2742	0.8782	66.3828
107	Lean right	30	40.6568	47.6004	3599	102.2337	47.1823	0.8871	67.6933
108	Lean right	30	43.3625	45.3052	3476	99.2222	47.0278	0.8805	66.5265
109	Lean right	30	43.2306	45.9697	3665	98.525	49.4115	0.8652	68.3112
285	Lean left	30	69.7533	44.3171	3393	96.7241	47.4319	0.8715	65.7275
286	Lean left	30	73.9715	44.5226	3542	98.1176	48.7383	0.8679	67.1552
287	Lean left	30	79.5218	45.7448	3530	95.4157	49.8202	0.8529	67.0413
394	Lean forward	30	47.0794	60.5017	4335	89.1385	64.1578	0.6942	74.2933
127	Look straight ahead	30	54.2326	44.6679	3397	98.6047	46.3332	0.8827	65.7662
422	Look straight ahead	30	49.1211	42.2809	3353	96.2671	46.9585	0.873	65.3389
424	Look straight ahead	30	48.1505	42.8787	3455	97.1725	47.7834	0.8707	66.3253
321	Lean right	30	44.4023	45.4701	3463	96.2363	48.4275	0.8642	66.402
338	Lean right	30	45.9278	43.5669	3489	97.0609	48.1042	0.8685	66.6508
339	Lean right	30	46.6681	43.9997	3603	99.2761	49.587	0.8663	67.731
288	Lean left	30	78.6243	45.344	3593	95.1352	50.2172	0.8493	67.6369
289	Lean left	30	76.7254	45.7034	3675	97.7849	50.2019	0.8582	68.4044
290	Lean left	30	74.99	46.3358	3586	97.9651	48.7048	0.8677	67.571
395	Lean forward	30	47.7939	48.6331	4036	95.5129	56.3902	0.8071	71.6854
74	Look straight ahead	30	0.34758	0.138518	0.221996	0.8834	0.083076	0.963711768	0.233471813
75	Look straight ahead	30	0.352621	0.185135	0.237271	0.985575	0.066133	0.98911353	0.2492741
126	Look straight ahead	30	0.339323	0.14119	0.10998	0.740959	0.052792	0.953862105	0.116579559
107	Lean right	30	0	0.291947	0.250509	1	0.047636	1	0.26293219
108	Lean right	30	0.069618	0.165981	0.125255	0.77003	0.038969	0.965785381	0.132627535
109	Lean right	30	0.066224	0.20245	0.317719	0.716789	0.1727	0.886469673	0.331937372
285	Lean left	30	0.748656	0.111751	0.040733	0.579266	0.06164	0.919129082	0.043397659
286	Lean left	30	0.85719	0.12303	0.192464	0.685679	0.134931	0.900466563	0.202838828
287	Lean left	30	1	0.190107	0.180244	0.479351	0.195629	0.822706065	0.190118824
394	Lean forward	30	0.165254	1	1	0	1	0	1
127	Look straight ahead	30	0.349307	0.131004	0.044807	0.722876	0	0.977190254	0.047719557
422	Look straight ahead	30	0.217787	0	0	0.544367	0.035081	0.926905132	0
424	Look straight ahead	30	0.192814	0.032809	0.10387	0.613507	0.081359	0.914981856	0.110158135
321	Lean right	30	0.096372	0.175031	0.112016	0.542015	0.117495	0.88128564	0.118723756
338	Lean right	30	0.135623	0.070579	0.138493	0.604985	0.099357	0.903576983	0.146508979
339	Lean right	30	0.154671	0.094332	0.254582	0.774146	0.182545	0.89217211	0.26714241
288	Lean left	30	0.976907	0.16811	0.244399	0.457931	0.217901	0.804043546	0.25663361
289	Lean left	30	0.928048	0.187835	0.327902	0.660272	0.217043	0.850181441	0.342345662
290	Lean left	30	0.883396	0.222542	0.237271	0.674033	0.133052	0.899429756	0.2492741
395	Lean forward	30	0.183638	0.348624	0.695519	0.486774	0.56422	0.585277346	0.708757706

Driver Volunteer 20
Name: Nukman ALL DATA

Frame number	Frame description	Face threshold value degree C	Centroid position x co-ordinate pixel	y co-ordnate pixel	Area pixel	Major Axis Length pixel	Minor Axis Length pixel	Eccentricity pixel	Equivdiameter pixel
107	Look straight ahead	30	54.4515	54.6764	1876	67.4779	42.198	0.7803	48.8733
109	Look straight ahead	30	53.172	53.9058	1953	66.837	43.1101	0.7642	49.8662
173	Look straight ahead	30	54.6147	54.4694	1975	68.2064	44.1988	0.7616	50.1463
182	Look right	30	49.1566	55.0817	2094	66.2943	45.1308	0.7325	51.6349
193	Look right	30	51.7181	55.8667	2160	67.9711	45.7755	0.7392	89.7027
691	Look right	30	51.3996	53.5955	2062	64.5097	42.8784	0.7471	51.2389
121	Look left	30	52.8679	54.2607	2029	64.8686	45.5231	0.7124	50.8272
128	Look left	30	52.8732	54.2208	2097	65.1486	45.7612	0.7118	51.6719
125	Look left	30	53.0059	54.2175	2041	64.7551	45.7613	0.7072	50.9773
330	Lean right	30	20.7813	56.1486	2099	73.0202	49.5486	0.7345	51.6965
331	Lean right	30	19.9696	56.4326	2136	68.3829	46.8361	0.7286	52.1502
332	Lean right	30	18.4881	58.227	2018	68.5453	43.944	0.7675	50.6892
523	Lean forward	30	96.024	62.2464	3202	96.5843	57.4746	0.8037	63.8507
702	Lean forward	30	67.8474	50.9568	3539	94.5547	55.8471	0.8069	67.1267
37	Look up	30	51.9601	54.5661	2028	65.2378	45.2587	0.7202	50.8147
38	Look up	30	50.904	54.5615	1895	64.2004	44.6477	0.7186	49.1201
39	Look up	30	50.9721	54.9594	2042	65.3649	45.7971	0.7135	50.9898
96	Look back	30	75.5097	64.9214	2417	65.2289	48.0045	0.677	55.4745
97	Look back	30	79.2982	64.8316	2435	65.7914	47.7685	0.6876	55.6807
98	Look back	30	82.5805	65.108	2286	63.3662	46.6648	0.6765	53.9502
66	Reach right	30	45.6469	64.8139	2628	76.9489	48.4148	0.7773	57.8453
67	Reach right	30	45.2705	64.9218	2673	77.1601	48.7576	0.775	58.3384
68	Reach right	30	45.0283	64.7748	2717	76.7848	49.8061	0.7611	58.8166
175	Look straight ahead	30	54.632	54.3646	2027	67.8255	44.3437	0.7567	50.8021
232	Look straight ahead	30	54.1837	55.2085	1938	66.4403	66.4403	0.7622	88.9556
423	Look straight ahead	30	55.8049	53.6706	1861	66.969	40.497	0.7964	48.6775
693	Look right	30	51.4728	53.1174	1984	62.5065	42.6806	0.7306	50.2604
694	Look right	30	50.9906	53.6718	2127	63.7654	43.6828	0.7255	52.0402
696	Look right	30	51.6975	53.4734	2106	53.4734	43.2843	0.7371	51.7626
126	Look left	30	52.9605	53.8611	2002	64.6978	44.6475	0.7237	50.4679
198	Look left	30	55.058	58.4224	2450	70.3719	49.1148	0.7162	75.2478
199	Look left	30	53.3328	57.4874	2302	67.7036	48.043	0.7046	54.1387
333	Lean right	30	19.6682	58.721	2179	68.8273	45.926	0.7448	52.6725
334	Lean right	30	19.3761	59.1307	2188	68.913	45.5573	0.7714	52.7811
335	Lean right	30	19.236	59.6243	2220	69.7368	44.9339	0.7647	53.1657
703	Lean forward	30	69.1359	52.0465	3443	93.9803	55.5886	0.8063	66.21
704	Lean forward	30	67.1158	48.3831	3213	89.7833	53.207	0.8055	63.9603
40	Look up	30	51.0804	54.5743	2152	65.29	46.2946	0.7051	52.3451
41	Look up	30	51.0153	54.6828	2090	64.9394	45.9475	0.7067	51.5856
42	Look up	30	51.2877	54.5736	2113	64.6792	46.1131	0.7012	51.8686
99	Look back	30	84.1974	65.0917	2280	63.5202	46.3744	0.6834	53.8794
100	Look back	30	84.035	65.8134	2283	63.5328	46.3996	0.6831	53.9148
101	Look back	30	77.1818	62.3859	2646	66.6886	50.1797	0.6851	58.043
69	Reach right	30	44.7348	65.1838	2626	75.2781	49.0945	0.7581	57.8453
70	Reach right	30	43.0969	66.0117	2745	77.2955	49.8226	0.7645	59.1189
71	Reach right	30	43.2374	66.4995	2729	75.9832	50.4799	0.7474	58.9463
107	Look straight ahead	30	0.463829	0.347381	0.008939	0.324848	0.065566	0.79601227	0.004772676
109	Look straight ahead	30	0.447327	0.304845	0.054827	0.309982	0.100724	0.67254601	0.028974874
173	Look straight ahead	30	0.465934	0.335955	0.067938	0.341747	0.142688	0.65260736	0.035802385
182	Look right	30	0.395539	0.369753	0.138856	0.297393	0.178613	0.42944785	0.0720874
193	Look right	30	0.428576	0.413084	0.178188	0.336289	0.203463	0.48082822	1
691	Look right	30	0.424468	0.287717	0.119785	0.255998	0.091792	0.54141104	0.062434796
121	Look left	30	0.443405	0.324435	0.100119	0.264323	0.193734	0.27530675	0.052399501
128	Look left	30	0.443473	0.322233	0.140644	0.270818	0.202912	0.27070552	0.072989285
125	*Look left*	*30*	*0.445185*	*0.322051*	*0.107271*	*0.26169*	*0.203687*	*0.23542945*	*0.056058228*
330	Lean right	30	0.029576	0.428645	0.141836	0.453407	0.348899	0.44478528	0.073588916
331	Lean right	30	0.019107	0.444321	0.163886	0.345841	0.244344	0.39953988	0.084647972
332	Lean right	30	0	0.54337	0.093564	0.349608	0.132867	0.69785276	0.049035715
523	Lean forward	30	1	0.765235	0.799166	1	0.654412	0.97546012	0.369850726
702	Lean forward	30	0.636599	0.142066	1	0.952921	0.591679	1	0.449704084
37	Look up	30	0.431697	0.341293	0.099523	0.272687	0.183543	0.3351227	0.05209481
38	Look up	30	0.418076	0.341039	0.020262	0.248623	0.159991	0.32285276	0.010788491
39	Look up	30	0.418954	0.363003	0.107867	0.275835	0.204296	0.28374233	0.056362918
96	Look back	30	0.735422	0.912891	0.331347	0.27268	0.289381	0.00383436	0.165678656
97	Look back	30	0.784283	0.907934	0.342074	0.285728	0.280284	0.0851227	0.170704835
98	Look back	30	0.826816	0.923191	0.253278	0.229473	0.237742	0	0.128523444
66	Reach right	30	0.350274	0.906957	0.457092	0.544537	0.305196	0.77300613	0.223467527
67	Reach right	30	0.345419	0.912913	0.483909	0.549436	0.31841	0.7563681	0.235486969
68	Reach right	30	0.342296	0.904799	0.510131	0.540731	0.358825	0.64877301	0.247143219
175	*Look straight ahead*	*30*	*0.466157*	*0.33017*	*0.098927*	*0.332911*	*0.148273*	*0.81503067*	*0.051787682*
232	Look straight ahead	30	0.460375	0.376753	0.045888	0.30078	1	0.65720859	0.933038718
423	Look straight ahead	30	0.481284	0.291863	0	0.313044	0	0.91947853	0
693	Look right	30	0.425412	0.261327	0.073302	0.209532	0.084168	0.4148773	0.038583602
694	Look right	30	0.419193	0.291929	0.158522	0.238733	0.130508	0.37576687	0.081966694
696	Look right	30	0.42831	0.280977	0.146007	0	0.107438	0.46472393	0.075687626
126	Look left	30	0.444599	0.302378	0.084029	0.260361	0.159984	0.36196319	0.044128974
198	Look left	30	0.471651	0.554155	0.351013	0.391977	0.332178	0.30444785	0.647658025
199	Look left	30	0.449401	0.502545	0.262813	0.330084	0.290865	0.2154908	0.133118181
333	Lean right	30	0.01522	0.570638	0.189511	0.356149	0.209264	0.52377301	0.097379172
334	Lean right	30	0.011453	0.593253	0.194875	0.358137	0.195052	0.72776074	0.100026325
335	Lean right	30	0.009646	0.620499	0.213945	0.377246	0.171023	0.67638037	0.109401051
703	Lean forward	30	0.653217	0.202325	0.942789	0.939598	0.581715	0.99539877	0.427359282
704	Lean forward	30	0.627164	0	0.805721	0.842244	0.489915	0.9892638	0.372522255
40	Look up	30	0.420351	0.341746	0.173421	0.274098	0.22348	0.21932515	0.089398711
41	Look up	30	0.419511	0.347735	0.138472	0.265965	0.210093	0.23159509	0.0708857
42	Look up	30	0.423025	0.341707	0.150179	0.25993	0.216476	0.18941718	0.077783899
99	Look back	30	0.847469	0.922291	0.249702	0.233045	0.226548	0.05291411	0.126797676
100	Look back	30	0.845375	0.962128	0.25149	0.233338	0.227519	0.0506135	0.12766056
101	Look back	30	0.756987	0.772935	0.467819	0.357571	0.373225	0.06595092	0.228286517
69	Reach right	30	0.33851	0.927375	0.457092	0.505782	0.331396	0.62576687	0.223467527
70	Reach right	30	0.317386	0.973074	0.526818	0.552577	0.359461	0.67484663	0.254511861
71	Reach right	30	0.319198	1	0.517282	0.522137	0.384797	0.54371166	0.250304691

Driver Volunteer 20
Name: Nukman OOP DATA

Frame number	Frame description	Face threshold value degree C	Centroid position x co-ordinate pixel	y co-ordnate pixel	Area pixel	Major Axis Length pixel	Minor Axis Length pixel	Eccentricity pixel	Equivdiameter pixel
107	Look straight ahead	30	54.4515	54.6764	1876	67.4779	42.198	0.7803	48.8733
109	Look straight ahead	30	53.172	53.9058	1953	66.837	43.1101	0.7642	49.8662
173	Look straight ahead	30	54.6147	54.4694	1975	68.2064	44.1988	0.7616	50.1463
330	Lean right	30	20.7813	56.1486	2099	73.0202	49.5486	0.7345	51.6965
331	Lean right	30	19.9696	56.4326	2136	68.3829	46.8361	0.7286	52.1502
332	Lean right	30	18.4881	58.227	2018	68.5453	43.944	0.7675	50.6892
523	Lean forward	30	96.024	62.2464	3202	96.5843	57.4746	0.8037	63.8507
702	Lean forward	30	67.8474	50.9568	3539	94.5547	55.8471	0.8069	67.1267
175	Look straight ahead	30	54.632	54.3646	2027	67.8255	44.3437	0.7567	50.8021
232	Look straight ahead	30	54.1837	55.2085	1938	66.4403	66.4403	0.7622	86.9556
423	Look straight ahead	30	55.8049	53.6706	1861	66.969	40.497	0.7964	48.6775
333	Lean right	30	19.6682	58.721	2179	68.8273	45.926	0.7448	52.6725
334	Lean right	30	19.3761	59.1307	2188	68.913	45.5573	0.7714	52.7811
335	Lean right	30	19.236	59.6243	2220	69.7368	44.9339	0.7647	53.1657
703	Lean forward	30	69.1359	52.0485	3443	93.9803	55.5886	0.8063	66.21
704	Lean forward	30	67.1158	48.3831	3213	89.7833	53.207	0.8055	63.9603
107	Look straight ahead	30	0.463829	0.453954	0.008939	0.034421	0.065566	0.66028097	0.005115196
109	Look straight ahead	30	0.447327	0.398368	0.054827	0.01316	0.100724	0.45466156	0.03105431
173	Look straight ahead	30	0.465934	0.439022	0.067938	0.058589	0.142688	0.42145594	0.038371811
330	Lean right	30	0.029576	0.560148	0.141836	0.218282	0.348899	0.07535121	0.078870163
331	Lean right	30	0.019107	0.580634	0.163886	0.064444	0.244344	0	0.090722894
332	Lean right	30	0	0.710069	0.093564	0.069831	0.132867	0.49680715	0.052554855
523	Lean forward	30	1	1	0.799166	1	0.654412	0.95913155	0.39639376
702	Lean forward	30	0.636599	0.185648	1	0.93267	0.591679	1	0.481977946
175	Look straight ahead	30	0.466157	0.431463	0.098927	0.045953	0.148273	0.35887612	0.055504322
232	Look straight ahead	30	0.460375	0.492336	0.045888	0	1	0.42911877	1
423	Look straight ahead	30	0.481284	0.381403	0	0.017539	0	0.86590038	0
333	Lean right	30	0.01522	0.745703	0.189511	0.079187	0.209264	0.20689655	0.104367772
334	Lean right	30	0.011453	0.775256	0.194875	0.08203	0.195052	0.54661558	0.107204903
335	Lean right	30	0.009646	0.81086	0.213945	0.109358	0.171023	0.46104725	0.117252424
703	Lean forward	30	0.653217	0.264396	0.942789	0.913615	0.581715	0.99233716	0.458029526
704	Lean forward	30	0.627164	0	0.805721	0.774383	0.489915	0.98212005	0.399257016

Driver Volunteer 21
Name: Masood

ALL DATA

Frame number	Frame description	Face threshold value degree C	Centroid position x co-ordinate pixel	y co-ordnate pixel	Area pixel	Major Axis Length pixel	Minor Axis Length pixel	Eccentricity pixel	Equivdiameter pixel
63	Look straight ahead	30	53.5215	66.131	5030	114.762	91.2736	0.6062	80.0275
66	Look straight ahead	30	54.1906	66.1018	5037	115.1625	92.5956	0.5946	80.0831
110	Look straight ahead	30	58.0956	69.0771	5304	115.7569	97.6238	0.5374	82.1782
176	Look right	30	54.7657	68.3122	5391	110.9353	91.6134	0.5639	82.8495
177	Look right	30	55.2775	70.1172	5419	109.865	96.0478	0.4855	83.0643
37	Look left	30	56.9571	66.3278	5156	115.5754	89.6874	0.6307	81.0236
38	Look left	30	54.7265	65.2476	4866	112.5627	82.4388	0.6809	78.712
31	Lean right	30	38.9914	71.7097	4857	127.7684	66.1116	0.8557	81.1289
32	Lean right	30	39.4779	68.74	4974	124.5632	67.0185	0.8429	79.5807
325	Lean left	30	75.1466	71.256	5382	113.3145	76.3933	0.7386	82.7803
326	Lean left	30	80.5292	73.5911	5395	112.3718	77.5285	0.7239	82.8802
327	Lean left	30	85.0654	74.2854	5427	114.0966	76.8797	0.7389	42.3584
273	Lean forward	30	58.0159	74.3887	6773	113.4888	96.263	0.5297	92.8636
274	Lean forward	30	57.1809	73.4059	7033	115.3534	97.737	0.5311	94.6292
272	Head on steering wheel	30	56.8697	77.5647	6361	113.6032	91.1159	0.5973	89.9949
53	Look back	30	87.1366	66.7318	4620	125.1023	77.8504	0.7828	76.6966
262	Use mobile phone	30	58.3174	68.0581	6043	102.045	92.6134	0.4199	87.7165
263	Use mobile phone	30	58.779	67.9598	6162	103.4427	93.9683	0.4181	88.576
264	Use mobile phone	30	59.6159	68.7998	6170	102.8701	94.9644	0.3844	70.941
208	Look straight ahead	30	58.4572	70.6661	5643	111.3243	99.4976	0.4485	84.7637
221	Look straight ahead	30	56.1633	70.049	5451	111.0235	95.9152	0.5036	83.3092
441	Look straight ahead	30	62.8997	74.8856	6259	123.3811	94.0542	0.6472	89.2704
408	Look right	30	60.2842	73.2064	5862	124.8603	85.6795	0.7274	86.3929
409	Look right	30	55.4352	74.2256	6176	127.8506	89.5299	0.7139	88.6765
35	Look left	30	54.2727	64.9521	4951	113.8855	81.2688	0.7006	79.3965
36	Look left	30	56.0984	66.2971	5183	117.4695	87.0892	0.6711	81.2355
25	Lean right	30	43.7046	68.985	5338	132.0539	74.6495	0.8249	82.4412
26	Lean right	30	38.9902	69.17	4795	127.5858	68.6735	0.8428	78.1357
328	Lean left	30	81.1149	73.521	5630	111.336	83.4654	0.6618	49.6369
332	Lean left	30	80.8328	73.6137	5615	110.7754	83.5178	0.6569	84.5532
333	Lean left	30	80.887	73.3795	5639	111.2628	83.6566	0.6593	84.7337
275	Lean forward	30	56.9272	74.5518	6886	115.8888	94.1242	0.5834	93.6351
282	Lean forward	30	45.9204	72.5857	6831	126.0587	89.5662	0.7037	93.2604
382	Head on steering wheel	30	67.3851	84.7469	5085	109.1676	63.6045	0.8127	80.4638
54	Look back	30	87.4689	67.2343	4926	123.9168	82.3893	0.747	79.1958
265	Use mobile phone	30	59.3606	68.731	6267	106.4763	94.3188	0.464	89.3274
266	Use mobile phone	30	61.2845	68.1894	6109	104.232	92.7033	0.4571	88.1942
267	Use mobile phone	30	60.2236	68.8959	6207	106.6133	93.6587	0.4778	88.8988
63	Look straight ahead	30	0.299746	0.059556	0.169913	0.423774	0.770875	0.470613198	0.720652831
66	Look straight ahead	30	0.313548	0.058081	0.172614	0.43712	0.807707	0.446000424	0.721716522
110	Look straight ahead	30	0.394099	0.208388	0.283465	0.456928	0.947795	0.324633991	0.761798174
176	Look right	30	0.325411	0.169747	0.319519	0.296255	0.780342	0.380861447	0.774640908
177	Look right	30	0.335968	0.260932	0.331123	0.260589	0.903887	0.214513049	0.778750277
37	Look left	30	0.370614	0.069498	0.22213	0.45088	0.726683	0.522597072	0.73970936
38	Look left	30	0.324602	0.014928	0.101948	0.350486	0.524733	0.62911097	0.695485816
31	Lean right	30	2.48E-05	0.341383	0.098218	0.857192	0.069849	1	0.741723869
32	Lean right	30	0.01006	0.191358	0.146705	0.750384	0.095116	0.972841078	0.712105038
325	Lean left	30	0.74582	0.318462	0.315789	0.375539	0.356302	0.751538298	0.773317034
326	Lean left	30	0.856851	0.436428	0.321177	0.344125	0.38793	0.720347974	0.775228235
327	Lean left	30	0.950422	0.471503	0.334438	0.401601	0.369854	0.752174836	0
273	Lean forward	30	0.392455	0.476721	0.89225	0.381347	0.909882	0.308296202	0.966222059
274	Lean forward	30	0.375231	0.427072	1	0.443482	0.950949	0.311266709	1
272	Head on steering wheel	30	0.368811	0.637167	0.721508	0.385159	0.766482	0.451729259	0.911340557
53	Look back	30	0.993145	0.089907	0	0.768349	0.396898	0.845321451	0.656928916
262	Use mobile phone	30	0.398674	0.15691	0.589722	0	0.808203	0.075323573	0.867752168
263	Use mobile phone	30	0.408196	0.151944	0.639039	0.046576	0.845951	0.07150435	0.884195383
264	Use mobile phone	30	0.425459	0.194379	0.642354	0.027495	0.873703	0	0.546817726
208	Look straight ahead	30	0.401558	0.288662	0.423954	0.309218	1	0.13600679	0.811261737
221	Look straight ahead	30	0.35424	0.257487	0.344365	0.299195	0.900193	0.252917462	0.783435494
441	Look straight ahead	30	0.493196	0.501824	0.679237	0.710992	0.848344	0.55760662	0.897480046
408	Look right	30	0.439244	0.416993	0.514712	0.760284	0.615021	0.727774241	0.84243019
409	Look right	30	0.339221	0.468482	0.64484	0.859932	0.722295	0.699130066	0.886118062
35	Look left	30	0.315242	0	0.137174	0.394566	0.492136	0.670910248	0.708581082
36	Look left	30	0.352901	0.067947	0.23332	0.513998	0.654296	0.60831742	0.743763248
25	Lean right	30	0.097247	0.203735	0.297555	1	0.307719	0.934648844	0.766829664
26	Lean right	30	0	0.213081	0.072524	0.851108	0.141225	0.972628899	0.68446054
328	Lean left	30	0.868932	0.432886	0.418566	0.309608	0.553335	0.588584766	0.139246004
332	Lean left	30	0.863113	0.437569	0.41235	0.290927	0.554795	0.578187991	0.807234632
333	Lean left	30	0.864231	0.425738	0.422296	0.307169	0.558662	0.583280289	0.810687803
275	Lean forward	30	0.369998	0.484961	0.93908	0.461323	0.850294	0.422236367	0.980981734
282	Lean forward	30	0.142954	0.385637	0.916287	0.800219	0.723306	0.6774878	0.973813295
382	Head on steering wheel	30	0.585719	1	0.192706	0.23735	0	0.908762996	0.728999747
54	Look back	30	1	0.115293	0.126813	0.728844	0.523354	0.769361341	0.704741462
265	Use mobile phone	30	0.420193	0.190904	0.682553	0.147666	0.855716	0.168894547	0.898570521
266	Use mobile phone	30	0.459878	0.163543	0.617074	0.072878	0.810707	0.154254191	0.876891113
267	Use mobile phone	30	0.437994	0.199234	0.657688	0.152232	0.837325	0.19817526	0.890370915

Driver Volunteer 21
Name: Masood OOP DATA

Frame number	Frame description	Face threshold value degree C	Centroid position x co-ordinate pixel	y co-ordnate pixel	Area pixel	Major Axis Length pixel	Minor Axis Length pixel	Eccentricity pixel	Equivdiameter pixel
63	Look straight ahead	30	53.5215	66.131	5030	114.762	91.2736	0.6062	80.0275
66	Look straight ahead	30	54.1906	66.1018	5037	115.1625	92.5956	0.5946	80.0831
110	Look straight ahead	30	58.0956	69.0771	5304	115.7569	97.6238	0.5374	82.1782
31	Lean right	30	38.9914	71.7097	4857	127.7684	66.1116	0.8557	81.1289
32	Lean right	30	39.4779	68.74	4974	124.5632	67.0185	0.8429	79.5807
325	Lean left	30	75.1466	71.256	5382	113.3145	76.3933	0.7386	82.7803
326	Lean left	30	80.5292	73.5911	5395	112.3718	77.5285	0.7239	82.8802
327	Lean left	30	85.0654	74.2854	5427	114.0966	76.8797	0.7389	42.3584
273	Lean forward	30	58.0159	74.3887	6773	113.4888	96.263	0.5297	92.8636
274	Lean forward	30	57.1809	73.4059	7033	115.3534	97.737	0.5311	94.6292
272	Head on steering wheel	30	56.8697	77.5647	6361	113.6032	91.1159	0.5973	89.9949
208	Look straight ahead	30	58.4572	70.6661	5643	111.3243	99.4976	0.4485	84.7637
221	Look straight ahead	30	56.1633	70.049	5451	111.0235	95.9152	0.5036	83.3092
441	Look straight ahead	30	62.8997	74.8856	6259	123.3811	94.0542	0.6472	89.2704
25	Lean right	30	43.7046	68.985	5338	132.0539	74.6495	0.8249	82.4412
26	Lean right	30	38.9902	69.17	4795	127.5858	68.6735	0.8428	78.1357
328	Lean left	30	81.1149	73.521	5630	111.336	83.4654	0.6618	49.6369
332	Lean left	30	80.8328	73.6137	5615	110.7754	83.5178	0.6569	84.5532
333	Lean left	30	80.887	73.3795	5639	111.2628	83.6566	0.6593	84.7337
275	Lean forward	30	56.9272	74.5518	6886	115.8888	94.1242	0.5834	93.6351
282	Lean forward	30	45.9204	72.5857	6831	126.0587	89.5662	0.7037	93.2604
382	Head on steering wheel	30	67.3851	84.7469	5085	109.1676	63.6045	0.8127	80.4638
63	Look straight ahead	30	0.315382	0.001566	0.105004	0.244443	0.770875	0.387278978	0.720652831
66	Look straight ahead	30	0.329904	0	0.108132	0.261943	0.807707	0.358791749	0.721716522
110	Look straight ahead	30	0.414657	0.159575	0.227435	0.287915	0.947795	0.218320236	0.761798174
31	Lean right	30	2.6E-05	0.300771	0.027703	0.812748	0.069849	1	0.741723869
32	Lean right	30	0.010585	0.141496	0.079982	0.672699	0.095116	0.968565815	0.712105038
325	Lean left	30	0.784726	0.276437	0.262288	0.181196	0.356302	0.712426326	0.773317034
326	Lean left	30	0.901548	0.401677	0.268097	0.140005	0.38793	0.67632613	0.775228235
327	Lean left	30	1	0.438914	0.282395	0.215369	0.369854	0.713163065	0
273	Lean forward	30	0.412927	0.444455	0.883825	0.188812	0.909882	0.199410609	0.966222059
274	Lean forward	30	0.394805	0.391744	1	0.270284	0.950949	0.202848723	1
272	*Head on steering wheel*	*30*	*0.38805*	*0.614794*	*0.699732*	*0.19381*	*0.766482*	*0.365422397*	*0.911340557*
208	Look straight ahead	30	0.422505	0.244799	0.37891	0.094235	1	0	0.811261737
221	Look straight ahead	30	0.372719	0.211702	0.293119	0.081092	0.900193	0.135314342	0.783435494
441	Look straight ahead	30	0.518923	0.471105	0.654155	0.621048	0.848344	0.487966601	0.897480046
25	Lean right	30	0.10232	0.154636	0.242627	1	0.307719	0.924361493	0.766829664
26	Lean right	30	0	0.164558	0	0.80477	0.141225	0.968320236	0.68446054
328	Lean left	30	0.91426	0.397917	0.373101	0.094747	0.553335	0.523821218	0.139246004
332	Lean left	30	0.908137	0.402889	0.366399	0.070252	0.554795	0.511787819	0.807234632
333	Lean left	30	0.909313	0.390328	0.377122	0.091548	0.558662	0.517681729	0.810687803
275	Lean forward	30	0.389298	0.453202	0.934316	0.293678	0.850294	0.331286837	0.980981734
282	Lean forward	30	0.150411	0.347754	0.909741	0.738044	0.723306	0.626719057	0.973813295
382	Head on steering wheel	30	0.616273	1	0.12958	0	0	0.894400786	0.728999747

Driver Volunteer 22
Name: Phil Bamforth ALL DATA

Frame number	Frame description	Face threshold value degree C	Centroid position x co-ordinate pixel	y co-ordnate pixel	Area pixel	Major Axis Length pixel	Minor Axis Length pixel	Eccentricity pixel	Equivdiameter pixel
14	Look straight ahead	30	55.0254	57.7694	3461	96.2098	47.6609	0.8687	66.3828
20	Look straight ahead	30	54.7242	57.4665	3524	97.0197	48.0597	0.8687	66.9843
115	Look straight ahead	30	58.8267	56.4591	3590	97.9873	48.254	0.8703	67.6087
401	Look right	30	50.8269	59.7991	3374	95.4411	46.9818	0.8704	65.5432
403	Look right	30	49.5114	59.7874	3457	96.4758	47.5324	0.8702	66.3445
434	Look right	30	55.612	57.2151	3552	98.3839	47.837	0.8738	67.2499
448	Look left	30	64.6569	59.0165	3573	97.3573	48.5213	0.867	67.4484
449	Look left	30	65.45	59.2047	3493	96.5915	47.7681	0.8692	66.689
457	Look left	30	61.2532	58.7961	3527	96.2021	48.0705	0.8662	67.0128
204	Lean right	30	41.9783	59.5885	3463	94.5465	47.9804	0.8617	66.402
205	Lean right	30	42.8106	59.3094	3516	94.3456	48.7527	0.8561	66.9082
206	Lean right	30	42.6924	59.8256	3394	93.4693	47.6108	0.8605	65.7372
201	Look straight ahead	30	59.0399	57.1782	3435	95.5537	47.8661	0.8655	66.133
693	Look straight ahead	30	58.2041	58.5935	3454	96.4568	47.7997	0.8686	66.3157
700	Look straight ahead	30	58.2677	57.2623	3500	98.6586	47.0283	0.8791	66.7558
435	Look right	30	53.7811	58.9348	3389	94.7764	47.3825	0.8661	65.6887
436	Look right	30	52.2331	58.4271	3505	96.0952	48.3616	0.8641	66.8035
437	Look right	30	52.7812	59.1851	3404	95.2136	47.3618	0.8675	65.8339
448	Look left	30	64.6569	59.0165	3573	97.3573	48.5213	0.867	67.4484
449	Look left	30	65.45	59.2047	3493	96.5915	47.7681	0.8692	66.689
268	Look left	30	60.3277	58.4117	3476	94.0719	48.1626	0.859	66.5265
207	Lean right	30	43.2368	59.072	3417	94.34	47.6331	0.8632	65.9595
208	Lean right	30	42.9545	59.6584	3498	95.0894	48.2197	0.8619	66.7367
209	Lean right	30	43.515	59.5124	3509	94.8521	48.4215	0.8599	66.8416
14	Look straight ahead	30	0.555865	0.389217	0.402778	0.528106	0.383477	0.54782609	0.406487533
20	Look straight ahead	30	0.543033	0.299243	0.694444	0.684177	0.608674	0.54782609	0.697700315
115	Look straight ahead	30	0.717818	0	1	0.870638	0.718392	0.6173913	1
401	Look right	30	0.37699	0.992128	0	0.379974	0	0.62173913	0
403	Look right	30	0.320944	0.988653	0.384259	0.579365	0.310915	0.61304348	0.387944808
434	Look right	30	0.580857	0.224566	0.824074	0.947064	0.482918	0.76956522	0.826289034
448	Look left	30	0.96621	0.759661	0.921296	0.749234	0.869332	0.47391304	0.922391673
449	Look left	30	1	0.815565	0.550926	0.601661	0.444012	0.56956522	0.55473251
457	Look left	30	0.821197	0.694193	0.708333	0.526622	0.614772	0.43913043	0.711498427
204	Lean right	30	0	0.929571	0.412037	0.207581	0.563894	0.24347826	0.415783103
205	Lean right	30	0.03546	0.846666	0.657407	0.168867	1	0	0.660856935
206	Lean right	30	0.030424	1	0.092593	0	0.355187	0.19130435	0.093923989
201	Look straight ahead	30	0.726901	0.213605	0.282407	0.401673	0.499351	0.40869565	0.285548293
693	Look straight ahead	30	0.691292	0.634012	0.37037	0.575704	0.461856	0.54347826	0.374001452
700	Look straight ahead	30	0.694002	0.238586	0.583333	1	0.026258	1	0.587073348
435	Look right	30	0.502852	0.735393	0.069444	0.251884	0.226269	0.43478261	0.070442992
436	Look right	30	0.436901	0.584583	0.606481	0.506022	0.779152	0.34782609	0.61016703
437	Look right	30	0.4594	0.809743	0.138889	0.336134	0.21458	0.49565217	0.140740741
448	Look left	30	0.96621	0.759661	0.921296	0.749234	0.869332	0.47391304	0.922391673
449	Look left	30	1	0.815565	0.550926	0.601661	0.444012	0.56956522	0.55473251
268	Look left	30	0.781767	0.580009	0.472222	0.116124	0.66678	0.12608696	0.476059066
207	Lean right	30	0.053618	0.776147	0.199074	0.167786	0.367779	0.30869565	0.201549262
208	Lean right	30	0.041591	0.950334	0.574074	0.3122	0.699023	0.25217391	0.577826192
209	Lean right	30	0.06547	0.906966	0.625	0.266471	0.812976	0.16521739	0.628612927

Driver Volunteer 22
Name: *Phil Bamforth* *OOP DATA*

Frame number	Frame description	Face threshold value degree C	Centroid position x co-ordinate pixel	y co-ordnate pixel	Area pixel	Major Axis Length pixel	Minor Axis Length pixel	Eccentricity pixel	Equivdiameter pixel
14	Look straight ahead	30	55.0254	57.7694	3461	96.2098	47.6609	0.8687	66.3828
20	Look straight ahead	30	54.7242	57.4665	3524	97.0197	48.0597	0.8687	66.9843
115	Look straight ahead	30	58.8267	56.4591	3590	97.9873	48.254	0.8703	67.6087
204	Lean right	30	41.9783	59.5885	3463	94.5465	47.9804	0.8617	66.402
205	Lean right	30	42.8106	59.3094	3516	94.3456	48.7527	0.8561	66.9082
206	Lean right	30	42.6924	59.8256	3394	93.4693	47.6108	0.8605	65.7372
201	Look straight ahead	30	59.0399	57.1782	3435	95.5537	47.8661	0.8655	66.133
693	*Look straight ahead*	30	58.2041	58.5935	3454	96.4568	47.7997	0.8686	66.3157
700	Look straight ahead	30	58.2677	57.2623	3500	98.6586	47.0283	0.8791	66.7558
207	Lean right	30	43.2368	59.072	3417	94.34	47.6331	0.8632	65.9595
208	Lean right	30	42.9545	59.6584	3498	95.0894	48.2197	0.8619	66.7367
209	Lean right	30	43.515	59.5124	3509	94.8521	48.4215	0.8599	66.8416
14	Look straight ahead	30	0.764706	0.389217	0.341837	0.528106	0.366852	0.54782609	0.344963933
20	Look straight ahead	30	0.747052	0.299243	0.663265	0.684177	0.598121	0.54782609	0.666363879
115	Look straight ahead	30	0.987504	0	1	0.870638	0.710798	0.6173913	1
204	*Lean right*	30	0	0.929571	0.352041	0.207581	0.552134	0.24347826	0.355223083
205	Lean right	30	0.048782	0.846666	0.622449	0.168867	1	0	0.625701309
206	Lean right	30	0.041854	1	0	0	0.337799	0.19130435	0
201	Look straight ahead	30	1	0.213605	0.209184	0.401673	0.48585	0.40869565	0.211488111
693	Look straight ahead	30	0.951013	0.634012	0.306122	0.575704	0.447344	0.54347826	0.309110339
700	Look straight ahead	30	0.95474	0.238586	0.540816	1	0	1	0.544269303
207	Lean right	30	0.073762	0.776147	0.117347	0.167788	0.350731	0.30869565	0.118781726
208	Lean right	30	0.057216	0.950334	0.530612	0.3122	0.690907	0.25217391	0.534063585
209	*Lean right*	30	0.090068	0.906966	0.586735	0.266471	0.807933	0.16521739	0.590114881

Driver Volunteer 23
Name: Nazli Ozkaya ALL DATA

Frame number	Frame description	Face threshold value degree C	Centroid position x co-ordinate pixel	y co-ordnate pixel	Area pixel	Major Axis Length pixel	Minor Axis Length pixel	Eccentricity pixel	Equivdiameter pixel
46	Look straight ahead	30	58.1989	42.886	1684	63.1314	34.7488	0.8349	46.3048
116	Look straight ahead	30	59.1827	65.2626	1790	65.2626	35.743	0.8367	47.7399
160	Look straight ahead	30	60.9489	43.7352	1624	64.2428	64.2428	0.8562	45.4724
140	Look right	30	56.6707	42.7827	1813	61.6927	38.4768	0.7665	48.0456
141	Look right	30	52.5714	43.1158	1848	61.9427	39.4574	0.7709	48.5072
144	Look right	30	59.4077	47.866	1940	61.0655	40.9133	0.7424	49.6999
152	Look left	30	62.9537	48.2888	2223	64.3275	44.7753	0.718	53.2016
200	Look left	30	68.4024	45.5324	2008	61.2576	42.3803	0.7221	50.5635
238	Look left	30	65.6407	45.5639	2004	63.0212	41.1148	0.7579	80.3976
22	Lean left	30	82.4588	64.9162	752	40.4005	37.0871	0.3966	30.9431
23	Lean left	30	87.1393	65.9131	725	45.0339	35.3443	0.6197	30.3825
24	Lean left	30	88.1437	63.5679	1016	46.0825	38.5022	0.5495	35.9668
423	Lean forward	30	66.7543	43.2654	2133	66.9223	41.0646	0.7896	52.1135
443	Head on steering wheel	30	45.7716	63.1151	556	31.3779	27.6793	0.471	26.6068
444	Head on steering wheel	30	37.5357	95.754	252	23.9136	17.5457	0.6795	17.9125
445	Head on steering wheel	30	18.2203	96.2161	472	30.6028	26.8164	0.4818	24.5147
163	Look straight ahead	30	59.4077	43.1574	1722	64.6225	34.8978	0.8416	46.8243
526	Look straight ahead	30	55.5972	45.5182	1785	63.4867	36.4023	0.8193	47.6732
528	Look straight ahead	30	54.1536	46.4637	1790	62.9227	36.9969	0.8089	47.7399
145	Look right	30	56.9284	50.5686	1787	59.2729	39.9106	0.7393	47.6999
150	Look right	30	54.236	45.2518	1763	60.6707	39.1255	0.7643	47.3785
459	Look right	30	56.0703	50.7622	1522	61.5575	32.1487	0.8528	44.0213
246	Look left	30	68.7931	45.5122	2054	62.0138	42.614	0.7265	51.1394
255	Look left	30	65.6255	44.7242	1936	62.6844	39.877	0.7716	83.521
257	Look left	30	67.2903	44.7561	1874	61.633	39.2157	0.7715	48.8472
25	Lean left	30	85.7335	48.932	1602	55.1593	38.7929	0.7109	45.1634
26	Lean left	30	86.0647	51.5162	1577	53.6044	39.8495	0.6688	44.8096
30	Lean left	30	91.9597	53.5322	1537	56.0174	36.3851	0.7603	44.2376
424	Lean forward	30	67.3096	59.0713	1763	79.481	32.3478	0.9134	47.4322
446	Head on steering wheel	30	24.0095	82.0474	739	59.926	31.2809	0.853	30.6745
447	Head on steering wheel	30	35.2408	72.6571	1009	89.4916	31.3871	0.9365	35.8427
448	Head on steering wheel	30	38.9121	70.7525	1309	105.7626	38.6329	0.9309	40.8249
46	Look straight ahead	30	0.542161	0.001933	0.726535	0.479148	0.368398	0.811817	0.432753378
116	Look straight ahead	30	0.555502	0.420709	0.780315	0.505186	0.389688	0.81515095	0.454627068
160	Look straight ahead	30	0.579454	0.017826	0.696093	0.492727	1	0.85126875	0.420065998
140	Look right	30	0.521436	0	0.791984	0.461571	0.448231	0.68512688	0.459286525
141	Look right	30	0.465845	0.006234	0.809741	0.464625	0.46923	0.69327653	0.466322199
144	Look right	30	0.558554	0.095133	0.856418	0.453908	0.500408	0.64048898	0.484501246
152	Look left	30	0.606642	0.103046	1	0.493762	0.583111	0.59529543	0.537873904
200	Look left	30	0.680533	0.05146	0.890918	0.456255	0.531823	0.60288942	0.497664175
238	Look left	30	0.643081	0.05205	0.888889	0.477802	0.504723	0.669198	0.952393364
22	Lean left	30	0.871156	0.414226	0.253678	0.201431	0.418471	0	0.19861146
23	Lean left	30	0.934629	0.432883	0.23998	0.25804	0.38115	0.41322467	0.190066836
24	Lean left	30	0.94825	0.388993	0.38762	0.270851	0.448775	0.28320059	0.275182332
423	Lean forward	30	0.658183	0.009034	0.954338	0.525464	0.503648	0.72791258	0.521289162
443	Head on steering wheel	30	0.373631	0.380519	0.154236	0.091196	0.217007	0.1378033	0.13251789
444	Head on steering wheel	30	0.261941	0.991352	0	0	0	0.52398592	0
445	Head on steering wheel	30	0	1	0.111618	0.081726	0.198528	0.157807	0.100630254
163	Look straight ahead	30	0.558554	0.007012	0.745814	0.497366	0.371588	0.82422671	0.440671559
526	Look straight ahead	30	0.506878	0.051195	0.777778	0.483489	0.403807	0.78292276	0.453610432
528	Look straight ahead	30	0.487301	0.068889	0.780315	0.476598	0.41654	0.76365994	0.454627068
145	Look right	30	0.524931	0.145712	0.778792	0.432006	0.478936	0.63474718	0.454017391
150	Look right	30	0.488419	0.046209	0.766616	0.449084	0.462123	0.68105205	0.449118636
459	Look right	30	0.513294	0.149335	0.644343	0.459919	0.312717	0.84497129	0.397948437
246	Look left	30	0.685831	0.051082	0.914257	0.465494	0.536828	0.61103908	0.506442001
255	Look left	30	0.642875	0.036335	0.854389	0.473687	0.478216	0.69457307	1
257	Look left	30	0.665452	0.036932	0.822933	0.460841	0.464055	0.69438785	0.471504454
25	Lean left	30	0.915585	0.115083	0.684932	0.381748	0.455	0.58214484	0.415356242
26	Lean left	30	0.920056	0.163446	0.672248	0.362751	0.477627	0.50416744	0.409963648
30	Lean left	30	1	0.201176	0.651953	0.392232	0.403438	0.67364327	0.401245265
424	Lean forward	30	0.665713	0.304839	0.766616	0.678901	0.316981	0.9572143	0.449937127
446	Head on steering wheel	30	0.078509	0.734834	0.247083	0.439986	0.294134	0.84534173	0.194517479
447	Head on steering wheel	30	0.23082	0.559096	0.384069	0.801207	0.298408	1	0.273290808
448	Head on steering wheel	30	0.280607	0.523452	0.536276	1	0.451574	0.98962771	0.34922914

Driver Volunteer 23
Name: Nazli Ozkaya OOP DATA

Frame number	Frame description	*Face* threshold value degree C	Centroid position x co-ordinate pixel	y co-ordnate pixel	Area pixel	Major Axis Length pixel	Minor Axis Length pixel	Eccentricity pixel	Equivdiameter pixel
46	Look straight ahead	30	58.1989	42.886	1684	63.1314	34.7488	0.8349	46.3048
116	Look straight ahead	30	59.1827	65.2626	1790	65.2626	35.743	0.8367	47.7399
160	*Look straight ahead*	*30*	*60.9489*	*43.7352*	*1624*	*64.2428*	*64.2428*	*0.8562*	*45.4724*
22	Lean left	30	82.4588	64.9162	752	40.4005	37.0871	0.3966	30.9431
23	Lean left	30	87.1393	65.9131	725	45.0339	35.3443	0.6197	30.3825
24	Lean left	30	88.1437	63.5679	1016	46.0825	38.5022	0.5495	35.9668
423	Lean forward	30	66.7543	43.2654	2133	66.9223	41.0646	0.7896	52.1135
443	Head on steering wheel	30	45.7716	63.1151	556	31.3779	27.6793	0.471	26.6068
444	*Head on steering wheel*	*30*	*37.5357*	*95.754*	*252*	*23.9136*	*17.5457*	*0.6795*	*17.9125*
445	Head on steering wheel	30	18.2203	96.2161	472	30.6028	26.8164	0.4818	24.5147
163	Look straight ahead	30	59.4077	43.1574	1722	64.6225	34.8978	0.8416	46.8243
526	Look straight ahead	30	55.5972	45.5182	1785	63.4867	36.4023	0.8193	47.6732
528	Look straight ahead	30	54.1536	46.4637	1790	62.9227	36.9969	0.8089	47.7399
25	Lean left	30	85.7335	48.932	1602	55.1593	38.7929	0.7109	45.1634
26	Lean left	30	86.0647	51.5162	1577	53.6044	39.8495	0.6688	44.8096
30	Lean left	30	91.9597	53.5322	1537	56.0174	36.3851	0.7603	44.2376
424	Lean forward	30	67.3096	59.0713	1763	79.481	32.3478	0.9134	47.4322
446	Head on steering wheel	30	24.0095	82.0474	739	59.926	31.2809	0.853	30.6745
447	Head on steering wheel	30	35.2408	72.6571	1009	89.4916	31.3871	0.9365	35.8427
448	Head on steering wheel	30	38.9121	70.7525	1309	105.7626	38.6329	0.9309	40.8249
46	Look straight ahead	30	0.542161	0	0.761297	0.479148	0.368398	0.811817	0.830159937
116	Look straight ahead	30	0.555502	0.419587	0.81765	0.505186	0.389688	0.81515095	0.872120698
160	Look straight ahead	30	0.579454	0.015923	0.729399	0.492727	1	0.85126875	0.805821467
22	Lean left	30	0.871156	0.413091	0.265816	0.201431	0.418471	0	0.381000556
23	Lean left	30	0.934629	0.431784	0.251462	0.25804	0.38115	0.41322467	0.364609222
24	Lean left	30	0.94825	0.387809	0.406167	0.270851	0.448775	0.28320059	0.527888073
423	Lean forward	30	0.658183	0.007114	1	0.525464	0.503648	0.72791258	1
443	Head on steering wheel	30	0.373631	0.379319	0.161616	0.091196	0.217007	0.1378033	0.254211865
444	Head on steering wheel	30	0.261941	0.991335	0	0	0	0.52398592	0
445	Head on steering wheel	30	0	1	0.116959	0.081726	0.198528	0.157807	0.193041139
163	Look straight ahead	30	0.558554	0.005089	0.781499	0.497366	0.371588	0.82422671	0.845349551
526	Look straight ahead	30	0.506878	0.049357	0.814992	0.483489	0.403807	0.78292276	0.870170463
528	Look straight ahead	30	0.487301	0.067086	0.81765	0.476598	0.41654	0.76365994	0.872120698
25	Lean left	30	0.915565	0.113369	0.717703	0.381748	0.455	0.58214484	0.796786644
26	Lean left	30	0.920056	0.161826	0.704413	0.362751	0.477627	0.50416744	0.786441917
30	Lean left	30	1	0.199628	0.683147	0.392232	0.403438	0.67364327	0.76971726
424	Lean forward	30	0.665713	0.303493	0.803296	0.678901	0.316981	0.9572143	0.863123885
446	Head on steering wheel	30	0.078509	0.734321	0.258905	0.439986	0.294134	0.84534173	0.373146984
447	Head on steering wheel	30	0.23082	0.558242	0.402446	0.801207	0.296408	1	0.524259525
448	Head on steering wheel	30	0.280607	0.522529	0.561935	1	0.451574	0.98962771	0.669933628

HEIGHT DETECTION DATA

			Centroid position						
Frame number	Frame description	Face threshold value	x co-ordinate	y co-ordnate	Area	Major Axis Length	Minor Axis Length	Eccentricity	Equivdiameter
		degree C	pixel	pixel	pixel	pixel	pixel	pixel	pixel
1	Look straight	30	47.8945	58.865	2200	91.6722	37.7847	0.9111	52.9257
482	Look straight	30	47.7816	55.0803	2441	89.7045	41.3338	0.8875	55.7492
51	Look straight	30	54.6153	45.9487	3683	108.28	44.7914	0.9104	68.4788
112	Look straight	30	56.5354	45.6779	3670	108.6373	44.7401	0.9113	68.3578
74	Look straight ahead	30	54.1655	44.8048	3571	100.7068	47.814	0.8801	67.4295
75	Look straight ahead	30	54.3614	45.6542	3586	102.0448	47.512	0.885	67.571
126	Look straight ahead	30	53.8446	44.8535	3461	98.8415	47.2742	0.8782	66.3828
85	Look straight ahead	30	57.4392	63.3274	2639	79.4537	43.6608	0.8355	57.9662
82	Look straight ahead	30	58.2237	62.0882	2597	79.8338	42.7401	0.8446	57.5031
129	Look straight ahead	30	61.7305	61.803	2731	80.1607	44.6596	0.8304	58.9679
22	Look straight ahead	30	58.0509	55.836	3202	94.3873	44.4771	0.882	63.8507
101	Look straight ahead	30	64.9264	57.132	3219	92.3526	45.6885	0.8691	64.02
207	Look straight ahead	30	67.9918	56.3925	3292	93.7775	46.3256	0.8695	64.7418
39	Look straight ahead	30	61.9435	75.9692	5749	114.7054	99.9229	0.4911	85.5561
60	Look straight ahead	30	70.5247	74.616	5542	114.4059	87.2291	0.647	84.0017
63	Look straight ahead	30	66.6774	80.0494	6556	119.1469	98.0888	0.5677	91.3639
75	Look straight ahead	30	50.3912	75.983	4992	109.7717	84.5181	0.6381	79.7246
150	Look straight ahead	30	50.7845	75.3797	5212	111.2846	87.4577	0.6184	81.4624
230	Look straight ahead	30	53.3307	75.6881	5056	110.2665	87.2086	0.612	80.234
3	Look straight	30	47.8707	58.5195	2227	92.6863	37.9878	0.9122	53.2495
500	Look straight	30	48.8132	54.8402	2441	93.1438	41.1166	0.8973	55.7492
361	Look straight	30	58.1637	46.729	3727	109.6181	44.9814	0.9119	68.8866
588	Look straight	30	53.7854	46.9632	3780	110.7842	45.2485	0.9128	69.3747
127	Look straight ahead	30	54.2326	44.6679	3397	98.6047	46.3332	0.8827	65.7662
422	Look straight ahead	30	49.1211	42.2809	3353	96.2671	46.9585	0.873	65.3389
424	Look straight ahead	30	48.1505	42.8787	3455	97.1725	47.7834	0.8707	66.3253
264	Look straight ahead	30	52.673	60.3482	2771	81.3781	44.5981	0.8365	59.3982
529	Look straight ahead	30	54.2782	60.0957	2768	82.3987	44.0303	0.8453	59.366
627	Look straight ahead	30	50.1433	62.0245	2812	81.9147	44.8279	0.837	59.836
315	Look straight ahead	30	71.9934	56.2032	3174	92.8653	45.1369	0.8739	63.5709
415	Look straight ahead	30	72.9223	55.3853	3190	93.694	45.2117	0.8759	63.731
612	Look straight ahead	30	70.6196	57.7438	3333	96.9205	45.7698	0.8815	65.1437
183	Look straight ahead	30	69.7157	78.3995	6300	120.086	98.3544	0.5737	89.5623
208	Look straight ahead	30	69.483	77.1447	5979	117.5148	98.6074	0.544	87.2508
307	Look straight ahead	30	68.7354	77.879	6040	115.8311	98.4591	0.5267	87.6947
382	Look straight ahead	30	54.1814	75.233	5871	121.6676	86.198	0.7057	86.4592
452	Look straight ahead	30	51.0512	75.8238	5427	112.9108	89.1908	0.6132	83.1256
570	Look straight ahead	30	50.8853	75.734	5041	108.6986	86.7013	0.6031	80.1149
1	Look straight	30	0.004491	0.439099	0	0.289443	0	0.9959687	0
482	Look straight	30	0	0.338891	0.055326	0.24283	0.057116	0.94000474	0.073455573
51	Look straight	30	0.271818	0.097113	0.34045	0.682863	0.11276	0.99430875	0.404626127
112	Look straight	30	0.348192	0.089943	0.337466	0.691327	0.111934	0.99644297	0.401478217
74	Look straight ahead	30	0.253927	0.066826	0.314738	0.503462	0.161403	0.92245672	0.377327762
75	Look straight ahead	30	0.261719	0.089315	0.318182	0.535158	0.156543	0.93407636	0.381008996
126	Look straight ahead	30	0.241163	0.068115	0.289486	0.459275	0.152716	0.91795115	0.350097039
85	Look straight ahead	30	0.384142	0.55725	0.100781	0	0.094565	0.81669433	0.131132571
82	Look straight ahead	30	0.415346	0.52444	0.091139	0.009004	0.079748	0.83827365	0.119084661
129	Look straight ahead	30	0.554833	0.516888	0.121901	0.016748	0.110639	0.80460043	0.157192584
22	Look straight ahead	30	0.408473	0.3589	0.230028	0.35376	0.107702	0.9269623	0.284222466
101	Look straight ahead	30	0.681954	0.393214	0.23393	0.30556	0.127197	0.89637183	0.288626939
207	Look straight ahead	30	0.803884	0.373634	0.250689	0.339315	0.13745	0.89732037	0.307405133
39	Look straight ahead	30	0.563306	0.891968	0.814738	0.835073	1	0	0.848905516
60	Look straight ahead	30	0.904633	0.856139	0.767218	0.827978	0.795717	0.3696941	0.808466578
63	Look straight ahead	30	0.751602	1	1	0.940287	0.970484	0.18164572	1
75	Look straight ahead	30	0.1038	0.892334	0.640955	0.718199	0.752088	0.34858904	0.697194458
150	Look straight ahead	30	0.119444	0.87636	0.69146	0.754038	0.799396	0.30187337	0.742404691
230	Look straight ahead	30	0.220722	0.884525	0.655647	0.729921	0.795387	0.2866967	0.710446899
3	Look straight	30	0.003544	0.429951	0.006198	0.313465	0.003269	0.99857719	0.008423912
500	Look straight	30	0.041033	0.332534	0.055326	0.324303	0.053621	0.96324401	0.073455573
361	Look straight	30	0.41296	0.117773	0.350551	0.714561	0.115818	0.99786578	0.415235365
588	Look straight	30	0.238808	0.123974	0.362718	0.742184	0.120116	1	0.42793367
127	Look straight ahead	30	0.256596	0.063201	0.274793	0.453666	0.137572	0.92862224	0.334055705
422	Look straight ahead	30	0.05328	0	0.264692	0.398291	0.147635	0.90562011	0.322939159
424	Look straight ahead	30	0.014673	0.015828	0.288108	0.419739	0.160911	0.90016599	0.348601131
264	Look straight ahead	30	0.194561	0.47837	0.131084	0.045587	0.109649	0.81906569	0.168387177
529	Look straight ahead	30	0.25841	0.471684	0.130395	0.069764	0.100511	0.8399336	0.167549469
627	Look straight ahead	30	0.093939	0.522753	0.140496	0.058298	0.113347	0.82025136	0.179776889
315	Look straight ahead	30	0.963052	0.368622	0.2236	0.317706	0.11832	0.90775433	0.276943249
415	Look straight ahead	30	1	0.346966	0.227273	0.337337	0.119524	0.91249704	0.281108377
612	Look straight ahead	30	0.908407	0.409413	0.260101	0.413769	0.128505	0.92577662	0.317860878
183	Look straight ahead	30	0.872454	0.956315	0.94123	0.962534	0.974758	0.19587384	0.953129959
208	Look straight ahead	30	0.863198	0.923092	0.867539	0.901625	0.978829	0.12544463	0.892994469
307	Look straight ahead	30	0.833461	0.942534	0.881543	0.86174	0.976443	0.0844202	0.904542877
382	Look straight ahead	30	0.254559	0.872476	0.842746	1	0.779123	0.50889258	0.872400373
452	Look straight ahead	30	0.130052	0.888118	0.740817	0.792561	0.827287	0.28954233	0.785674147
570	Look straight ahead	30	0.123453	0.885741	0.652204	0.692779	0.787223	0.26559165	0.707348419

Appendix 3 Tables of ANN Results

The following tables were used for creating the graphs shown in figure 6-4 to figure 6-14:

LOOK STRAIGHT		Simulation Outputs			Absolute errors between Target and simulation outputs		
Volunteer	Target	s1	s2	s3	s1	s2	s3
1	10	10.72	9.69		0.7170	-0.3059	-10.0000
2	10	21.94	12.52	24.75	11.9440	2.5150	14.7510
3	10	65.00	75.15	2.62	54.9990	65.1540	-7.3844
4	10	6.84	31.27	11.74	-3.1588	21.2700	1.7400
5	10	10.00	40.00		0.0000	29.9950	
6	10	15.67	13.23	18.33	5.6740	3.2280	8.3300
7	10	12.28	9.83	9.26	2.2820	-0.1660	-0.7397
8	10	16.74	13.49	11.59	6.7360	3.4920	1.5900
9	10	10.00	17.40	30.00	0.0000	7.4030	20.0000
10	10	10.09	10.00	10.00	0.0880	0.0000	0.0000
11	10	19.39	19.80	10.42	9.3910	9.7960	0.4200
12	10	10.00	10.04	10.00	0.0000	0.0350	0.0000
13	10	112.32	66.65	73.64	102.3200	56.6520	63.6360
14	10	42.62	10.00	9.93	32.6220	0.0040	-0.0666
15	10	36.36	58.93	45.95	26.3550	48.9330	35.9500
16	10	13.22	23.57	2.48	3.2240	13.5680	-7.5235
17	10	-0.46	-38.43		-10.4633	-48.4250	
18	10	10.13	8.17		0.1310	-1.8257	
19	10	15.45	41.26	41.10	5.4490	31.2550	31.0970
20	10	10.18	29.81	10.00	0.1750	19.8130	-0.0011
21	10	35.81	18.34	52.56	25.8060	8.3370	42.5580
22	10	4.58	9.81	5.36	-5.4163	-0.1947	-4.6387
23	10	10.08	9.99	9.88	0.0780	-0.0054	-0.1210

LOOK RIGHT		Simulation Outputs			Absolute errors between Target and simulation outputs		
Volunteer	Target	s1	s2	s3	s1	s2	s3
1	30	8.04	20.07		-21.9600	-9.9300	
2	30	28.41	29.43	50.52	-1.5900	-0.5700	20.5200
3	20	36.17	-2.81	43.46	16.1700	-22.8100	23.4600
4	30	30.85	45.32	33.61	0.8500	15.3200	3.6100
5	30	30	30		0.0000	0.0000	
6	30	13.28	40.044	45.36	-16.7200	10.0440	15.3600
7	20	13.33	12.73		-6.6700	-7.2700	
8	30	25.39	16.94	-6.64	-4.6100	-13.0600	-36.6400
9	30	40	39.99	97.58	10.0000	9.9900	67.5800
10	30	84.54	104.39	10	54.5400	74.3900	-20.0000
11	30	73.85	74.3		43.8500	44.3000	
12	20	11.53	70	70	-8.4700	50.0000	50.0000
13	20	-10.25	-4.94	-13.54	-30.2500	-24.9400	-33.5400
14	20	52.47	10		32.4700	-10.0000	
15	20	31.74	30.95	17.24	11.7400	10.9500	-2.7600
16	20	26.63	0.52		6.6300	-19.4800	
17	20	21.9	31.34		1.9000	11.3400	
18	20	70.44	21.83		50.4400	1.8300	
19	20	23.42	23.67		3.4200	3.6700	
20	20	21.53	22.08	33.83	1.5300	2.0800	13.8300
21	20	16.69	30.06		-3.3100	10.0600	
22	20	28.96	22.07	26.07	8.9600	2.0700	6.0700
23	20	3.14	10.92	10.5	-16.8600	-9.0800	-9.5000

LOOK LEFT Volunteer	Target	Simulation Outputs s1	s2	s3	Absolute errors between Target and simulation outputs s1	s2	s3
1	40	38.12	38.77		-1.8800	-1.2300	
2	40	40.00	65.20		0.0000	25.2000	
3	30	20.69	20.69	15.78	-9.3100	-9.3100	-14.2200
4	20	48.7	15.46	9.11	28.7000	-4.5400	-10.8900
5	20	0.01	0.57		-19.9900	-19.4300	
6	20	17.88	28.59		-2.1200	8.5900	
7							
8	20	17.58	19.04	18.8	-2.4200	-0.9600	-1.2000
9	20	20	20		0.0000	0.0000	
10	20	49.98	-21.95		29.9800	-41.9500	
11	20	15.42	8.03	20	-4.5800	-11.9700	0.0000
12	30	62.87	54.88		32.8700	24.8800	
13	30	58.23	74.88	29.65	28.2300	44.8800	-0.3500
14	30	29.95	29.98	29.96	-0.0500	-0.0200	-0.0400
15	30	65.2	22.63	17.6	35.2000	-7.3700	-12.4000
16	30	29.89	29.99		-0.1100	-0.0100	
17	30	22.1	30.02		-7.9000	0.0200	
18	30	68.05	76.28		38.0500	46.2800	
19	30	34.08	34.9	25.42	4.0800	4.9000	-4.5800
20	30	22.04	53.83	50.86	-7.9600	23.8300	20.8600
21	30	33.92	31.25		3.9200	1.2500	
22	30	30	30	30.52	0.0000	0.0000	0.5200
23	30	31.79	17.33	12.16	1.7900	-12.6700	-17.8400

LEAN FORWARD		Simulation Outputs			Absolute errors between Target and simulation outputs		
Volunteer	Target	s1	s2	s3	s1	s2	s3
1	50	9.67			-40.3300		
2	60	60.00			0.0000		
3	60	60	41		0.0000	-19.0000	
4	60	54.221			-5.7790		
5	40	40	37.03		0.0000	-2.9700	
6	40	54.02			14.0200		
7							
8	40	33.39	19.45		-6.6100	-20.5500	
9							
10							
11	40	15.53	11.55		-24.4700	-28.4500	
12							
13	60	23.86	70.177	60.59	-36.1400	10.1770	0.5900
14	50	21.5	67.95		-28.5000	17.9500	
15	50	46.83	28.181	8.998	-3.1700	-21.8190	-41.0020
16	60	81.7			21.7000		
17	40	43.44	43.11		3.4400	3.1100	
18	60	55.79	33.6		-4.2100	-26.4000	
19	60	74.7			14.7000		
20	50	56.34	-18.55		6.3400	-68.5500	
21	60	58.38	55.034		-1.6200	-4.9660	
22							
23	50	10.08			-39.9200		

HEAD ON WHEEL		Simulation Outputs			Absolute errors between Target and simulation outputs		
Volunteer	Target	s1	s2	s3	s1	s2	s3
1	60	52.69			-7.3100		
2							
3	70	18.366	78.116		-51.6340	8.1160	
4	70	76.13			6.1300		
5	50	24.94			-25.0600		
6	50	22.46	89.05		-27.5400	39.0500	
7							
8							
9							
10							
11							
12	60	49.58			-10.4200		
13	70	-1.663	30.951		-71.6630	-39.0490	
14	60	80.194			20.1940		
15	60	55.24	58.25	97.22	-4.7600	-1.7500	37.2200
16	70	83.25			13.2500		
17	50	58.7	45.31		8.7000	-4.6900	
18	70	32.04			-37.9600		
19							
20							
21	70	63.76			-6.2400		
22							
23	60	55.407	16.21	14.85	-4.5930	-43.7900	-45.1500

LEAN RIGHT		Simulation Outputs			Absolute errors between Target and simulation outputs		
Volunteer	Target	s1	s2	s3	s1	s2	s3
1							
2	20						
3	40	45.16	44.2	46.3	5.1600	4.2000	6.3000
4	50	50.6	40.72		0.6000	-9.2800	
5	60	42.71	58.72	60.5	-17.2900	-1.2800	0.5000
6	60	52.9	49.12	61.56	-7.1000	-10.8800	1.5600
7	30	45.9	52.9	32.28	15.9000	22.9000	2.2800
8							
9	40	40	40		0.0000	0.0000	
10	40	40	40	40.04	0.0000	0.0000	0.0400
11							
12	40	6.91	6.8	-6.96	-33.0900	-33.2000	-46.9600
13	40	41.67			1.6700		
14							
15	40	25.53	23.42	32.2	-14.4700	-16.5800	-7.8000
16	40	36.22	44.72		-3.7800	4.7200	
17							
18	40	40.04	39.74		0.0400	-0.2600	
19	40	38.04	38.74	37.73	-1.9600	-1.2600	-2.2700
20	40	40	40	40	0.0000	0.0000	0.0000
21	40	36.75	34.43		-3.2500	-5.5700	
22	40	36.83	37.12	37.5	-3.1700	-2.8800	-2.5000
23							

LEAN LEFT Volunteer	 Target	 Simulation Outputs s1	 s2	 s3	Absolute errors between Target and simulation outputs s1	 s2	 s3
1							
2							
3							
4	40	34.92	27.35		-5.0800	-12.6500	
5	70	69.97	109.84		-0.0300	39.8400	
6	70	40.15			-29.8500		
7	40	31.84	45.74		-8.1600	5.7400	
8	50	50	50.42		0.0000	0.4200	
9							
10							
11	50	49.99	50	49.99	-0.0100	0.0000	-0.0100
12	50	49.4			-0.6000		
13	50	51.03	84.7		1.0300	34.7000	
14	40	34.84	30.07	30.08	-5.1600	-9.9300	-9.9200
15							
16	50	46.89	39.9		-3.1100	-10.1000	
17							
18	50	22.53	18.01		-27.4700	-31.9900	
19	50	45.8	38.13	42.933	-4.2000	-11.8700	-7.0670
20							
21							
22							
23	40	-22.81	-18.47	-1.47	-62.8100	-58.4700	-41.4700

REACH RIGHT		Simulation Outputs			Absolute errors between Target and simulation outputs		
Volunteer	Target	s1	s2	s3	s1	s2	s3
1							
2							
3	80	52.69			-27.3100		
4							
5	80	35.31	9.96		-44.6900	-70.0400	
6	80	50.53	50.87		-29.4700	-29.1300	
7	50	51.52			1.5200		
8							
9	60	30	-28.44		-30.0000	-88.4400	
10	50	97.5	97.53		47.5000	47.5300	
11							
12							
13							
14							
15							
16	90	90	90		0.0000	0.0000	
17	80	45.58			-34.4200	-80.0000	
18	90	92.34	62.344		2.3400	-27.6560	
19	70	69.76	98.431	91.16	-0.2400	28.4310	21.1600
20	80	80	80	80	0.0000	0.0000	0.0000
21							
22							
23							

USE MOBILE PHONE		Simulation Outputs			Absolute errors between Target and simulation outputs		
Volunteer	Target	s1	s2	s3	s1	s2	s3
1							
2							
3							
4							
5							
6							
7							
8							
9							
10							
11							
12	70	70	70	70	**0.0000**	**0.0000**	**0.0000**
13	90	88.26	80.512		**-1.7400**	**-9.4880**	
14	80	80.02	99.291	80.041	**0.0200**	**19.2910**	**0.0410**
15	80	92.891	81.284	91.726	**12.8910**	**1.2840**	**11.7260**
16							
17	70	45.58			**-24.4200**		
18							
19							
20							
21	90	85.709	93.274	87.445	**-4.2910**	**3.2740**	**-2.5550**
22							
23							

LOOK BACK		Simulation Outputs			Absolute errors between Target and simulation outputs		
Volunteer	Target	s1	s2	s3	s1	s2	s3
1							
2							
3							
4							
5							
6							
7	60	56.9			**-3.1000**		
8	60	39.993	38.93		**-20.0070**	**-21.0700**	
9							
10							
11							
12							
13							
14	70	30.63			**-39.3700**		
15							
16	80	25.454			**-54.5460**		
17	60	3.88	3.8		**-56.1200**	**-56.2000**	
18							
19							
20	70	69.823	101.13	54.466	**-0.1770**	**31.1300**	**-15.5340**
21	80	51.43			**-28.5700**		
22							
23							